



**Grain characteristics of tephra from the
subglacial SILK-LN Katla eruption ~3400
years ago and the subaerial Hekla eruption
in 1947**

Edda Sóley Þorsteinsdóttir



**Faculty of Earth Sciences
University of Iceland
2015**

**Grain characteristics of tephra from the
subglacial SILK-LN Katla eruption
~ 3400 years ago and the subaerial Hekla
eruption in 1947**

Edda Sóley Þorsteinsdóttir

60 ECTS thesis submitted in partial fulfillment of a
Magister Scientiarum degree in Geology

Advisors
Esther Ruth Guðmundsdóttir
Guðrún Larsen

External examiner
Magnús Á. Sigurgeirsson

Faculty of Earth Sciences
School of Engineering and Natural Sciences
University of Iceland
Reykjavik, February 2015

Grain characteristics of tephra from the SILK-LN Katla eruption ~3400 years ago and the subaerial Hekla eruption in 1947

Characteristics of SILK-LN Katla and Hekla 1947 tephra

60 ECTS thesis submitted in partial fulfillment of a *Magister Scientiarum* degree in Geology

Copyright © 2015 Edda Sóley Þorsteinsdóttir
All rights reserved

Faculty of Earth Sciences
School of Engineering and Natural Sciences
University of Iceland
Askja, Sturlugata 7
101 Reykjavík
Iceland

Telephone: 525 4000

Bibliographic information:

Edda Sóley Þorsteinsdóttir, 2015, *Grain characteristics of tephra from the SILK-LN Katla eruption ~3400 years ago and the subaerial Hekla eruption in 1947*, Master's thesis, Faculty of Earth Sciences, University of Iceland, pp. 165.

Printing: Háskólaprent
Reykjavík, Iceland, February

Declaration

Hereby I declare that this thesis is written by me and that it has neither by part nor the whole been submitted previously to a higher degree.

Edda Sóley Þorsteinsdóttir
311079-3799

Abstract

In this project grain size and grain shape characteristics of silicic to intermediate tephra from two volcanoes, Katla and Hekla, are studied. Chemical composition of the tephra is similar but the eruption environment is quite different.

The ~3400 years old Katla SILK-LN and the Hekla 1947 tephra layers were studied with respect to grain size changes with distance from the source and their grain characteristics were compared. The main focus was on the finer fraction of the tephra grains. The results show obvious difference both in mean grain size and the fraction of finest particles from the two volcanoes. The Hekla 1947 tephra has significantly higher mean grain size and much lower content of material finer than $\leq 4 \Phi$ at all distances than in the SILK-LN tephra. The mean grain size of Hekla 1947 decreases more rapidly with distance than that of the SILK-LN tephra. The difference between the two layers regarding grain morphology is very clear. The grains from the Katla tephra are elongated and are even needle shaped, but the grains from the Hekla tephra are more equant.

A pilot study on silicic Katla layers (SILK) formed between 2800-8100 years ago was undertaken to examine whether their grain characteristics had changed with time and in such a case could indicate changes in eruption environment when the SILK layers formed. Neither mean grain size nor grain morphology of the SILK tephra layers changed with time but the second oldest tephra layer A11 stands out regarding the grain morphology not having the typical elongated grains and resembling more the 1947 Hekla tephra.

Útdráttur

Verkefnið fjallar um kornastærðareinkenni súrra til ísúrra gjóskulaga frá tveim eldfjöllum, Kötlu og Heklu. Efnasamsetning gjóskunnar er svipuð en gosumhverfið er ólíkt. Tvö gjóskulög, Kötulagið SILK-LN um 3400 ára gamalt og Heklulagið úr gosinu 1947 voru skoðuð með tilliti til kornastærðarbreytinga með fjarlægð frá upptökum og kornalögunareinkenni þeirra borin saman. Athygli var sérstaklega beint að finustu gjóskunni.

Greinilegur munur er bæði á meðalkornastærð og á hlutfalli fínefnis í gjóskulögunum frá þessum tveim eldfjöllum. Meðalkornastærð gjóskunnar úr Heklugosinu 1947 er talsvert hærri og hlutfall fínefnis, $\leq 4 \Phi$, er miklu minna í öllum fjarlægðum samanborið við SILK-LN gjóskulagið úr Kötlu. Munur á kornalögun Heklu- og Kötlugjóskunnar er mjög greinilegur, kornin í Kötlugjóskunni eru ílöng og jafnvel nárlaga en kornin í Heklugjóskunni fremur jafnása.

Kornalögun og kornastærð þekktra súrra til ísúrra Kötlugjóskulaga frá því fyrir 2800-8100 árum var rannsökuð með það að markmiði að kanna hvort kornaeinkenni gjóskulaganna gæfu upplýsingar um breytingar í umhverfi við gosstöðvarnar. Hvorki meðalkornastærð né kornalögun ísúru Kötluglaganna breytast með tíma en næstelsta gjóskulagið A11 sker sig nokkuð úr hvað kornalögun varðar. Það er ekki með hin dæmigerðu ílöngu korn og svipar fremur til Heklugjósku.

Table of Contents

List of Figures	xi
List of tables	xiii
Acknowledgements	xv
1 Introduction.....	1
2 Geological background and theory	3
2.1 Eastern Volcanic Zone	3
2.2 Katla Volcanic System	3
2.2.1 Geological setting and short overview	3
2.2.2 Volcanic activity and eruption history	4
2.2.3 The silicic Katla eruptions in Holocene time – previous work.....	6
2.2.4 The SILK-LN tephra	9
2.3 Hekla volcanic system	11
2.3.1 Geological setting and short overview	11
2.3.2 Volcanic activity and eruption history	12
2.3.3 Mixed explosive-effusive Hekla eruptions in historical time – previous work	14
2.3.4 The Hekla 1947 tephra.....	15
2.4 Explosive volcanism: Wet eruptions vs dry eruptions	17
2.4.1 Magmatic eruptions	17
2.4.2 Hydromagmatic/Phreatomagmatic eruptions.....	18
3 Methods.....	21
3.1 Field work – sample collection	21
3.2 Laboratory	25
3.2.1 Grain size analysis	25
3.2.2 Grain morphology analysis	25
4 Results	29
4.1 The SILK-LN tephra.....	29
4.1.1 Field characteristics (Macroscopic characteristics, bedding).....	29
4.1.2 Grain size characteristics	32
4.1.3 Grain Shape characteristics	37
4.2 The Hekla 1947 tephra	41
4.2.1 Field characteristics (Macroscopic characteristics, bedding).....	42
4.2.2 Grain size characteristics	43
4.2.3 Grain shape characteristics.....	49
4.3 Silicic Katla tephra layers: changes through the Holocene	54
4.3.1 Age range of silicic Katla tephra.....	54

4.3.2	Changes in grain size	54
4.3.3	Changes in grain shape	55
4.3.4	Changes in chemical composition with time	57
5	Discussion	61
5.1	Comparison of grain characteristics of silicic Katla and Hekla tephra	61
5.1.1	Grain size characteristics and changes with distance along axis of thickness	61
5.1.2	Changes with time	64
5.1.3	Grain morphology	65
5.2	Silicic Katla tephra layers: changes through the Holocene	67
5.3	Effects of fine tephra, 4Φ and smaller, on air traffic and health	69
6	Summary	71
	References	73
	Appendix I.....	81
	Appendix II.....	84
	Appendix III	102
	Appendix IV.....	122
	Appendix V	143
	Appendix VI.....	146
	Appendix VII	159

List of Figures

<i>Figure 2.1: Katla volcanic system</i>	<i>4</i>
<i>Figure 2.2: Tephra layer frequency of analysed basaltic Katla tephra, SILK tephra and unanalysed layers, partly Katla plotted against time (the 500 time interval).....</i>	<i>6</i>
<i>Figure 2.3: Axes of thickness of the silicic tephra layers from Katla</i>	<i>8</i>
<i>Figure 2.4: Isopach lines of the SILK-LN tephra layer.....</i>	<i>10</i>
<i>Figure 2.5: Hekla Volcanic System</i>	<i>11</i>
<i>Figure 2.6: Isopach map of the Hekla 1947 tephra layer</i>	<i>15</i>
<i>Figure 2.7: Mass ratio of water/magma versus efficiency and grain size</i>	<i>19</i>
<i>Figure 2.8: Plot of fragmentation</i>	<i>20</i>
<i>Figure 3.1: Sampling locations of the SILK layers</i>	<i>23</i>
<i>Figure 3.2: Map showing sampling locations of the Hekla 1947 layer</i>	<i>24</i>
<i>Figure 3.3: The Sedigraph III 5120 that was used in this study</i>	<i>25</i>
<i>Figure 3.4: Powers scale that shows few stages of grain roundness</i>	<i>26</i>
<i>Figure 3.5: Preparation work done in a microscope before using the computer image analyzing program Morphocop</i>	<i>27</i>
<i>Figure 4.1: SILK-LN tephra layer in Loðnugil</i>	<i>30</i>
<i>Figure 4.2: SILK-LN tephra layer collected at Varmárfell.....</i>	<i>31</i>
<i>Figure 4.3: SILK-LN tephra layer collected at Strútur hut.....</i>	<i>31</i>
<i>Figure 4.4: Grain size distribution of samples from Loðnugil.....</i>	<i>33</i>
<i>Figure 4.5: Mean grain size along the axis of thickness of SILK-LN plotted against distance from source.....</i>	<i>36</i>
<i>Figure 4.6: Finer particles of the SILK-LN tephra layer</i>	<i>37</i>
<i>Figure 4.7: Grain morphology of SILK-LN tephra versus distance from source</i>	<i>39</i>

<i>Figure 4.8: Selected pictures demonstrating the 6 categories and sub categories of grains photographed in the SEM electron microscope from samples collected in both Geldingasker and Varmárfell</i>	<i>41</i>
<i>Figure 4.9: Hekla 1947 tephra at Fljótsdalsheiði with tephra from Eyjafjallajökull eruption from 2010 at the top or just below the surface</i>	<i>42</i>
<i>Figure 4.10: Hekla 1947 tephra at Hamragarðaheiði</i>	<i>43</i>
<i>Figure 4.11: Examples of grain size distribution graphs of samples from Vestan Hafráfells (A), Fljótsdalsheiði (B) and Hamragarðaheiði (C).....</i>	<i>45</i>
<i>Figure 4.12: Mean grain size of Hekla 1947 plotted against distance from source</i>	<i>47</i>
<i>Figure 4.13: Finer particles of Hekla 1947 tephra layer.....</i>	<i>49</i>
<i>Figure 4.14: Grain morphology of Hekla 1947 tephra versus distance from source</i>	<i>51</i>
<i>Figure 4.15: Demonstration of 4 categories and sub categories of grains photographed in the SEM electron microscope from samples collected at Vestan Hafráfells, Fljótsdalsheiði and in Hamragarðaheiði</i>	<i>53</i>
<i>Figure 4.16: Examples of grain size distribution of the SILK layers.....</i>	<i>55</i>
<i>Figure 4.17: SEM images and shadow images (from Morphocop) showing the difference between the two oldest SILK tephra layers A12 and A11</i>	<i>57</i>
<i>Figure 4.18: Graph that shows CaO values plotted against FeO values</i>	<i>59</i>
<i>Figure 5.1: Mean grain size along the axis of thickness of the SILK-LN and Hekla 1947 tephra plotted against distance from source</i>	<i>62</i>
<i>Figure 5.2: Graph showing the fine material $\leq 4 \Phi$ (≤ 0.063 mm) in SILK-LN tephra and Hekla 1947 tephra, samples from all locations included.....</i>	<i>63</i>
<i>Figure 5.3: Graph showing particles equal and smaller than 6.5Φ (0.011 mm) in SILK-LN tephra and Hekla 1947 tephra</i>	<i>64</i>
<i>Figure 5.4: Ruggedness (lower values represent more rugged grains) of the SILK-LN and Hekla 1947 tephra plotted against distance</i>	<i>66</i>
<i>Figure 5.5: Elongation (lower values represent more elongated grains) of the SILK-LN and Hekla 1947 tephra plotted against distance</i>	<i>66</i>
<i>Figure 5.6: Circularity (higher values represent more circular grains) of the SILK-LN and Hekla 1947 tephra plotted against distance</i>	<i>67</i>

List of tables

<i>Table 2.1: Known prehistoric silicic Katla eruptions and their age</i>	<i>7</i>
<i>Table 2.2: Volumes of the youngest six SILK tephra layers on land.....</i>	<i>8</i>
<i>Table 2.3: Volumes of few historical Katla eruptions</i>	<i>9</i>
<i>Table 2.4: Thickness and distribution of the SILK-LN tephra</i>	<i>10</i>
<i>Table 2.5: Chemical analyses of the SILK-LN tephra layer.....</i>	<i>11</i>
<i>Table 2.6: Biggest prehistoric Hekla eruptions.....</i>	<i>13</i>
<i>Table 2.7: Thickness and distribution of the Hekla 1947 tephra</i>	<i>16</i>
<i>Table 2.8: Chemical analyses from the Hekla 1947 tephra layer</i>	<i>16</i>
<i>Table 3.1: Symbols used in field work for both the colors and the size of the tephra</i>	<i>22</i>
<i>Table 4.1: Results of grain morphology measurements</i>	<i>38</i>
<i>Table 4.2: Results of grain morphology measurements</i>	<i>50</i>
<i>Table 4.3: The 12 SILK tephra layers that were grain size and grain shape analyzed</i>	<i>54</i>
<i>Table 4.4: Results of grain shape measurements</i>	<i>55</i>
<i>Table 4.5: Average values (wt %) of chemical analyses performed on the SILK layers YN, UN, MN, LN, N4, N3, N2, N1, A1, A8 and A9.....</i>	<i>58</i>
<i>Table 5.1: Results of grain morphology measurements</i>	<i>65</i>

Acknowledgements

A lot of good people were involved in this project in one way or the other.

Firstly I would like to thank my advisors, Esther Ruth Guðmundsdóttir and Guðrún Larsen for excellent guidance.

This work was supported by the International Civil Aviation Organization as a part of the Catalog of Icelandic Volcanoes Project of the Icelandic Meteorological Office and the Institute of Earth Sciences, University of Iceland and would like to thank them sincerely.

Special thanks go to Bergrún Arna Óladóttir, Johanne Schmidt, Jón Eiríksson, Agnes Ösp Magnúsdóttir and Tinna Jónsdóttir. Last but not least I would like to thank my family for all their support and enthusiasm, especially Heiðar Vignir Pétursson and Hildur Grétarsdóttir.

1 Introduction

The recent eruptions in Eyjafjallajökull 2010 and Grímsvötn 2011 (Gudmundsson et al., 2012; Hreinsdóttir et al., 2014) have increased interest in the transport of fine-grained tephra and the proportion of particles 0.063 mm and smaller generated by different types of explosive eruptions. The fine-grained tephra particles tend to stay in the air for a long time and can be transported very far. Once an explosive eruption takes place and an ash cloud forms, these small fine particles can be carried to the level where air traffic takes place. Up in the air they can cause critical engine failure if an airplane encounters an ash cloud. Serious disturbances in flight transportations can therefore occur during an explosive eruption (e.g. Thorkelsson, 2012). The tephra can cause trouble in the area around the volcano for a long time after the eruption has ended due to wind blowing up the tephra into the air on windy days. Example of such windblown material is the fine tephra from the Eyjafjallajökull 2010 and Grímsvötn 2011 eruptions which reached Reykjavík on a number of occasions (Nicholson et al., 2014). During an eruption and afterwards on windy days the very fine glass grains can be harmful for the respiratory organs (Horwell and Baxter 2006). The surface of fine tephra grains is relatively big and if harmful chemical compound such as fluorine sticks to it, it can be carried into the nature and cause fluorine poisoning in grazing animals (e.g. Thorarinsson, 1970).

Tephra is a Greek word which Thorarinsson (1944) proposed as a collective term for all airborne material thrown out from a volcanic vent, regardless of size and shape. Tephra deposits are records of what has been left on the ground at varying distances from the volcanic vent. Nevertheless they are the only source that can provide information on the grain characteristics of the tephra from a particular eruption or type of eruption. There are obvious shortcomings - part of the material has travelled farther away and is missing. But these deposits can at least provide information on the minimum proportion of the fine material that was present in an eruption cloud at a particular distance and they can also provide information on variations in grain characteristics between different types of explosive eruptions.

The project described in the following chapters is a part of a larger project aimed at the characterization of tephra from different types of explosive Icelandic eruptions through analysis of grain sizes and grain shapes. This thesis deals with tephra of similar chemical composition from two eruptions occurring in different environmental settings, one from the ice-covered Katla volcano and the other from the ice-free Hekla volcano.

Among the questions of interest is whether the effect of the eruption environment is discernible in the grain characteristics of the tephra from these two eruptions? Of particular interest is the proportion of tephra 0.063 mm and smaller and how it changes with distance from source, as well as during the course of the eruptions. Also, will the grain types reflect the different eruptive environment they were generated in? And in such a case will the difference in grain shape have potential effects on the long-range transport?

A small pilot study, looking at potential changes in grain size and grain shape of silicic tephra layers from the ice-covered Katla volcano with time, was also carried out. The

period 8100-2800 years ago includes the Holocene climate optimum followed by a gradual cooling and the question of interest is whether changes in the eruption environment can be discerned in the grain characteristics.

This work has been supported by the International Civil Aviation Organization as a part of the Catalog of Icelandic Volcanoes Project of the Icelandic Meteorological Office and the Institute of Earth Sciences, University of Iceland.

2 Geological background and theory

2.1 Eastern Volcanic Zone

In Iceland and on the continental shelf of Iceland there have been around 41 active volcanic systems in the Holocene and late-Pleistocene (Jakobsson et al., 2008). Since AD 870 just over half of these systems have been active. The simplest way of describing a volcanic system is that it consists of a central volcano, where eruptions are frequent and the magma is evolved, and a fissure swarm where eruptions are less frequent and the magma erupted is solely basalt. In central volcanoes a caldera may have formed along with geothermal activity. The products vary from basalts to rhyolites but are mostly basalt or basaltic andesite (Jakobsson et al., 2008; Larsen & Eiríksson, 2008; Thordarson & Larsen, 2007).

The Eastern Volcanic Zone (EVZ) is the most productive volcanic zone in Iceland and eruption frequency is also highest there (Thordarson and Larsen, 2007; Thordarson and Höskuldsson, 2008). Eight volcanic systems lie within the EVZ and four of them are the most active in Iceland, the Grímsvötn, Katla, Bárðarbunga and Hekla systems. In this project, product of two volcanic systems, Katla and the Hekla volcanic system, situated in the Eastern Volcanic Zone are being investigated.

2.2 Katla Volcanic System

2.2.1 Geological setting and short overview

Substantial parts of the volcanic zones in Iceland are covered with ice. Eruptions that start below glaciers are therefore nowhere more common than here in Iceland (e.g. Thordarson & Larsen, 2007). One of those partly ice-covered volcanic systems is the Katla volcanic system which is situated in the southern part of the Eastern Volcanic Zone, and has been one of the most active ones during Holocene. Katla volcanic system is about 80 km long and with a southwest-northeast direction. The system is widest in the southwestern part and narrows down to less than a 1 km at its northeast tip just west of Vatnajökull glacier (Figure 2.1) (Jakobsson, 1979; Larsen, 2000, 2010; Óladóttir et al., 2005, 2008).

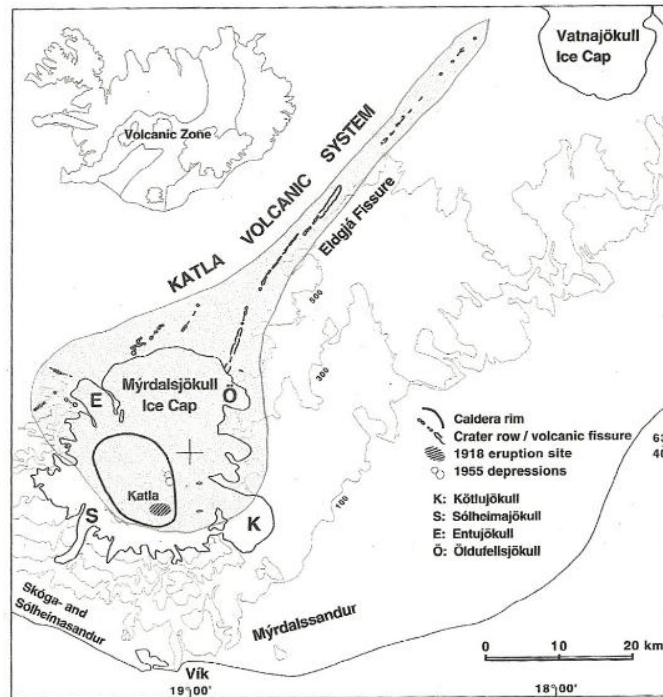


Figure 2.1: Katla volcanic system (shaded area) (from Larsen, 2000).

Katla volcanic system is comprised of a central volcano which is situated in the southern part of the system, under the 600 km² Mýrdalsjökull ice cap, and a fissure swarm located mostly outside the glacier (Figure 2.1). The Katla volcanic system has most likely been active for several hundred thousand years (Björnsson et al., 2000; Óladóttir et al., 2007, 2008). The Katla central volcano is a hyaloclastic massif ca 30-35 km in diameter and has a 110 km² ice filled caldera (Björnsson et al., 2000; Larsen, 2000; Óladóttir et al., 2007, 2008). The volume of the ice in the caldera has been calculated to be ca 45 km³ (Björnsson et al., 2000). The caldera age is not known. A silicic explosive eruption that created the Sólheimar ignimbrite and the Vedde Ash (Lacasse et al., 1995) may have contributed to its formation. A shallow magma chamber is thought to lie at ca 3 km below the surface (Guðmundsson et al., 1994; Brandsdóttir & Menke, 2008). Earthquakes that are connected to the Katla central volcano are mostly tied to the caldera but there is also some activity in the western part of Goðabunga (Einarsson & Brandsdóttir, 2000). Earthquake activity connected to Goðabunga may possibly be an indication of a another magma chamber which is not connected to the magma chamber situated under the Katla caldera (Einarsson & Brandsdóttir, 2000). Based on changes in the chemical composition of the basaltic Katla tephra layers, Óladóttir et al., (2008) postulated that the plumbing system below the Katla caldera changes with time.

2.2.2 Volcanic activity and eruption history

The Katla volcanic system has been one of the most active systems in Iceland during the Holocene (Larsen, 2000, 2010; Larsen et al., 2001; Björnsson et al., 2000; Óladóttir et al., 2005, 2008; Thordarson and Höskuldsson, 2008). Volcanic activity in Katla volcanic system in Holocene time has been divided into three categories (Larsen, 2000, 2010).

1. Explosive hydromagmatic/phreatomagmatic basaltic eruptions see chapter 2.4.2, which are the most frequent type of Katla eruptions in Holocene time. This type of

eruption begins under the ice cap as a short volcanic fissure and usually takes place within Mýrdalsjökull caldera. Once the ice has been melted away, which takes about 1-4 hours, they become subaerial. Tephra fall usually follows and is usually greatest in the beginning of an eruption (Larsen, 2000, 2010). “They appear to be the typical Katla eruptions as far back as the record from soil-sections goes” (Larsen, 2000, 3). In the past centuries the activity has mostly been located in the eastern part of the caldera.

2. Explosive silicic eruptions. The silicic eruptions are believed to be the second most common eruption type from Katla volcano in Holocene time. Silicic eruptions have their origin from a vent under the ice cap, either inside the caldera or possibly on the caldera fracture (Larsen, 2000, 2010). Compared to the explosive basaltic eruptions that occur within Mýrdalsjökull caldera the explosive silicic eruptions are generally smaller/less voluminous.
3. Effusive basaltic eruptions, the least common, mostly take place outside the glacier on the fissure swarm. Some fissures lie partly under the glacier, which has caused some explosive activity as well. Katla events do not get any bigger than those eruptions, and there have only been two events in Holocene time that fit this description (Larsen, 2000, 2010).

When eruptions take place in Katla volcano, melt-water flows out from under three glaciers: Entujökull, Kötlujökull and Sólheimajökull. In historical time or since late in the 12th century most Katla jökulhlaups have emerged from Kötlujökull and headed down to Mýrdalssandur or 18 in total. In prehistoric time and before the Eldgjá fires in the 10th century the jökulhlaups also broke out from Entujökull outlet which is situated in the northwestern part of Mýrdalsjökull ice cap. Katla jökulhlaups are quite large, for example the maximum flow in the Katla 1918 eruption was ca 300.000 m³/s (Tómasson, 1996; Larsen, 2000, 2010).

Katla eruption history in the Holocene is fairly well known and especially the history of the basaltic eruptions. What characterizes the Katla eruptions in the Holocene is that the majority of the eruptions start below the icecap, both basaltic and silicic eruptions.

Tephrochronological studies from the area east of Mýrdalsjökull demonstrate that the frequency of the basaltic eruptions is higher in prehistoric time than in the historical time (Óladóttir et al., 2005, 2008). A total of 172 basaltic tephra layers were assigned to the Katla volcanic system, representing 8400 years of activity. The historical basaltic Katla eruptions are thought to be 21, that is, the ones that have reached the ice surface, and left behind a tephra layer (Larsen, 2000, Óladóttir et al., 2005). If the prevailing wind directions have remained approximately the same in the last 8400 years the number of basaltic eruptions in Holocene could be at least 300 (Óladóttir et al., 2005, 2008). Silicic Katla explosive eruptions have not occurred in historical time that is in the last 11 centuries. At least 17 silicic eruptions have occurred in prehistoric time (Newton, 1999; Larsen, 2010).

Eruption frequency of basaltic eruptions in historical time has been ca 1-3 eruptions per century and for prehistoric time the eruption frequency is estimated at ca. 4 eruptions per century (Óladóttir et al., 2005, 2008).

When closely observing the silicic and the basaltic frequency changes in prehistoric time, two eruption peaks are noticed where there is increased activity (Óladóttir et al., 2005).

Five different time intervals were investigated, 200, 400, 500, 700 and 1000 years and in all the intervals the tephra layer frequency distribution appears to have two peaks, possibly even three peaks. In Figure 2.2 an example of the 500 years interval is shown, which demonstrates clearly two peaks in the tephra layer frequency in between 2.5-4.5 ka and 6.5-8.5 ka (Óladóttir et al., 2005).

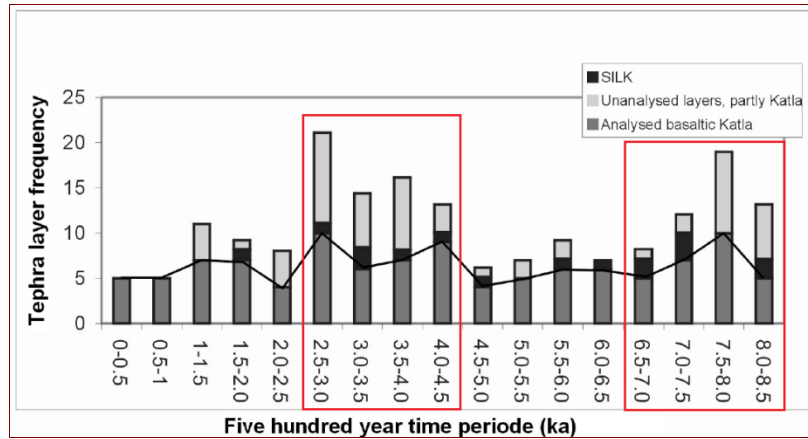


Figure 2.2: Tephra layer frequency of analysed basaltic Katla tephra, SILK tephra and unanalysed layers, partly Katla plotted against time (the 500 time interval). On this graph we see the eruption frequency peaks between (2.5-4.5ka) and between (6.5-8.5 ka) (after Óladóttir et al., 2005).

2.2.3 The silicic Katla eruptions in Holocene time – previous work

The subject of investigation among other are the silicic Katla (SILK) tephra layers and the SILK-LN tephra layer. Published material about the silicic tephra from the Katla volcanic system is scant. Hitherto most of the papers have focused on the basaltic volcanism (e.g. Larsen, 2000; Óladóttir et al., 2005, 2008).

Of the 17 known silicic tephra layers (Table 2.1) four have been dated by radiocarbon measurements on peat immediately below the tephra and 12 have been given an approximate age using soil accumulation rates (SAR) between tephra layers of known age (Table 2.1 and references therein). All are prehistoric and the most recent one erupted/produced is called SILK-YN and is about 1620 years old (1675 ± 12 ^{14}C BP). Slight amount of silicic material is present in basaltic tephra from both historical and prehistoric time. It is not considered sufficient enough to be categorized as mixed eruptions since the amount is less than 1% (Larsen et al., 2001).

Table 2.1: Known prehistoric silicic Katla eruptions and their age.

SILK Tephra	¹⁴ C age BP	¹⁴ C age cal b2k & SAR age	Rounded age	References
YN	1676±12	1622±40	~1600	Dugmore et al., 2000
UN	2660±50	2850±70	~2800	Larsen et al., 2001
MN	2975±12	3230±30	~3200	Larsen et al., 2001
LN	3139±40	3440±75	~3400	Larsen et al., 2001
N4		~3920	~3900	Estimated after Óladóttir et al., 2008
N3		~4050	~4100	G. Larsen unpublished data
N2		~4960	~5000	After Óladóttir et al., 2005, Table 1b
N1		~5830	~5800	After Óladóttir et al., 2005, Table 1b
A1		~6010	~6000	After Óladóttir et al., 2005, Table 1b
A2		~6700	~6700	Estimated after Óladóttir et al., 2005, 2008
A3		~6900	~6900	Estimated after Óladóttir et al., 2005, 2008
A5		~7100	~7100	Directly above Hekla-5, 7125 cal b2k
A7		~7180	~7200	Estimated after Óladóttir et al., 2008
A8		~7400	~7400	Estimated after Óladóttir et al., 2008
A9		~7500	~7500	
A11		~8000	~8000	Estimated after Óladóttir et al., 2008 Estimated after Óladóttir et al., 2008
A12		~8100	~8100	Estimated after Óladóttir et al., 2008

The source of the silicic eruptions is believed to be inside the Katla caldera. On Figure 2.3 it is demonstrated how the axes of thickness of six silicic layers intersect more or less inside the caldera. It is also possible that the source of some of the silicic eruptions is at the caldera fracture (Larsen et al., 2001). There are silicic rocks that crop out, e.g. at Austmannsbunga, but the geochemistry of the outcrops does not support this (Lacasse et al., 2007). Óladóttir et al., (2007) have shown that during the last 8400 years the sulphur degassing of the basaltic Katla tephra has been arrested, indicating that the basaltic Katla tephra was quenched by contact with water in hydromagmatic/phreatomagmatic eruptions. This indicates that the caldera was never ice-free during the last 8400 years, or at least there was water present. It is therefore believed that when the silicic eruptions occurred the volcano/area was covered with ice, and the environmental conditions were ice and meltwater. Thus the silicic eruptions have been taking place under similar conditions as the basaltic eruptions.

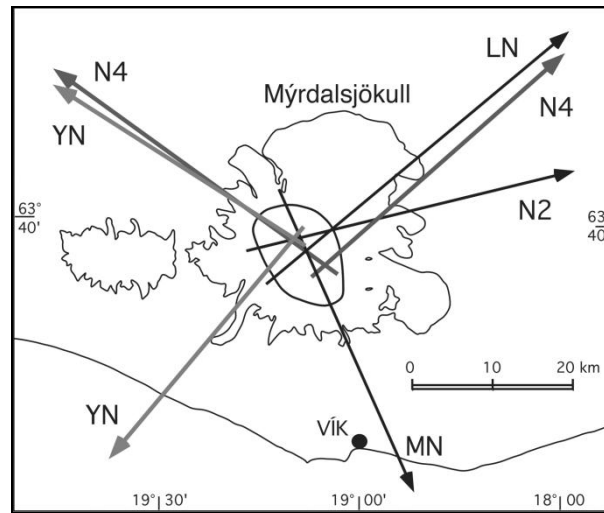


Figure 2.3: Axes of thickness of the silicic tephra layers from Katla (Larsen, 2000).

Dispersal maps exist for six silicic tephra layers (Larsen et al., 2001). The distribution and the shape of the tephra lobes of these silicic eruptions suggest that they have been rather short lived and small with a small eruption plume. Volume calculations of six silicic tephra layers (Table 2.2) show that the silicic eruptions were generally smaller than the known basaltic eruptions (Table 2.3) (Larsen et al., 2001; Larsen, 2010). Silicic Katla tephra has nevertheless been found overseas, e.g. in the Faroe Islands and Ireland (Hall and Pilcher, 2002; Wastegård, 2002). The basaltic Katla eruptions have lasted from few days to several months. The basaltic tephra has also dispersed beyond Iceland and has been reported from the Faroe Islands, Shetland Islands and the mainland of Europe (Thorarinsson, 1981; Larsen et al., 2001; Larsen, 2010).

Table 2.2: Volumes of the youngest six *SILK* tephra layers on land. *CPT* stands for compacted tephra volume and *UCP* uncompacted or freshly fallen tephra (Larsen et al., 2001).

SILK Tephra	CPT km³	UCP km³
Layer YN	0.04	0.08
Layer UN	0.16	0.27
Layer MN	0.03	0.05
Layer LN	0.12	0.20
Layer N4	0.07	0.11
Layer N2	0.04	0.06

Table 2.3: Volumes of few historical Katla eruptions (UCP: uncompactd or freshly fallen tephra)(Larsen, 2010).

Tephra layer	UCP km ³
K-1755	0.8
K-1721	0.33
K-1660	0.26
K1625	0.5
K-1612	0.04
K-1500	0.5
K ca. 1357	Ca. 0.2
K-1262	0.48
E ca. 934	Ca. 4.5
K ca. 920	0.27

The silicic tephra from Katla volcano has specific characteristics in the field. Most of them are of olive-green to gray-green color and have elongated glass grains in varying amounts. Three out of the 17 known silicic prehistoric tephra layers have more distinct characteristics than the others. This difference lies both in the size and shape of the grains but the grains are prominently needle shaped. The term “needle layer” was first used about these layers (Ólafsson et al., 1984), in English UN (upper needle layer), MN (middle needle layer) and LN (lower needle layer). The prefix SILK (silicic Katla layer) was added later (Larsen, 2000). The needles form when vesicles are drawn out into tubes, often flattened, with very thin walls that break into needle-like grains or thin glass plates. The needle grains are very sensitive and brittle because of the thin walls. The elongated grains have measured up to more than 8 cm long and 1-2 cm wide. More equant grains, sometimes massive, occur as well in most of the layers. The needle layers have very unusual appearance and no other Icelandic tephra layer looks like the needle layers, although there are some characteristic features in these layers, thin flat like grains, that are similar to the tephra that was formed in the Öraefajökull eruption in 1362 (Larsen, 2000; Thorsteinsdóttir, 2012). It is worth mentioning that Dr Grant Heiken, author of the Atlas of volcanic ash (1974) and Volcanic Ash (1992) who kindly inspected a sample of the SILK-LN tephra in 2014, did not know of any tephra having this characteristics. Even though basaltic eruptions are more common in Katla volcanic system than silicic, investigation on silicic tephra is just as important for future volcano hazard assessment. Investigations carried out on silicic Katla tephra are therefore of great importance.

2.2.4 The SILK-LN tephra

The source of the SILK-LN tephra layers is believed to be under the ice cap of Mýrdalsjökull, as explained earlier. Dispersal, volume and chemical composition of the SILK-LN tephra layer has been investigated previously by Larsen et al (2001) (Figure 2.4; Table 2.4 & 2.5).

The SILK-LN tephra layer is the second largest silicic tephra layer from Katla. The volume of compacted tephra has been calculated and it is about 0.12 km³ and for uncompactd tephra about 0.2 km³. Thickness has only been measured beyond ca 22 km distance,

because large part of the tephra fell straight on to Mýrdalsjökull ice cap and was not preserved. In the case of SILK-LN the maximum thickness is therefore not known. The greatest thickness that was measured at ca 22 km distance was about 12 cm. The eruption site has not been exactly located, i.e. whether it is inside the caldera or along the caldera rim (Larsen et al., 2001). The dispersal/distribution map of the SILK-LN tephra layer shows one narrow main lobe, which is mostly directed to the northeast and a minor lobe towards southeast (Figure 2.4).

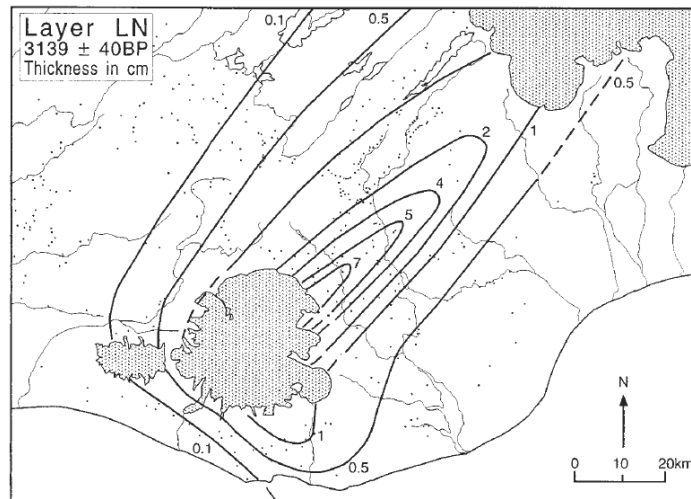


Figure 2.4: Isopach lines of the SILK-LN tephra layer (Larsen et al., 2001).

The area on land which the SILK-LN tephra layer covers is $>15000 \text{ km}^2$ within the 0.1 cm isopach line see Table 2.4. The narrow isopachs of SILK-LN could indicate a rather short-lived eruption and/or strong wind during deposition. Explosive activity in the silicic eruptions has been considered to be of relatively low intensity with relatively low eruption columns (Larsen et al., 2001).

Table 2.4: Thickness and distribution of the SILK-LN tephra (Larsen et al., 2001).

Isopach,	Km ²
Within 10cm	100
Within 7 cm	150
Within 5 cm	360
Within 4 cm	610
Within 2 cm	1115
Within 1 cm	2640
Within 0,5 cm	4980
Within 0,1 cm	15000

The majority of the silicic tephra layers from Katla volcano have been chemically analysed. Chemical analyses on the tephra have revealed that the major element composition is similar, with SiO₂ content between ca 63 – 67 % (Appendix VII). The average SiO₂ content in the SILK-LN tephra layer is 65.23 % (Table 2.5).

Table 2.5: Chemical analyses of the SILK-LN tephra layer (Larsen et al., 2001).

Tephra	SiO ₂	TiO ₂	Al ₂ O ₃	FeO	MnO	MgO	CaO	Na ₂ O	K ₂ O	Total
SILK-LN	65.93	1.25	14.32	5.83	0.20	1.12	3.06	4.51	2.91	99.13
	65.84	1.26	14.34	5.80	0.18	1.09	3.15	4.45	2.83	98.94
	65.63	1.27	14.09	5.48	0.20	1.09	3.02	4.54	2.86	98.18
	65.58	1.12	14.38	5.73	0.23	1.18	2.95	4.40	2.74	98.31
	65.34	1.24	14.29	5.69	0.10	1.14	3.06	4.51	2.76	98.31
	65.30	1.20	14.19	5.38	0.15	1.12	3.08	4.28	2.79	97.49
	65.01	1.23	14.45	5.42	0.18	1.19	2.90	4.09	2.64	97.11
	64.28	1.14	14.03	5.65	0.20	1.08	3.03	4.49	2.60	96.50
	64.12	1.22	14.13	5.60	0.25	1.11	2.92	4.54	2.71	96.60
Average	65.23	1.21	14.25	5.62	0.19	1.12	3.02	4.42	2.76	97.84

2.3 Hekla volcanic system

2.3.1 Geological setting and short overview

The Hekla volcanic system is situated in the Eastern Volcanic Zone. Unlike Katla volcano Hekla is not ice covered, however perennial snow is found on the top and upper slopes. Hekla volcanic system is about 40 km long and about 7 km wide as defined by Jakobsson (1979). The fissure swarm of the system lies across the highest point of Hekla volcano and has a southwest-northeast direction. Another fissure swarm is situated to the southeast of the Hekla volcanic system and is possibly thought to belong to the Hekla volcanic system due to similar chemical composition of its basalt, see Figure 2.5 (Jakobsson, 1979; Jóhannesson and Einarsson, 1992; Sigmarsson et al., 1992; Thordarson and Larsen, 2007). If the Vatnafjöll fissure swarm belongs to the Hekla system it is about 60 km long and 20 km wide (Jóhannesson and Sæmundsson, 1998; Larsen et al., 2013).

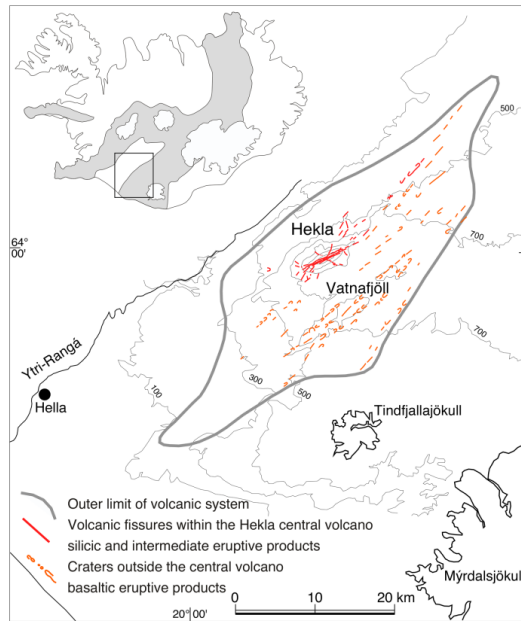


Figure 2.5: Hekla Volcanic System (after Larsen et al., 2013 and Jóhannesson & Sæmundsson 1998).

Hekla volcano itself consists mostly of lava flows and pyroclastic material with a tuff/palagonite foundation, the lava and pyroclasts being mostly basalt and andesite. Hekla volcano has been categorized as an intermediate stage between stratovolcano and crater row according to the classification scheme of Icelandic volcanoes (Thorarinsson 1967). About 6 km long fissure on top of Hekla ridge reaches out to the shoulders of the mountain. In large eruptions the fissure opens on the top in the beginning of the eruption then progresses in both directions away from the top and out towards the shoulders. This fissure is called Heklugjá.

Most fissures that have opened up in Hekla eruptions have had the main direction east-northeast – west-southwest along the Heklugjá but in the recent eruptions fissures have opened up on the flanks as well. Palagonite ridges and hills in the vicinity of Hekla suggest that eruptions took place in the Hekla volcanic system back in the ice age (Jakobsson, 1979). The postglacial history of the Hekla volcano we know today began about 7000 years ago.

A magma chamber is believed to be situated below Hekla. What supports the existence of a magma chamber is that the chemical composition of the magma changes with time, the longer the repose between eruptions the more silicic is the first erupted material in the next eruption (Thorarinsson, 1967; Sverrisdóttir, 2007). The one who first brought up the idea of a magma chamber situated under below Hekla was Jens Tómasson (1967). He did not only assume that there was one magma chamber, he mentioned the possibility of two magma chambers (Tómasson, 1967). The magma chamber is now believed to be situated below 10-14 km depth (Soosalu & Einarsson, 2004; Höskuldsson et al., 2007).

Basaltic to intermediate material from Hekla is thought to belong to the transitional alkalic series and the intermediate to silicic material is thought to belong to the tholeiitic series. (Jakobsson et al., 2008). The material that has been produced in historical Hekla eruptions has mostly been of intermediate composition. Material produced in Hekla tends to be more silicic the longer the eruption interval is (Thorarinsson, 1968).

2.3.2 Volcanic activity and eruption history

Postglacial activity of Hekla volcanic system can be divided into three eruption types: purely explosive eruptions; mixed explosive-effusive eruptions, both occurring within the Hekla central volcano; and effusive fissure eruption occurring mostly outside the Hekla central volcano.

The magma erupted in the explosive- and the mixed eruptions ranges from rhyolite to basaltic andesites. However in the effusive fissure eruptions the magma is basaltic (Larsen & Thorarinsson, 1977; Larsen et al., 2013). More detailed description of these three different eruption types of Hekla is as following:

1. Purely explosive eruptions in Hekla are magmatic see chapter 2.4.2 of plinian type and are almost solely tephra producing eruptions. The biggest eruptions in Iceland are of this type and they have formed more than 10 km³ of freshly fallen tephra. The biggest prehistoric Hekla eruptions, including the one from 1104 is of the type described here. What characterizes these eruptions is high initial silica content (Larsen & Thorarinsson, 1977).

2. Mixed eruptions start with an explosive phase but then the eruption develops towards effusive eruption. In the initial explosive phase the eruptive material is predominantly tephra. Lava emission begins very soon and takes place simultaneously with the explosive activity but once the effusive phase takes over mostly lava is produced. The initial explosive phase of the mixed eruptions can be either Plinian or Sub-Plinian. A good example of mixed eruption with powerful opening phase is the Hekla 1947 eruption where the eruptive column reached 30 km height in the explosive beginning phase (Thorarinsson, 1968). Example of Sub-Plinian eruption is the Hekla 2000 eruption where the eruptive column only reached about 11-12 km height (Lacasse et al., 2004).
3. The last group comprises the basaltic fissure eruptions. The material produced is mostly basaltic lava which is low in silica content and tephra production is usually small. Most of these fissure eruptions lie outside of Hekla volcano on the fissure swarm. These fissures are not long and often discontinuous. The tephra produced in the fissure eruptions does not travel far away from the source, in most cases. (Larsen & Thorarinsson, 1977; Larsen et al., 2013).

Eruption history of Hekla is over all well known and written documents exist on most historical Hekla eruptions. In the book Heklueldar the history of Hekla eruptions since 1104 is treated in detail (Thorarinsson, 1968).

The biggest Hekla eruptions took place in the prehistoric time and are from the oldest to the youngest the H5, HÖ, H4, HS and H3 eruptions (Table 2.6). Two of them, H3 ~3000 years old and H4 ~4300 years old, are the biggest tephra layers formed in Hekla in prehistoric time, see table 2.6 (Larsen & Thorarinsson, 1977; Guðmundsdóttir et al., 2011). All of these largest Hekla tephra layers erupted between 7000-3000 years ago. The silica content was high in the beginning phase (ca 74-72 % SiO₂) and decreased gradually towards lower silica content as the eruption went on (ended in ca 57 % SiO₂). After the eruption that formed the H3 tephra layer changes took place in the eruptive activity. In the next 2000 years or up to the settlement in the 9th century AD the eruptions were relatively small in comparison to the big events that occurred earlier. These eruptions are believed to be around 30 and belong to three eruption periods (Róbertsdóttir et al., 2002). What characterizes these eruption periods is mainly the chemical composition (dacite to basaltic andesite; andesite to basaltic andesite; and basaltic stages), which displays in the color of the tephra. Repose intervals in this time period are from 15 years to 300 years (Larsen & Vilmundardóttir, 1992; Róbertsdóttir et al., 2002).

Table 2.6: Biggest prehistoric Hekla eruptions, within 0.1 cm isopach line except 0.2 cm for H-1104 (Larsen & Thorarinsson, 1977; Guðmundsdóttir et al., 2011; Larsen et al., 2013).

Volcanoe Hekla	Age of tephra layer	Volume on land mill. m³	Total volume mill. m³	Tephra fall area on land km²	% SiO₂ of initial tephra
H5	~7100	~2500	~3000	62000	74
HÖ	~6100	~1000	Unknown	59000	60-76
H4	~4300	~6700	~10000	78000	74
HS	~3900	~1500	>2000	19000	~70
H3	~3000	~8000	~10000	80000	73

Total of 18 eruptions has taken place in the Hekla volcano in historical time (Kjartansson, 1945; Thorarinsson, 1967, 1968, 1970; Grönvold et al., 1983; Larsen et al., 1992; Höskuldsson et al., 2007). One silicic explosive eruption has occurred in the historical time, in the year 1104. The other 17 eruptions are mixed eruptions, which begin with an explosive phase followed by lava effusion (Thorarinsson, 1967, 1968; Larsen & Thorarinsson, 1977; Thordarson & Larsen, 2007). Also there have been at least 5 basaltic fissure eruptions on the fissure swarm or outside of Hekla itself (Jakobsson, 1979).

2.3.3 Mixed explosive-effusive Hekla eruptions in historical time – previous work

The Hekla 1947 eruption, investigated in this study, is of the mixed explosive-effusive category.

Many eruptions from the historical time are well known from written documents. Some of these sources give information on year, date and even the time of an eruption. These eruptions have been treated by e.g. Sigurður Þórarinnsson, Guðmundur Kjartansson and Jens Tómasson (Kjartansson, 1945; Thorarinsson, 1968). The Hekla eruption in 1947 and following eruptions have been observed and documented by numerous geoscientists (e.g. Thorarinsson, 1954, 1967, 1968, 1970; Grönvold et al., 1983; Larsen et al., 1992; Höskuldsson et al., 2007).

These eruptions begin by a plinian (e.g. Hekla 1947) or sub-plinian phase (e.g. Hekla 2000) lasting for several hours. In most eruptions a fissure opens up along the Hekla ridge and on the upper slopes, as in 1947 and 1991, but in some cases fissures open up on the lower slopes of Hekla as in 1970. Tephra production comes mostly from the fissure along the ridge. Lava production begins almost immediately from the fissure on the ridge but is then concentrated at the lower parts on the shoulders (Thorarinsson, 1968; Höskuldsson et al., 2007).

The SiO₂ content of the first erupted magma increases with the length of the preceding interval. This is also seen in the characteristics of the tephra erupted after long repose. The 1947, 1845 and 1510 tephra layers have a brown or grayish brown tephra at the bottom and brownish black tephra at the top, reflecting change in composition of the magma with time (Thorarinsson 1967, 1968). The tephra in the 1970, 1980, 1991 and 2000 layers is black (Sverrisdóttir, 2007).

Documented eruption column height is 30 km above sea level in 1947 but has not exceeded 16 km in later eruptions (16 km 1970, 15 km 1980, 12 km 1991, 11-12 km 2000). Volumes of tephra in historical eruptions, excluding Hekla 1104, range from 0.01 km³ (10 million m³) in Hekla 2000 to 0.5 km³ (500 million m³) in Hekla 1300, calculated as freshly fallen. By far the largest lava flow was extruded in 1766-68 or 1.3 km³ (Thorarinsson, 1968; Grönvold et al., 1983; Larsen et al., 1992; Höskuldsson et al., 2007).

Several Hekla eruptions have sent tephra overseas, in 1947 (Finland, Ireland), in 1845 (Faroe Islands, Orkneys) in 1510 (Scotland, Ireland), in 1158 (Norway, Ireland) and in 1104 (Norway, Ireland) (Wastegård & Davies, 2009 and references therein).

2.3.4 The Hekla 1947 tephra

The 1947-Hekla eruption started at 06:41 on March 29 in the summit of Hekla volcano and ended on 21 of April 1948. The eruption plume rose slowly at first but after a strong earthquake there was a quite an increase in energy of the eruption. In early stages the eruption plume was about 27 km high and later it had reached up to 30 km height. Close to 08:00 it was down to 10 km height. The main direction of the Hekla 1947 eruption plume was to the south.

The pumice fall in Fljótshlíð, 30 km to the south, started around 07:10. In the beginning the color of the pumice was grey brown then about half an hour later the color changed to brownish black and finer grain size than in the grey brown material. The boundary between the grey brown pumice (SiO_2 64-61%) and the brownish black pumice (SiO_2 58-56%) was sharp. In the end, for a short while more delicate black tephra fell down. The thickness of evenly distributed tephra in the inner part of the region is ca 10 cm, but ca 3 cm in the western part of the region close to Hlíðarendi. In Vestmannaeyjar the thickness was 0.13 cm. Close to Hekla or in between Vatnafjöll and Hekla the thickness was ca 0.5 – 1 m (Figure 2.6). To the north of Hekla no tephra- or pumice fall took place in the beginning of the eruption. Some tephra was transported all the way to Finland. It is also possible that tephra reached Russia (Thorarinsson 1954, Thorarinsson 1968).

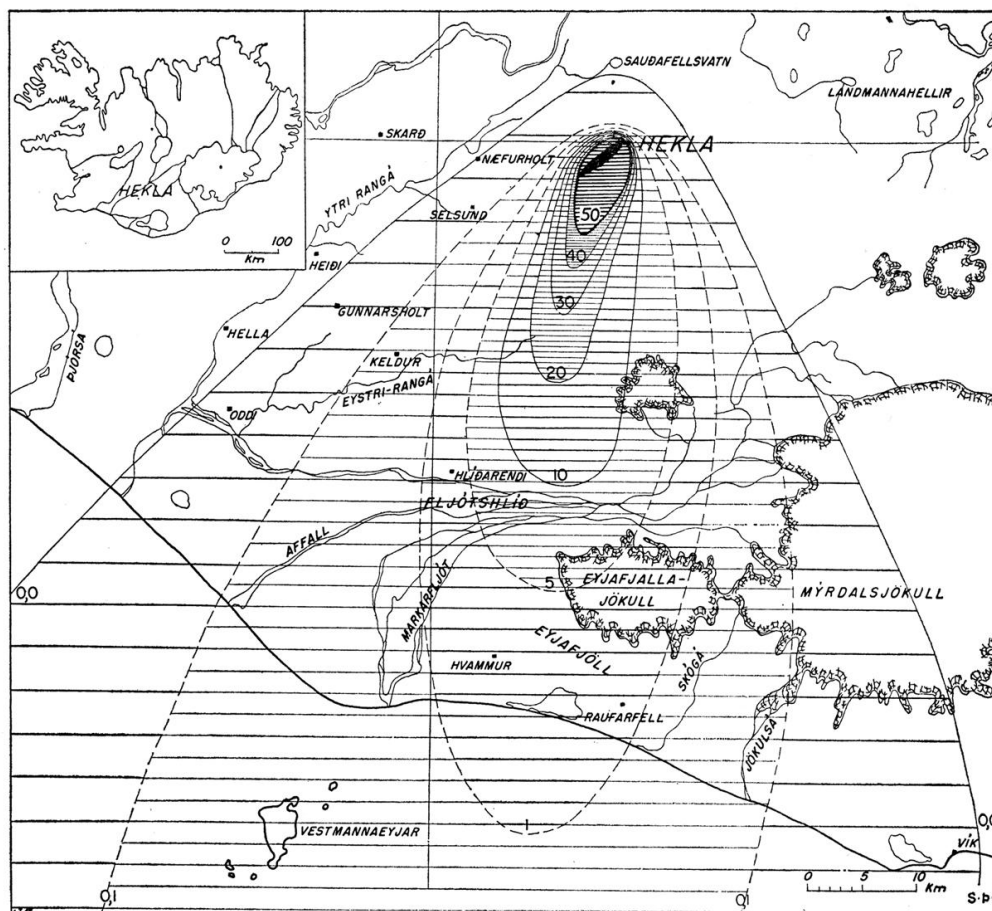


Figure 2.6: Isopach map of the Hekla 1947 tephra layer (thickness in cm) (after Thorarinsson, 1968).

The total volume of pumice and tephra in the beginning phase of the eruption and for the first few hours has been calculated and is believed to be around 180 million m³. The tephra from the first eruption phase covered about 3130 km² of land. The amount of tephra that fell on land has been calculated to be around 120 million m³. Table 2.7 contains the thickness and distribution from the beginning phase of the Hekla 1947 tephra. Most of the tephra was deposited during the first day of the eruption (Thorarinsson, 1968).

Table 2.7: Thickness and distribution of the Hekla 1947 tephra (after Thorarinsson, 1968).

Isopach line	Km ²
Within 100 cm	15
Within 50 cm	30
Within 40 cm	50
Within 30 cm	76
Within 20 cm	139
Within 10 cm	311
Within 5 cm	605
Within 1 cm	1310
Within 0.5 cm	2040
Within 0.2 cm	12000
Within 0.006 cm	70000

Chemical analyses on Hekla tephra from 1947 are presented in Table 2.8. The samples come from the first phase of the eruption (bottom unit) and do not show those changes with time regarding the concentration changes in SiO₂ (Larsen et al., 1999). The glass analyses were performed with electron probe micro analyser (EPMA).

Table 2.8: Chemical analyses from the Hekla 1947 tephra layer (Larsen et al., 1999).

	SiO ₂	TiO ₂	Al ₂ O ₃	FeO	MnO	MgO	CaO	Na ₂ O	K ₂ O	Total
	63.91	1.03	15.12	7.80	0.21	1.25	4.17	4.18	1.66	99.33
	63.34	0.98	14.96	7.46	0.22	1.23	4.30	4.27	1.75	98.51
	62.97	0.92	15.34	7.72	0.24	1.25	4.42	4.83	1.88	99.50
	62.56	1.03	15.13	8.12	0.27	1.36	4.66	4.25	1.71	99.08
	62.51	0.88	15.30	8.09	0.20	1.14	4.54	4.77	1.65	99.08
	62.14	0.96	15.02	7.88	0.24	1.18	4.28	3.95	1.73	97.39
	62.01	0.91	15.28	7.99	0.20	1.32	4.40	4.26	1.77	98.13
	61.03	0.92	15.11	8.12	0.22	1.31	4.52	4.59	1.66	97.49
	60.07	1.33	15.13	8.63	0.26	1.73	5.15	2.88	1.61	96.76
	59.09	1.15	15.19	8.98	0.24	1.71	4.99	4.52	1.69	97.48
<i>Mean</i>	62.15	0.98	15.13	8.01	0.22	1.28	4.46	4.38	1.73	98.48

2.4 Explosive volcanism: Wet eruptions vs dry eruptions

Explosive eruptions are of two different kinds, magmatic explosive eruptions where the explosive activity is first and foremost caused by gas expansion in the magma and secondly hydromagmatic/phreatomagmatic eruptions which are caused by interaction between external water and magma. (White & Houghton, 2000; Morrissey et al., 2000; Vergnolle & Mangan, 2000; Cashman et al., 2000; Francis, 2001; Francis & Oppenheimer, 2004).

Eruptions in Iceland can be phreatomagmatic, wet or magmatic, dry. As discussed previously, Katla volcanic system is partly covered by ice and the majority of the eruptions in Katla occur under ice, i.e. under wet conditions. Thus volcanism in Katla is characterized by phreatomagmatic eruptions. Volcanism in Hekla volcanic system is characterized by dry eruptions.

2.4.1 Magmatic eruptions

Magmatic eruptions (sometimes called dry eruptions), are divided into several types, for example Hawaiian, Strombolian and Plinian eruptions. They are as mentioned earlier, eruptions where only volatiles take place in the explosive activity. The two basic processes of tephra formation are fragmentation of the magma and the cooling of the fragments or clasts. In purely magmatic eruptions fragmentation is caused by exsolution and expansion of gases belonging to the magma itself. The fragments are then cooled during flight through the air.

In the Hawaiian and Strombolian eruptions the magma is basaltic or basaltic andesite but usually intermediate or silicic in plinian eruptions. The Hawaiian magma is less viscous than magma in Strombolian eruptions so the volatiles escape more easily. Therefore the explosiveness is greater in the Strombolian eruptions. In addition the magma in the Hawaiian eruptions is hotter and less viscous because of higher temperature. Intermediate and silicic magma is much more viscous which prevents the volatiles from escaping easily. This, together with generally higher volatile content, is the main reason for the much higher explosiveness of plinian and subplinian eruptions (Cashman et al., 2000; Vergnolle & Mangan, 2000; Francis & Oppenheimer, 2004).

In the following only silicic magma is considered. Fragmentation of magma may occur when the tensile strength of the melt is exceeded. If strain rates acting on the magma are so high that they cannot respond fast enough the melt can break as a solid matter would, in a brittle fashion (e.g. Cashman et al., 2000; Zhang, 1999). Fragmentation in magmatic eruptions where the magma is high-viscosity silicic magma may result either from rapid acceleration or rapid decompression of magma according to Cashman et al., (2000). In the former vesiculation and growth of bubbles causes the expansion and acceleration of the magma through a conduit. The vesiculating magma forms foam and fragmentation occurs by the disintegration of the magma foam when its tensile strength is exceeded during rapid acceleration. In the latter case fragmentation of already vesiculated magma, that may be stationary or moving slowly, occurs by rapid decompression resulting in bubble rupture and explosive eruption of the fragments. Cashman et al., (2000) also mention that both fragmentation mechanisms may be acting simultaneously in plinian eruptions, and that

pumice clasts may result from the fragmentation by rapid acceleration and fine ash may be the result of fragmentation by sudden decompression. Accordingly, the proportions of pumice and fine ash may indicate the relative importance of these fragmentation mechanisms in magmatic eruptions. Fine material can also form as a result of abrasion of pumice clasts as they collide with each other or conduit walls during ascent and ejection (Rose & Durant, 2009).

In pumice from plinian eruptions vesicularity is commonly 70-85% (Cashman et al., 2000) indicating that this was the vesicularity of the magma upon fragmentation. The mixture of fragments and gas leaves the vents at high speed, up to 600 m/sec, producing high eruption columns that can reach as high as 45-55 km in extreme cases (Cas & Wright, 1987). Plinian eruptions produce widespread fall deposits that can cover very large areas ($>100\,000\text{ km}^2$).

2.4.2 Hydromagmatic/Phreatomagmatic eruptions

Eruptions that begin under ice caps, wet eruptions, are the most common ones in Iceland. The reason is that many volcanic systems in Iceland are partly covered with glaciers. Phreatomagmatic/hydromagmatic eruptions therefore characterize the volcanic activity in Iceland (Thordarson & Larsen, 2007; Thordarson & Höskuldsson, 2008). These eruptions are mainly basaltic.

Hydromagmatic eruptions are divided into three categories: Phreatic eruptions where magma is not directly involved, phreatomagmatic eruptions and phreatoplinian eruptions where the magma fragments as a result of interaction with water and becomes extremely fine grained tephra. Characteristic feature of phreatic eruptions is steam explosion that causes the bedrock to explode and blow up into the air.

Fragmentation in hydromagmatic eruptions is much more complex process than in magmatic eruptions. The presence of external water can affect both fragmentation and cooling at various stages in an eruption.

Phreatomagmatic basaltic eruptions (including surtseyan eruptions) are the most common and the best known hydromagmatic eruptions. Considerable knowledge exists from direct observations of such eruptions and their deposits and from experiments involving the interaction of water and basaltic melts, resulting in fragmentation as in Molten Fuel Coolant Interaction (e.g. Morrissey et al., 2000; White & Houghton, 2000; Zimanowsky et al., 1997; Wohletz, 1983).

Wohletz (1983) did a research on eruptive material that had formed by interaction of magma and water. From these investigations he designed a graph that shows maximum and minimum fragmentation caused by external water (Figure 2.7). This graph demonstrates the mass ratio of water and magma against efficiency and approximate median grain size. With increased fragmentation the grain size decreases. If the mass ratio of water/magma is less than 0.3 the efficiency decreases and the grains get bigger. In that kind of situation there are two things that maintain the explosive activity of the eruption; on the one hand volatiles and on the other hand steam. Once the mass ratio of water/magma is about 0.3 and even slightly more than 0.3 the water and magma maintain the explosions in the eruption.

At this stage the efficiency is as high as it gets, the fragmentation of magma is as much as it gets and the smallest grains are produced (Cas & Wright, 1987; Wohletz, 1983).

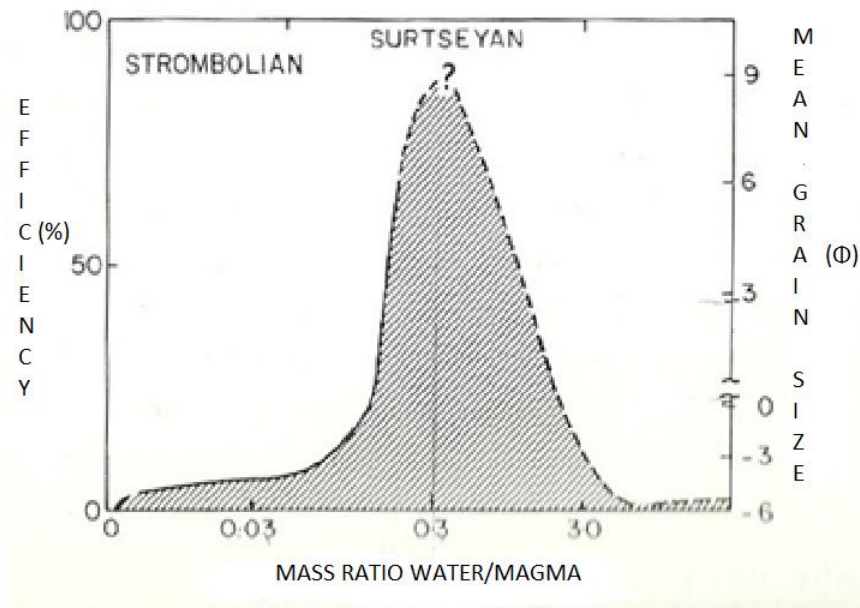


Figure 2.7: Mass ratio of water/magma versus efficiency and grain size (Wohletz, 1983).

Grains formed in phreatomagmatic basaltic eruptions have been classified into five main types and their formation has been clarified by experiments (e.g. Morrissey et al., 2000; Wohletz, 1983). The blocky grains form by brittle fracture when deformation rates exceed the tensile strength of the melt and also by thermal contraction in quenched portions of the melt. Fusiform grains with fluidal surfaces form from portions of melt that fragment prior to quenching. Moss-like grains form by viscous deformation under tensional stress conditions but drop-like grains develop from the effect of surface tension from fluid melt. Plate-like grains are thought to be pieces stripped off quenched crust. One of the characteristics of phreatomagmatic basaltic eruptions is the presence of lithics from substrata of the vents and from conduit walls.

Phreatoplinian eruptions are very rare compared to the other two types and not as well known phenomena (White & Houghton, 2000; Morrissey et al., 2000; Francis, 2001; Francis & Oppenheimer, 2004). This category was first recognized and named by Self and Sparks (1978), partly based on observations of the widespread unit C in the Askja 1875 eruption. The characteristics described by them were abundant fine ash, even near the source, well bedded deposits and accretionary lapilli, all indicating the presence of water. Self and Sparks (1978) concluded that the extreme fragmentation was due to magma/water interaction superimposed on fragmentation caused by vesiculation and expansion of gases in the magma itself. The wide dispersal indicated deposition from a high eruption column. About 90% of the total grains size in Askja unit C was smaller than 1 mm (Sparks et al., 1981) see Figure 2.8.

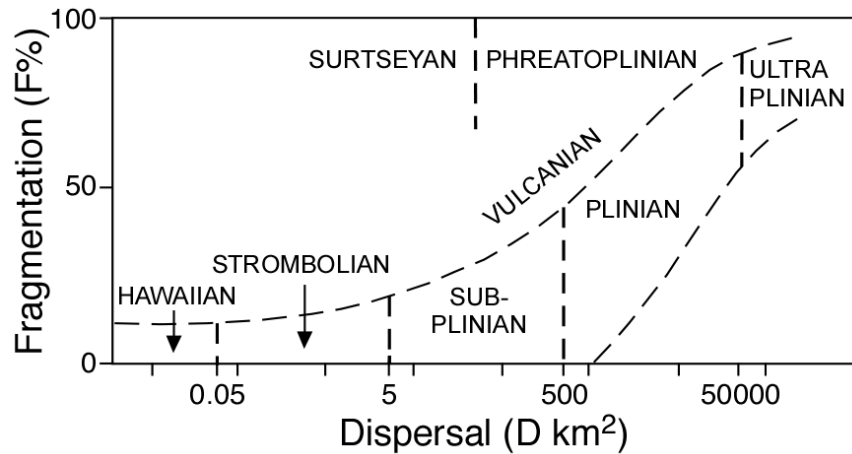


Figure 2.8: Plot of fragmentation index F (weight % finer than 1 mm where the isopach for 0.1 T_{max} crosses dispersal axis) against dispersal index D (area enclosed by the isopach for 0.01 T_{max}). After Walker (1980).

Fragmentation in most of the phreatoplinian eruptions described by Houghton et al., (2000) was brought about by vesiculation and bubble expansion as well as by quenching by external water. The pumice clasts were vesicular enough to imply that the magma had already formed foam and perhaps begun to fragment or disintegrate when it first encountered external water. The fragmentation resulting from the magma-water interaction could be the result of thermal contraction upon quenching, brittle failure caused by high shear rate resulting from expansion of steam or both these mechanisms. Lithics appear to be less common in phreatoplinian eruptions than in the basaltic ones. This could suggest that the fragmentation caused by water takes place at the interface between the magma and ice/water, rather than deeper in the conduit (Dellino et al., 2012).

Knowledge about phreatoplinian eruption columns or plumes is limited. It has been suggested that limited amount of water will have little effect on the height and dispersive power but excessive amount will cause column collapse and pyroclastic flows or surges (Houghton et al., 2000).

Only two examples of recent explosive silicic (>63% SiO_2) eruptions within a glacier was found in literature (Guðmundsson et al 2012; Kratzmann et al., 2009). It is suggested that some phases of the 1991 Hudson eruption were phreatoplinian because of the fine ash produced. However, no phase of the Eyjafjallajökull eruption was classified as phreatoplinian although about 94% of the tephra from the first phase (14-16 April) was smaller than 1 mm and up to 50% smaller than 0.063 mm.

3 Methods

A detailed description on all the methods used can be found in Appendix II.

3.1 Field work – sample collection

The tephra samples come from two volcanoes, the subglacial Katla volcano and the Hekla volcano. The Katla tephra samples are silicic in composition. Sample locations are shown on Figure 3.1, a total of 12 places. Most of the samples were collected from the Katla layer SILK-LN (SILicic Katla - Lower Needle layer). From other SILK layers only one sample was collected from each eruption/layer, the main focus with Katla is therefore the SILK-LN layer.

The Hekla samples are silicic to intermediate and only one tephra layer is investigated, or the Hekla 1947 eruption. The Hekla 1947 samples were collected in total of 3 places (Figure 3.2) as a complement to the field and laboratory measurement of Thorarinsson were used (Thorarinsson, 1954).

Sampling locations or soil sections in the case of SILK-LN and Hekla 1947 were collected in the thickness axis and were the tephra deposits and soil was undisturbed. Samples in two cross sections over the thickness axis of SILK-LN tephra were collected. The sections and the tephra layers were cleaned, photographed, measured and macroscopic features described such as bedding, grading, color, texture, grain size and grain types using modified Atterberg scale (Atterberg, 1903; Table 3.1; Appendix II). The classification after Schmidt (1981) modified by Thordarson is commonly used in Fisher & Schmincke, 1984. Following logging, samples were collected from the tephra layers either bulk samples and/or samples from particular units within the layers (Appendix II and chapter 4).

Table 3.1: Symbols used in field work for both the colors and the size of the tephra.

Tephra color	Tephra size terms*	Type
S: black	f: < 0.2 mm	a: tephra/ash
Grgr: grey green	s: 0.2 til 2.0 mm	b: berg (rock fragm.)°
Grá: grey	m: 2 mm til 2 cm	
B: brown	g: > 2 cm	
Ólgr: olive green	<i>Further divisions into s ÷ & s+ and m ÷ & m+indicate grain sizes in the lower and upper part of each class</i>	<i>°Not relevant here</i>

*Modified from grade scale of Atterberg (1903). Names in Swedish and Icelandic: Fine material <0.2 mm is named mo, lättler, ler (méla, leir, here denoted by f); sand 0.2-2 mm (sandur - s); grus 2-20 mm (möl - m); sten 20-200 mm (grjót - g); block >200 mm. On drawings of tephra sections Thorarinsson (e.g.1967) and Larsen (e.g. 1996) only use three size categories, <0.2 mm, 0.2-2 mm, >2 mm, larger grains are drawn to scale. In fieldwork the last category is omitted and g is used for grains >20 mm, three to five largest grains are measured individually in the field or in samples collected.

SILK tephra

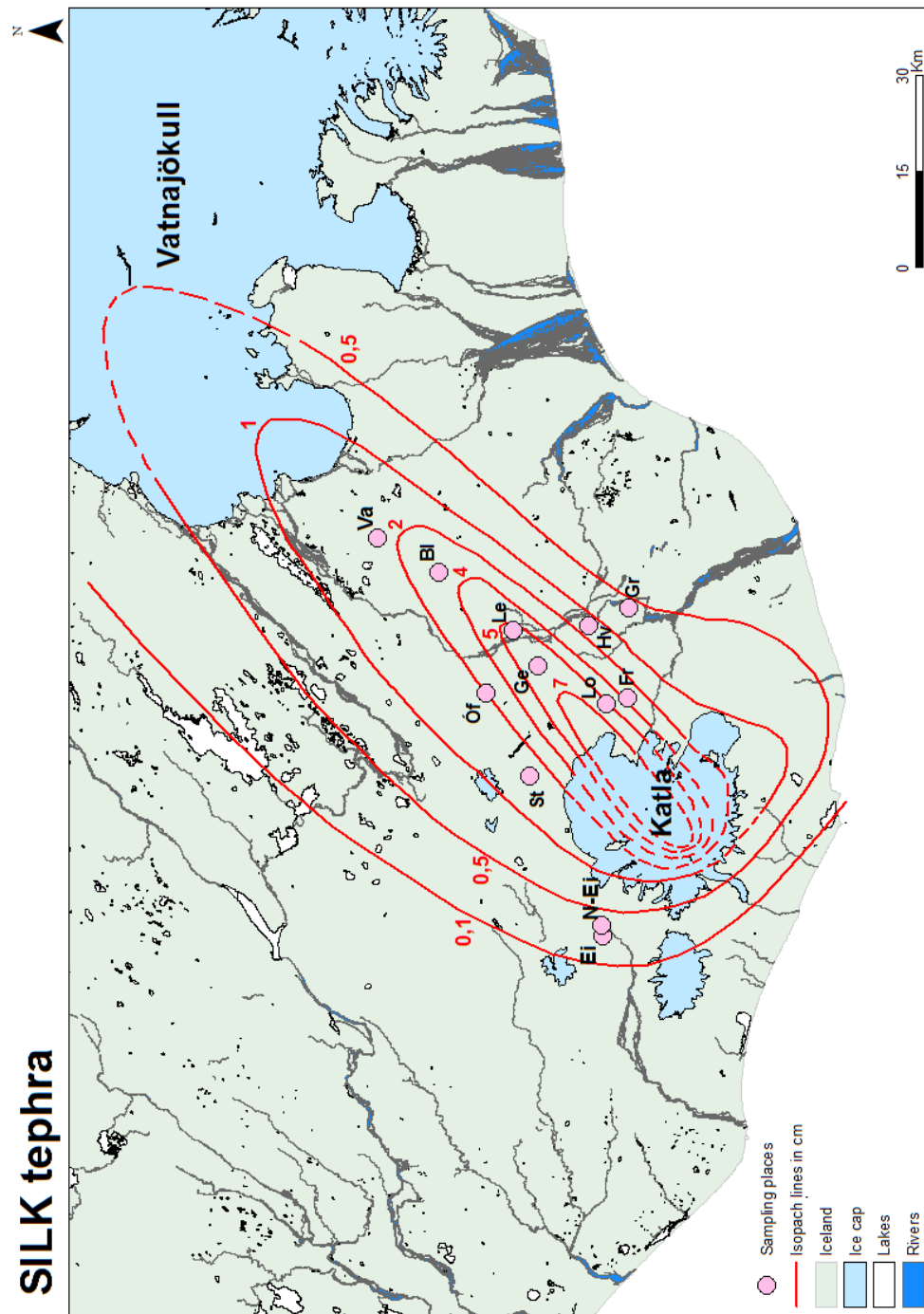


Figure 3.1: Sampling locations of the SILK layers (pink circles). SILK-LN samples were collected at following locations, (Va) Varmárfell, (Bi) Blálgil, (Le) Leiðólfssfell, (Óf) Ófeyri, (Ge) Geldingasker, (St) Strútur, (Lo) Lochnúgl, (Hv) Hvannmur and (Gr) Grófar. SILK samples through time were collected at following locations, (Fr) Frangil, (Ei) Einhyrningur and (N-Ei) Hill N of Einhyrningur. Map worked by: Edda Sóley Þorsteinsdóttir, References: Landmælingar Íslands, ISV50 Landgagnagrunnur Landmælinga Íslands. Projection, ISN_93.

Hekla-1947

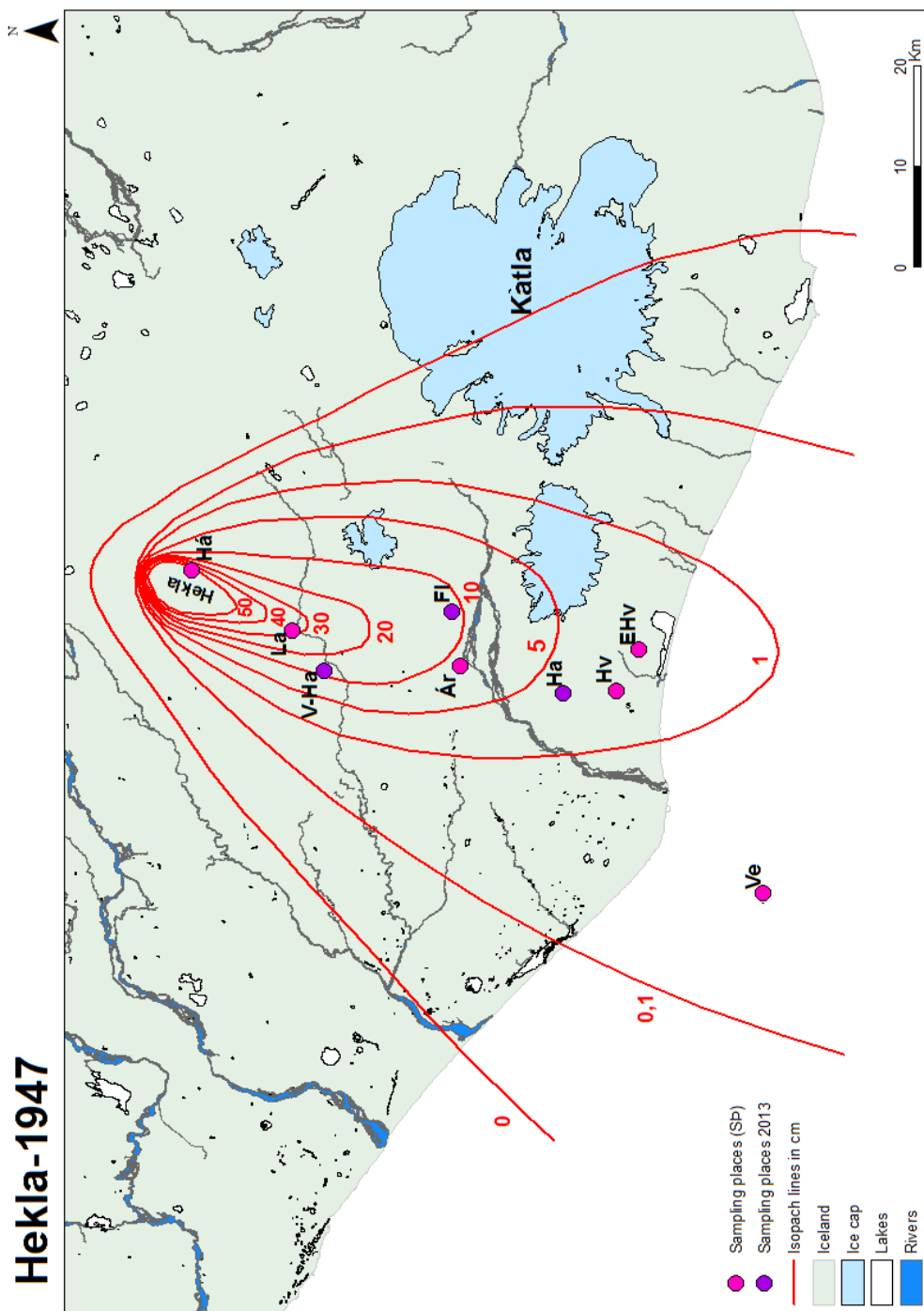


Figure 3.2: Map showing sampling locations of the Hekla-1947 layer (dark pink and purple circles). Hekla-1947 samples collected in 2013 were collected at following locations, (V-Ha) Vestan Hafið, (FI) Fjótalsheiði and (Ha) Hamragarðheiði. Hekla-1947 samples obtained by Sigurður Þórinsson, freshly fallen were collected at following locations, (Há) Háabrunn, (La) Langvuhraun, (Ar) Árkrönn, (Hv) Hvammur, (EHv) 4 km east of Hvammur and (Ve) Vestmannaeýjar. Map worked by: Edda Sóley Þorsteinsdóttir, References: Landmælingar Íslands, ISV50 Landgagnagrunnur Landmælinga Íslands, projection: ISN_93.

3.2 Laboratory

3.2.1 Grain size analysis

When analysing tephra grain size few methods can be used. The method chosen depends on the grain size. The most common ones are sieving and settling velocity measurements. Sieving is mostly used for size fractions larger than 4Φ and settling velocity for smaller than 4Φ (e.g. Fisher & Scmincke, 1984; Eiríksson, 1993; Boggs, 2013). In this study both sieving and settling velocity methods are used. A Sedigraph (Micromeritics, 2010) is used for the smaller grains (smaller than 4Φ) (Figure 3.3). The sedigraph can measure from 300 μm down to 0.1 μm .

After having both sieved the tephra layers and measured in the Sedigraph the results from both methods were combined and plotted on a graph, showing the complete/total grain size distribution of each tephra layer.

Grain size analysis can help to understand the eruption that produced the tephra in question (Appendix II and chapter 4). Grain size distribution can provide important information about an eruption because different eruption conditions, such as plume height, eruption intensity, changes in wind strength and fragmentation are all factors that influence both size and shape of the grains. Grain size influences the way of transport and how far the grains have travelled (e.g. Carey & Sparks, 1986; Dellino & Volpe, 1996; Rose & Durant, 2009; Bonadonna & Haughton, 2005; Eiríksson, 1993; Guðmundsdóttir, 1998; Óladóttir, 2003; Thorsteinsdóttir, 2012) Grain size analysis have been used to see what kind of operative mechanism drives the fragmentation process in different phases of an eruption (Dellino & Volpe, 1996).

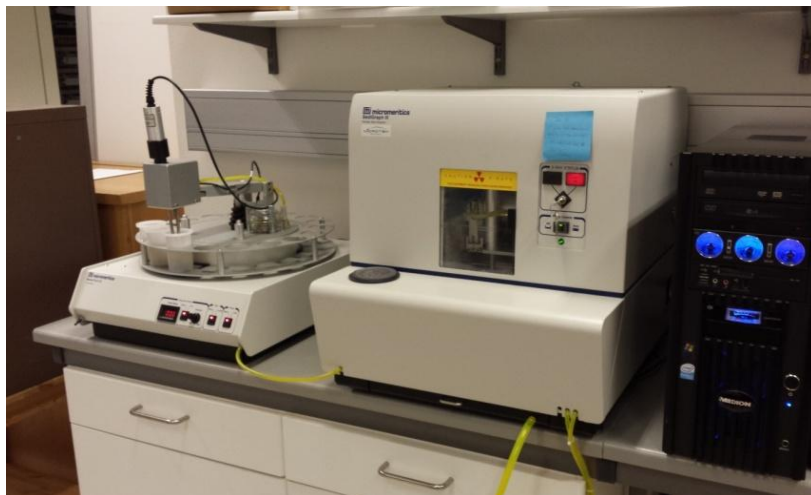


Figure 3.1: The Sedigraph III 5120 that was used in this study. To the left is the mastertech or a carousel, in the middle is the analysing instrument and to the right is the computer that contains the program that controls the instrument (Photo Thorsteinsdóttir, 2013).

3.2.2 Grain morphology analysis

When eruptions take place, most of them produce some tephra. Chemical composition, viscosity of the magma and the type of eruption influence the shape of the tephra grains that are produced (Eiríksson, 1993; Eiríksson, et al., 1994; Eiríksson & Wigum, 1989). Tephra grain morphology has been used to obtain information on whether the grains are a

product of fragmentation by hydromagmatic activity or due to exsolution of magmatic gases and to distinguish between different phases within an eruption (e.g. Eiríksson & Wigum, 1989; Dellino & Volpe, 1995; Gudmundsdóttir, 1998; Óladóttir, 2003; Dellino & Liotino, 2002; Büttner et al., 2002; Thorsteinsdóttir, 2012; Cioni et al., 2014). In addition grain morphology studies have been used to investigate the flight properties of tephra particles. i.e. how far and for how long they stay up in the air. Mele et al (2011) concluded that settling velocity of tephra grains is highly influenced by shape, it does not only depend on size and density. Such information is important with respect to international air traffic as evident from the Eyjafjallajökull eruption in 2010.

When defining the shape of tephra grains, several different parameters can be used. Among them are form, elongation, circularity, sphericity, roundness, ruggedness and surface texture which all are defined in their own way. The form concept (Zingg 1935) describes the ratio between length (L), width (I) and thickness (S) of sediment particles. Elongation is the ratio I/L . Circularity relates to the difference between area and perimeter. The roundness concept describes the outlines of sediment grains, how well-rounded they are and has been categorized from being very angular to well rounded (Figure 3.4, after Powers 1953) The more angular sediment grains, the smaller the roundness coefficient gets. Ruggedness relates to how rough the grain surface is. The surface texture concept describes the texture of sediment grains (Eiríksson, 1993).

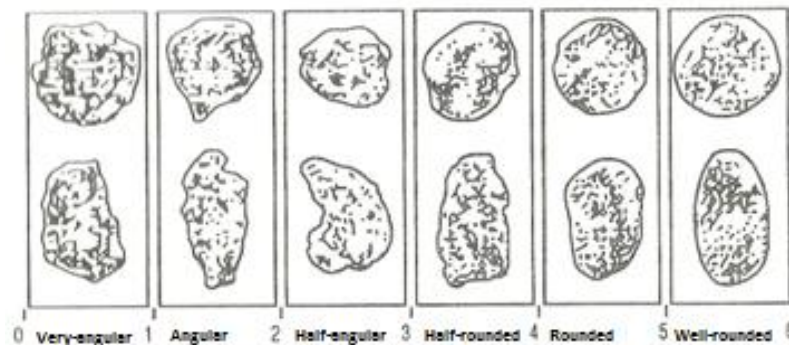


Figure 3.2: Powers scale that shows few stages of grain roundness (Eiríksson, 1993, after Powers 1953).

Grain morphology analysis was carried out on selected samples from both Hekla 1947 and silicic Katla tephra.

An attempt was made to use the new Particle Shape Analyzer (Particle Insight User Manual) at the Institute of Earth Sciences to measure grain morphology of SILK-LN tephra and Hekla 1974. However the instrument was unable measure the light colored tephra grains from Katla volcano. Therefore it was decided to measure the grain morphology by microscope imagery. About 50 grains, from 3 and 3.5 Φ fractions, were picked randomly, placed on a slide and photographed through a microscope. The photographs were processed and converted to grey-scale and run through an image analysis program (Morphocop) that measures morphological parameters such as ruggedness, elongation, and circularity etc. using definitions given by Schwartz (1980) (Figure 3.5). The Hekla tephra was cleaned using an ultrasonic bath to remove organic material adherent to the grains. The cleaning was successful and no organic matter was noticed afterwards.



Figure 3.3: Preparation work done in a microscope before using the computer image analyzing program Morphocop (Photo Thorsteinsdóttir, 2014).

4 Results

4.1 The SILK-LN tephra

In this chapter the results from the investigations on the SILK-LN (Silicic Katla – lower needle layer) tephra layer are discussed.

4.1.1 Field characteristics (Macroscopic characteristics, bedding)

Results of the investigations on the SILK-LN tephra in the field show that there are changes in macroscopic characteristics i.e. bedding, grain size, color etc. between sampling locations.

The locations where the SILK-LN tephra showed bedding lie in most cases along the axis of thickness, except in Blágil section, which shows no bedding. Other locations where the SILK-LN showed no signs of bedding are from the two cross sections of the SILK-LN tephra layer (Figure 3.1 & 3.2). Altogether 23 samples were collected, both bulk samples and samples from single units within the layer. At four locations, Loðnugil, Geldingasker, Leiðólfssfell and at Varmárfell, the layer was bedded and sample from each unit was collected. Where no bedding was apparent only a bulk sample was collected.

Sample locations from the axis of thickness are as follows, from closest to furthest away from the source: Loðnugil, Geldingasker, Leiðólfssfell, Blágil and Varmárfell. With the exception of Blágil the SILK-LN tephra in these different sampling places were divided into two to four units based on changes in macroscopic characteristics.

Loðnugil: The SILK-LN tephra at Loðnugil (22 km from the source) showed distinct bedding and was divided into four units (Figure 4.1). The bottom unit is 2 cm thick and grey to olive green. The lower middle unit is 4-4.5 cm thick and the color is grey green. The upper middle unit is 2-2.5 cm thick and the color is dark grey green. The top unit is 3.5-4 cm thick and the color is grey green. Total thickness of the layer is 11.5-13 cm.



Figure 4.1: SILK-LN tephra layer in Loðnugil (Photo Thorsteinsdóttir, 2012).

Geldingasker: The SILK-LN tephra at Geldingasker (33 km from the source) showed bedding and was divided into two units. The bottom unit is 5 cm thick and the color is grey green. The middle unit is 3-3.5 cm thick and the color is grey green. Total thickness of the layer is 11cm.

Leiðólfssfell: The SILK-LN tephra at Leiðólfssfell (40 km from the source) showed bedding and was divided into three units. Each unit was 2-3 cm thick. The color is grey green but slightly darker green in the middle unit. Thickness varies from 2.5 to 8.5 cm.

Varmárfell: The SILK-LN tephra at Varmárfell (65 km from the source) showed bedding and was divided into three units (Figure 4.2). The bottom unit is 0.5 cm thick and the color of the tephra is light grey green. The middle unit is 2-3 cm thick and the color is grey green. The top unit is 4 cm thick and the color is yellow green, possibly indicating some reworking. Total thickness of the layer is 6.5-7.5 cm.

Locations that showed no signs of bedding were as following: Blágil, Strútur hut, Ford at Syðri Ófæra, Hvammur and Grófará.

Blágil: At Blágil (54 km from the source) no sign of bedding was noticed. Bulk sample was collected. The color is grey green and total thickness of the layer is between 0 - 4 cm.

Strútur hut: At Strútur (24 km from the source) no sign of bedding was noticed. Bulk sample was collected (Figure 4.3). The color is olive green and total thickness of the layer is between 1 - 4 cm.

Ford at Syðri Ófæra: At Syðri Ófæra (36 km from the source) no sign of bedding was noticed. Bulk sample was collected. The color is grey green and the total thickness from all three locations is 1 - 2 cm.

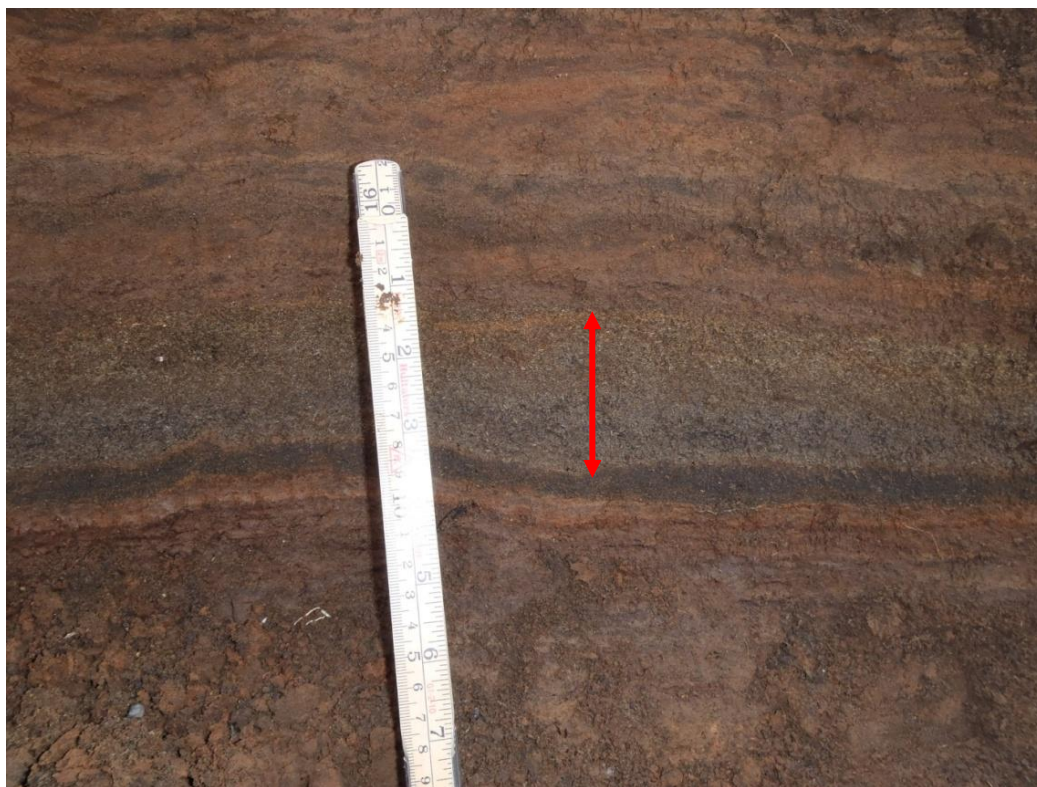


Figure 4.2: SILK-LN tephra layer collected at Varmárfell (Photo Thorsteinsdóttir, 2012).



Figure 4.3: SILK-LN tephra layer collected at Strútur hut (scale: table knife to the left) (Photo Óladóttir, 2013).

Hvammur: At Hvammur (34 km from the source) no sign of bedding was noticed. Bulk sample was collected. Total thickness is 1 – 2 cm and the color is olive-green.

Grófará: At Grófará (35 km from the source) no sign of bedding was noticed. Bulk sample was collected. The color is olive green and total thickness is 0.2 – 0.5 cm.

4.1.2 Grain size characteristics

For the grain size measurements of the SILK-LN tephra samples from 10 different locations were collected at about 22 to 65 km distance from the source. The samples were hand sieved down to 63 μm or 4 Φ and material finer than that was analysed in a Sedigraph. The program GradiStad was used to calculate mean grain size and sorting of each layer and each unit inside a bedded layer. A more detailed description of the grain size measurement can be viewed in chapter 3 and Appendix II – IV.

Changes in grain size with time

Loðnugil: In Loðnugil, closest to the source, five samples were collected, one bulk sample representing the whole layer and four samples from individual beds or units of the layer. The grain size distribution of individual units are shown on the graphs in Figure 4.4.

The bottom unit has a bimodal distribution and the peaks appear in 3 Φ and 5 Φ , where 3 Φ is more prominent. The mean grain size of the unit is 2.73 Φ (0.15 mm) and the fine fraction ($\leq 4 \Phi$ or $\leq 0.063 \text{ mm}$) is close to 35 wt %. The sorting is 2.40 and falls under the definition of very poorly sorted.

The lower middle unit has a trimodal distribution and the peaks appear in 0 Φ , 3 Φ and 5 Φ , where 3 Φ is most prominent. The mean grain size of the unit is 2.83 Φ (0.14 mm) and the fine fraction is almost 38 wt %. The sorting is 2.36 and falls under the definition very poorly sorted.

The upper middle unit has a trimodal distribution and the peaks appear in -1 Φ , 2 Φ and 5 Φ , where -1 Φ is most prominent. The mean grain size of the unit is 1.20 Φ (0.43 mm) and the fine fraction decreases to about 25 wt %. The sorting is 3.19 and falls under the definition very poorly sorted.

The top unit has a trimodal distribution with peaks in 0 Φ , 3 Φ and 5 Φ , none of them prominent. The mean grain size of the unit is 1.72 Φ (0.30 mm). As in the other units the sorting is very poor or 2.96.

It is possible that the peak at 5 Φ in these samples results from or is enhanced by the change of analyzing methods, at least in some cases. The bar graphs are described as they appear on the plots but may in some cases be classified as unimodal instead bimodal, et cetera.

In summary the development of the grain size of the SILK-LN tephra with time at this location (Figure 4.4) is from unimodal distribution to bimodal, developing a peak in the coarser fraction and reducing the wt % of fines. The sorting remains very poor and gets worse with time.

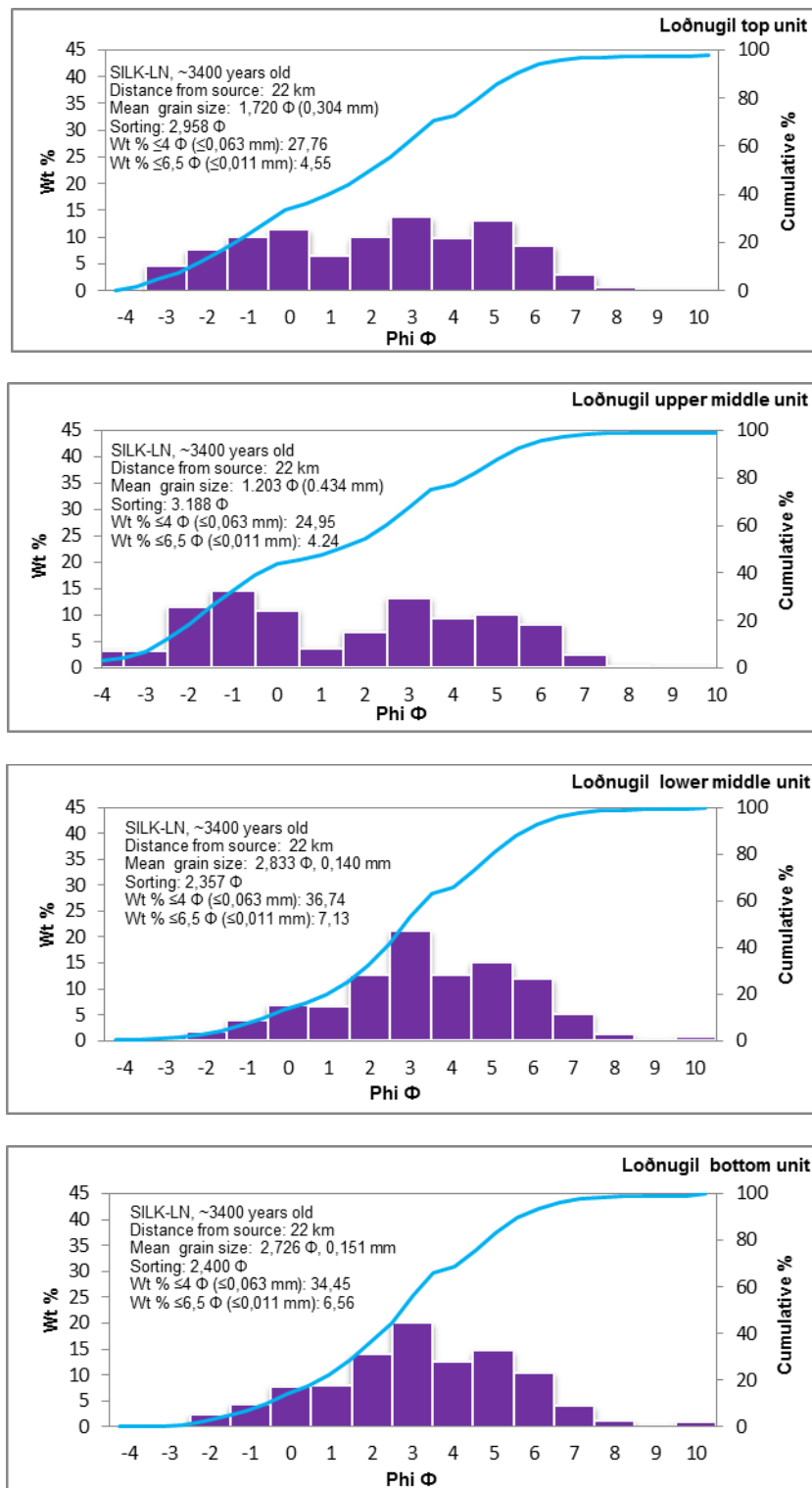


Figure 4.4: Grain size distribution of samples from Loðnugil. The purple bars represent the grain size distribution weight % plotted against Φ and the blue colored line represents the cumulative % plotted against Φ .

Geldingasker: In Geldingasker two samples were collected, one from each of the two units within the tephra layer. Graphs of the grains size distributions are presented in Appendix III.

The bottom unit has a bimodal distribution and the peaks appear in 3 Φ and 5 Φ , where 3 Φ is most prominent. The mean grain size of the unit is 2.61 Φ (0.16 mm) and the fine fraction ($\leq 4 \Phi$ or ≤ 0.063 mm) is close to 30 wt %. The sorting is 2.23 and falls under the definition of very poorly sorted.

The middle unit has a trimodal distribution and the peaks appear in -4 Φ , 2 Φ and 5 Φ , where 2 Φ is most prominent. The mean grain size of the unit is 2.52 Φ (0.17 mm) and the fine fraction is close to 29 wt %. The sorting is 3.51 and falls under the definition of very poorly sorted.

In summary the development of the grain size of the SILK-LN tephra with time at this location is from bimodal distribution to trimodal, the grains tend to get coarser grained with time but the fine wt % changes are little. The sorting remains very poor and gets worse with time.

Leiðólfssfell: At Leiðólfssfell three samples were collected, one from each of the three units within the tephra layer. Graphs of the grains size distributions are presented in Appendix III.

The bottom unit has a bimodal distribution and the peaks appear in 3 Φ and 5 Φ , where the 3 Φ is most prominent. The mean grain size of the unit is 3.07 Φ (0.12 mm) and the fine fraction ($\leq 4 \Phi$ or ≤ 0.063 mm) is close to 37 wt %. The sorting is 1.75 and is defined as poorly sorted.

The middle unit has a bimodal distribution and the peaks appear in 3 Φ and 5 Φ , where 3 Φ is more prominent. The mean grain size of the unit is 3.03 Φ (0.12 mm) and the fine fraction is close to 40 wt %. The sorting is 2.02 and is defined as very poorly sorted.

The top unit has a bimodal distribution and the peaks appear in 2 Φ and 5 Φ , where 2 Φ is more prominent. The mean grain size of the unit is 2.13 Φ (0.23 mm) and the fine fraction decreases to about 24 wt %. The sorting is 2.04 and is defined as very poorly sorted.

In summary the development of the grain size of the SILK-LN tephra with time at this location shows that all the units have bimodal distribution, the tephra tends to get coarser grained with time and the fine wt % decreases significantly with time. The sorting remains very poor and gets worse with time.

Varmárfell: In Varmárfell, furthest away from the source, four samples were collected in two locations, one bulk sample representing the whole layer and three samples from individual beds or units of the layer. Graphs of the grains size distributions are presented in Appendix III.

The bottom unit has a trimodal distribution and the peaks appear in 3 Φ , 5 Φ and 9 Φ , where both 3 Φ and 5 Φ are most prominent. The mean grain size of the unit is 3.29 Φ (0.10 mm) and the fine fraction ($\leq 4 \Phi$ or ≤ 0.063 mm) is close to 43 wt %. The sorting is 1.98 and is defined as poorly sorted.

The middle unit has a bimodal distribution and the peaks appear in 3 Φ and 5 Φ , where 3 Φ is more prominent. The mean grain size of the unit is 3.14 Φ (0.11 mm) and the fine fraction is close to 37 wt %. The sorting is 1.85 and is defined as poorly sorted.

The top unit has unimodal distribution and the peak appears in 3 Φ . The mean grain size is 2.37 Φ (0.19 mm) and the fine fraction decreases to about 11wt %. The sorting is 1.20 and is defined as poorly sorted. Top unit is possibly reworked.

In summary the development of the grain size of the SILK-LN tephra with time at this location is from trimodal to bimodal (except the top unit which is unimodal), the tephra tends to get coarser grained with time and the fine wt % decreases significantly with time. The sorting remains very poor but gets better with time.

Changes in grain size with distance

Grain size changes of the SILK-LN tephra layer with respect to distance from source were investigated. To do so grain size distributions graphs from sampling places that lie in the axis of thickness were analyzed. Also the medium grain size was studied with respect to distance. Those sampling places that lie in the axis of thickness from closest to furthest away from the source are as following: Loðnugil, Geldingasker, Leiðólfssfell, Blágil and Varmárfell. The grain size distribution graphs show how much (in wt %) there are of grains in each phi category or on the size range from 16 mm to 0.00098 mm (-4 Φ to 10 Φ). The biggest grains in this study fall in the -4.5 Φ category, but it was combined in the -4 Φ category since the phi categories are presented on a whole phi interval. The grain size distribution graphs only show measurements down to 10 Φ . All the graphs are presented in Appendix III (p.27-34) and the Tables are presented in Appendix IV.

The grain size distribution shows clear changes in grain size of the SILK-LN layer with distance from source. Coarser material is observed at locations closest to the eruption source and the material becomes finer with increasing distance from the source. Closest to source, at Loðnugil the largest grains that were found belonged to the size categories of -4 Φ and -3 Φ and in Varmárfell, furthest away the biggest grains belong to the 0 Φ size category.

Mean grain size is also a convenient way to examine changes in grain size with respect to distance from source (Figure 4.5). Mean grain size (through axis of thickness) was therefore calculated and plotted against distance from source. The result show that the mean grain size changes with distance with prominent changes within the tephra layers where bedding is visible. In 40 km distance from the source the mean grain size of the SILK-LN Katla tephra is about 2.74 Φ (0.15 mm) but in ca 65 km distance the mean grain size is 2.94 Φ (0.13 mm). The mean grain size closest to the source (22 km distance from source) is 2.12 Φ (0.23 mm). These mean grain size values are average values from all samples collected at each location, bulk samples not included, for example: the mean grain size at Varmárfell was calculated from three samples collected from the tephra layer (same with other locations).

The graph indicates, if excluding the possibly reworked top sample at Varmárfell, that the mean grain size decreases by 1 Φ (halving of the grain size in mm) every 70-75 km for the fine-grained bottom units but every 20-22 km for the coarser upper units.

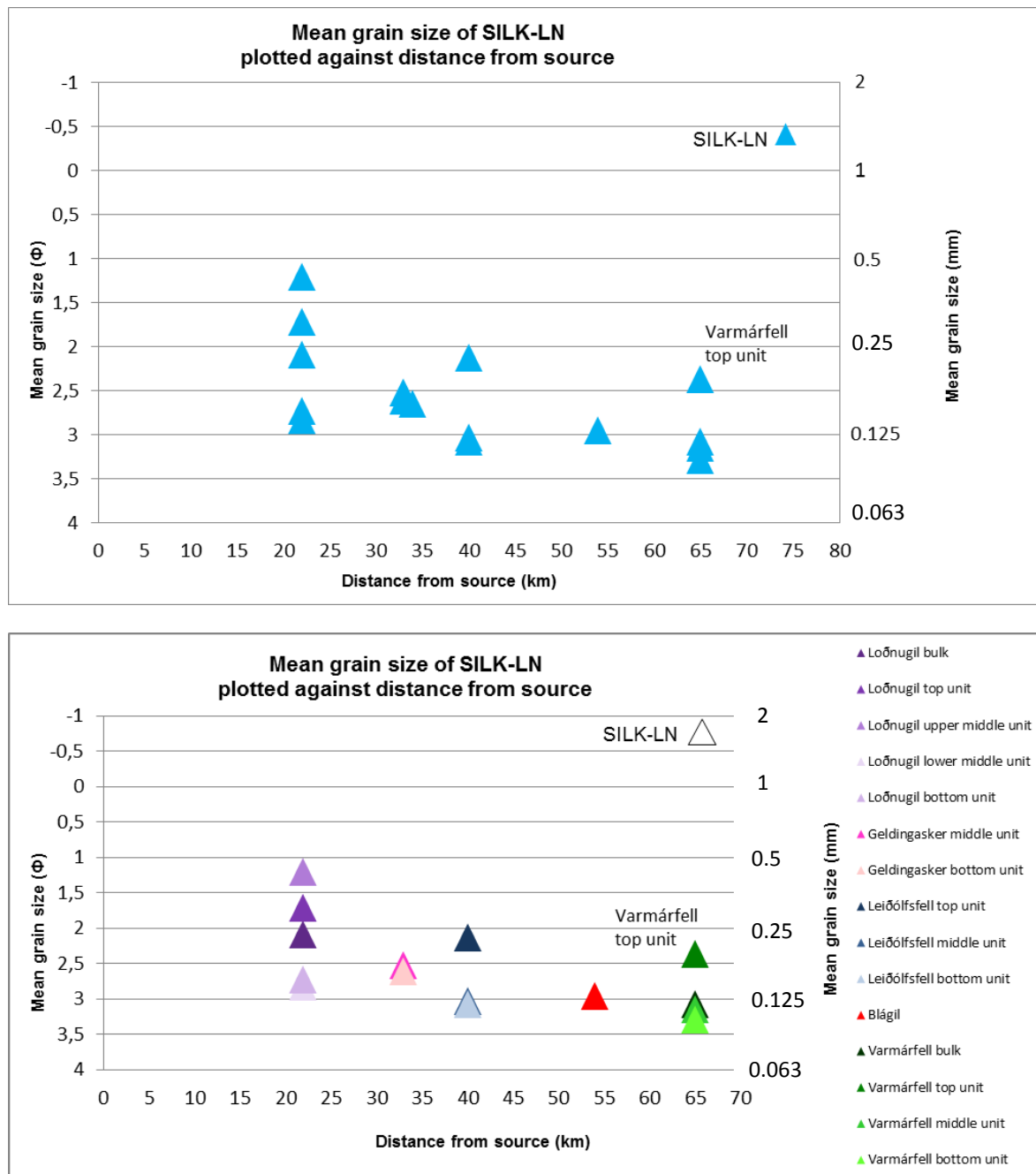


Figure 4.5: (A) Mean grain size along the axis of thickness of SILK-LN plotted against distance from source. Blue triangles stand for Katla. (B) Mean grain size of SILK-LN plotted against distance from source, illustrating individual units and bulk samples at the different sampling places of the SILK-LN tephra.

Proportion of ash equal to and finer than 4 Φ

When the proportion of ash equal to and finer than 4 Φ (≤ 0.063 mm) is viewed it is very prominent how much fine material the SILK-LN tephra layer contains. The fine proportion results were plotted against distance from source in three different ways: material equal and smaller than 4 Φ , equal and smaller than 5 Φ (≤ 0.031 mm) and equal and smaller than 6.5 Φ (≤ 0.011 mm) (Figure 4.6).

The proportion of fine ash equal and smaller than 4Φ (≤ 0.063 mm) in the SILK-LN tephra at about 40 km from the source is ca 24 – 40% of the samples total weight (variable in bedded tephra layers). At about 65 km distance from source this proportion is ca 37 – 43% of the samples total weight (variable in bedded tephra layers), that is if the potentially reworked top unit in Varmárfell is omitted.

The proportion of fine ash equal and smaller than 5Φ (≤ 0.031 mm) at about 40 km distance from the source is ca 16 – 27% of the samples total weight (variable in bedded tephra layers). At about 65 km distance from source this proportion is about 26 – 31% of the samples total weight (variable in bedded tephra layers), omitting the top unit of Varmárfell as previously done.

It is interesting that the ratio of finer particles equal and smaller than 6.5Φ (≤ 0.011 mm) changes very little with distance. At about 20 km distance from the source the Katla tephra layer has about 3-7 wt % for material equal and smaller than 0.011 mm and 1-8 wt % at about 65 km distance.

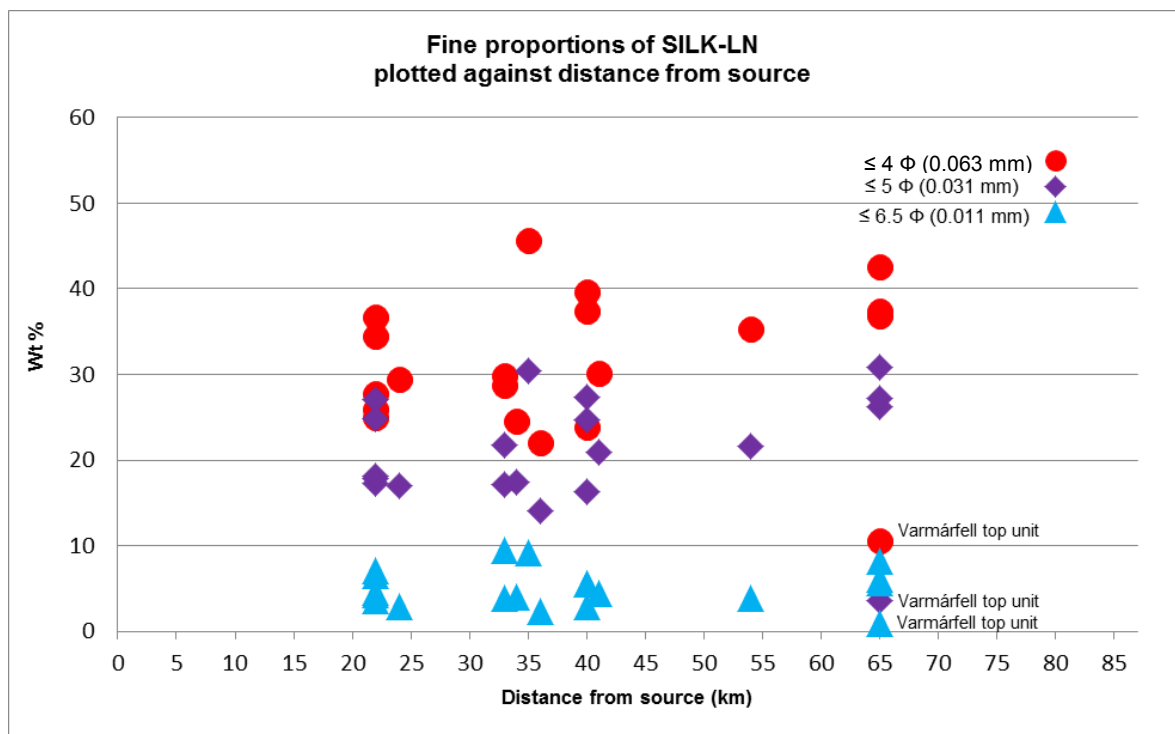


Figure 4.6: Finer particles of the SILK-LN tephra layer equal and smaller than 4Φ (≤ 0.063 mm) (red circles), equal and smaller than 5Φ (≤ 0.031 mm) (purple diamonds) and equal and smaller than 6.5Φ (≤ 0.011 mm) (blue triangles) plotted against distance from source.

4.1.3 Grain Shape characteristics

Grain shape analyses were carried out on SILK-LN tephra. The samples that were used for analyses were collected at two locations; one location close to Katla, at Geldingasker and the second location further away from Katla, at Varmárfell. Two samples from Varmárfell were analysed for grain shape, the bottom unit and the middle unit. Two samples from Geldingasker were analysed for grain shape, the bottom unit and the middle unit. The

sample from Geldingasker that is used in this study has been previously analysed by Thorsteinsdóttir (2012).

Grain parameters

Samples were collected at two locations as mentioned earlier in Geldingasker and Varmárfell. Geldingasker is at about 33 km distance from the source and Varmárfell is at about 65 km distance from the source. The results from the grain shape analyses can be seen in Figure 4.7 and Table 4.1. More detailed results can be viewed in Appendix V & VI.

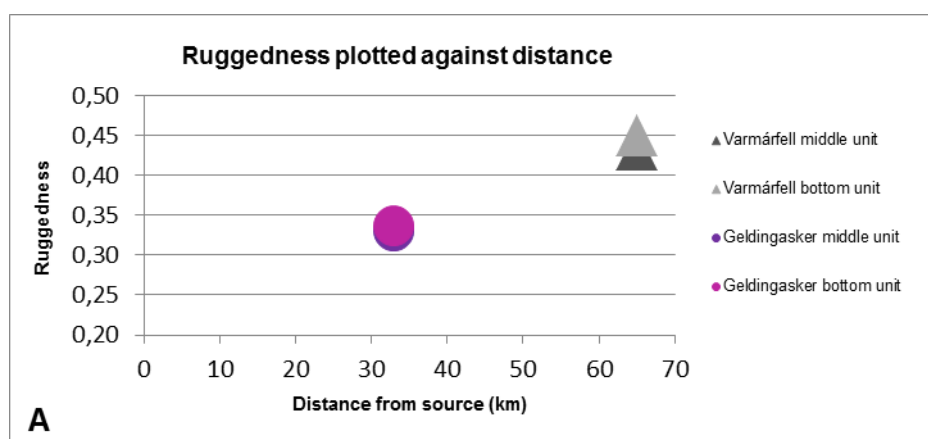
Table 4.1: Results of grain morphology measurements. The parameters measured are Elongation (lower values represent more elongated grains), Ruggedness (lower values represent more rugged grains) and Circularity (higher values represent more circular grains).

Unit	Elongation	Ruggedness R2	Circularity	Distance (km)
Varmárfell bottom unit	0.53	0.45	0.62	65
Varmárfell middle unit	0.51	0.43	0.57	65
Geldingasker bottom unit	0.55	0.36	0.63	33
Geldingasker middle unit	0.68	0.33	0.67	33

Geldingasker: The ruggedness value in Geldingasker ranges from 0.36 in the bottom unit to 0.33 in the middle unit, the elongation is from 0.55 in the bottom unit to 0.68 in the middle unit and the circularity increases from bottom unit to the middle unit or from 0.63 to 0.67

Varmárfell: The ruggedness value in Varmárfell ranges from 0.45 in the bottom unit to 0.43 in the middle unit, the elongation is from 0.53 in the bottom unit to 0.51 in the middle unit and the circularity decreases from bottom unit to the middle unit or from 0.62 to 0.57.

Grains closer to source, in Geldingasker, are more rugged, shorter and also closer to a circular form than further away from source in Varmárfell (Figure 4.7 A-C). In simple terms this indicates that long smooth grains tend to travel farther than short/circular, rugged grains.



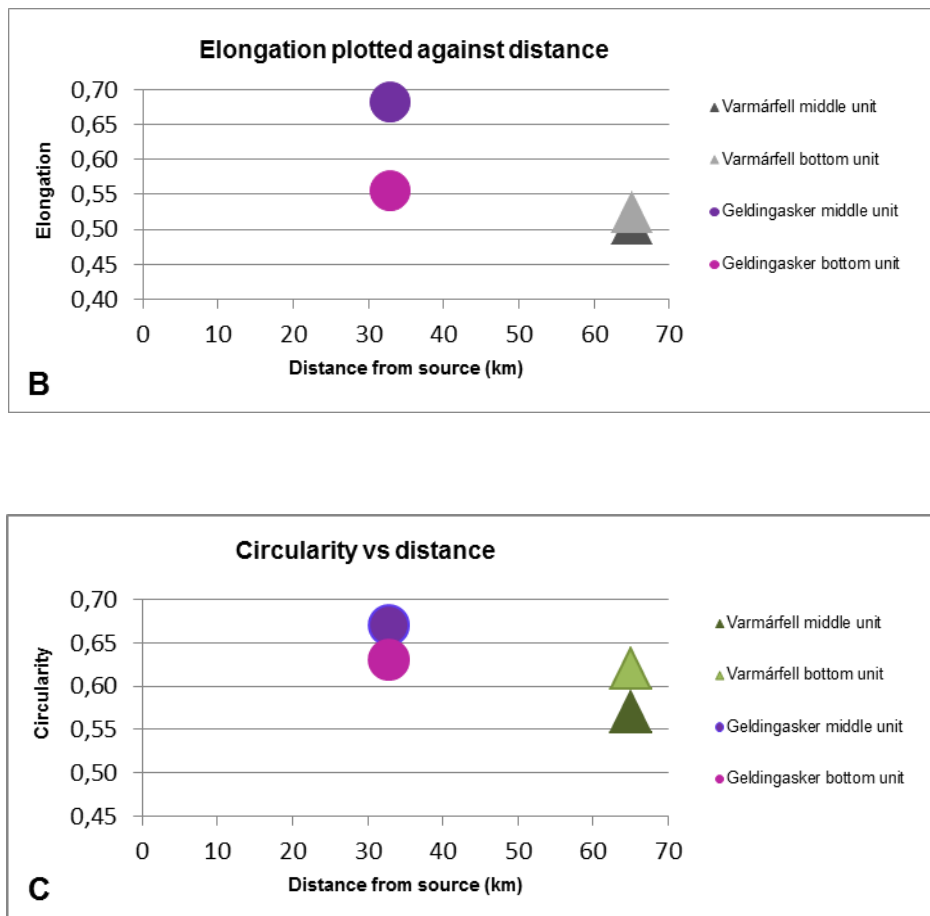


Figure 4.7: Grain morphology of SILK-LN tephra versus distance from source. A: Ruggedness of the SILK-LN tephra layer plotted against distance (lower values represent more rugged grains). B: Elongation of the SILK-LN tephra layer plotted against distance (lower values represent more elongated grains). C: Circularity of the SILK-LN tephra layer plotted against distance (higher values represent more circular grains). Grey triangles represent the location of Varmárfell and purple circles represent the location of Geldingasker.

At both locations the grains tend to become more rugged (with more uneven outline) with time but such systematic change is not seen in the other two parameters. In case of the basaltic and basaltic-andesite tephra, the grains tend to be more rugged in magmatic eruptions than in hydromagmatic eruptions (Eiríksson & Wigum, 1989). This could therefore indicate that the effects of water became less prominent with time.

Grain properties seen in SEM – a preliminary study

The electronic microscope TM3000 was used to photograph the SILK-LN tephra grains (Hitachi High-Technologies Corporation, 2010). Samples used came from Geldingasker and Varmárfell. The size of the grains analyzed was 3.5Φ (0.088 mm). Several photographs were taken of each sample or from four samples. The SEM observations were carried out to visually demonstrate the grain shapes found in the SILK-LN tephra. When the samples were observed in the electronic microscope five to six different types of grains along with few sub categories were noticed (Figure 4.8). These types are as following:

I Elongated needle- or rod-like.

- a. Long, narrow-drawn out- elongate tube-like vesicles.
- b. Shorter, medium-elongate tube-like vesicles.

II Equant with elongated/tubelike vesicle. Thicker walls than in I.

- a. Straight.
- b. Curved.

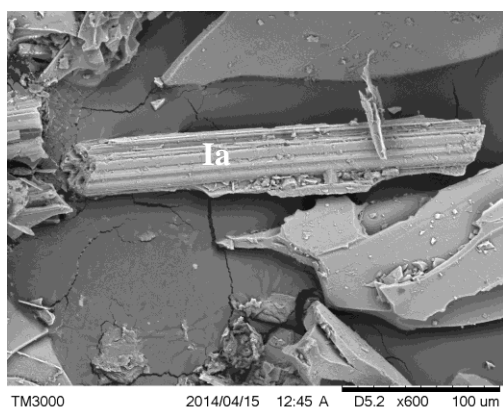
III Plates, thin flat or curved, sometimes with vesicles. (c axis much smaller than the others).

IV Equant more massive with oval to spherical vesicles.

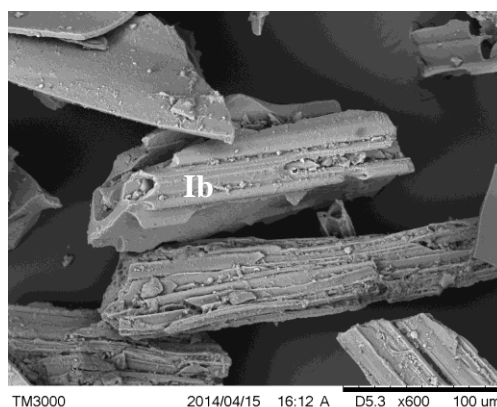
V Massive equant without vesicles.

VI Grains with fluidal surface.

*more images and information on SEM work procedure in Appendix II and VIII.



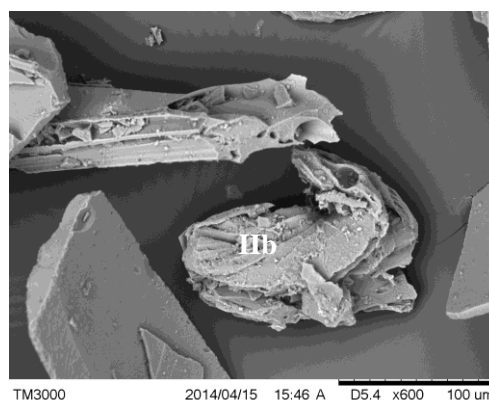
Ia (Geldingasker bottom unit)



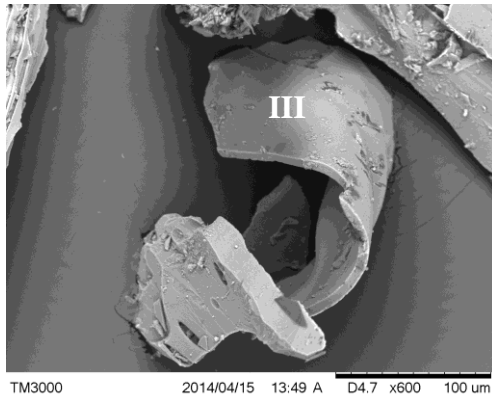
Ib (Geldingasker middle unit)



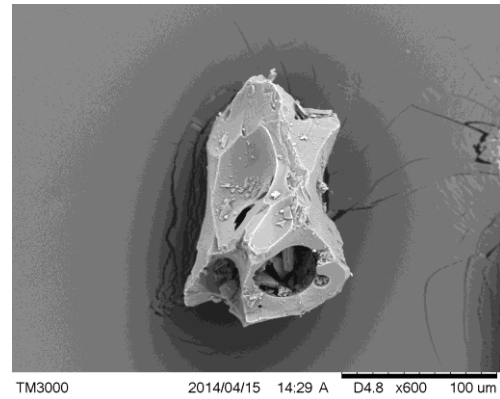
IIa (Geldingasker middle unit)



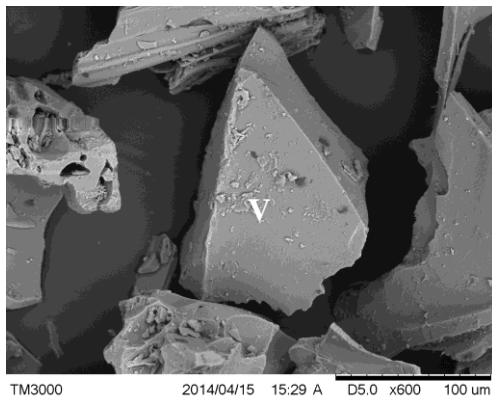
IIb (Geldingasker middle unit)



III (Varmárfell bottom unit)



IV (Varmárfell bottom unit)



V (Varmárfell middle unit)



VI (Varmárfell middle unit)

Figure 4.8: Selected pictures demonstrating the 6 categories and sub categories of grains photographed in the SEM electron microscope from samples collected in both Geldingasker and Varmárfell.

The pictures shown here were selected to visually represent different grain types of the SILK-LN tephra. Statistical grain counts to document changes with time or distance were not carried out this time. Type I-III are the most common and type VI is definitely the least common according to visual estimate. The characteristic grains are the type I and II grains. No examples of type I and II tephra, with such elongate needle- or rod-shaped grains, were found in literature.

Studies tackling the effects of differing magma-water interaction on the grain shape of the SILK tephra will have to be carried out in another project.

4.2 The Hekla 1947 tephra

In this chapter the results from the investigations on the Hekla 1947 tephra layer are discussed.

4.2.1 Field characteristics (Macroscopic characteristics, bedding)

The Hekla 1947 tephra layer did not show any bedding out in the field although descriptions of the tephra fall explicitly describe changes both in color and grain size of the tephra. Therefore the Hekla 1947 samples collected for this project were bulk samples. Where lateral changes in thickness were observed more than one sample was collected and treated individually. Total of eight bulk samples were collected. The sampling locations all lie in the axis of thickness. They are as following from closest to furthest away from the source: Vestan Hafrafells, Fljótsdalsheiði and Hamragarðaheiði, 19 km, 29.5 km and 42 km from Hekla summit, respectively.

Vestan Hafrafells: The color of the tephra is mostly black but few red colored grains are noticed and total thickness of the layer is 1-2.5 cm.

Fljótsdalsheiði: The color of the tephra is mostly brownish black with grey brown grains in between. Total thickness of the layer is from 2 – 6.5 cm (Figure 4.9).



Figure 4.9: Hekla 1947 tephra at Fljótsdalsheiði with tephra from Eyjafjallajökull eruption from 2010 at the top or just below the surface (Photo Thorsteinsdóttir, 2013).

Hamragarðaheiði: The color is mostly brownish black with grey brown grains in between. Total thickness is from 0.8 – 5 cm (Figure 4.10).



Figure 4.10: Hekla 1947 tephra at Hamragarðaheiði (Photo Thorsteinsdóttir, 2013).

4.2.2 Grain size characteristics

The Hekla 1947 samples were collected at three locations in ca 19 – 42 km distance from the source. These samples were hand sieved down to 63 μm or 4 Φ . The rest in both the 4 Φ sieve and in the collecting pan was analyzed in the SediGraph. The results from the grain size analyse will be discussed below. A more detailed description of the grain size measurements and results can be viewed in Chapter 3 and Appendix II – IV.

Changes with time

Although descriptions of the 1947 tephra fall mention changes in grain size with time, most prominent when the chemical composition and the color of the tephra changed, no such changes through the Hekla 1947 tephra were observed at the sample locations. It is likely that the finer material at the top of the tephra layer had mixed into the coarser lower part or possibly eroded away. Figure 4.11 A shows that the grain size distribution in sample from location “Vestan Hafrafells” forms two distinct groups, which at least partly represent this change in grain size with time.

Grain size analyses performed on samples of the lower grey brown and upper brownish black tephra collected shortly after the tephra fall were published by Thorarinsson (1954). Three such “pairs” collected from bedded 1947 deposit at 32, 49 and 68 km from Hekla summit were included in this study and the mean grain size re-calculated. The mean Φ of the lower unit was -1.00 Φ , -0.07 Φ and 1.19 Φ at 32, 49 and 68 km, respectively. The mean Φ of the upper unit was -0.01 Φ , 0.48 Φ and 2.62 Φ at 32, 49 and 68 km, respectively. See also Figure 4.12.

Changes with distance

Results from the grain size analyses (Figure 4.11) show changes with respect to distance from source in samples from Vestan Hafrafells, Fljótsdalsheiði and Hamragarðaheiði. The grain size distribution graphs show how much wt % of material there is in each phi fraction

in the size range of -4Φ to 10Φ (16 mm to 0.00098 mm). The biggest Hekla 1947 grains in this study fall in the -4Φ size fraction.

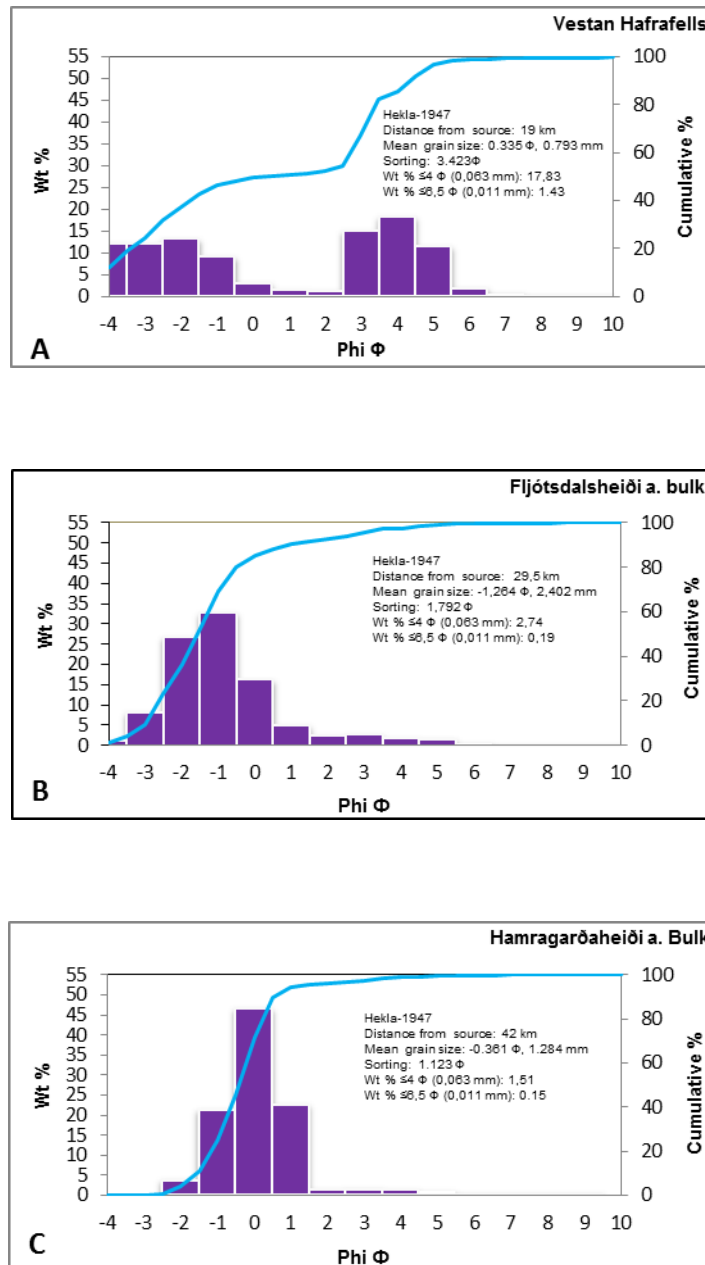


Figure 4.11: Examples of grain size distribution graphs of samples from Vestan Hafrafells (A), Fljótsdalsheiði (B) and Hamragarðaheiði (C). The purple bars represent the grain size distribution weight % plotted against Φ , the blue line represents the cumulative % plotted against Φ .

When grain size distribution graphs of Hekla 1947 tephra are observed, obvious changes are noticed when comparing locations closest and furthest away from the source (Figure 4.11).

Vestan Hafrafells:

The layer has a bimodal distribution and the peaks appear in -2 Φ and 4 Φ , where 4 Φ is more prominent (Figure 4.11 A). The mean grain size of the unit is 0.34 Φ (0.79 mm) and the fine fraction ($\leq 4 \Phi$ or ≤ 0.063 mm) is close to 18 wt %. The sorting is 3.423 and falls under the definition of very poorly sorted.

Fljótsdalsheiði:

Samples here were collected at three locations and the layers shows unimodal distribution in two samples and bimodal distribution in one sample. The peaks of the unimodal distribution appear in -1 Φ and the bimodal distribution peak appears in -2 Φ and 3 Φ , where -2 Φ is more prominent. The average mean grain sizes for these three units is -1.25 Φ (2.38 mm) and the fine fraction ($\leq 4 \Phi$ or ≤ 0.063 mm) is between ca 1 – 3 wt %. The average sorting for these three units is 1.73 and falls under the definition from moderately sorted to very poorly sorted.

Hamragarðaheiði:

The layer has unimodal distribution in all four samples and the peaks appear in two samples in 0 Φ and in two samples in 1 Φ . The average mean grain size for these four samples is 0.45 Φ (0.73 mm) and the fine fraction ($\leq 4 \Phi$ or ≤ 0.063 mm) is between ca 1.5 – 9 wt %. The average sorting for these four units is 1.49 and falls under the definition from moderately sorted to poorly sorted.

In addition to the samples from Vestan Hafrafell, Fljótsdalsheiði and Hamragarðaheiði the mean grain size of freshly fallen Hekla 1947 samples collected by Sigurður Þórarinnsson were also looked at. Mean grain size was recalculated, based on graphs and tables in Thorarinsson (1954), and plotted against distance from source, see Figure 4.12.

The mean grain size of Hekla 1947 tephra layer shows obvious changes with distance, getting gradually smaller with distance. Also a systematic variability appears in samples collected from the two units where the bottom grey brown unit of the tephra layer is always more coarse grained than the bulk samples and the bulk samples are always more coarse grained than the top brownish black unit in the same location. The Hekla samples that were collected freshly fallen (dark red on Figure 4.12A) were only sieved down to 4 Φ (0.063 mm) and the finer particles ≤ 0.063 mm were not measured in the SediGraph. Therefore the mean grain size in the Hekla 1947 samples collected freshly fallen is probably slightly smaller than it would be otherwise.

From the graph on Figure 4.12 A and B it appears that the mean grain size decreases by one Φ (is halved in mm) every 13 to 14 km out to 68 km from source, at least in case of the grey brown and possibly also the black tephra. Thorarinsson (1954) shows on his Figure 6 how median grain size of his bulk samples decreases with distance, there it is halved every 12 km (on average) out to 68 km. Figure 4.12 A and B show that most samples collected in 2013 fit reasonably well to the general trend. Two samples diverge from it. The bulk sample collected in 2013 at 19 km may not be representative due to reworking. A possible explanation for the sample collected at 74 km in 1947 from the grey brown tephra is that it did not represent the whole unit, lacking the finer material.

The multiple samples collected in 2013 at 29 km and 42 km distance show variation of up to one and half Φ in the mean grain size at each site. All are bulk samples and the variation reflects varying proportions of the grey brown and black tephra. Nevertheless these samples fall on the general trend defined by the samples collected in 1947. They are therefore considered to be informative although not representative of undisturbed tephra.

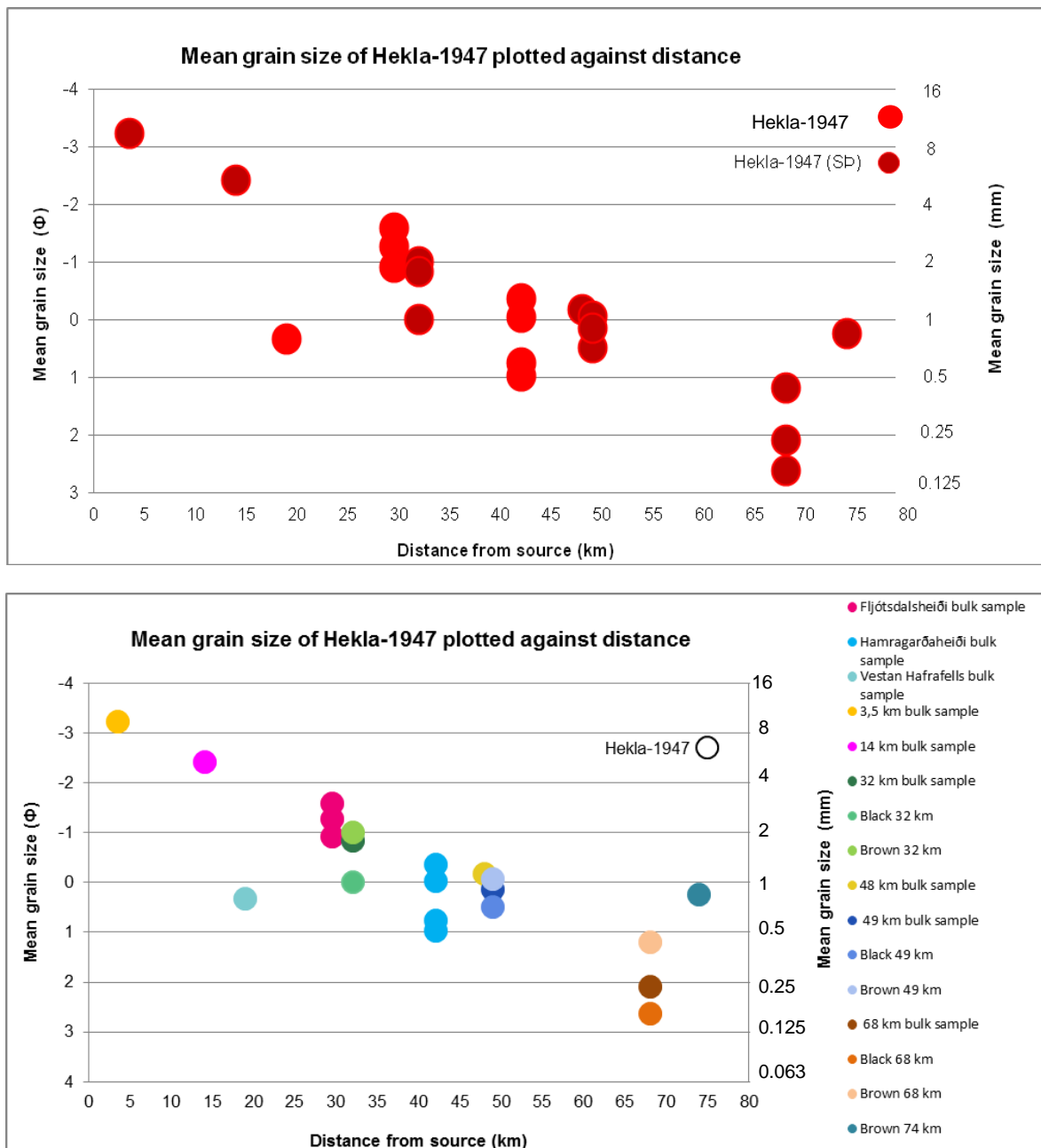


Figure 4.12: (A) Mean grain size of Hekla 1947 plotted against distance from source. Lighter red colored circles stand for Hekla 1947 tephra samples collected in 2013 and darker red colored circles stand for Hekla 1947 samples collected by Thorarinsson (1954). (B) Mean grain size of Hekla 1947 plotted against distance from source, illustrating individual units and bulk samples at the different sampling locations of Hekla 1947.

Proportion of ash equal and finer than 4 Φ

The proportion of ash $\leq 4 \Phi$ or (≤ 0.063 mm) in the Hekla 1947 layer is not very prominent. The fine proportion results were plotted against distance from source in three different ways: material equal and smaller than 4 Φ (including the samples from Sigurður Þórarinnsson), equal and smaller than 5 Φ (≤ 0.031 mm) equal and smaller than 6.5 Φ (≤ 0.011 mm). The graphs with the fine material equal and smaller than 5 Φ and equal and smaller than 6.5 Φ do not include samples from Sigurður Þórarinnsson since no measurements were carried out on the finer particles.

The proportion of fine ash $\leq 4 \Phi$ in the Hekla 1947 tephra (Figure 4.13 A) has to be looked at separately, first in the bulk samples and then in the grey brown and black tephra pairs of Thorarinsson (1954). In the bulk samples the proportion of $\leq 4 \Phi$ is less than 10 wt %, except at 68 km where it is about 24 wt % (excluding the possibly reworked tephra collected at 19 km in 2013). In samples of the grey brown tephra the proportion of $\leq 4 \Phi$ does not exceed 8 wt % and changes irregularly with distance, e.g. it is only 5.6 wt % at 74 km. In samples of the black tephra it varies significantly, from about 8 to 33 wt %, but changes irregularly with distance.

The samples from 42 to 49 km distance, both those from 1947 and 2013, have conspicuously low proportion of fine ash $\leq 4 \Phi$ (Figure 4.13 A). In case of the 2013 samples this could be explained by reworking and/or the sampling. But the samples collected as freshly fallen in 1947 also have such low proportion of fine ash. No explanation for this can be offered here.

The samples of bulk tephra and in particular the black tephra at 68 km, collected in 1947, have the highest proportion of fine ash $\leq 4 \Phi$, 24 and 33 wt %. Increase with distance in proportion of finer grains is expected and in case of the black tephra could fit with the results at 32 km, but not those at 49 km. A secondary thickening caused by particle aggregation (e.g. Brazier et al., 1983) of the black tephra could explain the sudden increase.

The proportions of fine ash which are equal and smaller than 5Φ in the Hekla 1947 tephra at about 19 km distance from the source is ca 8 wt % of the samples total weight, at about 42 km distance from the source this proportion is ca 1 – 6 % (Figure 4.13 B).

The ratio of finer particles equal and smaller than 6.5Φ changes very little with distance. At about 19 km distance from the source Hekla 1947 tephra layer has about 1 wt % of the samples total weight, and this proportion is also ca 1% for Hekla 1947 at about 42 km distance from the source (Figure 4.13 C). These results from the samples collected in 2013 are considered to be informative although not representative of undisturbed tephra.

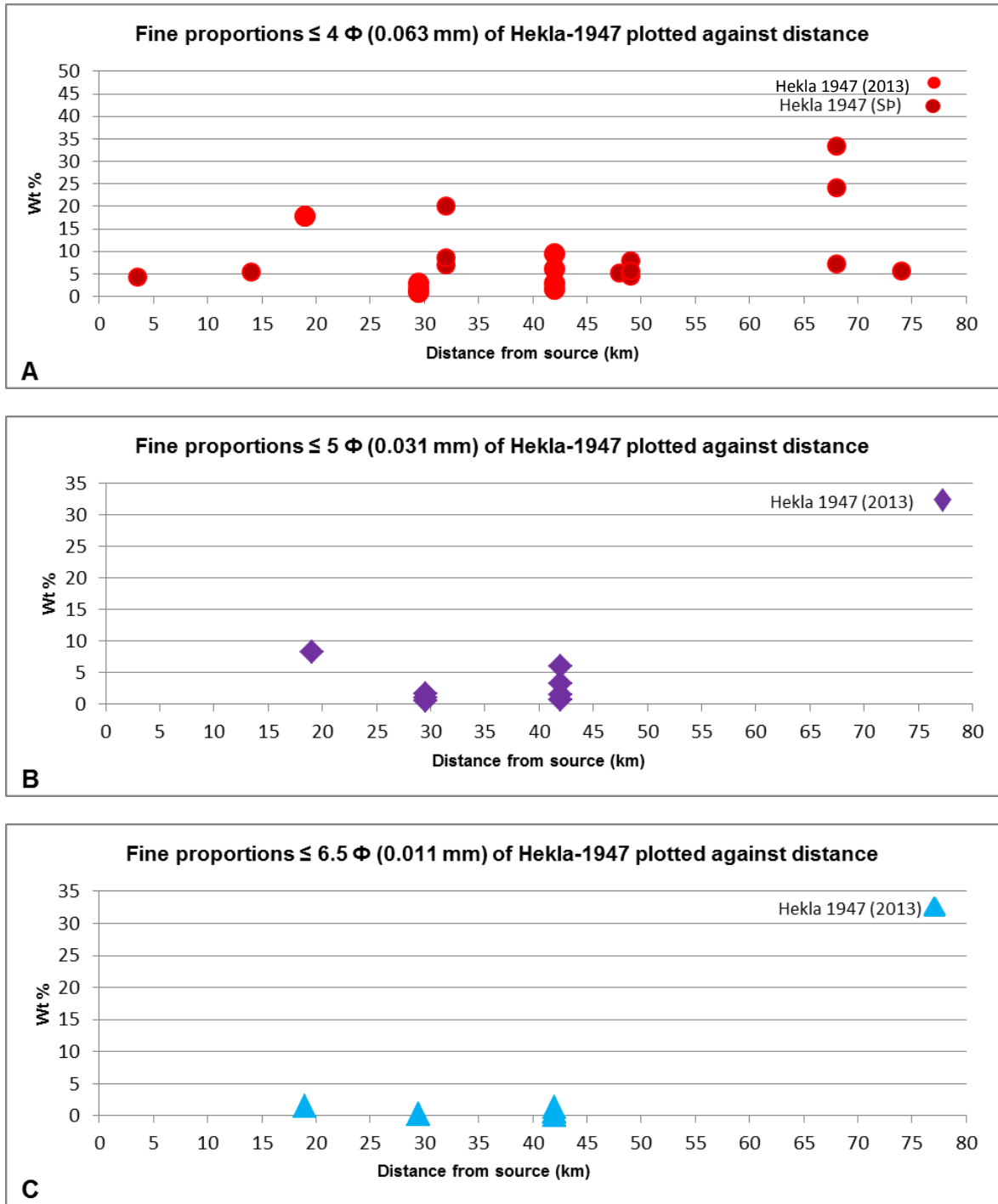


Figure 4.13: Finer particles of Hekla 1947 tephra layer. Figure A: particles equal and smaller than 4Φ (≤ 0.063 mm). Figure B: particles equal and smaller than 5Φ (≤ 0.031 mm) and Figure C: particles equal and smaller than 6.5Φ (≤ 0.011 mm) plotted against distance from source. Red circles represents particles $\leq 4 \Phi$, purple diamonds represents particles $\leq 5 \Phi$ and blue triangles represents particles $\leq 6.5 \Phi$.

4.2.3 Grain shape characteristics

Grain shape analyses were carried out on Hekla 1947 tephra. The samples that were analyzed were collected at two locations, Vestan Hafrafell and at Hamragarðaheiði. One bulk sample from each location was analyzed since no bedding was visible. None of the

samples collected in 1947 that were used in the grain size study were available for grain shape measurements.

Grain parameters

The shape of the tephra grains from the Hekla 1947 tephra layer was analyzed with the image analyzing program Morphocop developed by Jón Eiríksson as discussed in Chapter 3 and in more detail in Appendix II, V and VI.

Changes in grain shape with distance

Samples were collected at two locations. The locality Vestan Hafrafells is at about 19 km distance from the source and Hamragarðaheiði is at about 42 km distance from the source. The results are shown in Table 4.2. Also more detailed results regarding the grain shape analyses can be found in Appendix V and VI.

Table 4.2: Results of grain morphology measurements. The parameters measured are Elongation (lower values represent more elongated grains), Ruggedness (lower values represent more rugged grains) and Circularity (higher values represent more circular grains).

Unit	Elongation	Ruggedness	Circularity	Distance (km)
Vestan Hafrafells	0.73	0.40	0.73	19
Hamragarðaheiði	0.73	0.41	0.75	42

Vestan Hafrafells: The ruggedness at Vestan Hafrafells is 0.40, the elongation is 0.73 and circularity is 0.73 (Figure 4.14).

Hamragarðaheiði: The ruggedness value at Hamragarðaheiði is 0.41, the elongation value 0.73 and circularity is 0.75 (Figure 4.14).

Between the two locations, slight decrease is observed in ruggedness or slight increased ruggedness value. That is the grains from Vestan Hafrafells have slightly more uneven outlines than the grains from Hamragarðaheiði. These changes are very little. The elongation values are exactly the same between the two layers, both with the value 0.73 so there is no change with distance. The higher the number represent the less elongated the grains are. These grains are closer to being equant than elongated. Circularity values increases with distance, with increased value the grains get more circular in shape (Figure 4.14).

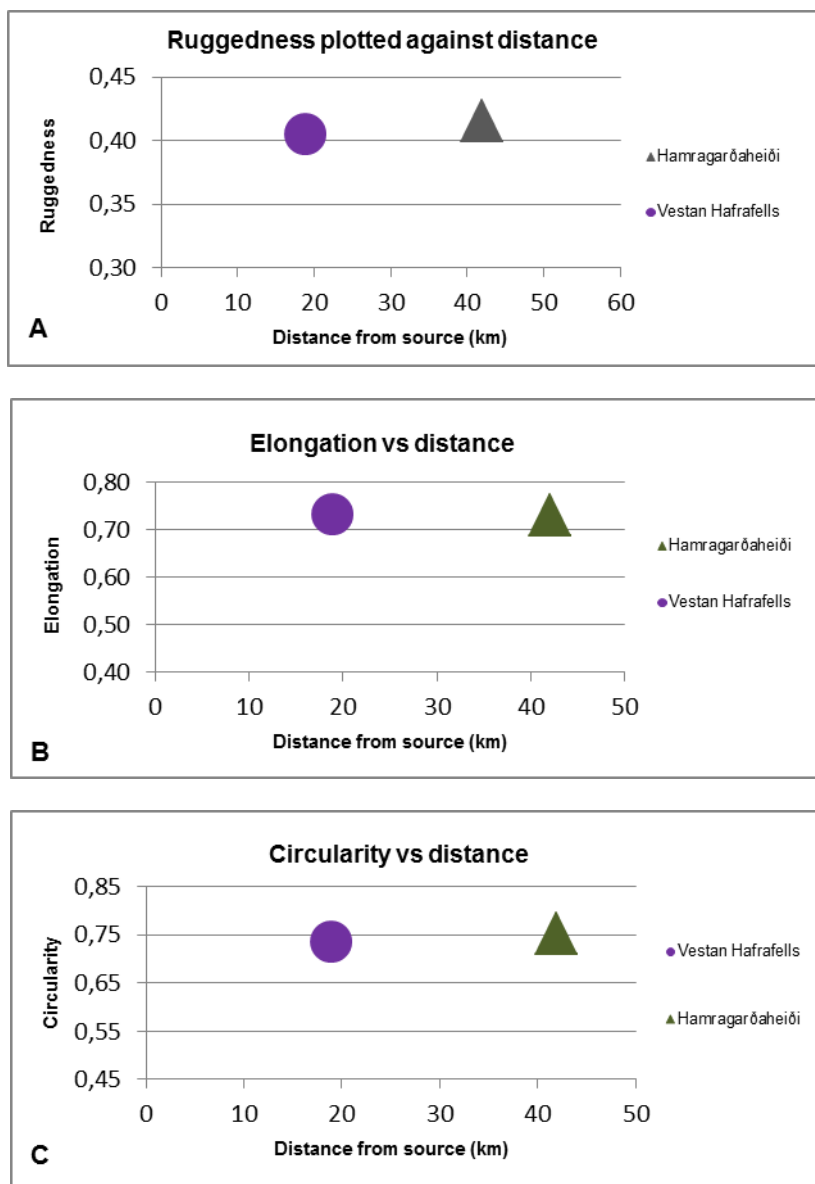


Figure 4.14: Grain morphology of Hekla 1947 tephra versus distance from source . A: Ruggedness of the Hekla 1947 tephra layer plotted against distance (lower values represent more rugged grains). B: Elongation of the Hekla 1947 tephra layer plotted against distance (lower values represent more elongated grains). C: Circularity of the Hekla 1947 tephra layer plotted against distance (higher values represent more circular grains). Grey triangle represents the location of Hamragarðaheiði and purple circle represent the location Vestan Hafráfells.

In summary the Hekla 1947 tephra grains are closer to being equant/circular in shape than elongated and have rather uneven surface. Changes within the distance covered, 23 km, are very small.

Grain properties seen in SEM – a preliminary study

The electronic microscope TM3000 was used to photograph the Hekla 1947 tephra grains (Hitachi High-Technologies Corporation, 2010). Samples used came from Vestan Hafráfells, Hamragarðaheiði and Fljótisdalsheiði. The size of the grains analyzed was 3.5 Φ (0.088 mm). Several photographs were taken of each of the 3 samples. As in case of the

Katla tephra the SEM observations were carried out to demonstrate the grain shapes found in the Hekla 1947 tephra.

Once the samples were observed in the electronic microscope 4 different types of grains along with few sub categories were noticed (Figure 4.15). These types are as following:

I Massive grains

- a. With few large vesicles, thick walls
- b. With more vesicles, oval or spherical
- c. Plate like

II Grains with irregularly wrought glass strands

III Massive grains with fluidal surface

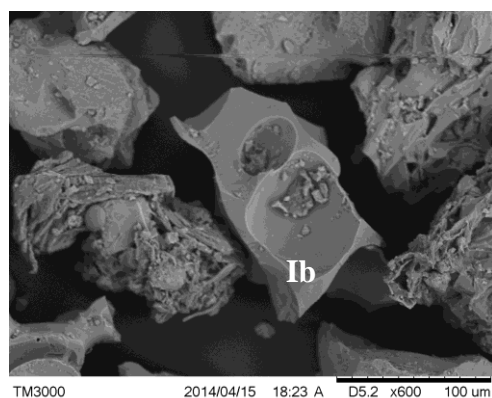
- a. Smooth, sinous surface
- b. Smooth surface but with rodlike bumps (possibly plagioclase rods)

IV Grains with crusted surfaces, sometimes partly broken off, possibly post-depositional

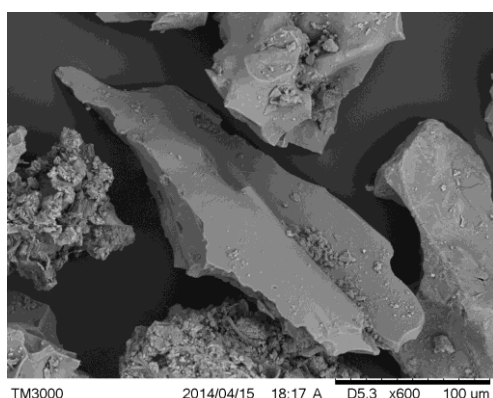
*more images and information on SEM work procedure in Appendix II and VIII.



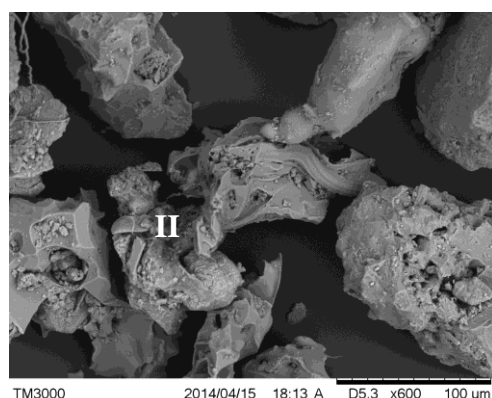
Ia Hamragarðaheiði



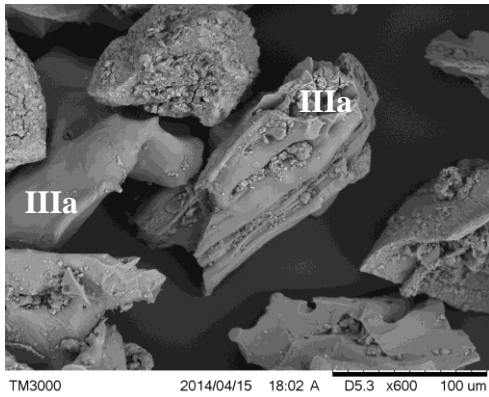
Ib (Hamragarðaheiði)



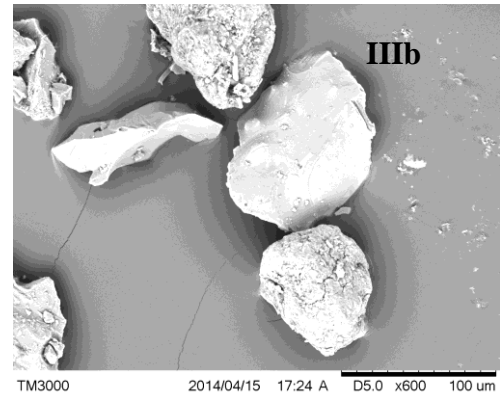
Ic (Hamragarðaheiði)



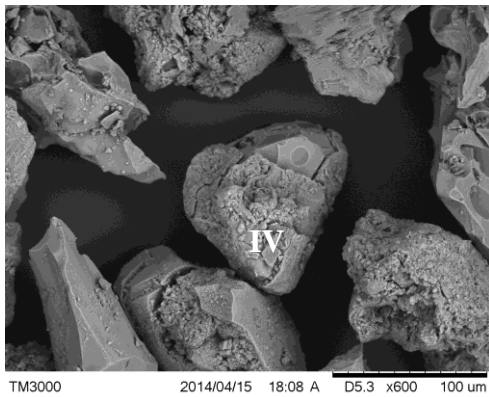
II (Hamragarðaheiði)



IIIa (Hamragarðaheiði)



IIIb (Vestan Hafráfells)



IV (Hamragarðaheiði)

Figure 4.15: Demonstration of 4 categories and sub categories of grains photographed in the SEM electron microscope from samples collected at Vestan Hafráfells, Fljótsdalsheiði and in Hamragarðaheiði.

The pictures shown here were selected to visually represent different grain types. Statistical grain counts to document changes with distance were not carried out. However, types Ia and Ib were more common closest to source and type II and Ic were more common farther from source, according to visual estimate. Type III grains were present in all the samples.

The different grain types are taken to reflect the state of degassing of the magma upon fragmentation and cooling. However, all the samples are bulk samples and no discrimination was made between the grey brown and black tephra. Changes in grain shape that may be related to decreasing SiO_2 content of the magma with time were therefore not looked for but will hopefully be part of a later study.

4.3 Silicic Katla tephra layers: changes through the Holocene

4.3.1 Age range of silicic Katla tephra

In this part of the project 10 SILK tephra layers, in addition to SILK-LN, were analyzed for grain size and grain shape. Here the main focus was on possible changes through time in the period 2800 to 8100 years ago. The tephra layers were collected at similar distance, 20-22 km, from the center of Katla caldera. The thickness axes are, however, not known for all the layers. These tephra layers, including their age in cal BP, are shown in Table 4.3. Three SILK layers were not investigated, the youngest one called SILK-YN, SILK-MN and SILK-A9. The remaining layers except SILK-A11 were grain size analyzed, and samples SILK-N1, SILK-A8, SILK-A11 and A12 were grain shape analyzed.

Table 4.3: The 12 SILK tephra layers that were grain size^Δ and grain shape analyzed. Consult Table 2.1 for details on the age and associated references.*

Tephra layer	Rounded age	Largest Φ	Mean Φ
SILK-UN ^Δ	~2800	-3	1.62
SILK-LN ^{Δ*}	~3400	-3	2.24
SILK-N4 ^Δ	~3900	-1	3.96
SILK-N3 ^Δ	~4100	-3	1.12
SILK-N2 ^Δ	~5000	-1	2.01
SILK-N1 ^{Δ*}	~5800	-1	3.03
SILK-A1 ^Δ	~6000	0	3.52
SILK-A5 ^Δ	~7100	0	3.47
SILK-A7 ^Δ	~7200	-2	1.61
SILK-A8 ^{Δ*}	~7400	0	3.88
SILK-A11 [*]	~8000	-	-
SILK-A12 ^{Δ*}	~8100	0	2.96

4.3.2 Changes in grain size

The largest Φ interval and mean grain size of the SILK layers are shown in Table 4.3. The upper and younger part of the sequence appears coarse grained while the lower part and older one is fine grained. The largest grains in the top coarser part belong to the grain size categories from -3 Φ to -1 Φ but the largest grains from the lower finer grained part all except from one layer belong to the grain size category 0 Φ . The exception is SILK-A7 where the biggest grain belongs to the grain size category -2 Φ . This “change” occurs between 5800 and 6000 years ago. The mean grain size, however, does not clearly follow this trend. Yet it can be said that the majority of tephra layers younger than 5000 years have mean grain size of 2.2 to 1.1 Φ (0.2 to 0.45 mm). SILK-N4 has the most fine grained distribution of the younger layers and there we see very prominent peak in the 5 Φ grain size category (Appendix III and IV). It can also be said that the majority of SILK layers older than 5000 years have mean grain size of ~3 to ~4 Φ , or smaller than 0.125 mm, the exception being SILK-A7. Examples on both fine and coarse grain size distribution are shown in Figure 4.16. More grains size distribution graphs are presented in Appendix III.

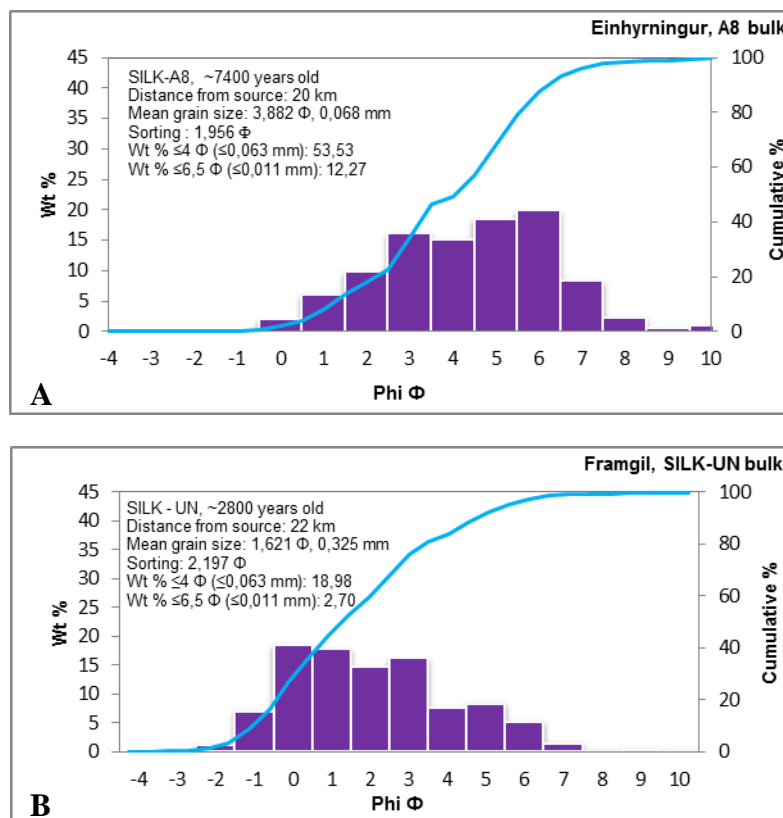


Figure 4.16: Examples of grain size distribution of the SILK layers. A) SILK-A8 fine grained and B) SILK-UN coarse grained.

4.3.3 Changes in grain shape

Grain shape analyses were performed on the following SILK tephra layers, SILK-N1, SILK-A8, SILK-A11 and SILK-A12, all of them sampled at about 20 km distance from source and collected at Einhyrningsflátir. The results from Morphocop are shown in (Table 4.4). Grain shape analyses on SILK-LN tephra layer (Geldingasker, Table 4.1) will also be considered.

Table 4.4: Results of grain shape measurements. The parameters measured are Elongation (lower values represent more elongated grains). Ruggedness (lower values represent more rugged grains) and Circularity (higher values for more circular grains).

Layer/Unit	Elongation	Ruggedness R2	Circularity	Age
SILK-N1 bottom unit	0.58	0.40	0.66	5800
SILK-N1 middle unit	0.69	0.41	0.73	5800
SILK-N1 average	0.64	0.40	0.70	5800
SILK-A8	0.69	0.42	0.74	~7400
SILK-A11	0.78	0.35	0.78	~8000
SILK-A12	0.52	0.42	0.65	~8100

When the grain shape results for SILK-N1, SILK-A8, SILK-A11 and SILK-A12 layers are observed it is quite obvious that SILK-A11 is significantly different from the other layers. Also in the field the SILK-A11 grains looked different from the other SILK layers. First and foremost this difference is in the elongation values. The elongation of the SILK grains

in the oldest layer A12 has the value 0.52 then changes in the SILK-A11 layer to 0.78. which means that the grains are less elongated. This is even higher than elongation values for Hekla 1947 grains which were 0.73. In fact the A11 grains are closer to a circular shape (a circle has the value 1).

When we look at how the elongation changes with time we see that the grains are very elongated in the oldest A12 layer with the value being 0.52 and then suddenly changes to the value of 0.78 in the second oldest A11 layer. In SILK-A8 and SILK-N1 (average) the grains become more elongated again. Within the bedded layer the elongation changes with time where the value goes from 0.58 in the bottom unit to 0.69 in the middle layer. But in these four SILK layers no systematic change with time is seen. Adding the ~3400 old SILK-LN (Geldingasker, Table 4.1) to the list and omitting SILK-A11 does not change this result.

The ruggedness values are all quite similar except for SILK-A11. and if we would exclude SILK-A11 the ruggedness increases slightly with time (the ruggedness values get lower). The ruggedness value for SILK-A11 is 0.35 so the grains in SILK-A11 have more uneven outlines than in the other three layers. The difference between A12, A8 and N1 is small. from 0.42 in the oldest layer to average of 0.40 in the youngest layer. The values of the N1 layer do not change very much internally or from 0.40 in the bottom unit to 0.41 in the middle unit. No systematic change in ruggedness with time is seen even though SILK-LN is included and SILK-A11 omitted.

The circularity value is lowest in the oldest layer A12 then it increases significantly in the A11 layer as observed in both elongation and ruggedness. Then the values slowly trend away from circular shape. The value of the oldest layer SILK-A12 is 0.65 and it is furthest away from having circular shape. the SILK-A11 value is 0.78 which is also the highest circularity value measured in all tephra layers investigated. for example compared to Hekla 1947 where the circularity values are 0.73 and 0.75. The values for SILK-A8 and SILK-N1 (average) are 0.74 and 0.70. respectively. Within bedded layer circularity increases with time. the value in the bottom unit is 0.66 and 0.73 in the middle layer. Overall there is no systematic change in circularity with time in the tephra layers investigated even though SILK-LN is included and SILK-A11 omitted.

In summary the SILK-A11 tephra layer is very different from the other three SILK layers in all parameters measured. The grains are not elongated but rather circular in shape and have more uneven surface. The other grains from the SILK layers including the SILK-LN layer have much more elongated shape. less circularity and smoother surface. This difference is demonstrated in Figure 4.17. During the period investigated (between ~3400 and ~8100 years ago) no systematic changes with time were seen in the grain parameters of the SILK layers.

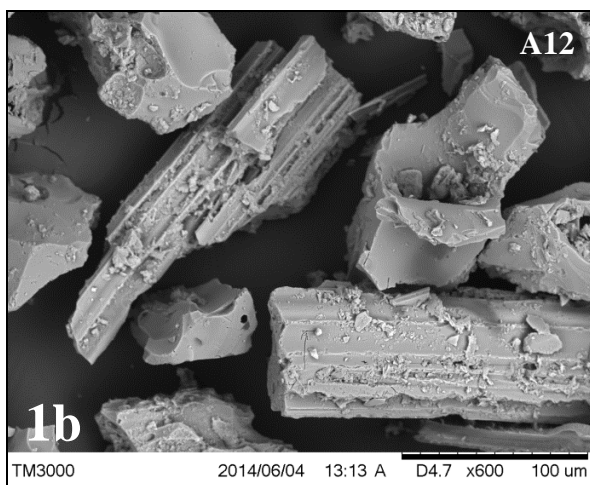
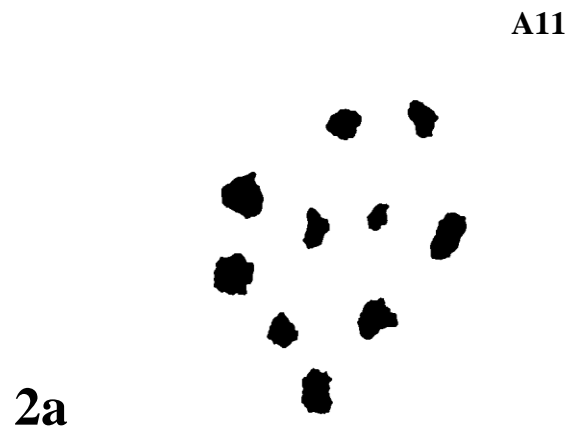
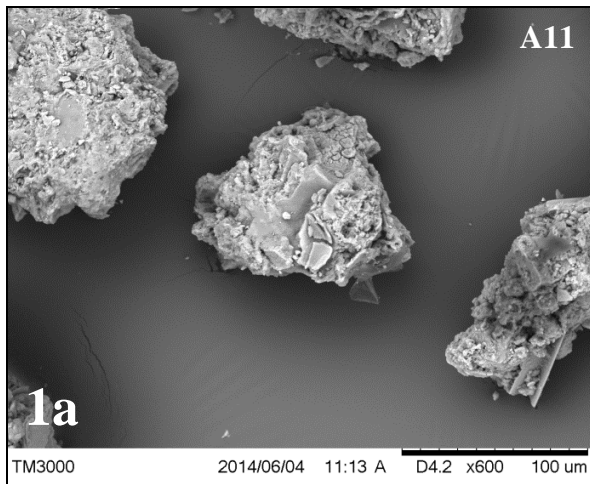


Figure 4.17: SEM images and shadow images (from Morphocop) showing the difference between the two oldest SILK tephra layers A12 and A11. 1a: Example of SEM image from the SILK-A11 tephra sample. 2a: Example of shadow image from the SILK-A11 tephra sample. 1b: Example of SEM image from the SILK-A12 tephra sample. 2b: Example of shadow image from the SILK-A12 tephra sample.

4.3.4 Changes in chemical composition with time

Thirteen silicic tephra layers from Katla volcano have been chemically analyzed or the majority of the silicic tephra layers. The average values of the major element composition of the SILK layers YN, UN, MN, LN, N4, N3, N2, N1, A1, A8, A9 (Larsen et al., 2001) A11 and A12 (new analyses) are shown in Table 4.5.

Table 4.5: Average values (wt %) of chemical analyses performed on the SILK layers YN, UN, MN, LN, N4, N3, N2, N1, A1, A8 and A9. Layers UN, N3, N2 and A8 show higher TiO₂, MgO and CaO and lower SiO₂ concentration than the other 8 layers (red colored numbers). A11 and A12 show higher SiO₂ and lower TiO₂, MgO and CaO concentration than the other 11 layers (purple colored numbers) (Larsen et al., 2001 and unpublished data). Grain size^Δ and grain shape analysed* material.

Tephra	SiO ₂	TiO ₂	Al ₂ O ₃	FeO	MnO	MgO	CaO	Na ₂ O	K ₂ O	Total
SILK-YN	65.31	1.19	14.15	6.04	0.19	1.06	2.94	4.55	2.70	98.12
SILK-UN ^Δ	64.16 ↓	1.33 ↑	13.95	5.94	0.20	1.36 ↑	3.40 ↑	4.37	2.59	97.30
SILK-MN	65.39	1.19	14.21	5.54	0.21	1.13	2.96	4.22	2.63	97.48
SILK-LN ^{Δ*}	65.23	1.21	14.25	5.62	0.19	1.12	3.02	4.42	2.76	97.84
SILK-N4 ^Δ	66.19	1.23	14.10	5.57	1.79	1.14	2.90	4.50	2.80	98.61
SILK-N3 ^Δ	64.69 ↓	1.48 ↑	14.15	5.96	2.02	1.35 ↑	3.35 ↑	4.25	2.60	98.02
SILK-N2 ^Δ	63.59 ↓	1.52 ↑	13.94	6.35	0.21	1.44 ↑	3.60 ↑	4.32	2.53	97.49
SILK-N1 ^{Δ*}	65.34	1.37	13.67	5.78	0.19	1.19	3.03	4.52	2.78	97.83
SILK-A1 ^Δ	65.83	1.21	14.15	5.52	0.18	1.15	3.07	4.41	2.80	98.22
SILK-A8 ^{Δ*}	64.44 ↓	1.25 ↑	14.00	5.78	0.17	1.23 ↑	3.34 ↑	4.61	2.65	97.46
SILK-A9	64.88	1.14	14.00	5.45	0.14	1.14	3.10	4.60	2.70	97.17
SILK-A11*	68.59	0.88	13.86	4.26	0.17	0.74	2.09	4.41	3.13	98.38
SILK-A12 ^{Δ*}	69.07	0.85	13.98	4.21	0.15	0.80	2.07	5.03	3.10	99.40

The chemical composition of the tephra from the SILK layers reveals discrete changes between individual layers as indicated by colors and arrows in Table 4.5. The compositional changes of SILK-YN, -UN, -MN, -LN, -N4, -N3, -N2, -N1, -A1, -A8 and -A9 have been treated by Larsen et al (2001) and an example is demonstrated on Figure 4.18 where two groups are apparent. SILK-UN, SILK-N3, SILK-N2 and SILK-A8 tephra layers have somewhat lower SiO₂, higher MgO and CaO and generally higher TiO₂ than SILK-YN, SILK-MN, SILK-LN, SILK-N4, SILK-N1, SILK-A1 and SILK-A9.

Here new EPMA analyses of the two oldest tephra layers, SILK-A11 and SILK-A12, are presented. Their values of TiO₂, MgO and CaO are considerably lower than in all the other SILK layers (Table 4.5). This difference between the tephra layers is presented in Figure 4.18. where CaO is plotted against FeO. The oldest tephra layers form the third group on the plot.

Tephra samples analyzed for grain size and grain shape characteristics came from the three “groups” as indicated in Tables 4.3. and 4.5.

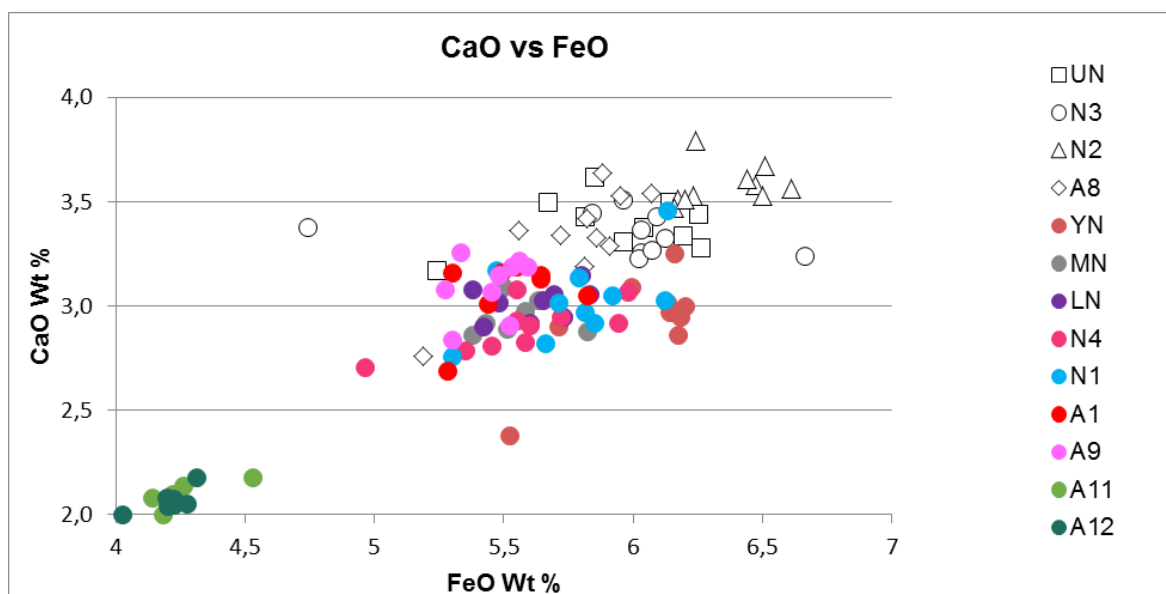


Figure 4.18: Graph that shows CaO values plotted against FeO values. The UN, N3, N2 and A8 have higher values in CaO than the other 9 layers (Guðrún Larsen et al., 2001).

There appears to be potential correlation between grain sizes and chemical composition of the 11 SILK tephra layers analyzed for grain size (Tables 4.3 and 4.5). When considering the largest Φ (Table 4.3) the tephra layers with lower SiO_2 and higher MgO , CaO and TiO_2 tend to be more coarse grained than the others. Sample from only five SILK tephra layers have been analyzed for grain shape so far. There seems to be no correlation between chemical composition and the grain shape parameters measured in this study. This is best demonstrated by very significant difference in grain shape parameters between SILK-A11 and -A12 (Table 4.4) although their chemical composition is very similar, as obvious from Figure 4.17 & 4.18 and table 4.5.

5 Discussion

5.1 Comparison of grain characteristics of silicic Katla and Hekla tephra

5.1.1 Grain size characteristics and changes with distance along axis of thickness

There is a prominent difference in the mean grain size and the proportion of the fine material in the tephra layers investigated here from these two volcanoes. The Hekla 1947 tephra is much coarser than the Katla SILK-LN tephra compared to similar distance from the source (Figure 5.1).

The mean grain size of the SILK-LN tephra changes fairly regularly with distance but varies within bedded layers. The mean grain size of the bottom units is halved every 70-75 km and that of the coarser units is halved every 20-22 km. The mean grain size of Hekla 1947 does however change much more with distance and is halved every 13-14 km, apparently in both units. This rapid change with distance was pointed out by Thorarinsson (1954). These differences can at least partly be explained by the proportion of fine material (Figure 5.2).

In 40 km distance from the source the mean grain size of the Hekla 1947 tephra is about 0.79 mm (0.34 Φ) but the mean grain size of the Katla tephra is about 0.15 mm (2.74 Φ). At about 68 km distance the mean grain size of Hekla 1947 is about 0.23 mm (2.10 Φ) however in the SILK-LN Katla tephra it is about 0.13 mm (2.94 Φ). Katla mean grain size values are average values from all samples collected at each location, bulk samples not included. For example: the mean grain size at Varmárfell was calculated from three samples collected from the tephra layer (same with other locations). Hekla 1947 mean grain size values are average values from all bulk samples collected in 2013 at each location. For the Hekla samples collected freshly fallen by Thorarinsson (1954) the bulk samples are used for the mean grain size. Those samples were only sieved down to 0.063 mm (4 Φ) and the fines ≤ 0.063 mm not analysed as mentioned previously.

Changes in mean grain size between units collected at the same location appear greater in the case of SILK-LN tephra than in the Hekla 1947 tephra (Figure 5.1). It should however be kept in mind that the sample localities are at different distances and therefore not directly comparable.

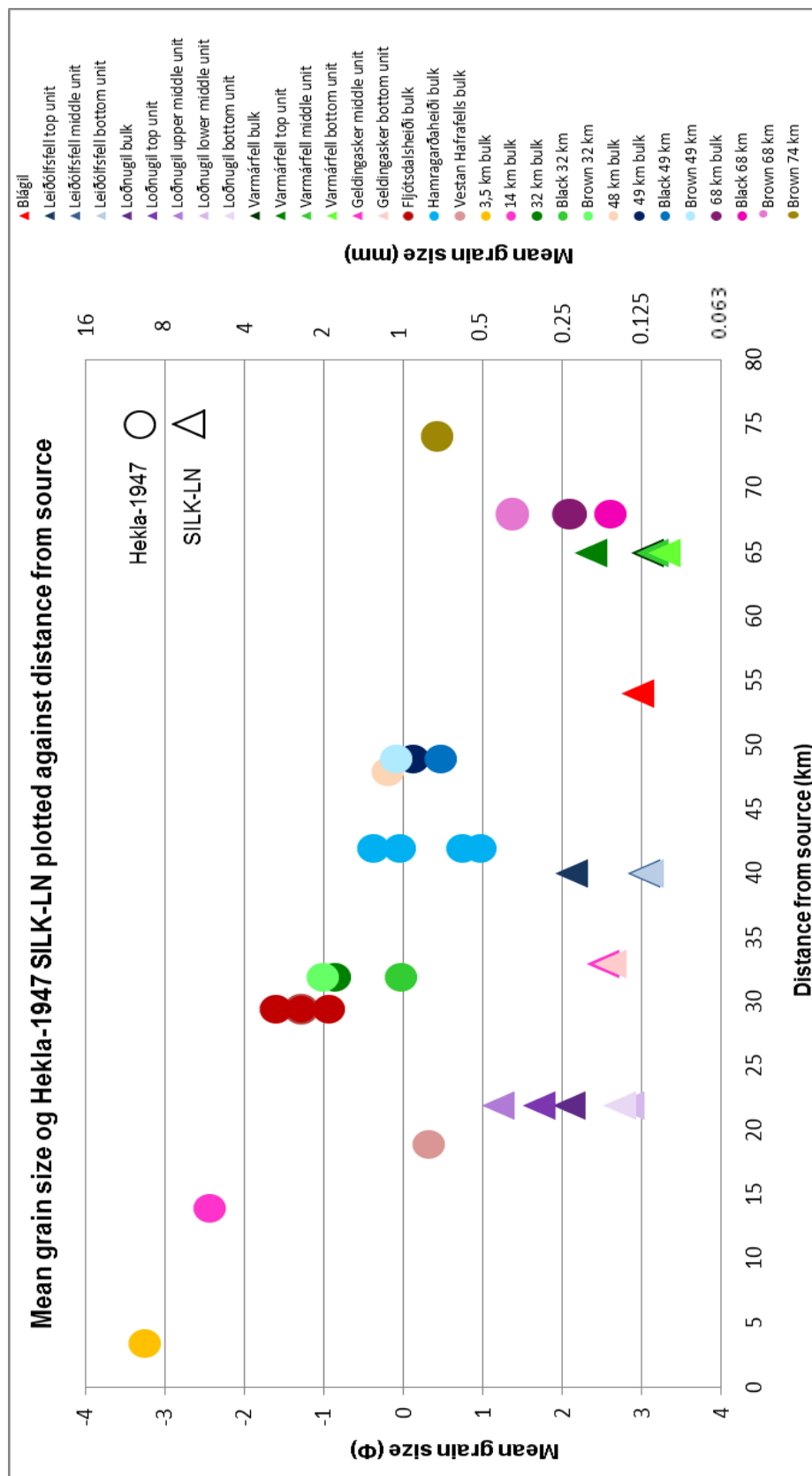


Figure 5.1: Mean grain size along the axis of thickness of the SILK-LN and Hekla 1947 tephra plotted against distance from source. Circles represent Hekla 1947 and triangles represent SILK-LN tephra. Different colors and shades illustrate individual units and bulk samples at different sampling locations. Note that the mean grain size of the SILK-LN at 22 km and Hekla 1947 at 68 km is very similar, both for the bulk samples and individual units.

There is much more fine material in the Katla tephra than in the Hekla tephra. The range in proportion of fines $\leq 4 \Phi$ (≤ 0.063 mm) is 24 to 43 wt % at distances between 22 and 65 km in the SILK-LN tephra (samples from axis of thickness) but in the Hekla tephra this proportion is 1 to 33 wt % at the same distance (excluding samples within 19 km distance because no Katla tephra could be obtained at that distance and potentially remobilized samples). If only the grey brown (the coarser material) Hekla tephra is looked at this proportion is 4.5 to 7.3 wt %. Possible reasons for greater proportion of finer material in the SILK-LN tephra close to source (22 km) compared to the Hekla 1947 tephra could be aggregation of particles and lower, colder and more humid eruption column. It is interesting that the changes in proportion of fine material smaller than 6.5Φ (≤ 0.011 mm) with distance, are little to none. In the Katla tephra the proportion of the samples total weight is about 3-7 % at 20 km distance and 1-8 % at 65 km distance from the source. In the Hekla 1947 tephra the proportion is only about 0.15 – 1.5 % of the samples total weight (Figure 5.3).

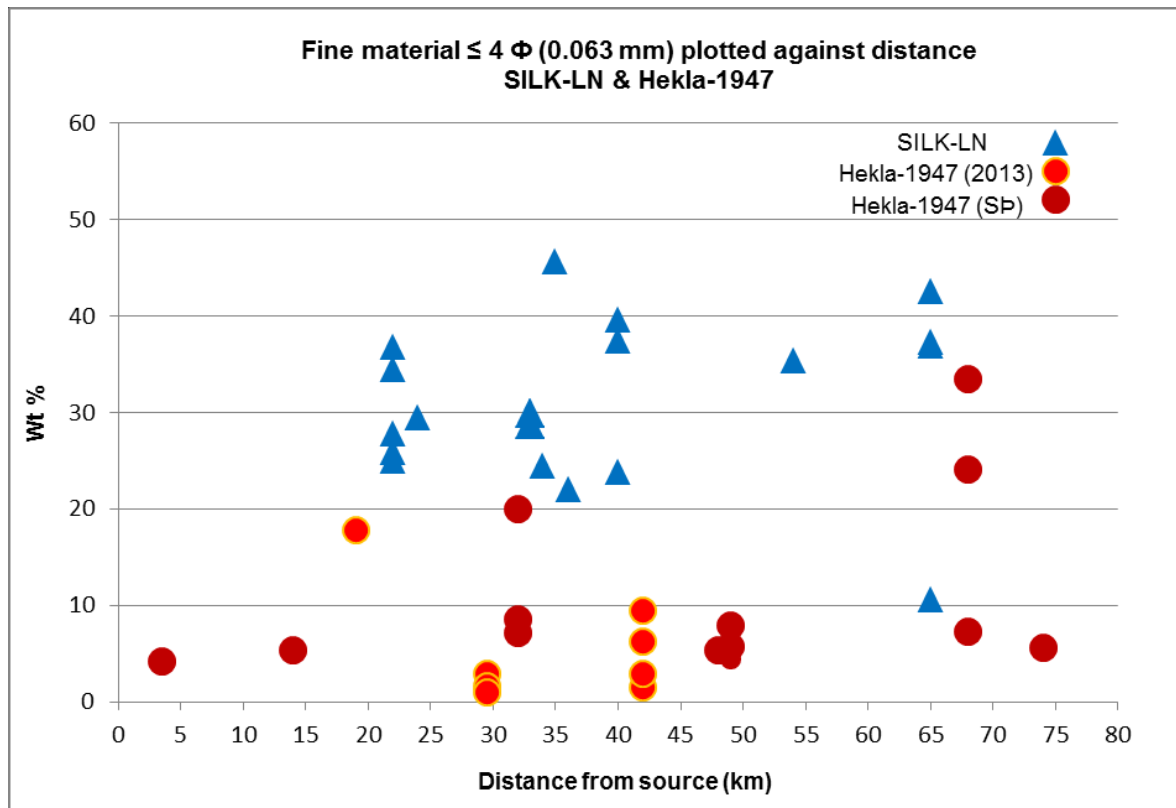


Figure 5.1: Graph showing the fine material $\leq 4 \Phi$ (≤ 0.063 mm) in SILK-LN tephra and Hekla 1947 tephra, samples from all locations included. Blue triangles stand for SILK-LN tephra layer, lighter red colored circles stand for Hekla 1947 tephra samples collected for this research and darker red colored circles stand for Hekla 1947 samples collected by-Thorarinsson (1954).

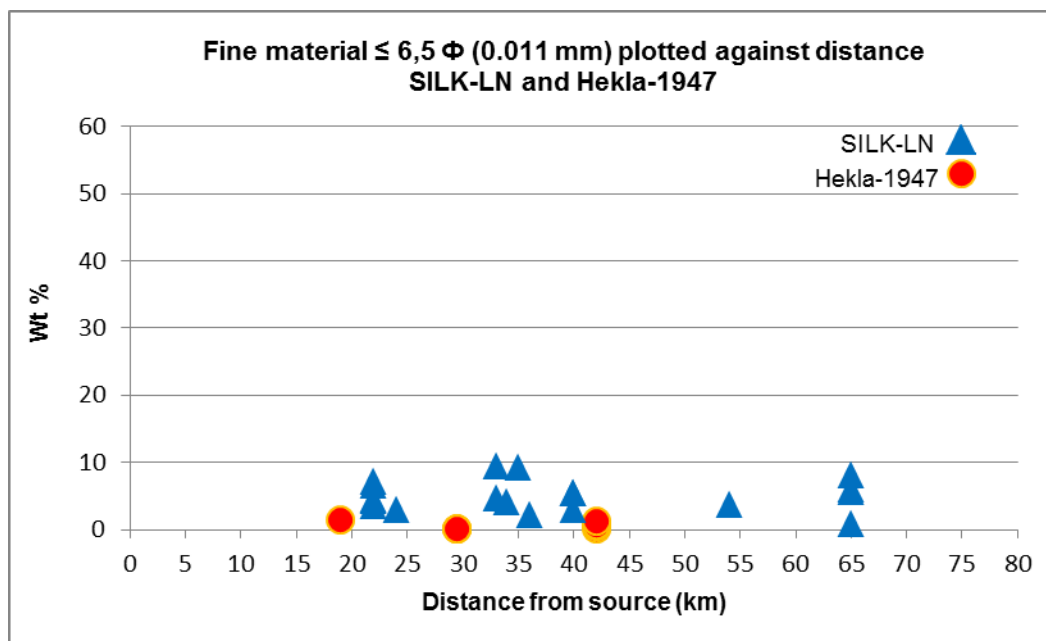


Figure 5.2: Graph showing particles equal and smaller than 6.5Φ (0.011 mm) in SILK-LN tephra and Hekla 1947 tephra. Blue triangles stand for SILK-LN tephra layer, red colored circles stand for Hekla 1947 tephra samples collected for this research.

The main differences in grain size between the SILK-LN and the Hekla 1947 tephra can be summed up in the following way. The Hekla 1947 tephra has significantly higher mean grain size and much lower content of material finer than 4Φ at all distances than in the SILK-LN tephra. The mean grain size of Hekla 1947 decreases more rapidly with distance than that of the SILK-LN tephra.

5.1.2 Changes with time

The grain size measurements of the SILK-LN tephra show an evolution from finer grained material in the beginning phase toward a coarser grained material in the latter part of the eruption. The amount of fine ash changes from ca 30 - 43 wt % in the bottom unit, 25 - 40 wt % in the middle unit and from ca 11 - 29 wt % in the top unit.

A possible reason for finer grained tephra in the beginning phase of the eruption could be due to vigorous fragmentation caused by great amount of external water and the fact that SILK-LN tephra layer is high in SiO_2 . The large amount of fine ash supports the idea that external water existed at the eruption site during the eruption. In this particular case the external water is caused by glacier melt water. When a lot of external water and high viscosity magma come together in an eruption vast amount of fines are produced (Self & Sparks 1978) which is likely in the case of the SILK-LN tephra layer. According to Rose and Durant (2009) silicic eruptions produce high proportions of fine material (30 to >50%) in comparison to basaltic eruptions (~1 to 4 %). In the latter part of the SILK-LN eruption when the grains are bigger depletion of external water is believed to be part of the cause, either due to isolation of the magma/vent from the melt water or due to draining of water in a jökulhlaup. Increased height of the eruption column late in the eruption, allowing larger grains to travel further, is less likely.

No internal layering was observed within the Hekla 1947 tephra layer in the field in 2013 and only bulk samples were collected. According to Thorarinsson (1954 and 1968) changes with time were observed at several locations where the Hekla 1947 tephra was collected freshly fallen by Thorarinsson. In the lower part (beginning phase) the color of the tephra was grey brown and coarse grained, then changed to brownish black and a finer grained top part. Reason for not seeing changes with time in the samples collected in 2013 could be that the fine material had been blown away and the rest got mixed into the coarser part below. In the samples measured by Thorarinsson (recalculated for this study) the mean grain size of the lower unit was -1.00Φ , -0.07Φ and 1.19Φ at 32, 49 and 68 km, respectively and that of the upper unit was -0.01Φ , 0.48Φ and 2.62Φ at the same locations (Figure 5.1).

Hekla is not covered with a glacier although perennial snow was present and also there is not sufficient amount of water in the area that could have caused a hydromagmatic eruption. The coarse grained grey brown tephra in the bottom unit was most likely produced during a magmatic eruption (dry eruption) such as is commonly with Hekla volcano. The change to finer brownish black tephra was related to decreasing SiO_2 content (Thorarinsson 1968) and most likely to lower eruption column.

5.1.3 Grain morphology

The grain shape results show a difference between the Hekla 1947 and SILK-LN tephra layers. In case of the ruggedness there is not a significant difference between Hekla and Katla tephra in the way that one contains more rugged grains than the other. In fact the value of Hekla 1947 samples lie between the two SILK-LN samples (Table 5.1 and Figure 5.4). The SILK-LN sample from Geldingasker which is closest to the source has the most rugged grains of all the samples. The Hekla samples on the other hand are less rugged than the samples from Geldingasker but more rugged than the Varmárfell grains.

Table 5.1: Results of grain morphology measurements. The parameters measured are Elongation (lower values represent more elongated grains), Ruggedness (lower values represent more rugged grains) and Circularity (higher values for more circular grains).

Tephra layer	Unit	Elongation	Ruggedness R2	Circularity	Distance (km)
SILK-LN	Varmárfell bottom unit	0.53	0.45	0.62	65
SILK-LN	Varmárfell middle unit	0.51	0.43	0.57	65
SILK-LN	Geldingasker bottom unit	0.55	0.36	0.63	33
SILK-LN	Geldingasker middle unit	0.68	0.33	0.67	33
Hekla 1947	Vestan Hafráfells	0.73	0.40	0.73	19
Hekla 1947	Hamragarðaheiði	0.73	0.41	0.75	42

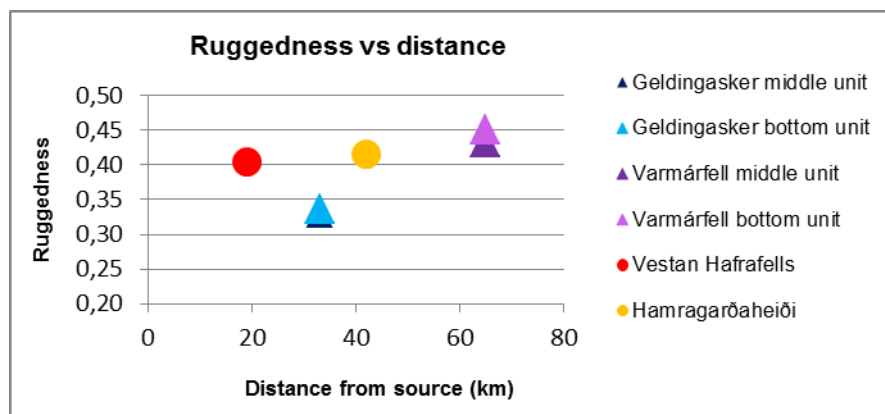


Figure 5.3: Ruggedness (lower values represent more rugged grains) of the SILK-LN and Hekla 1947 tephra plotted against distance. Triangles represent the SILK-LN tephra and the circles represent the Hekla 1947 tephra.

There is a prominent difference between the elongation values of the Katla tephra and the Hekla tephra (Table 5.1 and Figure 5.5). The Hekla elongation values are significantly higher than those of the Katla tephra, which indicates that the Katla grains have much more elongated shape than the Hekla grains that have more equant and stocky shape. The elongation values in the Hekla tephra stays exactly the same at a location close to the source and at a location further away from the source whereas those of the Katla tephra change with distance. The Katla grains that travel furthest away from the source have smoother surface and more elongated shape while the ones traveling shorter distances have more uneven surface and are less elongated. Therefore it appears that small, elongated, smooth surfaced grains settle more slowly and travel further through the air than bigger grains with more rounded shape and uneven surface. Walker et al., (1971) found that down to a diameter of 1 mm cylinders have lower terminal velocity than spheres. Here this seems also to be the case for grains smaller than 1 mm.

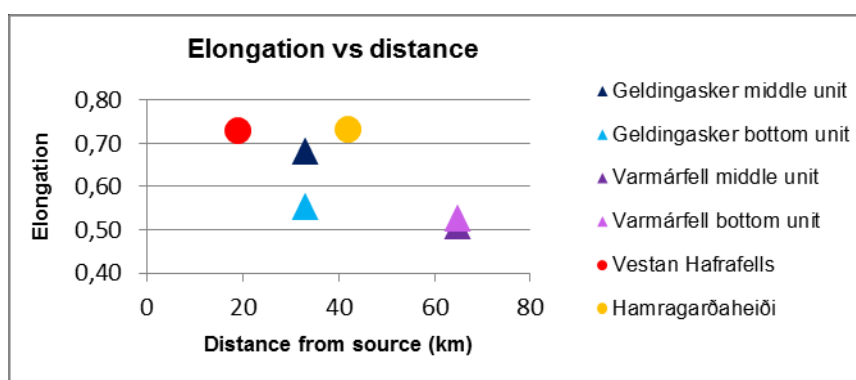


Figure 5.4: Elongation (lower values represent more elongated grains) of the SILK-LN and Hekla 1947 tephra plotted against distance. Triangles represent the SILK-LN tephra and the circles represent the Hekla 1947 tephra.

The circularity values of the SILK-LN and Hekla 1947 tephra show some difference. The circularity value of the Hekla 1947 tephra is higher which means more circular grains than in the Katla tephra, as expected keeping the elongation values in mind. When the SILK-LN tephra and Hekla 1947 tephra are compared we see that the circularity decreases in the

SILK-LN tephra with distance whereas the circularity increases slightly with distance in the Hekla 1947 tephra (Figure 5.6).

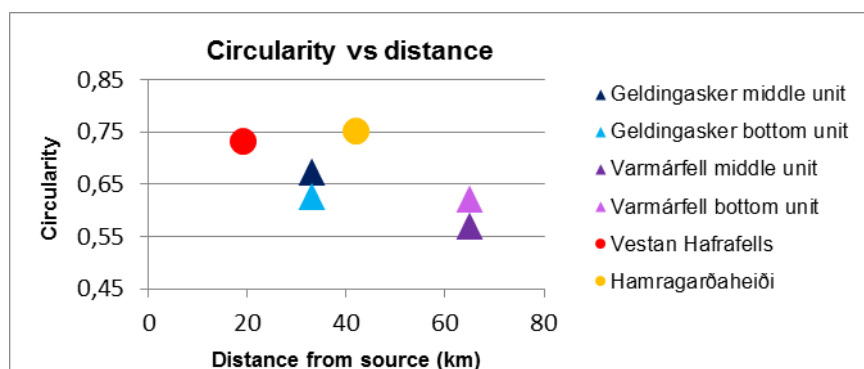


Figure 5.5: Circularity (higher values represent more circular grains) of the SILK-LN and Hekla 1947 tephra plotted against distance. Triangles represent the SILK-LN tephra and the circles represent the Hekla 1947 tephra.

When looking at the differences in grain shape as seen in the SEM the needle- or rod-like grains that characterize the SILK-LN tephra are almost completely missing in the Hekla 1947 tephra where equant grains are most common. Another difference is that grains with smooth, fluidal surface are much more common in the Hekla tephra than in the SILK-LN tephra.

The main difference between the silicic Katla tephra SILK-LN and the Hekla 1947 tephra regarding grain morphology can be summed up in the following way. The grains of the SILK-LN tephra are significantly more elongated than those of the Hekla 1947 tephra but the ruggedness appears to be similar. Both the Hekla and Katla tephra grains become less rugged with distance from source. The Katla tephra becomes more elongated farther from source, contrary to the Hekla tephra that becomes more circular farther from source.

5.2 Silicic Katla tephra layers: changes through the Holocene

The main changes in the 12 SILK layers from Katla volcano through the Holocene (time period between 2800 and 8100 years ago) regarding the grain size are that the upper younger layers (2800-5800 year old) appear to be more coarser grained than the older layers (6000-8100 year old). An exception is the SILK-A8 which belongs to the older layers, which is coarser grained than the other older layers.

The factors that could cause differences in grain size and grain morphology are 1) external factors, in particular the presence and availability of melt water and 2) internal factors, such as changing composition of the magma and the volume erupted.

The eruptive material that is produced in phreatomagmatic eruptions (wet eruptions) is often characterized by highly fragmented fine tephra. The ratio of water to magma affects the explosive activity and the fragmentation of the magma (e.g. Wohletz 1983; White & Houghton 2000; Morrisay et al., 2000; Francis, 2001; Francis & Oppenheimer, 2004). The reason for less fragmentation of the erupting magma and consequently coarser grained

tephra in a sub-glacial environment could be the results of thinner ice cover and less melt water for interaction with the magma.

A trend towards more coarse grained tephra in the younger SILK layers can be argued for, based on the data in Table 4.3. This could suggest a thinner ice cover 2800-5800 years ago than when the older SILK layers were forming. The two largest SILK layers are among the coarse grained younger layers, so the length of the eruption could also be important. Long eruption could create a less wet environment. The location of eruption sites may have changed within the caldera to an area of less ice thickness. It should also be kept in mind that not all tephra samples came from axes of thickness which could affect the result.

Grain shape analyses were performed on four SILK layers other than SILK-LN and what was revealed is that the SILK-A11 tephra layer is very dissimilar from the other SILK tephra layers that were analyzed for grain shape. Firstly the elongation value, the SILK-A11 grains are far from being considered elongated, this is also supported by the circularity value of A11 indicating that the A11 grains are closer to having a circular shape rather than elongated shape like the other SILK layers. And finally the A11 grains have much rougher surface than the grains from the other layers. The reasons why this particular layer is so different from the other SILK layers are not obvious. Was there a lot less water involved than in the other eruptions or is this connected to the chemical composition of the A11 tephra layer? Chemical composition analysis of the A11 layer reveals that it differs from all the other SILK layers except for SILK-A12. A11 and A12 have very similar chemical composition, and SILK-A12 has the typical elongated grains so this grain shape difference is not caused by a difference in chemical composition. The small age difference between A11 and A12 eruptions (~100 years) makes major changes in the glacier thickness unlikely. A different source area where the ice was thin and less melt water was present at the vents is more likely explanation.

In Dellino & Volpe (1996) grain shapes were analyzed with the purpose of identifying the origin of the grains i.e if they were of hydromagmatic or magmatic origin. According to them spherical shaped grains are thought to originate from hydromagmatic eruptions. According to Eiríksson & Wigum (1989) grains from silicic magma are readily more elongated than the basaltic ones and magmatic grains tend to be more elongated than the hydromagmatic grains. According to the elongation values (Chapter 4) the SILK grains are very elongated which fits the description above regarding viscous silicic magma producing more elongated grains. The high proportion of fine material supports phreatomagmatic activity (Self & Sparks 1978).

The elongated SILK grain shape is here believed to connect to the phreatomagmatic explosive activity. It is suggested that the reason for the very elongate shape is the break-up of viscous silicic magma with abundant elongate vesicles as a result of a shock caused either by cooling contraction, a sudden expansion of steam, or both. The lack of lithics in the SILK tephra (Thorsteinsdóttir 2012) could according to Dellino et al., (2012) suggest that the fragmentation caused by interaction with water occurred at the interface between magma and ice/water rather than deeper in the conduit.

5.3 Effects of fine tephra, 4Φ and smaller, on air traffic and health

The grain size data represents material deposited on the ground and therefore gives minimum values for the amount of material that was erupted, in particular for material $\leq 4\Phi$ ($\leq 63\mu\text{m}$ or 0.063 mm) that can travel over long distances, as exemplified by the Hekla 1947 tephra deposited in Finland with grain size of 3 to $15\mu\text{m}$ ($0.003\text{-}0.015\text{ mm}$, Salmi, 1948) and the Eyjafjallajökull 2010 tephra (Gudmundsson et al., 2012). Most samples from the SILK-LN tephra are considered representative of what was deposited (with one or two exceptions). The Hekla 1947 tephra samples of Thorarinsson (1954) are considered representative, the Hekla samples collected in 2013 less so.

The data shows that silicic Katla eruptions produce greater quantities of material $\leq 4\Phi$ ($\leq 63\mu\text{m}$) than Hekla eruptions of similar composition and are therefore more likely to affect air traffic and the health of people. These small grain sizes can reach up to the stratosphere where air traffic takes place. The air must not contain more than 4 mg of tephra per m^3 for air traffic to be safe (EASA Safety Information Bulletin, 2013). At distances of 65-70 km from source the proportion of deposited material $\leq 4\Phi$ ($\leq 63\mu\text{m}$) was up to 42 wt % and 33 wt % for Katla and Hekla tephra, respectively.

In case of the SILK-LN tephra the data shows that grains equal and smaller than 6.5Φ or $11\mu\text{m}$ were present in amounts greater than 1-8 wt % at distances of 65 km. These grains are thoracic, i.e. can be inhaled (Horwell and Baxter 2006). The elongate shape of the grains could be of concern because fibrous material, with length-diameter ratio of 3, can be hazardous when the fibers are longer than $5\mu\text{m}$ (Horwell and Baxter 2006). Checking the presence of such grains will have to be carried out in another study.

6 Summary

The SILK-LN tephra

- Changes with time: grain size of the SILK-LN tephra changes from being more prominently finer grained in the beginning phase and developing towards a coarser grained tephra.
- Changes with distance: The tephra becomes gradually more finer grained away from the source. The mean grain size (bulk samples) changes from 2.12 Φ (0.23 mm) at 22 km to 2.94 Φ (0.13 mm) at 65 km.
- The portion of fine material 4 Φ and smaller increases with distance but the changes are not very prominent. The fine material 6.5 Φ and smaller shows almost no sign of changes with distance.
- Grains found closer to the source have more rugged surface and less elongated shape than the ones further away.

The Hekla 1947 tephra

- Changes with time were observed at three locations (collected freshly fallen by Thorarinsson (1954)). The lower part of the tephra is grey brown and coarser grained, upper part is brownish black and finer grained.
- Changes in grain size with distance are very prominent the mean grain size (bulk samples) is halved every 13-14 km.
- There was a clear evidence of deficiency in fine material 4 Φ and smaller in the samples collected especially for this study which can possibly be explained by reworking.
- Changes in grain shape with distance are not very prominent. Results show that grains both close to and further away from the source is very similar. Grains further away from the source have slightly smoother surface and circular shape than the ones closer to the source.

Comparison of grain characteristics of silicic Katla and Hekla tephra

- The mean grain size of Hekla 1947 tephra layer changes more prominently with distance than in the SILK-LN tephra layer.
- In both tephra layers where bedding is visible considerable changes are noticed with time.
- The proportion of fines equal and smaller than 4 Φ is considerably higher in the SILK-LN tephra layer than in Hekla 1947 tephra layer. At a distance between 22 and 65 km this portion is 24-43 wt % along axis of thickness of SILK-LN but 1-33 wt % for Hekla 1947.

- Obvious difference was noticed in the grain shape results. The biggest difference observed was in the elongation and circularity values, the grains of the SILK-LN layer are more elongated than the Hekla 1947 grains. The Hekla 1947 grains have smoother surface than the SILK-LN grains at 33 km from the source but more uneven surface than the SILK-LN grains at 65 km.

Silicic Katla tephra layers: changes through the Holocene

- The younger SILK tephra layers appears to be coarser grained, i.e. have larger maximum grain size, while the older layers appears to be finer grained, except SILK-A7 which is one of the older layers. These changes occur between SILK-N1 (~5800 year old) and SILK-A1 (~6000 year old). However the mean grain size does not clearly follow this trend.
- Grain shape results of SILK-N1, SILK-A8, SILK-A11 and SILK-A12 layers show that the SILK-A11 is significantly different from the other three layers. This difference lies first and foremost in the elongation values.
- No systematic changes with time were observed in the shape parameters (elongation, ruggedness and circularity) in the measured SILK layers. Even though SILK-A11 is omitted and the ~3400 old SILK-LN is added to measurements it does not change these results.
- Chemical composition of the SILK-A11 and SILK-A12 show higher SiO₂ value and lower TiO₂, MgO and CaO values than in all the other SILK layers.
- A possible correlation appears to be between grain size and chemical composition, where the SILK tephra layers with the lowest SiO₂ and highest FeO and CaO tend to be coarser grained than the others but no correlation appears to be between grain shape (parameters measured in this study) and chemical composition.

References

- Atterberg, A. 1903. Studier i jordanalysen (Studies in soil analyses). Kongl. Landtbruks-akademiens handlingar och tidskrift 42, pp. 183-253.
- Björnsson, H., Pálsson, F. and Guðmundsson, M.T. 2000. Surface and bedrock topography of the Mýrdalsjökull ice cap, Iceland: The Katla caldera, eruption sites and routes of jökulhlaups. *Jökull* 49, pp. 29-46.
- Blott, S.J. and Pye, K. 2001. Gradistat: A grain size distribution and statistics package for the analysis of unconsolidated sediments [electronic version]. *Earth Surface Processes and Landforms*, 26, pp. 1237–1248.
- Bonadonna, C. and Houghton, B.F. 2005. Total grain-size distribution and volume of tephra-fall deposits. *Bulletin of Volcanology* 67, pp. 441-456.
- Brandsdóttir, B. and Menke, W.H. 2008. The seismic structure of Iceland. *Jökull* 58, pp. 17-34.
- Boggs, S. 2013. *Principles of Sedimentology and Stratigraphy, 5th Edition*. Edinburgh: Pearson Education Limited. 566 pp.
- Brazier, S., Sparks, R.S.J., Carey, S.N., Sigurdsson, H. and Westgate, J.A. 1983. Bimodal grain size distribution and seconsary thickening in air-fall ash layers. *Nature* 301, pp. 115-119.
- Büttner, R., Dellino, P., La Volpe, L., Lorenz, V. and Zimanowski, B. 2002. Thermohydraulic explosions in phreatomagmatic eruptions as evidenced by the comparison between pyroclasts and products from Molten Fuel Coolant Interaction experiments. *Journal of Geophysical Research: Solid Earth (1978–2012)*, 107(B11), ECV 5-1-ECV 5-14.
- Carey, S. and Sparks, R.S.J. 1986. Quantative models of the fallouts and dispersal of the tephra fom volcanic eruption columns. *Bulletin of Volcanology* 48, pp. 109-125.
- Carver, R.E. 1971. Procedures in sedimentary petrology. Robert E. Carver (Eds). Wiley-interscience. pp. 3-365
- Cas, R.A.F. and Wright, J.V. 1987. *Volcanic successions, modern and ancient*. London: Allen and Unwin.
- Cashman, K., Stuertervant, B., Papale, P. and Navon, O. 2000. Magmatic fragmentation. In: Sigurðsson, H., Houghton, B., McNutt, S.R., Rymer, H. and Stix, J. (Eds.), *Encyclopedia of Volcanoes*. San Diego: Academic press. pp. 421-430.

- Cioni, R., Pistolesi, M., Bertagnini, A., Bonadonna, C., Hoskuldsson, A. and Scateni, B. 2014. Insights into the dynamics and evolution of the 2010 Eyjafjallajökull summit eruption (Iceland) provided by volcanic ash textures. *Earth and Planetary Science Letters* 394, pp. 111-123.
- Dellino, P. and Volpe, L. La. 1995. Fragmentation versus transportation mechanisms in the pyroclastic sequence of Monte Pilato-Rocche Rosse (Lipari, Italy). *Journal of Volcanology and Geothermal Research* 64, pp. 211-231.
- Dellino, P. and Volpe, L. La. 1996. Image processing analysis in reconstructing fragmentation and transportation mechanisms of pyroclastic deposits. The case of Monte Pilato-Rocche Rosse eruptions, Lipari (Aeolian islands, Italy). *Journal of Volcanology and Geothermal research* 71, pp. 13-29.
- Dellino, P. and Liotino, G. 2002. The fractal and multifractal dimension of volcanic ash particles contour: a test study on the utility and volcanological relevance. *Journal of Volcanology and Geothermal Research* 113, pp. 1-18.
- Dellino, P., Gudmundsson, M.T., Larsen, G., Mele, D., Stevenson, J.A., Thordarson, T. and Zimanowski, B. 2012. Ash from the Eyjafjallajökull eruption (Iceland): Fragmentation processes and aerodynamic behavior. *Journal of Geophysical Research* 117, 10 pp.
- Dugmore, A.J., Newton, A.J., Larsen, G. and Cook, G.T. 2000. Tephrochronology, environmental change and the Norse settlement of Iceland. *Environmental archaeology* 5, pp. 21-34.
- EASA Safety Information Bulletin SIB: 201017RS, issued March 11, 2013.
- Einarsson, P. and Brandsdóttir, B. 2000. Earthquakes in the Mýrdalsjökull area, Iceland, 1978-1985: seasonal correlation and connection with volcanoes. *Jökull* 49, pp. 59-73.
- Eiríksson, J. and Wigum, B.J. 1989. The Morphometry of Selected Tephra Samples from Icelandic Volcanoes. *Jökull* 39, pp. 57-74.
- Eiríksson, J. 1993. Inngangur að setlagafraði. Reykjavík: Ísland.
- Eiríksson, J., Sigurgeirsson, M.Á. and Hoelstad, T. 1994. Image analysis and morphometry of hydromagmatic and magmatic tephra grains, Reykjanes volcanic system, Iceland. *Jökull* 44, pp. 41-55.
- Fisher, R.V. and Schmincke, H.U. 1984. *Pyroclastic Rocks*. New York: Springer-Verlag, 472 pp.
- Folk, R.L. 1980. Petrology of sedimentary rocks. Hemphill Publishing Company, Austin, Texas, 182 pp.
- Francis, P. 2001. *Volcanoes A planetary perspective*. Oxford: Clarendon Press. 443 pp.

- Francis, P. and Oppenheimer, C. 2004. *Volcanoes*. New York: Oxford University Press Inc. 521 pp.
- Grönvold, K., Larsen, G., Thorarinsson, S. and Sæmundsson, K. 1983. The Hekla Eruption 1980-1981. *Bulletin Volcanologique* 46 (4), pp. 349-363.
- Guðmundsdóttir, E.R. 1998. Gjóska úr Kötlugosi 1755. Ásýnd, kornastærð og kornalögun. B.Sc. Thesis, University of Iceland, Reykjavík, 64 pp.
- Guðmundsdóttir, E.R., Larsen, G. and Eiríksson, J. 2011. Two new Icelandic tephra markers: The Hekla Ö tephra layer, 6060 cal. yr BP, and Hekla DH tephra layer, ~6650 cal. yr BP. Land-sea correlation of mid-Holocene tephra markers. *The Holocene* 21 (4), pp. 629-639.
- Guðmundsson, O., Brandsdóttir, B., Menke, W. and Sigvaldason, G.E. 1994. The crustal magma chamber of the Katla volcano in south Iceland revealed by 2-D seismic undershooting. *Geophysical Journal International* 119, pp. 277-296.
- Guðmundsson, M.T., Thordarson, T., Höskuldsson, Á., Larsen, G., Björnsson, H., Prata, F.J., Oddson, B., Magnússon, E., Högnadóttir, Th., Petersen, G.N., Heyward, C.L., Stevenson, J.A. and Jónsdóttir, I. 2012. Ash generation and distribution from the April-May 2010 eruption of Eyjafjallajökull, Iceland. *Scientific reports* 2 (572), 12 pp.
- Hall, V.A. and Pilcher, J.R. 2002. Late-Quaternary Icelandic tephras in Ireland and Great Britain: detection, characterization and usefulness. *The Holocene* 12, pp. 223-230.
- Heiken, G. 1974. An Atlas of Volcanic Ash. Smithsonian Contr. Earth Sci., no 12.
- Heiken, G. and Wohletz, K. 1992. Volcanic Ash. University of California press. 246 pp.
- Hitachi High-Technologies Corporation. 2010. Instruction manual for model TM3000 Tabletop Microscope.
- Horwell, C.J. and Baxter, P.J. 2006. The respiratory health hazards of volcanic ash: a review for volcanic risk mitigation. *Bulletin of Volcanology* 69, pp. 1-24.
- Houghton, B., Wilson, C., Smith, R. and Gilbert, J. (2000). Phreatoplinian eruptions. In: H. Sigurdsson, B. Houghton, S.R. McNutt, H. Rymer, J. Stix (eds), *Encyclopedia of Volcanoes*, Academic Press, San Diego, pp. 513-525.
- Hreinsdóttir, S., Sigmundsson, F., Roberts, M.J., Björnsson, H., Grapenthin, R., Arason, Th., Árnadóttir, Th., Hólmjárn, J., Geirsson, H., Bennett, R.A., Guðmundsson, M.T., Oddson, B., Ófeigsson, B.G., Villemín, T., Jónsson, Th., Sturkell, E., Höskuldsson, Á., Larsen, G., Thordarson, T. and Óladóttir, B.A. 2014. Volcanic plume height correlated with magma-pressure change at Grímsvötn Volcano, Iceland. *Nature Geoscience* 7, pp. 214-218.

- Höskuldsson, Á., Óskarsson, N., Pedersen, R., Grönvold, K., Vogfjörð, K. and Ólafsdóttir, R. 2007. The millennium eruption of Hekla in February 2000. *Bulletin of Volcanology* 70, pp. 169-182.
- Jakobsson, S.P. 1979. Petrology of recent basalts of the Eastern Volcanic Zone, Iceland. *Acta Naturalia Islandica* 26, pp. 1-103.
- Jakobsson, S.P., Jónasson, K. and Sigurðsson, I.A. 2008. The three igneous rock series of Iceland. *Jökull* 58, pp. 117-138.
- Jóhannesson, H. and Einarsson, S. 1992. Hekla fjall með fortíð. *Náttúrufræðingurinn* 61, pp. 177-191.
- Jóhannesson, H. and Sæmundsson, K. 1998. Geological map of Iceland. 1:500 000. Tectonics. Icelandic Institute of Natural history, Reykjavík.
- Kratzmann, D.J., Carey, S., Scasso, R. and Naranjo, J.A. 2009. Compositional variations and magma mixing in the 1991 eruptions of Hudson volcano, Chile. *Bulletin of Volcanology* 71, pp. 419-439.
- Kjartansson, G. 1945. *Hekla. Árbók Ferðafélags Íslands* 1945. Ferðafélag Íslands, Reykjavík.
- Lacasse, C., Sigurdsson, H., Jóhannesson, H., Paterne, M. and Carey, S. 1995. Source of Ash Zone 1 in the North Atlantic. *Bulletin of Volcanology* 57, pp. 18-32.
- Lacasse, C., Karlsdóttir, S., Larsen, G., Soosalu, H., Rose, W.I. and Ernst, G.G. 2004. Weather radar observations of the Hekla 2000 eruption cloud, Iceland. *Bulletin of Volcanology* 66, pp. 457-473.
- Lacasse, C., Sigurdsson, H., Carey, S.N., Jóhannesson, N., Thomas, L.E. and Rogers, N.W. 2007. Bimodal volcanism at the Katla subglacial caldera, Iceland: insight into the geochemistry and petrogenesis of rhyolitic magmas. *Bulletin of Volcanology* 69 (4), pp. 373-399.
- Larsen, G. and Thorarinsson, S. 1977. Hekla 4 and other acid Hekla tephra layers. *Jökull* 27, pp. 28-46.
- Larsen, G. and Vilmundardóttir, E. 1992. Tvílit gjóskulög austan Heklu: H-X, H-Y, H-Z. *Vorráðstefna Jarðfræðafélags Íslands, Yfirlit og ágríp*, pp. 28-30.
- Larsen, G., Vilmundardóttir, E.G. and Thorkelsson, B. 1992. Heklugosið 1991: Gjóskufallið og gjóskulagið frá fyrsta degi gossins. *Náttúrufræðingurinn* 61, pp. 159-176.
- Larsen, G. 1996. Gjóskutímatal og gjóskulög frá tíma norræns landnáms á Íslandi. In: Grímsdóttir, G.Á. *Landnám á Íslandi*. Vísndafélag Íslendinga, Ráðstefnurit V. pp. 81-106.

- Larsen, G., Dugmore, A. and Newton, A. 1999. Geochemistry of historical-age silicic tephra in Iceland. *The Holocene* 9, pp. 463-471.
- Larsen, G. 2000. Holocene eruptions within the Katla volcanic system, south Iceland: Characteristics and environmental impact. *Jökull* 49, pp. 1-28.
- Larsen, G., Newton, A.J., Dugmore, A.J. and Vilmundardóttir, E.G. 2001. Geochemistry, dispersal, volumes and chronology of Holocene silicic tephra layers from the Katla volcanic system, Iceland. *Journal of Quaternary Science* 16, pp. 119-132.
- Larsen, G. and Eiríksson, J. 2008. Holocene tephra archives and tephrochronology in Iceland - a brief overview. *Jökull* 58, pp. 229-250.
- Larsen, G. 2010. Katla: Tephrochronology and eruption History. *Developments In Quaternary Sciences* 13, pp. 23-49.
- Larsen, G., Sverrisdóttir, G., Jóhannesson, H., Hjartarson, Á. and Einarsson, P. 2013. Hekla. In: Sigmundsson, F. (Eds.), *Náttúruvá á Íslandi – Eldgos og Jarðskjálftar*. Reykjavík: Viðlagatrygging Íslands and Háskólaútgáfan. pp. 189-209.
- Micromeritics. 2010. SediGraph III 5120 Operator's Manual (V1.04). Norcross, GA.
- Mele, D., Dellino, P., Sulpizio, R. and Braia, G. 2011. A systematic investigation on the aerodynamics of ash particles. *Journal of Volcanology and Geothermal Research* 203, pp. 1-11.
- Morrisay, M., Zimanowski, B., Wohletz, K. and Buetner, R. 2000. Phreatomagmatic fragmentation. In: Sigurðsson, H., Houghton, B., McNutt, S.R., Rymer, H. and Stix, J. (Eds.), *Encyclopedia of Volcanoes*. San Diego: Academic press. pp. 431-445.
- Newton A.J. 1999. Ocean-transported pumice in the North Atlantic. PhD thesis, University of Edinburgh: Edinburgh, 394 pp.
- Nicholson, E., Cashman, K., Beckett, F., Witham, C., Leadbetter, S. and Hjort, M. 2014. Brown snow: Remobilisation of volcanic ash from recent Icelandic eruptions. 31st Nordic Geological Winter Meeting, Abstracts, 163.
- Óladóttir, B.A. 2003. Gjóskulagið E2 úr Kötlu kornalögun og kornastærð. B.Sc. Thesis, University of Iceland, Reykjavík, 90 pp.
- Óladóttir, B.A., Larsen, G., Þórðarson, Þ. and Sigmarsson, O. 2005. The Katla volcano S-Iceland: Holocene tephra stratigraphy and eruption frequency. *Jökull* 55, pp. 53-74.
- Óladóttir, B.A., Thórðarson, Th., Larsen, G. and Sigmarsson, O. 2007. Survival of the Mýrdalsjökull ice cap through the Holocene thermal maximum: evidence from sulphur contents in Katla tephra layers (Iceland) from the last ~8400 years. *Annals of Glaciology* 45, pp. 183-188.

- Óladóttir, B.A., Sigmarsson, O., Larsen, G. and Thordarson, Th. 2008. Katla volcano, Iceland: magma composition, dynamics and eruption frequency as recorded by Holocene tephra layers. *Bulletin of Volcanology* 70, pp. 475-493.
- Ólafsson, M., Imsland, P. and Larsen, G. 1984. Nornahár II (Pelé's hair II). *Náttúrufræðingurinn* 53, pp. 135-144.
- Powers, M. C. 1953. A new roundness scale for sedimentary particles. *Journal of Sedimentary Petrology* 23, pp. 117-119.
- Rose, W. I. and Durant, A. J. 2009. Fine ash content of explosive eruptions. *Journal of Volcanology and Geothermal Research* 186, pp. 32-39.
- Róbertsdóttir, B.G., Larsen, G. and Eiríksson, J. 2002. 30 gos í Heklu og nágrenni á tímabilinu 2980-850 cal. BP. *Vorráðstefna Jarðfræðafélags Íslands 15. apríl 2002. Ágrip erinda og veggspjalda*. Jarðfræðafélag Íslands, Reykjavík, p. 11.
- Salmi, M. 1948. The Hekla ashfalls in Finland. *Suomen Geologinen Seura* 21, pp. 87-96.
- Schmid, R. 1981. Descriptive nomenclature and classification of pyroclastic deposits and fragments: Recommendations of the IUGS subcommission on the Systematics of Igneous Rocks. *Geology* 9, pp. 41-43.
- Schwarz, H. 1980. Two-Dimensional Feature-Shape Indices. *Mikroskopie (Wien)* 37 (Suppl.): 64-67.
- Self, S. and Sparks, R.S.J. 1978. Characteristics of Widespread Pyroclastic Deposits Formed by the Interaction of Silicic Magma and water. *Bulletin of Volcanology* 41 (3), pp. 196-212.
- Sparks, R.S.J., Wilson, L. and Sigurdsson, H. 1981. The Pyroclastic Deposits of the 1875 Eruption of Askja, Iceland. *Phil. Trans. Royal Soc. London*, v. 29, pp. 241-273.
- Sigmarsson, O., Condomines, M. and Fourcade, S. A. 1992. Detailed Th, Sr and O isotope study of Hekla: differentiation processes in an Icelandic volcano. *Contributions to Mineralogy and Petrology* 112, pp. 20-34.
- Soosalu, H. and Einarsson, H. 2004. Seismic constraints on magma chambers at Hekla and Torfajökull volcanoes, Iceland. *Bulletin of Volcanology* 66 (3), pp. 276-286.
- Sverrisdóttir, G. 2007. Hybrid magma generation preceding Plinian silicic eruptions at Hekla, Iceland; Evidence from mineralogy and chemistry of two zoned deposits. *Geological Magazine* 144, pp. 643-659.
- Thorarinsson, S. 1944. Tefrokronologiska studier på Island. *Geografiska Annaler* 26, pp. 1-217.
- Thorarinsson S. 1954. The tephra-fall from Hekla on March 29th 1947. In: Einarsson T, Kjartansson G and Thorarinsson S (Eds.), *The Eruption of Hekla 1947-48*. II, Reykjavík: Societas Scientiarum Islandica, 3, pp. 1-68.

- Thorarinsson, S. 1967. The eruptions of Hekla in historical times. In: Einarsson, T., Kjartansson, G. and Thorarinsson, S. (Eds.), *The eruption of Hekla 1947-48*. I, Reykjavík: Societas Scientiarum Islandica, pp. 1-177.
- Thorarinsson, S. 1968. *Heklueldar*. Sögufélag, Reykjavík. 185 pp.
- Thorarinsson, S. 1970. *Hekla*. Almenna bókafélagið, Reykjavík.
- Thorarinsson, S. 1981. Greetings from Iceland. *Geografiska Annaler* 63A, pp. 109-118.
- Thordarson, T. 1990. *Skaftáreldar 1783-1785 Gjóska og framvinda gossins*. 4. year essay, University of Iceland, Reykjavík, 187 pp.
- Thordarson, T. and Larsen, G. 2007. Volcanism in Iceland in historical time: Volcano types, eruption styles and eruptive history. *Journal of Geodynamics* 43, pp. 118-152.
- Thordarson, Th. and Höskuldsson, Á. 2008. Postglacial volcanism in Iceland. *Jökull* 58, pp. 197-228.
- Thorkelsson, B. (ed.) 2012. *The 2010 Eyjafjallajökull eruption, Iceland. Report to ICAO*. Icelandic Meteorological Office, Institute of Earth Sciences, University of Iceland and The National Commissioner of the Icelandic police, Reykjavík.
- Thorsteinsdóttir, E.S. 2012. Súr gjóska úr Kötlu. Kornastærð, kornalögun og þáttagreining. B.Sc. Thesis, University of Iceland, Reykjavík, 54 pp.
- Tómasson, J. 1967. Hekla's magma. In: Björnsson, S., (ed.), *Iceland and Mid-Ocean ridges*. Vísindafélag Íslendinga, Reykjavík, pp. 180-188.
- Tómasson, H. 1996. The Jökulhlaup from Katla in 1918. *Annals of Glaciology* 22, pp. 249-254.
- Vergnolle, S. and Mangan, M. 2000. Hawaiian and strombolian eruptions. In: Sigurðsson, H., Houghton, B., McNutt, S.R., Rymer, H. and Stix, J. (Eds.), *Encyclopedia of Volcanoes*. San Diego: Academic press. pp. 447-461.
- Walker, G.P.L., Wilson, L. and Bowell, E.L.G. 1971. Explosive Volcanic Eruptions - I. The Rate of Fall of Pyroclasts. *Geophysical Journal of the Royal Astronomical Society* 22, pp. 377-383.
- Walker, G.P.L. 1980. The Taupo pumice: product of the most powerful known (ultraplinian) eruption? *Journal of Volcanology and Geothermal Research* 8, pp. 69-94.
- Wastegård, S. 2002. Early to middle Holocene silicic tephra horizons from the Katla volcanic system, Iceland: new results from the Faroe Islands. *Journal of Quaternary Science* 17, pp. 723-730.
- Wastegård, S. and Davies, S.M. 2009. An overview of distal tephrochronology in northern Europe during the last 1000 years. *Journal of Quaternary Science* 24, pp. 500-512.

- White, J.D. and Houghton, B. 2000. Surtseyjan and related phreatomagmatic eruptions. In: Sigurðsson, H., Houghton, B., McNutt, S.R., Rymer, H. and Stix, J. (Eds.), *Encyclopedia of Volcanoes*. San Diego: Academic press. pp. 495-411.
- Wohletz, K.H. 1983. Mechanisms of hydrovolcanic pyroclast formation: grain-size, scanning electron microscopy, and experimental studies. *Journal of Volcanology and Geothermal Research* 17, pp. 31-63.
- Zhang, Y. A. 1999. Criterion for the fragmentation of bubbly magma based on brittle failure theory. *Nature* 402, pp. 648-650.
- Zimanowski, B., Büttner, R., Lorenz, V. and Häfele, H.-G. 1997. Fragmentation of basaltic melts in the course of explosive volcanism. *Journal of Geophysical Research* 102, pp. 803-814.
- Zingg, Th. 1935. Beiträge zur Schotteranalyse. *Schweizerische Mineralogische und Petrographische Mitteilungen* 15, pp. 39-140.

Webpage

- National Technical University of Athens. Data from webpage (2015) http://www.istone.ntua.gr/Training_courses/wp1/density__pycnometer.html /January 2015.

Appendix I

Sampling locations

SILK-LN tephra layers

Name of tephra layer	Locality	Distance.km*	District	Longitude Latitude
SILK-LN	Loðnugil	22	Álftaversafréttur	63.730432. -18.746435
SILK-LN	Ford at Sydri ófæra	36	Skaftártunguafréttur	63.899263. -18.708447
SILK-LN	Gully at Varmárfell	65	Síðuafréttur	64.052040. -18.212098
SILK-LN	Blágil gully	54	Síðuafréttur	63.965642. -18.321034
SILK-LN	Grófará-v. Múla	35	Skaftártunga	63.698686. -18.441746
SILK-LN	Hvammur	34	Skaftártunga	63.747426. -18.496500
SILK-LN	Leiðólfsfell	40	Síðuafréttur	63.861389. -18.510669
SILK-LN	Geldingasker	33	Skaftártunguafréttur	63.826170. -18.622029
SILK-LN	Strútur Hut	24	Mælifellssandur	63.838080. -018.97553

*Distance from center of Katla caldera (approx. 63°38'N 19°08'W).

SILK tephra layers

Name of tephra layer	Locality	Distance.km*	District	Longitude Latitude
SILK-N7/UN	Framgil	22	Álftaversafréttur	63.700262. -18.726672
SILK-N6	Framgil	22	Álftaversafréttur	63.700262. -18.726672
SILK-N5/LN	Framgil	22	Álftaversafréttur	63.700262. -18.726672
SILK-N4	Framgil	22	Álftaversafréttur	63.700262. -18.726672
SILK-N3	Framgil	22	Álftaversafréttur	63.700262. -18.726672
SILK-N2	Framgil	22	Álftaversafréttur	63.700262. -18.726672
SILK-N1	Framgil	22	Álftaversafréttur	63.700262. -18.726672

Name of tephra layer	Locality	Distance.km*	District	Longitude Latitude
SILK-N1	Einhyrningsflatir	20	Fljótshlíðarafréttur	63.735412. -19.482729
SILK-A1	Einhyrningsflatir	20	Fljótshlíðarafréttur	63.735412. -19.482729
SILK-A5	Einhyrningsflatir	20	Fljótshlíðarafréttur	63.735412. -19.482729
SILK-A7	Einhyrningsflatir	20	Fljótshlíðarafréttur	63.735412. -19.482729
SILK-A8/9	Einhyrningsflatir	20	Fljótshlíðarafréttur	63.735412. -19.482729
SILK-A12 II	Einhyrningsflatir	20	Fljótshlíðarafréttur	63.735412. -19.482729
SILK-A11	Hill N of Einhyrningsflatir	20	Fljótshlíðarafréttur	63.736018. -19.448736
SILK-A12	Hill N of Einhyrningsflatir	20	Fljótshlíðarafréttur	63.736018. -19.448736

*Distance from center of Katla caldera (approx. 63°38'N 19°08'W).

Hekla 1947 tephra layer

Tephra layer	Sampling locality	Distance*. km	District	Latitude Longitude
Hekla 1947	Hamragarðaheiði 1	42	Eyjafjöll	63.623750 -19.885566
Hekla 1947	Hamragarðaheiði 2	42	Eyjafjöll	63.624040 -19.885879
Hekla 1947	Hamragarðaheiði 3	42	Eyjafjöll	63.624769 -19.087049
Hekla 1947	Fljótisdalsheiði	29.5	Fljótshlíð	63.723520 -19.723650
Hekla 1947	Vestan Hafrafells	19	Rangárvallafréttur	63.837130 -19.847840

*Distance from Hekla's top crater (approx 63°59.52'N 19°40.00'W).

Hekla 1947 tephra layer. Approx location (after lmi.is) from Sigurður Þórarinnsson 1954

Tephra layer	Sampling locality	Distance*. km	District	Latitude Longitude
Hekla 1947	Háahraun	3.5	Hekla area	63.956178 -19.646022
Hekla 1947	Langvíuhraun	14	Rangárvallafréttur	63.865760 -19.765724
Hekla 1947	Árkvörn	32	Fljótshlíð	63.715176 -19.834018
Hekla 1947	Hvammur	47	Eyjafjöll	63.576687 -19.878508
Hekla 1947	4 km E of Hvammur	49	Eyjafjöll	63.557044 -19.796837
Hekla 1947	Vestmannaeyjakaupst	68	Vestmannaeyjar	63.442944 -20.277850

*Distance from Hekla's top crater (approx 63°59.52'N 19°40.00'W).

Appendix II

Methods

Methods

This chapter is divided into two subchapters. Discussing field- and laboratory work. It is complementary to Chapter 3 in the main text.

Field work

Documenting and sampling of tephra deposits in the field requires certain working procedures. The first thing to do is finding a suitable undisturbed soil section. The tephra has to be in its original state so that certain features can be seen. for example the bedding, grading, color and color changes, texture, grain size and grain types. This information can also give an idea on what type of eruption formed this specific tephra layer (Larsen, 1996; Óladóttir et al., 2005). When suitable soil section has been located, the section is opened (without unnecessary disturbance of soil and vegetation) and cleaned with a shovel. After the coarse cleaning the section is cleaned and smoothed out with finer tools such as trowel or a table knife, to make it easier to see the characteristics of the layers and bring out contacts between beds, etc. Next step is to photograph the section before the sampling takes place, both up close and further away, with a scale and possibly indicating the layer to be studied by inserting a knife. Although photographs can be very usefull they can show colors and texture differently in digital format compared to the appearance in nature. Careful logging of the details of the section in a field book is then carried out, example shown in Table 1. In this case the thickness, bedding, color, type of material and the grain size was logged. The categorizing method used in the fieldwork in this research is shown in Table 2 (modified Atterberg scale) (Atterberg, 1903). Another size categorizing method can also be used and is shown in Table 3 (Thordarson, 1990). Prominent features such as clearly needle shaped grains are also noticed.

When logging and photographing have been done the sampling can begin. When collecting multiple samples the general rule is to start from the top of the section and work your way down, to minimize contamination between layers. Where possible, samples were collected from individual beds. From thin layers without bedding a bulk sample was collected from the whole layer. Always make sure to take enough samples for the planned analyses. The sample collected is then put in to a well labelled plastic bag with the name and/or number of the tephra layer, sample number, sample location and date.

Table 1: Field book notes from place called Loðnugil, silicic Katla tephra: Nearly all the section is matrix supported, which means that there is more of finer material that holds up the coarser grains, also this layer has an uneven top. This sample is bedded and divided into four units. Total thickness of the layer is 11-13 cm.

Section	Thickness	Color	Type	Grain size
Lowest	2 cm	Grgr	a	S ÷ - M (Matrix supported)
Second lowest	4-4.5 cm	Grgr	a	F -S
Second highest	2-2.5 cm	Dark grgr	a	S ÷ - M +
Highest	3.5-4 cm	Grgr	a	S ÷ - G

Table 2: Symbols used in field work for both the colors and the size of the tephra.

Tephra color	Tephra size terms*	Type
S: black	f: < 0.2 mm	a: tephra/ash
Grgr: grágræn	s: 0.2 til 2.0 mm	b: berg (rock fragm) ^o
Grá: grey	m: 2 mm til 2 cm	
B: brown	g: > 2 cm	
Ólgr: olive green	<i>Further divisions into s÷ & s+ and m ÷ & m+ indicate grain sizes in the lower and upper part of each class</i>	^o Not relevant here

*Modified from grade scale of Atterberg (1903). Names in Swedish and Icelandic: Fine material <0.2 mm is named mo, lättler, ler (méla, leir, here denoted by f); sand 0.2-2 mm (sandur - s); grus 2-20 mm (möl - m); sten 20-200 mm (grjót - g); block >200 mm. On drawings of tephra sections Thorarinsson (e.g.1967) and Larsen (e.g. 1996) only use three size categories, <0.2 mm, 0.2-2 mm, >2 mm, larger grains are drawn to scale. In fieldwork the last category is omitted and g is used for grains >20 mm, three to five largest grains are measured individually in the field or in samples collected.

Table 3: Tephra classification (Thordarson, 1990).

Grain size mm	Grain size Φ	Tephra terms
> 64	< -6	Blocks and bombs
32-64	-5 to -6	Coarse lapilli
16-32	-4 to -5	Medium lapilli
2-16	-1 to -4	Fine lapilli
1-2	0 to -1	Coarse ash
0.064-1	4 to 0	Medium ash
< 0.064	> 4	Fine ash

The tephra samples come from two volcanoes. the subglacial Katla volcano and the Hekla volcano . The Katla tephra samples are silicic in composition. Sample locations are shown on Figure 1, a total of 12 places. Most of the samples were collected from the Katla layer SILK-LN (SILicic Katla - Lower Needle layer). From other SILK layers only one sample was collected from each eruption, so the main focus with Katla is the SILK-LN layer.

The Hekla samples are silicic to intermediate and only one eruption is under observation or the Hekla 1947 eruption. The Hekla 1947 samples were only collected in total of 3 places (Figure 2) as a complement to the field and laboratory measurement of Thorarinsson (1954).

SILK tephra

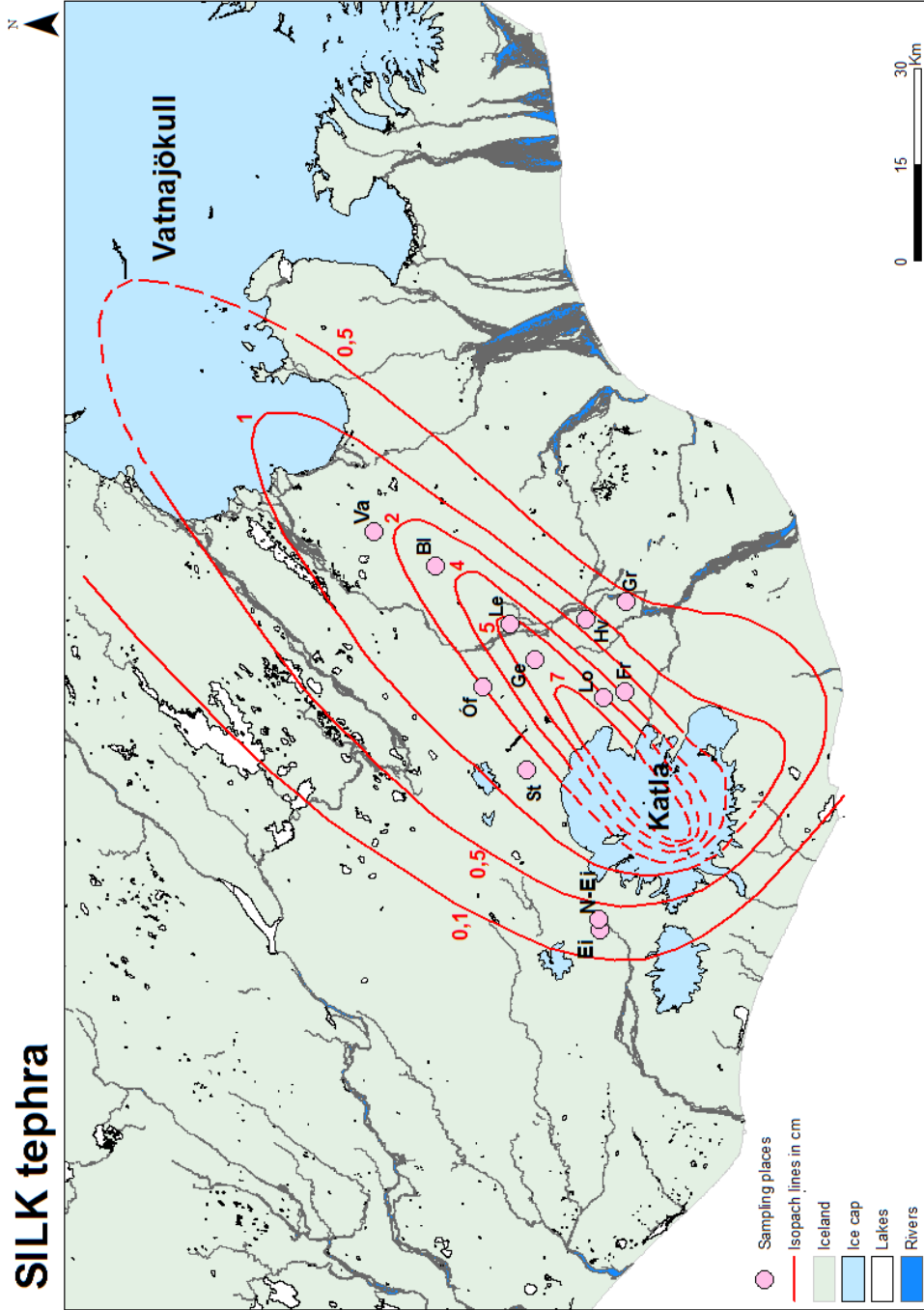


Figure 1: Sampling locations of the SILK layers (pink circles). SILK-LN samples were collected at following locations. (Va) Varmárfell. (Bi) Blágil. (Le) Leiðólfssfell. (Óf) Öfri Ófæra. (Ge) Geldingasker. (St) Strútur the hut. (Lo) Lodnugil. (Hv) Hvammur and (Gr) Gröfara. SILK samples through time were collected at following locations. (Fr) framgil. (Ei) Einhyrningur and (N-Ei) Hill N of Einhyrningur. Map worked by: Edda Sóley Þorsteinsdóttir, References: Landmælingar Íslands, ISV50 Landgagnagrunnur Landmælinga Íslands, projection: ISN_93.

Hekla-1947

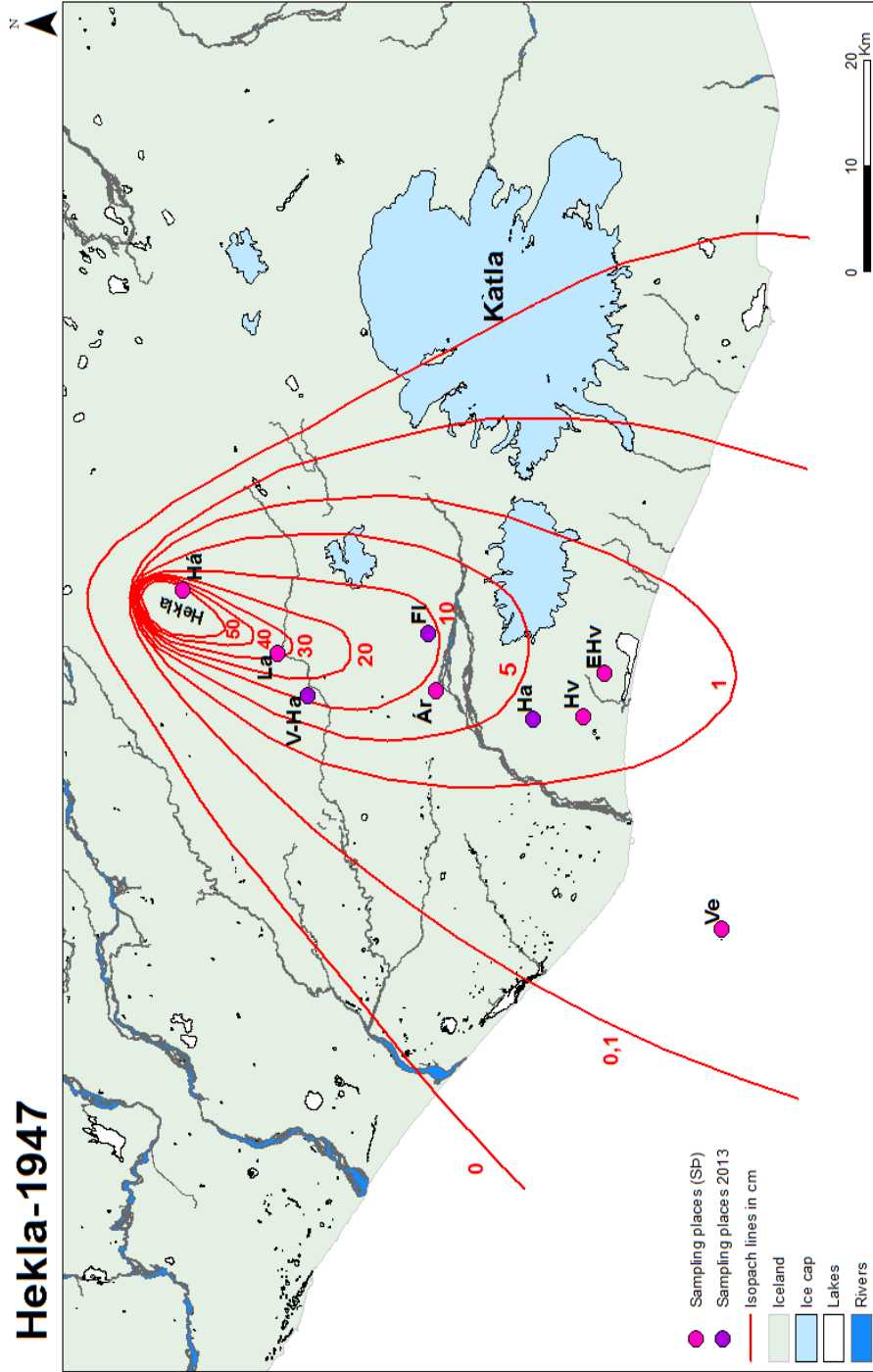


Figure 2: Map showing sampling places of the Hekla-1947 layer (dark pink and purple circles). Hekla-1947 samples collected in 2013 were collected at following locations. (V-Ha) Vestan Hafrafells. (FI) Fliótsdalsheiði and (Ha) Hamragarðsheiði. Hekla-1947 samples collected by Sigurður Þórarinnsson freshly fallen were collected at following locations. (Há) Háahraun. (La) Langvúhlaun. (Ar) Árkvörn. (Hv) Hvammur. (EHv) 4 km east of Hvammur and (Ve) Vestmannaeyjar. Map worked by: Edda Sóley Þorsteinsdóttir, References: Landmælingar Íslands, ISV50 Landgagnagrunnur Landmælinga Íslands, projection: ISN_93.

Laboratory

This chapter is divided into two subchapters. Grain size analysis and grain morphology analysis.

Grain size analysis

When analysing tephra grain size few methods can be used, the method chosen depends on the grain size. The most common ones are sieving and settling velocity measurements, both of them together analyze the coarser and finer grains (e.g. Eiríksson, 1993). In this study we use the hand sieving to avoid breaking the tephra grains, as explained below. It is necessary to use two methods because the finer grains and the coarser grains cannot be analyzed in the same way, the SediGraph cannot analyze the bigger grains and vice versa the sieving is not an option for analyzing the smallest grains. Therefore we have to use two different analyzing methods, hand sieving for the bigger grains (4Φ and bigger) and a machine called SediGraph for the smaller grains (smaller than 4Φ) (Micromeritics, 2010). Before the SediGraph the size of the smallest grains was measured by sampling particles settling through water columns by pipette (Eiríksson, 1993). In this study the smallest grains are analyzed with the SediGraph which can measure from $300\text{ }\mu\text{m}$ down to $0.1\text{ }\mu\text{m}$ in a faster and a more convenient way.

All sieving results from the hand sieving and from the SediGraph were put into the Gradistat. Gradistat gives us various statistical information. In addition to the mean grain size we also get information on sorting, skewness and kurtosis. The Gradistat gives us statistical results or methods of moment (Blott & Pye, 2001).

Grain size analysis can provide important information about an eruption because different eruption conditions can affect the grain size characteristics of the tephra layers, also the way of transport and how far the sediment has travelled (Eiríksson, 1993). The results therefore can help us understand the eruption that produced the tephra in question.

Grain size analysis (hand sieving)

The first part of the grain size analysis consists of hand sieving a sample (in this case tephra). The sieving gives us the weight retained in each sieve with an interval of $0.5\text{ }\Phi$ in between sieves. Grain size analysis is one of the most used methods when sediments are being analyzed (Eiríksson, 1993). The sieve column has a collecting pan at the bottom that catches everything that does not stop on the way down through the sieve column. On top of the pan we have varying number of sieves with an interval of $0.5\text{ }\Phi$ in between. The size of the finest sieve on top of the pan is $4\text{ }\Phi$ (mesh size is 0.063 mm), coarser sieves then come on top of each other. The coarsest sieve depends on the grain size of the sample (Jón Eiríksson, 1993). The number of sieves used is therefore not always the same, for example in this study the coarsest sieve used was $-4.5\text{ }\Phi$ (mesh size is 22.63 mm).

The tephra samples were allowed to dry in open bags and aluminium trays. When the samples are all completely dried the analysis can begin.

The sample is then divided, usually into two halves, sometimes it is divided again depending on the amount of sample collected. Sometimes the sample is too small to divide and the

whole sample is sieved. To divide the sample a „splitter“ (a metal box with ridge in the middle and two openings at the bottom) is usually used. Another simple way to divide a sample is to pour the sample onto a sheet of paper then use stiff cardboard to split up the sample, two halves or more. After dividing the sample the half used for the sieving is randomly chosen and put on the scale to obtain the total weight (g). Sample is then hand sieved (hand power to shake the sieve column) through the sieve column. Hand sieving is used instead of mechanical shaking because the tephra grains are very sensitive, they can break apart and therefore the shape and size distribution can change when using the electrical shaker. The sieves used in this study were from -4.5 Φ down to 4 Φ or total of 18 sieves. When all the grains have settled to their place in the sieve column the amount of sediment in each sieve and in the collecting pan is weighted and put into a carefully labeled bag. The finest grains from the collecting pan on the bottom of the sieve column were analyzed in a SediGraph which will be described in the following section.

The sieves must be cleaned thoroughly between the sample runs to prevent contamination from previous sieving. The tools to clean the sieves are mainly brushes and cloths and when using a brush it should be applied from corner to corner of the mesh to prevent damaging the sieves.

Once the grain size analysis has been completed for both the coarser and the finer grains the results are joined together on a graph where weight percentage is plotted against size in Φ .

Grain size analyze (SediGraph analyse)

To be able to analyze the finest tephra particles (4 Φ and smaller) an equipment is needed since hand/mechanical sieving is not an option. In this study an instrument called SediGraph (Micromeritics, 2010) was used to analyze the finest grain sizes. The SediGraph (Figure 3) uses both settling velocity of particles based on Stokes' Law and the amount of X-ray absorption to measure the grain size (Appendix E in Owners manual). The amount of X-ray absorption where the beam crosses the SediGraph sample analyzing cell is determined as a percentage of the absorption at the highest particle concentration of the sample and related to the maximum particle size above that point at different times (after Appendix E in Owners manual, see detailed explanations E-1 to E-13).

The results from the SediGraph are numerous sets of numbers, but what we focus on in this study are the Cumulative Mass Coarser Percent for each phi category. The SediGraph measures the finer particles in a sample or from maximum of 300 μm (0.300 mm) down to 0.1 μm (0.0001 mm) but the hand sieving method is only applied down to 63 μm (0.063 mm). In this study the “starting” diameter was set to 100 μm (for overlap) and the “ending” diameter was set to 1 μm . The results were from 3.5 Φ down to 10 Φ . but the SediGraph did not always measure down to 10 Φ like he was adjusted to do before each measurement. It was quite common that the measurements ended in 8 – 8.5 Φ and in few occasions the measurements only went down to 7 – 7.5 Φ . In this study the samples consisted of a mixture of 4 phi and the material in the collecting pan. The amount of sample used in the SediGraph must be between 0.001 and 4 grams according to the SediGraph manual. Best results are obtained if the sample size is not much smaller than 3 grams but this is not always possible. In this study the Hekla tephra samples were usually significantly smaller or on average 1.69 grams (4 Φ + sample in the collecting pan). The SILK tephra samples

from Katla were almost always larger than 3 grams. If the sample was too small like with almost all of the Hekla samples, the computer came up with a notice that the sample analyse was low but would continue the measurements. This also happened to a few small Katla samples when they were being analyzed. According to the SediGraph manual it is supposed to be able to measure a sample size of 0.001 g – 4 g, but nevertheless it issues warnings when the sample size is ca 0.3 g – 1.2 g. Two Hekla samples that were at least 3 g did not get this warning. Four Katla samples got this warning, and they were all smaller than 1 g.

When using the SediGraph, certain information is needed in the beginning to adjust the SediGraph correctly. These parameters are listed as following: specific weight, mixture's proportions, starting diameter and ending diameter. The Reynolds number on the other hand is automatically adjusted to these parameters. One of the fundamental adjustment is the specific weight. The specific weight of the sample is needed since it gives you information on how the proportions of the mixture into which the sample is blended should be. In this case the mixture is glycerole (40%) and deionized water (60%). Another important matter when setting up an analyse in the SediGraph is the Reynolds number and once you got your sample specific weight you adjust the mixture of glycerole and deionized water and try to get the Reynolds number to be between 0.1 and 3, the closer it is to 0.1 the better. What changes the Reynolds number is the specific weight, starting diameter, ending diameter and the mixture's proportions. The temperature of the liquid must also be known.

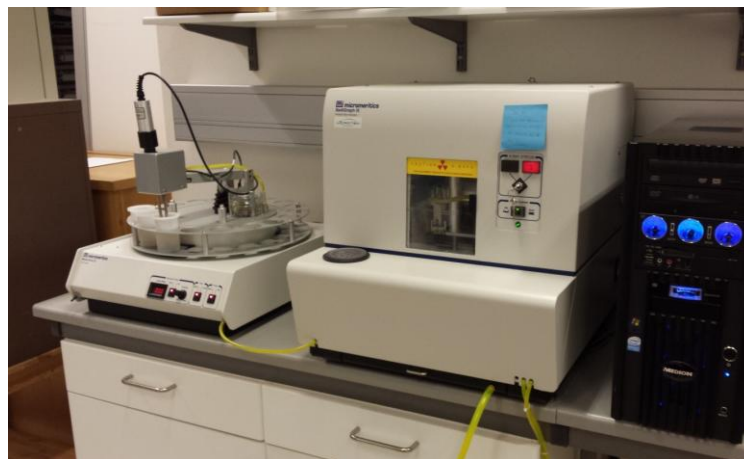


Figure 3: The SediGraph III 5120 that was used in this study. to the left is the mastertech or a carousel. in the middle is the analysing equipment and to the right the computer that contains the program to control the equipment (Photo Thorsteinsdóttir. 2013).

Specific weight measurements

Specific weight is an important number when starting to use the SediGraph. The material's specific weight therefore has to be determined before using the SediGraph. For example in this study the source of the tephra samples that are being analyzed have their origin from two volcanoes. The Katla tephra has rather low specific weight or 2.38, here we have silicic tephra. The Hekla tephra has a higher specific weight or 2.75, here we have intermediate tephra which is in between the mafic and the silicic one. In this study, samples from most of the silicic Katla tephra produced through time is being analyzed, but the

specific weight measurements only had to be carried out once since the geochemical composition of the silicic Katla tephra has remained similar (Larsen et al., 2001).

To do a specific weight measurements you need a pycnometer bottle (or specific gravity bottle (100 cm³), deionized water, a scale and a thermometer. A demonstration of a pycnometer bottle can be seen in Figure 4. The specific weight measurements/calculations are performed in four steps. Formulas used to calculate the specific weight are shown below along with a calculation demonstration (Carver, 1971) (Table 4). Results are shown in (Table 5 & 6).



Figure 4: An example of a pycnometer bottle (From the webpage of the Technical University of Athens).

The process of specific weight measurements

- A pycnometer bottle is cleaned with deionized water and then weighted (m_0).
- The sample is put into the pycnometer bottle (at least 1 g for better results) and the bottle is put on the scale again (m_1).
- The pycnometer bottle with the sample, is filled up with deionized water and weighted (m_2).
- Finally the bottle is cleaned with deionized water and filled up again with deionized water and weighted. Then we have all the numbers for the specific weight calculations (m_3).

Equations that were used to calculate the specific weight of the tephra from both Hekla and Katla volcano are listed here below along with calculation demonstrations.

Table 4: list of symbols and what they represent in the following specific weight measurement equations.

m_0	The weight of the pycnometer bottle cleaned with deionized water
m_1	The weight of the pycnometer bottle cleaned with deionized water + the sample (tephra)
m_2	The weight of the pycnometer bottle cleaned with deionized water + the sample (tephra) +filled up with deionized water
m_3	The weight of the the pycnometer bottle filled with deionized water
Γ	Specific weight of water at 22 °C =0.99777

1. Volume of the bottle

$$\frac{m_3 - m_0}{\gamma}$$

2. Volume of the water

$$\frac{m_2 - m_1}{\gamma}$$

3. Volume of the tephra

Volume of the tephra: volume of the bottle – volume of the water

4. Specific weight of the tephra

$$\frac{m_1 - m_0}{\text{Volume of the tephra}}$$

Katla experiment 1. demonstration on calculation

$$\text{Volume of the bottle: } \frac{(145.8017 - 46.0610)g}{0.99777} = 99.9636 \text{ cm}^3$$

$$\text{Volume of the water: } \frac{(146.2912 - 46.9242)g}{0.99777} = 99.5891 \text{ cm}^3$$

$$\text{Volume of the tephra: } (99.9636 - 99.5891) \text{ cm}^3 = 0.3745 \text{ cm}^3$$

$$\text{Specific weight of the tephra: } \frac{(46.9242 - 46.0610)g}{0.3745 \text{ cm}^3} = \underline{\underline{2.3049}}$$

Table 5: Results from the specific weight measurements performed on silicic Katla tephra. Measured by using pan+4 Φ from the sample SILK- A8 taken at Einhyrningsflatir.

Katla	Experiment 1	Experiment 2	Experiment 3	Experiment 4	Average specific weight
m₀	46.0610 g	46.0482 g	46.0721 g	46.0455 g	
m₁	46.9242 g	47.0747 g	47.1359 g	47.0635 g	
m₂	146.2912 g	146.4103 g	146.4206 g	146.4052 g	
m₃	145.8017 g	145.8079 g	145.8042 g	145.8050 g	
Specific weight	2.3049	2.4147	2.3724	2.4308	2.3807

Table 6: Results from the specific weight measurements performed on Hekla 1947 tephra. Measured by using pan + 4 Φ from the sample taken at a place vestan Hafrafells.

Hekla	Experiment 1	Experiment 2	Experiment 3	Experiment 4	Average specific weight
m_0	46.2564 g	46.1493 g	46.0831 g	46.0670 g	
m_1	47.0082 g	47.0254 g	47.0107 g	47.0005 g	
m_2	146.2625 g	146.3434 g	146.3675 g	146.3765 g	
m_3	145.7758 g	145.7752 g	145.7882 g	145.7863 g	
Specific weight	2.8295	2.8380	2.6578	2.7129	2.7596

SediGraph work

After turning on the SediGraph and before starting the work, the SediGraph must be heated up, or until 35 °C cell temperature has been reached. To be able to see the temperature status a special status window is opened. Also a good rule is to rinse the instrument before use to be sure that there is no contamination from earlier analysis. Then finally a baseline is performed which is necessary to do before loading tephra samples. To do the baseline a mixture of glycerole (40%) and deionized water (60%) ca 60-80 ml is put straight in to a special liquid compartment on the SediGraph but not in the mastertech (carousel) as is usually done with the samples. Sometimes with samples like Hekla 1947 tephra we have to put the samples straight into the liquid compartment on the SediGraph and measure it ca 3 times and get an average result of these three measurements. Then the SediGraph gets the whole sample (not just part of it like in the carousel) for analysis which would not occur if it first went to the carousel and from the carousel to the SediGraph for analysis. When forming the baseline sometimes the X-ray counts are just stuck in 0 and we get error message, the counts should always be higher than 0, If this happens the X-rays must be turned off and after checking if the window on front is securely closed, we have to form a new baseline. Also if the liquid compartment has some liquid inside before creating the baseline and after the rinse, it is possible to do a drain and load process to empty the liquid compartment. Once the baseline is completed a sample is prepared and as mentioned before it is best to mix at least 3 g with the glycerole/deionized water mixture to avoid getting the error report that the sample analyse is low. When the sample has been prepared, information on the sample can be loaded in the computer, the specific weight number, starting and ending diameter etc. Then finally the sample is put into the mastertech/carousel (Figure 5) and sample analysis is started by opening the mastertech schedule. If the mastertech (the carousel) is not used, as with most of the Hekla samples every command has to be done manually. For example rinsing in between samples which is a necessary action, for manual analyse you have to make sure to rinse in between samples yourself but in automatic analysis you just set up the SediGraph to rinse ca 3 times in between. Once the SediGraph has finished measuring one sample it gives you results which you save as an excel file to be able to work with the results.

When working with silicic tephra, like in this case with the silicic Katla tephra some adjusting is needed due to low specific weight of the sample. Stirrier time needs to be lowered to 45 sek instead of 60 sek, stirrier speed is set to low instead of high and finally mixing chamber speed is lowered to 4.

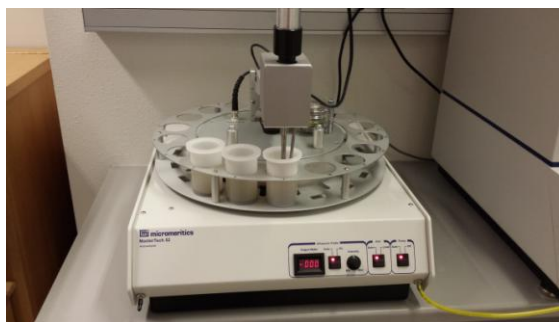


Figure 5: Mastertech (carousel) (Photo Thorsteinsdóttir, 2013).

Combining grain size results from two different analyzing methods

After having both sieved the tephra and measured in the SediGraph the results from both methods were joined to show the combined grain size distribution of each tephra layer. How this was done will be described briefly here below and based on Folk (1980).

To combine the results from both the sieving and the SediGraph we need to convert the SediGraph results to grams and weight percent (wt %). The mass frequency % results from each size fraction from the SediGraph is multiplied with total sample weight (7.6 gr see table 7 below) from the 4 Φ and the pan then divide by 100 and finally divided with the total sample weight (11.96 gr see table 7) including all size fractions and multiplied by 100. The results from the SediGraph and the hand sieving is combined in the 3.5 Φ fraction because this size fraction was measured both in the SediGraph and the hand sieving. This is done by adding up the wt% from the sieving and the SediGrp (0.02 gr (SediGraph) + 1.41 gr (hand sieving))(Table 8). The the amount of remaining material which contains finer particles than what the SediGraph measured was distributed equally on the phi categories of 8.5 down to 14 Φ . Example on calculations shown in (Table 7).

The results show that most of the finer material falls into the phi categories 3.5-5 Φ . Which lies exactly at the size range where the two methods overlap. The method we therefore use to combine these two analyzing methods is by using the results from the SediGraph upto 3.5 Φ and results from the sieving method down to 3.5 Φ . The results from each 3.5 phi analyzing methods are combined and used for the 3.5 size category in the final graph (Table 8).

Table 7: An example of calculations performed on SILK-N4 SediGraph results to show conversion from mass frequency (%) to weight (g).

Phi (Φ)	Mass frequency (%)	Converted (Wt g)	Wt %
3.5	0.3	$:(0.3/100)*7.6$ =0.02	$:(0.02/11.96*100)$ =0.19
4	9.3	0.71	5.91
4.5	22.2	1.69	14.11
5	24.7	1.88	15.70
5.5	18.8	1.43	11.95
6	10	0.76	6.35
6.5	4.4	0.33	2.80
7	2.4	0.18	1.53
7.5	1	0.08	0.64
8	5.7	0.43	3.62
	98.8	Measured=7.51 (Total=7.60)	62.78
		7.6-7.51=0.09	

Table 8: An example on the joining of two methods from the tephra layer SILK-N4.

Phi (Φ)	Weight g
-1.5 to 2.5	...
3	0.83
3.5	1.41g (sieving) 0.02g (SediGraph/converted) = 1.43g
4	0.71
4.5	1.69
5-14	...

Grain morphology analysis

When eruptions take place, most of them produce some tephra. Chemical composition, viscosity of the magma and the type of eruption influence the shape of the tephra grains that are produced (Eiríksson, 1993). Measurements by Eiríksson & Wigum (1989) showed that in silicic tephra the grains usually had more cylindrical shape compared to the basaltic grains. Grains that have formed in explosive eruptions in sea, water or within glacier (grains that belong to the same tephra layer) showed the least diversity regarding the shape of the tephra grains (Eiríksson & Wigum, 1989; Eiríksson, 1993).

When defining the shape of tephra grains, several different parameters can be used. Among them are form, elongation, circularity, sphericity, roundness, ruggedness and surface

texture which all are defined in their own way. The form concept (Zingg, 1935) describes the ratio between length (L), width (I) and thickness (S) of sediment particles. Elongation is the ratio I/L . Circularity relates to the difference between area and perimeter. The roundness concept describes the outlines of sediment grains, how well-rounded they are and has been categorized from being very angular to well rounded (Figure 6 after Powers 1953). The more angular sediment grains the smaller the roundness coefficient gets. Ruggedness relates to how rough the grain surface is. The surface texture concept describes the texture of sediment grains (Eiríksson, 1993).

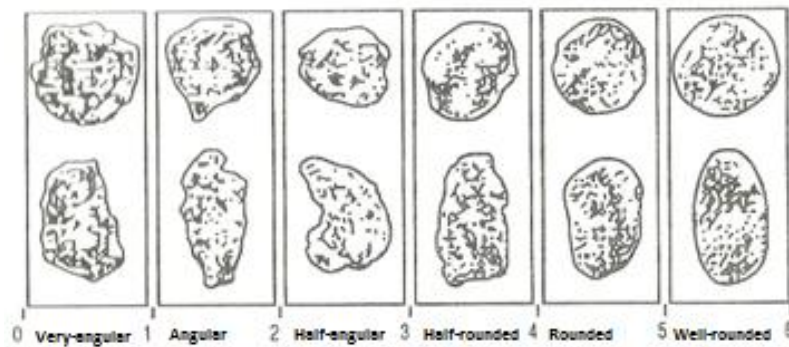


Figure 6: Powers scale that shows few stages of grain roundness (Eiríksson, 1993, after Powers 1953).

Grain morphology analysis was carried out on selected samples from both Hekla 1947 and silicic Katla tephra. Table 9 shows what samples were analysed, what analysing method was used and where the samples were collected.

Table 9: Samples and methods used for grain shape analyse.

Sample location	Sample	method	Sample	Method
Vestan Hafrafells	H-1947	Morphocop		
Hamragarðaheiði	H-1947	Morphocop		
Einhyrningsflatir			SILK A12, -A11, -A8 and -N1	Morphocop
Varmárfell			SILK-LN lower two section out of three	Morphocop
Geldingasker for comparison to the varmárfell sample			SILK-LN lower section out of two	Morphocop

Two different methods were used for the grain morphology analysis, the Particle Shape Analyzer equipment and the image analyzing program Morphocop. The reason for not using both of these two methods is because the Particle Shape Analyzer could not measure the light colored tephra grains from Katla volcano, no matter how the equipment was adjusted. The darker grains were much better documented since the the Particle Shape Analyzer takes shadow pictures and as a result only part of the sample is being analyzed. Therefore it was decided to do the grain morphology analysis on the silicic Katla tephra with Morphocop.

Particle Shape Analyzer

Grain morphology analyses were carried out with two different methods. The method described here uses an instrument called Particle Shape Analyzer. Basically it takes pictures of the grains and sends them to a computer connected to the analyzer. Single grains are analyzed based on the size and shape of the grains shadow or silhouette. When the equipment is in run mode the camera takes 30 images per second that are analyzed as they enter the computer. The software then accumulates statistics while pictures are being analyzed. Numerous parameters can be measured, such as equivalent circular area diameter (ECAD), equivalent circular perimeter diameter (ECPD, diameter of a circle with the same perimeter as the grain) and bounding circle diameter (BCD). Then circularity, form factor and compactness can be calculated (ParticleInsight 1.0 User Manual).

This equipment was not useful to analyze the translucent silicic Katla tephra, but worked for the darker intermediate Hekla 1947 tephra. Comparison of tephra from the two eruption was not possible. Decision was therefore made to do grain morphology analyses only in the image analyzing program Morphocop.

Ultrasonic cleaning

In two samples which were shape analysed, or from vestan Hafrafell and Hamragarðaheiði, fine organic material was cleaned out of the tephra by putting the samples in ultrasonic bath (Figure 7). The cleaning process was as following. Half of each sample that was being analyzed (both 3 and 3.5 Φ) was put into separate beaker glasses. These four beaker glasses were then labeled and filled up with water (not deionized). Into each beaker glass a small amount of dishwasher liquid was added. The beaker glasses were then arranged in the ultrasonic bath (Figure 7), a tub half-filled with water where the beaker glasses stand in. When the ultrasound bath has been turned on a vibration or ultrasound, which ranges usually from 20-400 kHz, oscillates the grains. The temperature of the water ranges between 20-32 °C. Each phase of the cleaning process in the ultrasonic bath took around 15 minutes. In between each phase the organic matter that was floating on top of the water in each beaker glass was cleaned of with a spoon. Then almost all of the turbid water was poured carefully (not to lose any sample) out of the beaker glass and new clean water poured into the glasses. This was repeated four times until the sample was clean enough. Once the Hekla 1947 tephra samples had been cleaned, no organic threads were measured in the particle shape analyser.



Figure 7: Ultrasonic bath (Photo Thorsteinsdóttir. 2014).

Grain morphology analyze in Morphocop

Grain morphology analyses were performed by using microscope, the image editing program photoshop and image analyzing program called Morphocop. Morphocop was adapted for measuring of tephra grains by Jón Eiríksson. This program measures roughness coefficient, circularity, elongation and facet among others (Eiríksson et al., 1994).

Originally the plan was to use both Particle Shape Analyzer and the Morphocop to analyze the shape of the grains and compare the results of two different methods. Because the Particle Shape Analyzer did not work on the silicic tephra Morphocop was used to analyze the shape of the silicic Katla tephra along with the Hekla 1947 tephra.

When grain morphology analysis is performed it has been customary to use a mixture of two grain size groups, 3 and 3.5 Φ . A small portion of 3 and 3.5 Φ from each sample that was going to be analyzed was mixed together. To analyze a sample in the microscope, only a very small amount of sample is needed. It is put onto a white cardboard paper, divided into four portions and part of $\frac{1}{4}$ is used for the microscope analysis, 50 grains from each sample were then chosen randomly and arranged on slide with the help of a microscope. When arranging the grains on the slide it is necessary to make sure that the grains do not lie too close together so that the image analyzing program does not take two or more grains as one grain. Once the grains are arranged on the slide a digital image is taken with a video camera and transported into a computer for further work in both Photoshop and Morphocop. In photoshop the grains are turned completely black with a white background to form a stark contrast between the background and the grains. This is necessary to do so

the Morphocop can process the images. Also the colors have to be black and white because Morphocop does not handle other colors well. The Morphocop program then calculates various parameters that provide information on the shape of the grains. In this study area, perimeter, L, I, R1, R2, circularity, elongation, facet and roundness were documented.

SEM images

SEM (scanning electron microscope) images were taken in TM3000 an electron microscope (Figure 8) on selected Hekla 1947- and silicic Katla tephra samples. These images show the difference between the tephra produced in these two volcanoes and different eruptive environments. The procedure to acquire SEM images is described below. The samples are placed onto a sample holder or a SEM mounts. On top of each SEM mount a Carbon Conductive Tape was plastered (double coated). Sample was then placed onto the mounts which got stuck on the tape. The sample was not evenly distributed to be able to take images of single grains and more clustered grains. After all samples had been prepared this way they were coated with gold. Both the Carbon Conductive tape and the gold coating are necessary for conductivity. Once the samples have been loaded into the SEM analyser and the computer program has been turned on an image appears on the computer screen. The sample is moved around with a joystick. In the computer program certain commands are available. For example zooming in and out, changing the contrast and brightness, slowing down the recording to get more clear image for taking a picture. Magnification in the TM3000 is from 15 to 30000x (TM3000 manual). Information on pictures are for example; what magnification was used and the size of the grains. An example of such an image can be seen in Figure 9.

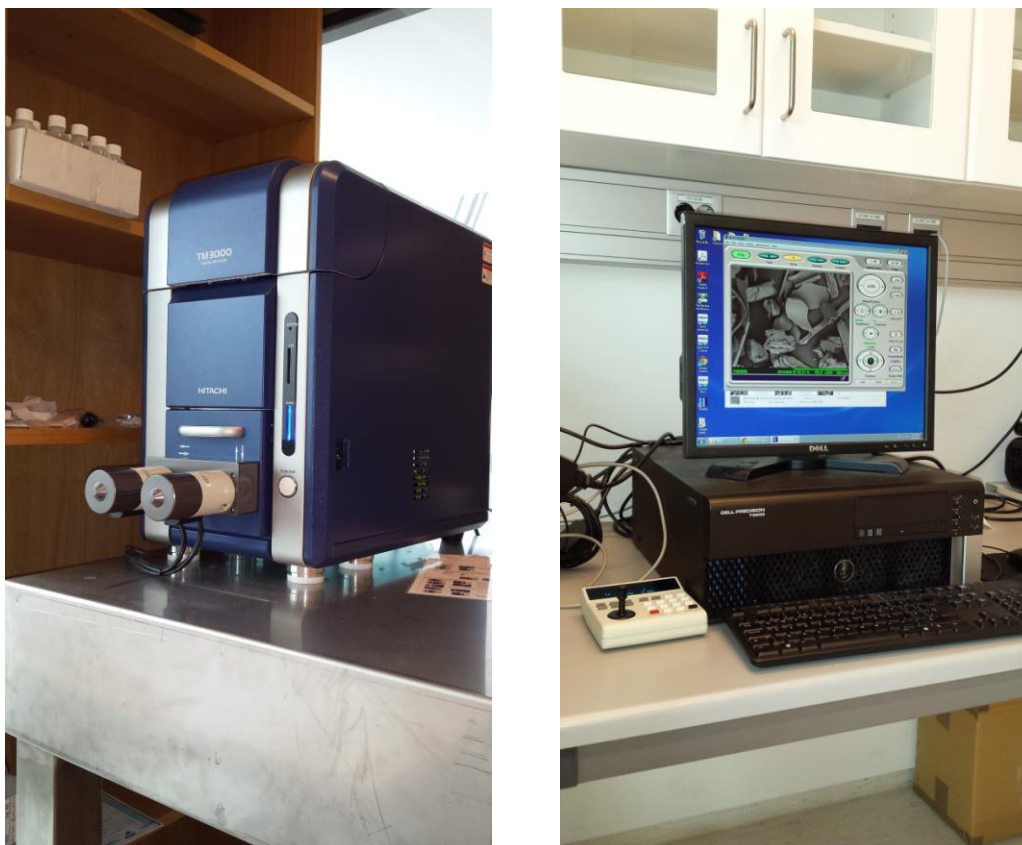


Figure 8: From left TM3000 analyser and TM3000 computer program at work (Photo Thorsteinsdóttir, 2014).

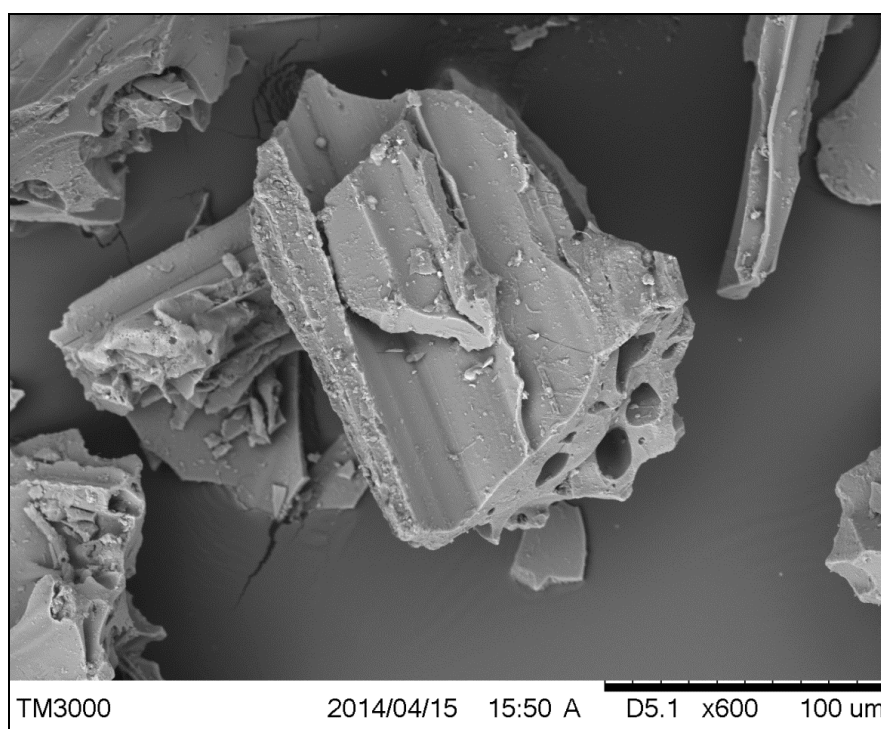


Figure 9: SEM image example from SILK-LN taken from Geldingasker middle unit in magnification of $\times 600$.

Appendix III

Grain size results: Distribution graphs

Tephra layer SILK-LN. ~3400 years old
Grain size characteristics SW to NE along axis of thickness

Loðnugil section. 22 km from source*

Top unit
Upper middle unit
Lower middle unit
Bottom unit
Bulk sample

Geldingasker section. 33 km from source*

(Top unit discarded)
Middle unit
Bottom unit

Leiðólfssfell section. 40 km from source*

Top unit
Middle unit
Bottom unit

Blágil section. 54 km from source*

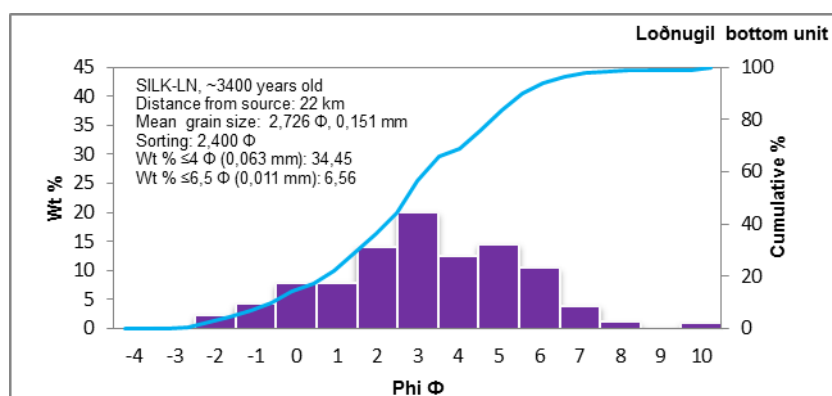
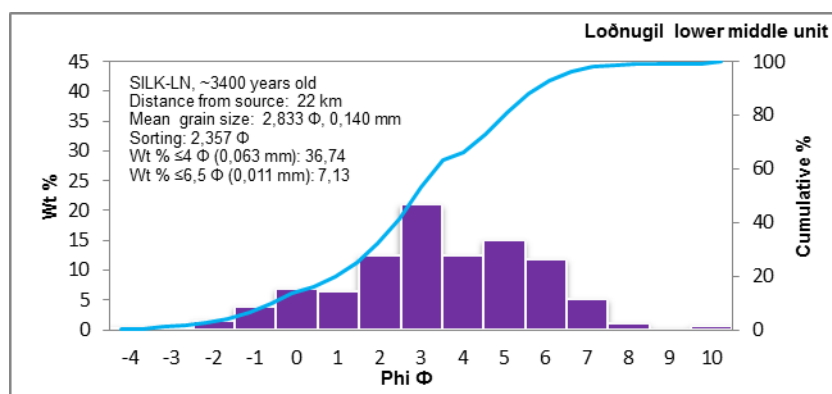
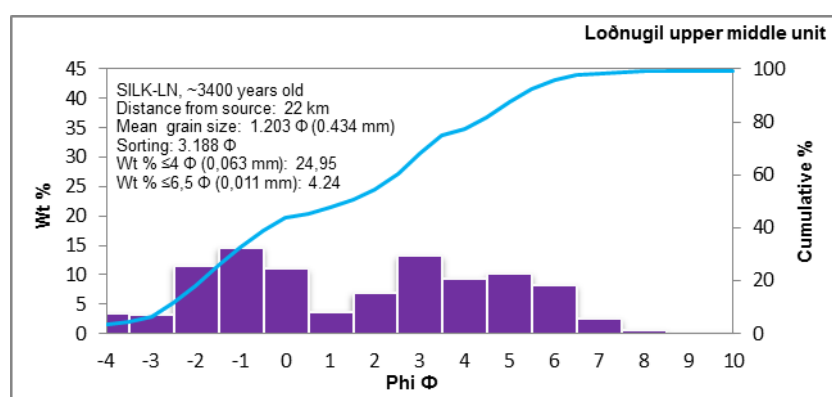
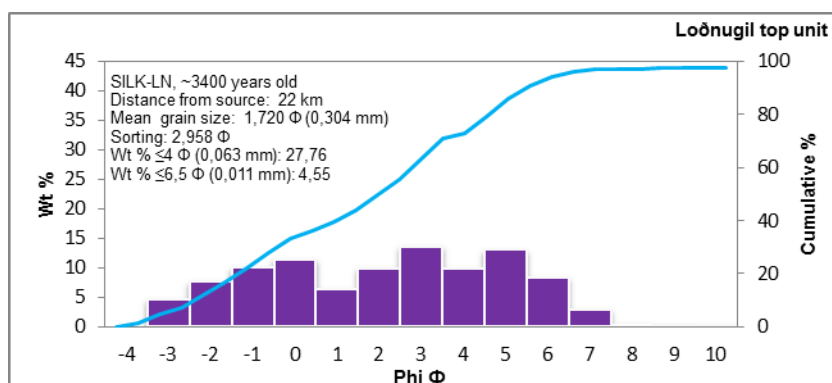
Bulk sample

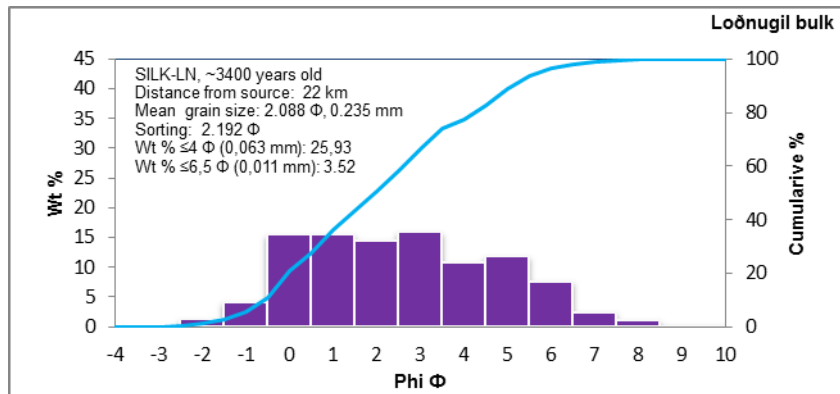
Varmárfell section. 65 km from source*

Top unit
Middle unit
Bottom unit
Bulk sample

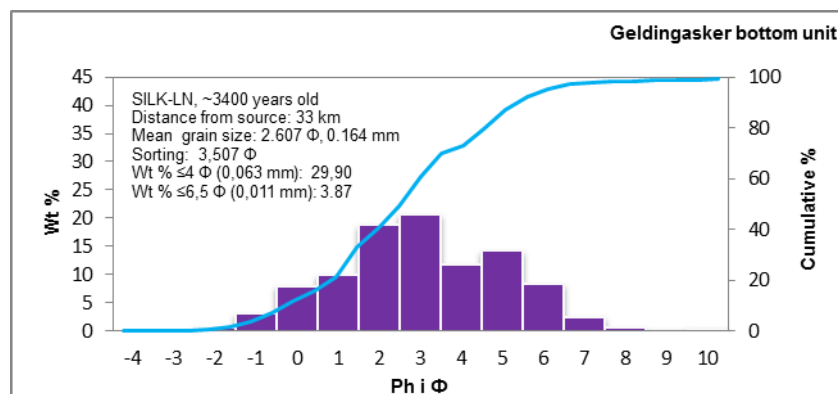
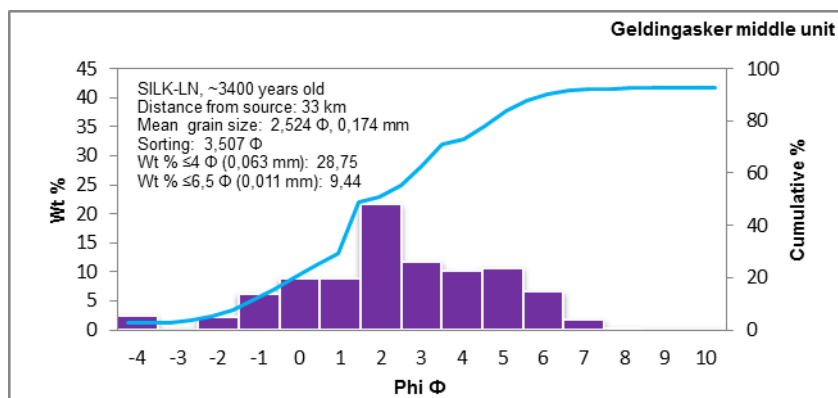
*Vent location within the Katla caldera is not known. distance is measured from central part of caldera

Tephra layer SILK-LN. ~3400 years old
Grain size distribution SW to NE along axis of thickness
GPS coordinates: N63.730432° N18.746435°

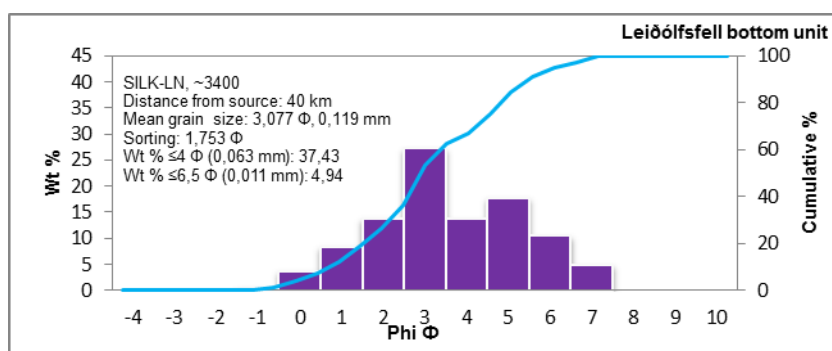
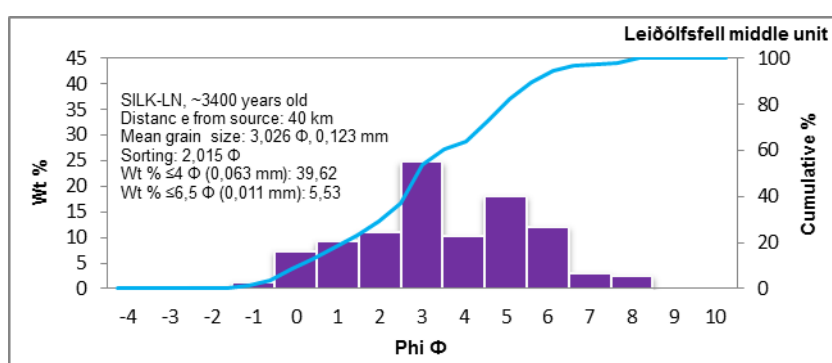
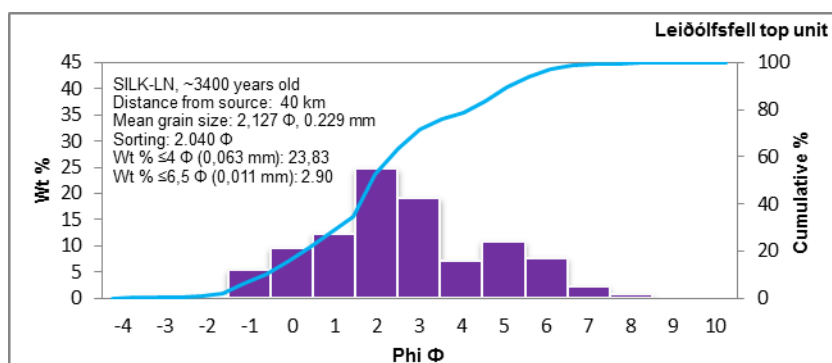




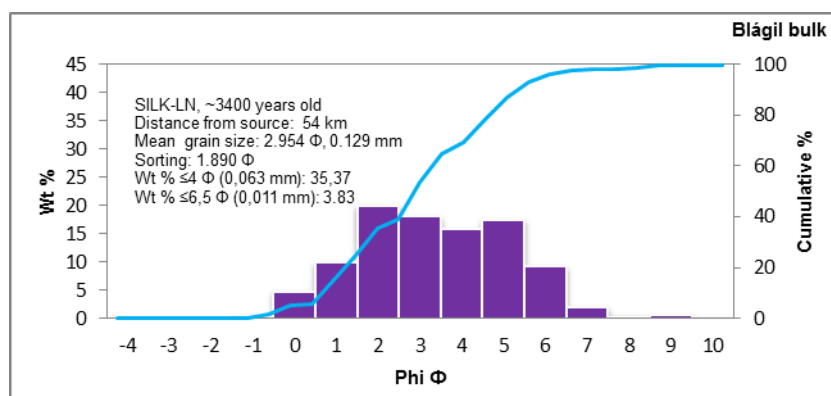
Tephra layer SILK-LN. ~3400 years old
 Grain size distribution SW to NE along axis of thickness
 GPS coordinates: N63.826170°. W18.622029°



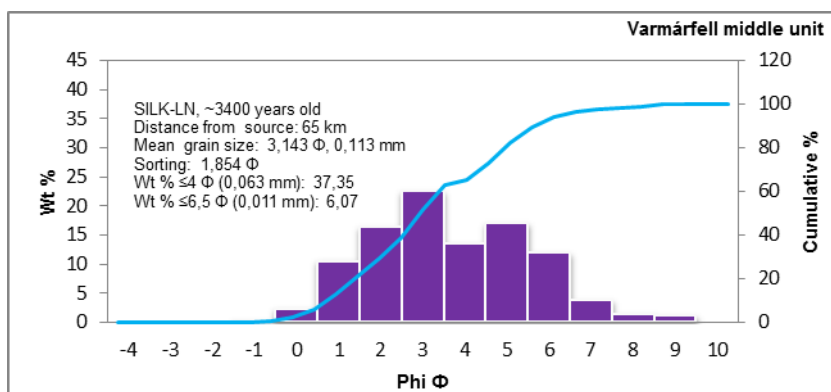
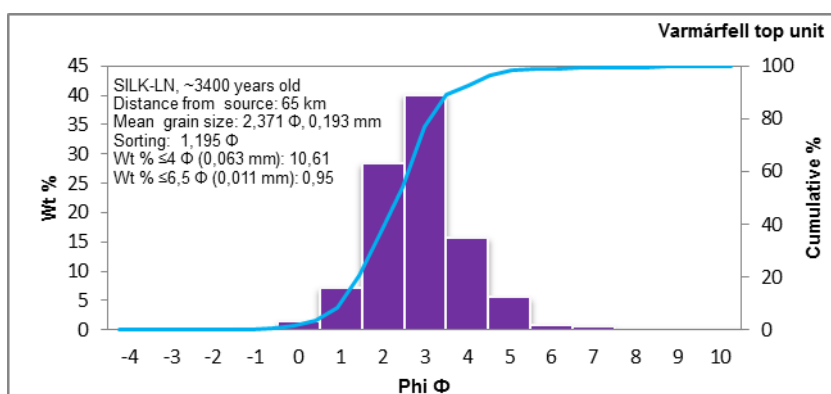
Tephra layer SILK-LN. ~3400 years old
 Grain size distribution SW to NE along axis of thickness
 GPS coordinates: N63.861389° N18.510669°

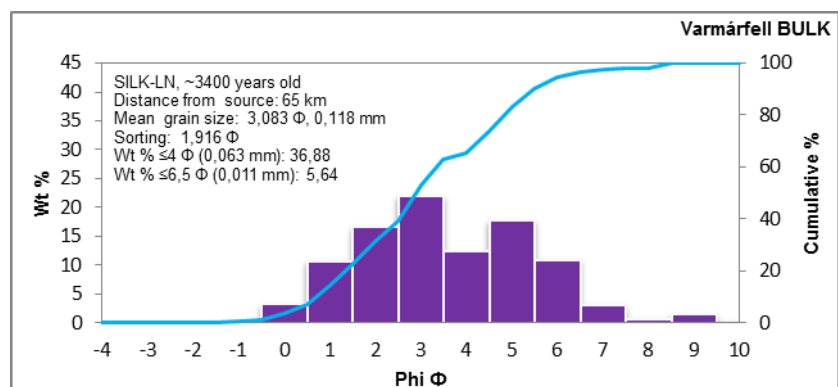
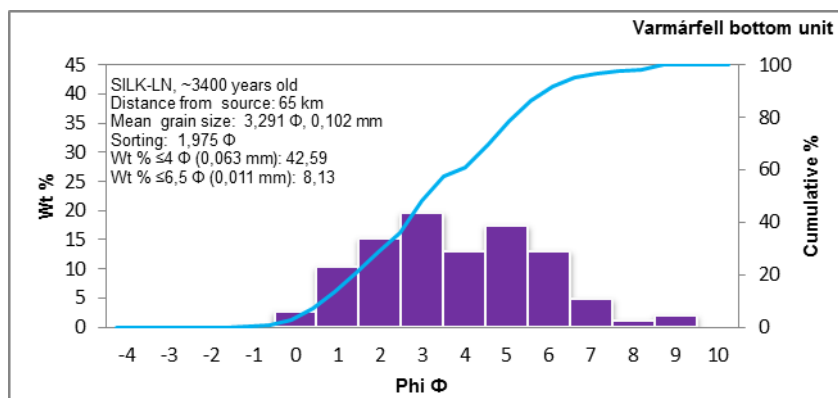


Tephra layer SILK-LN. ~3400 years old
 Grain size distribution SW to NE along axis of thickness
 GPS coordinates: N63.965642°. W18.321034°



Tephra layer SILK-LN. ~3400 years old
 Grain size distribution SW to NE along axis of thickness
 GPS coordinates: N64.052040°. W18.212098°





Tephra layer SILK-LN. ~3400 years old
Grain size characteristics N-S across the tephra layer

1. Distance from central part of the Katla caldera 22-24 km

Strútur section. 24 km from source*
Bulk Sample

Loðnugil section. 22 km from source*
Bulk sample

Framgil section. 22 km from source*
Bulk sample

2. Distance from central part of the Katla caldera 33-36 km

S-Ófæra section. 36 km from source*
Bulk sample

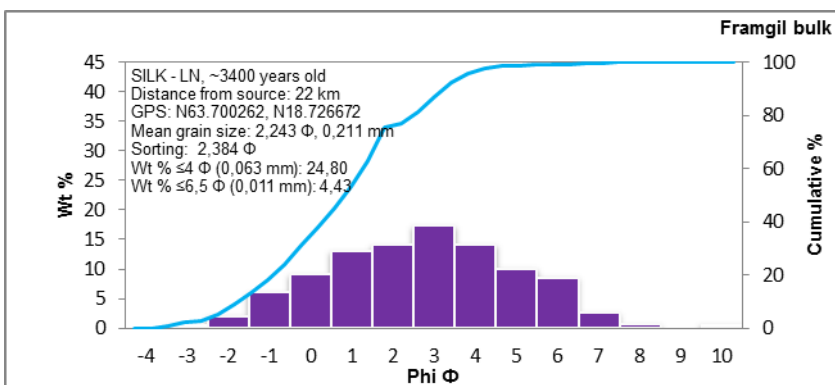
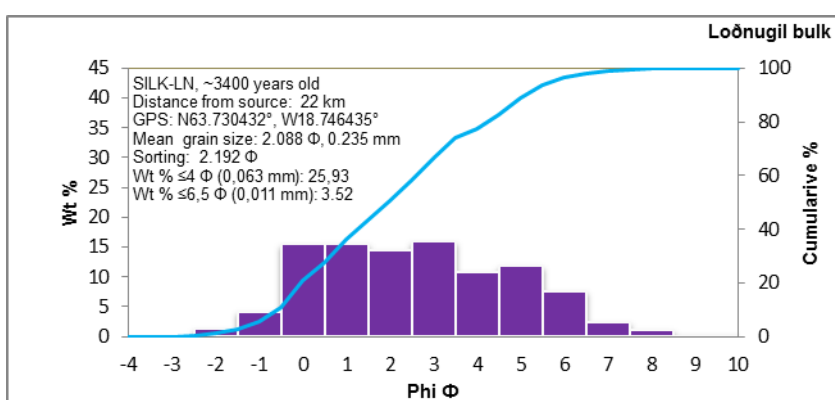
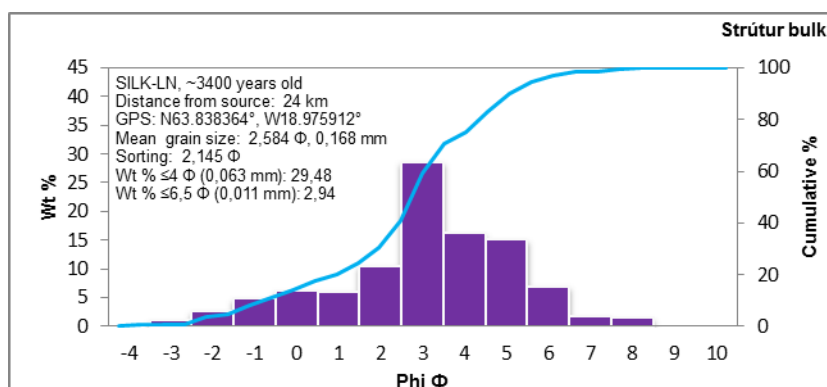
Geldingasker section. 33 km from source*
Middle unit
Bottom unit

Hvammur section. 34 km from source*
Bulk sample

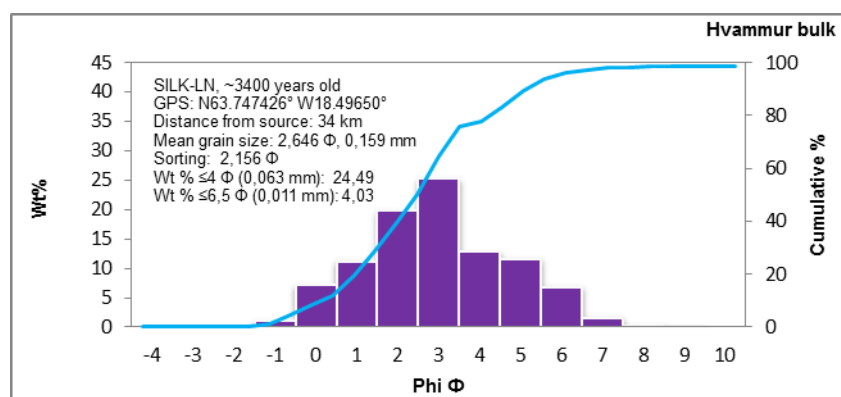
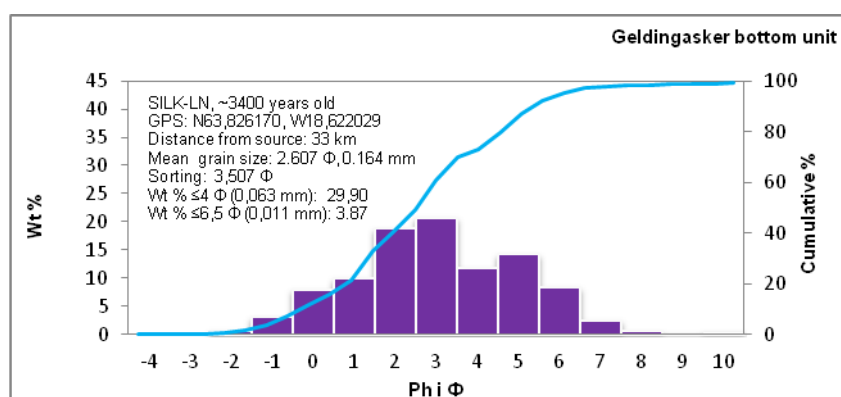
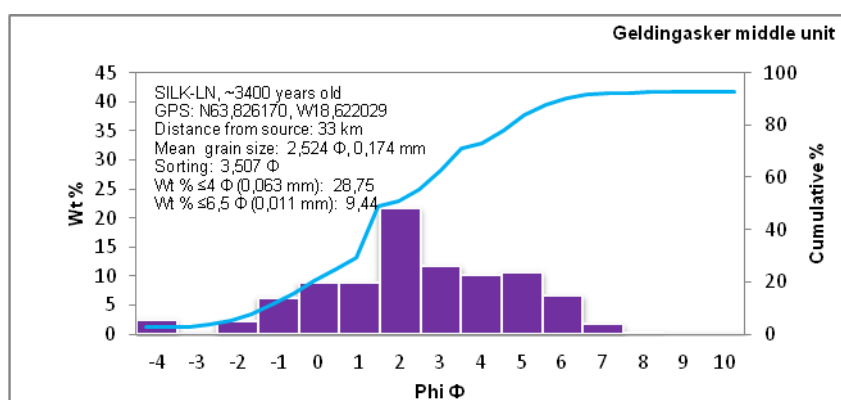
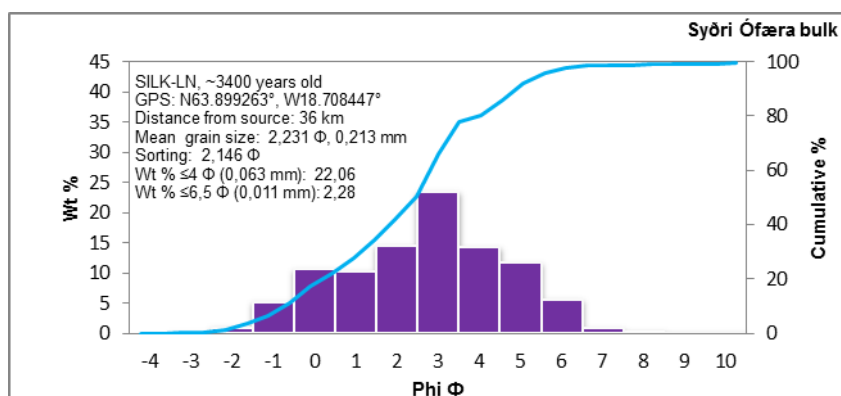
Grófará section. 35 km from source*
Bulk sample

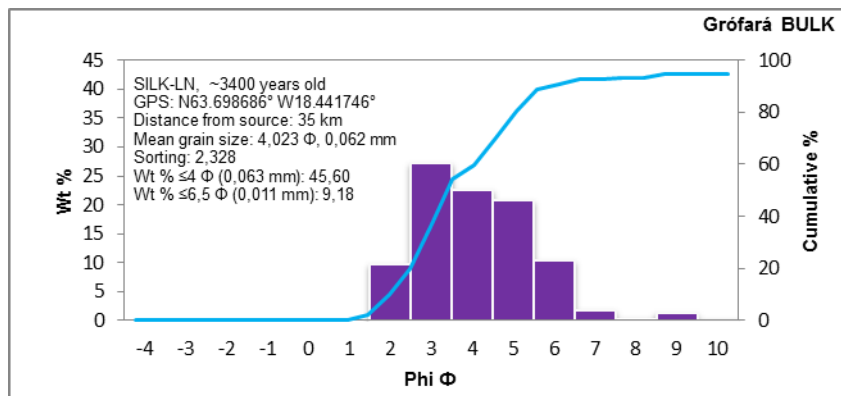
*Vent location within the Katla caldera is not known. distance is measured from central part of caldera

Tephra layer SILK-LN. ~3400 years old
Grain size distribution N-S across the tephra layer
Distance from central part of the Katla caldera 22-24 km



Tephra layer SILK-LN. ~3400 years old
Grain size distribution N-S across the tephra layer
Distance from central part of the Katla caldera 33-36 km





SILK tephra layers. erupted between ~8100 & 2800 years
ago

Grain size characteristics

1. Framgil. 22 km from source*

SILK-UN. ~2800 years

SILK-LN. ~3400 years

SILK-N4. ~3900 years

SILK-N3. ~4100 years

SILK-N2. ~5000 years

2. Einhyrningur. 20 km from source*

SILK-N1. ~5800 years

SILK-A1. ~6000 years

SILK-A5. ~7100 years

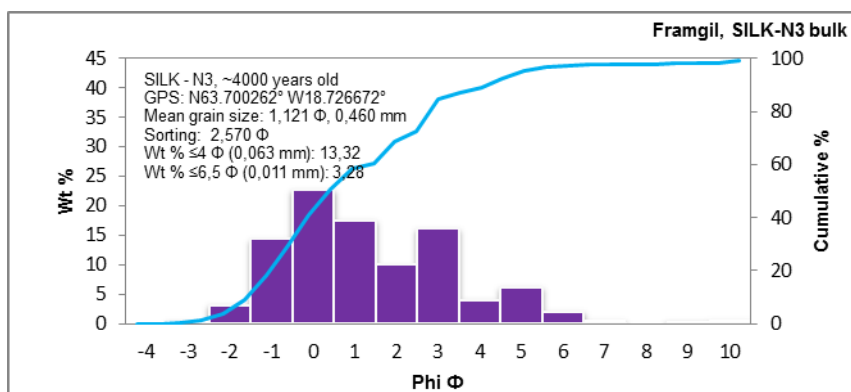
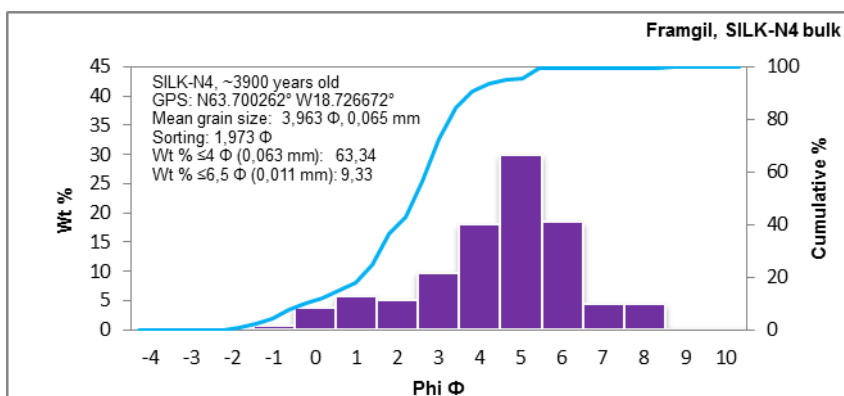
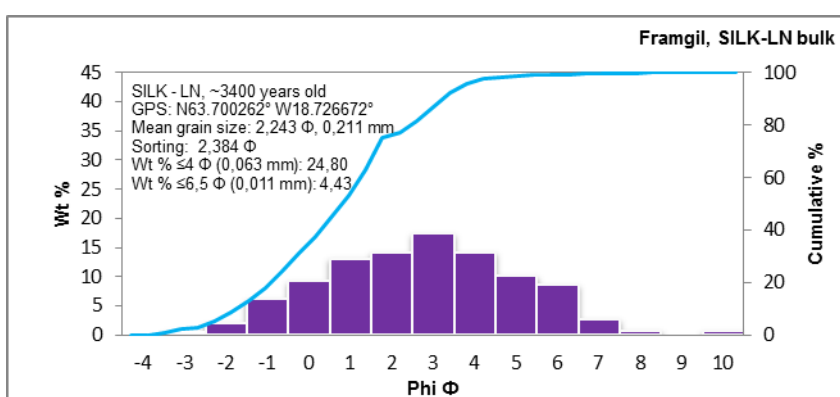
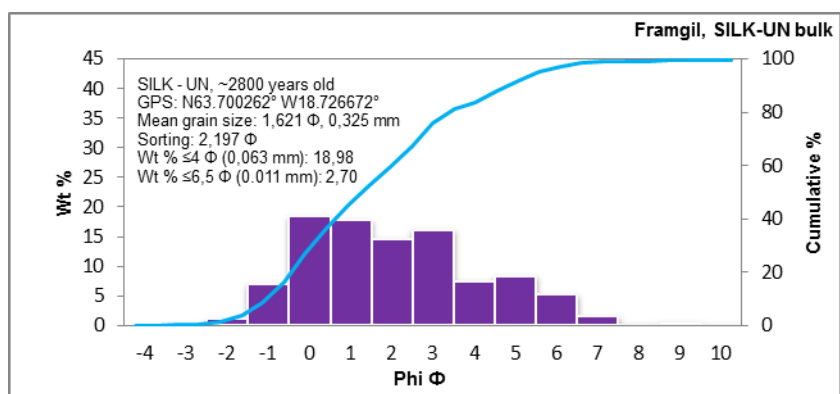
SILK-A7. ~7200 years

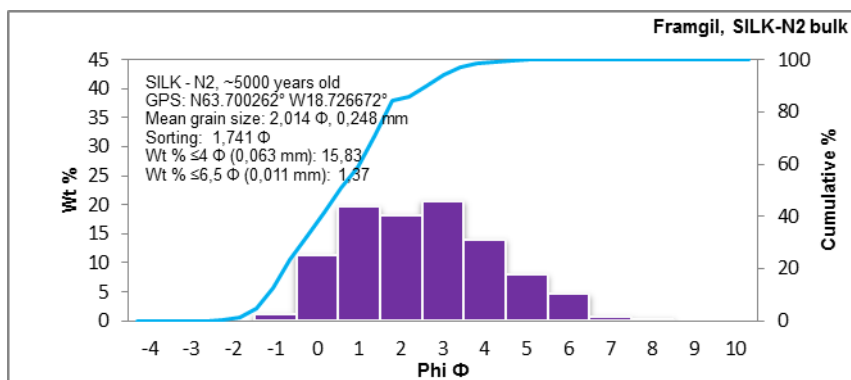
SILK-A8. ~7400 years

SILK-A12. ~8100 years

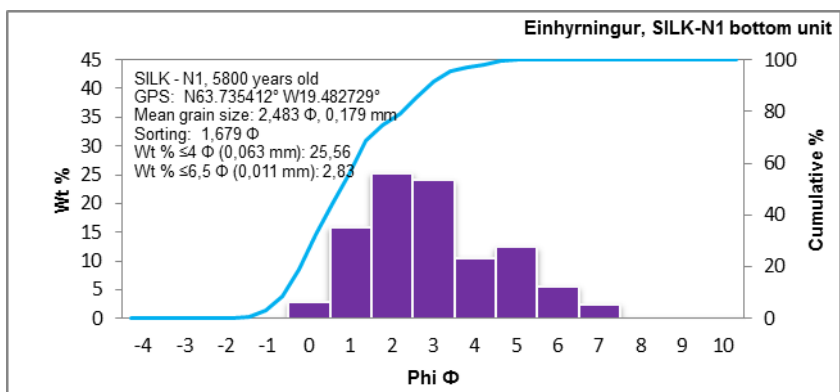
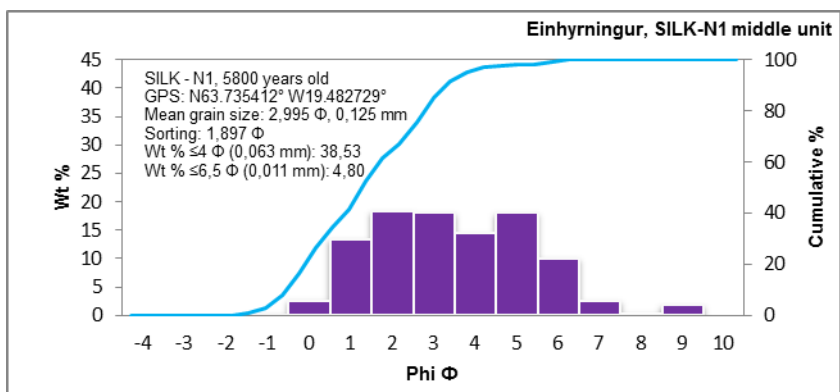
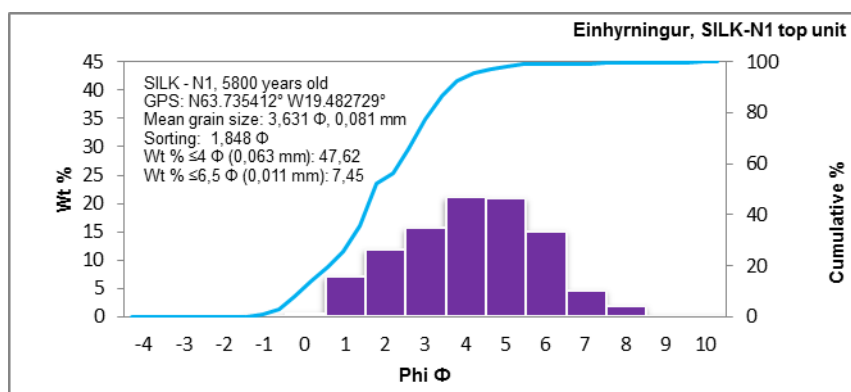
*Vent location within the Katla caldera is not known. distance is measured from central part of caldera

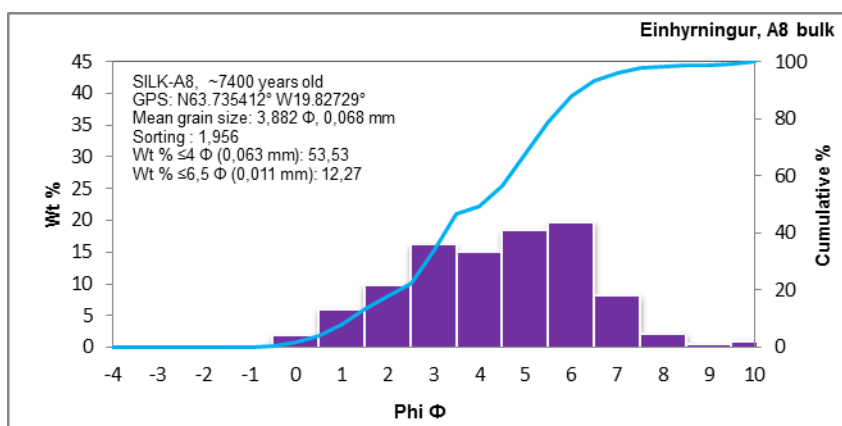
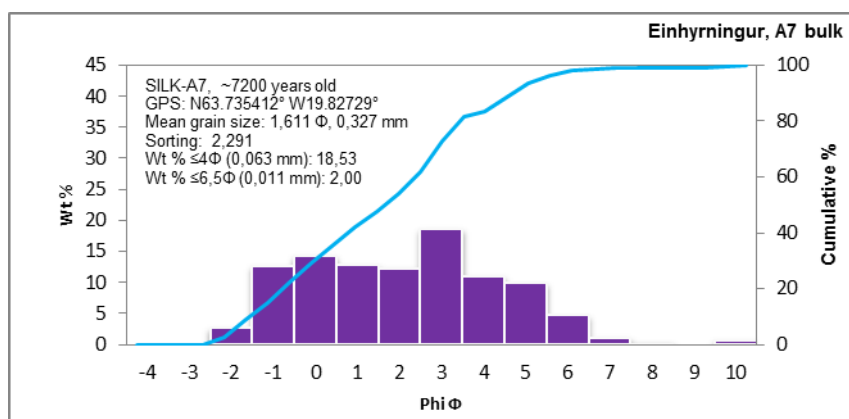
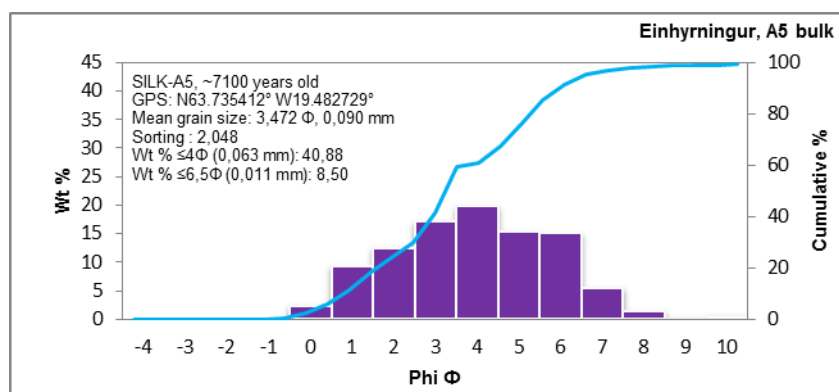
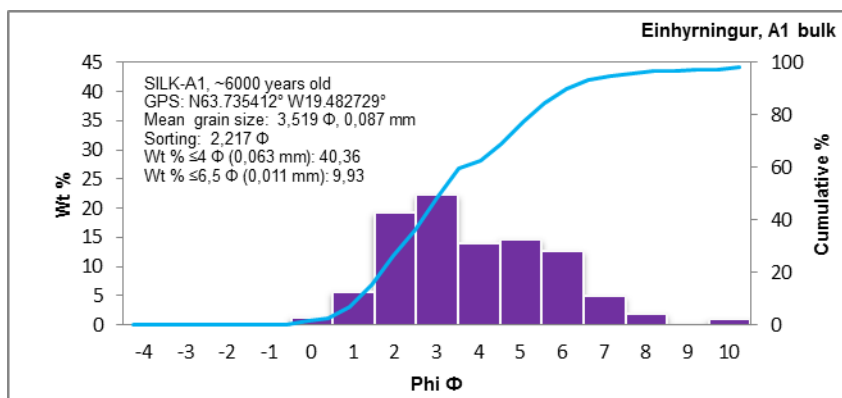
SILK tephra layers. erupted between ~2800 and ~5000 years ago
 Framgil. distance from source 22 km.

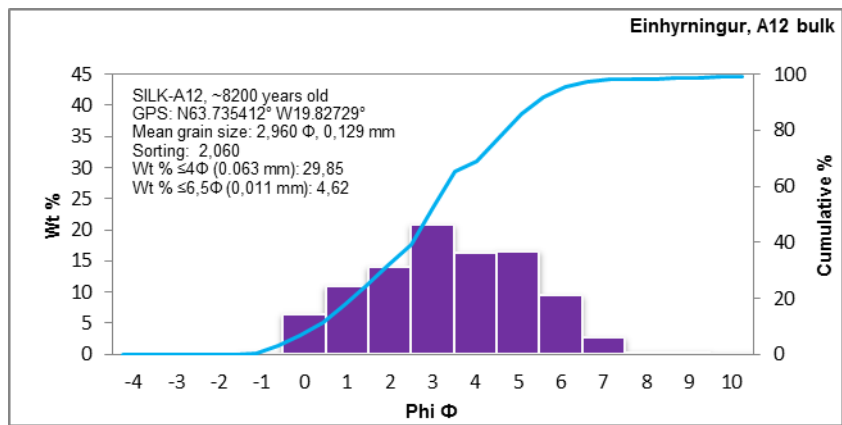




SILK tephra layers. erupted between ~5800 and ~8100 years ago
 Einhyrningur. distance from source 20 km.







Tephra layer Hekla 1947

Grain size characteristics N-S along axis of thickness

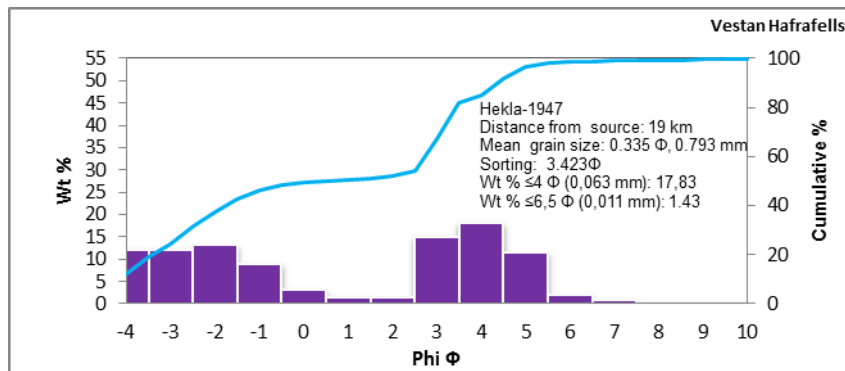
Vestan Hafrafells section. 19 km from source*
Bulk sample

Fljótisdalsheiði section. 29.5 km from source*
Bulk sample

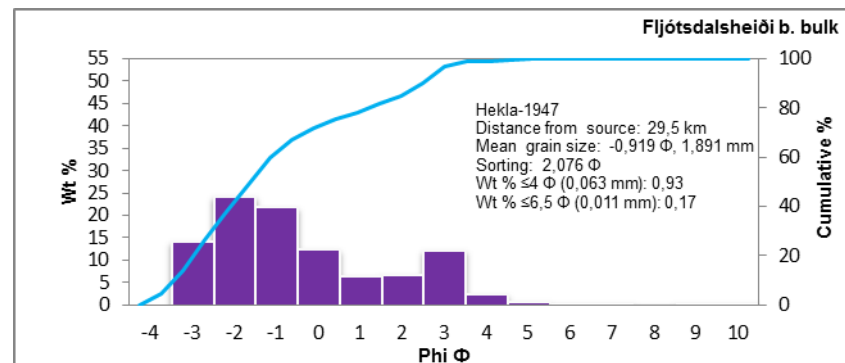
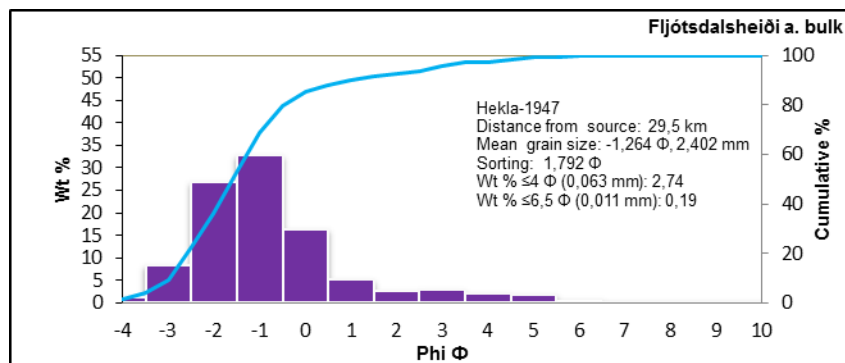
Hamragarðaheiði section. 42 km from source*
Bulk sample

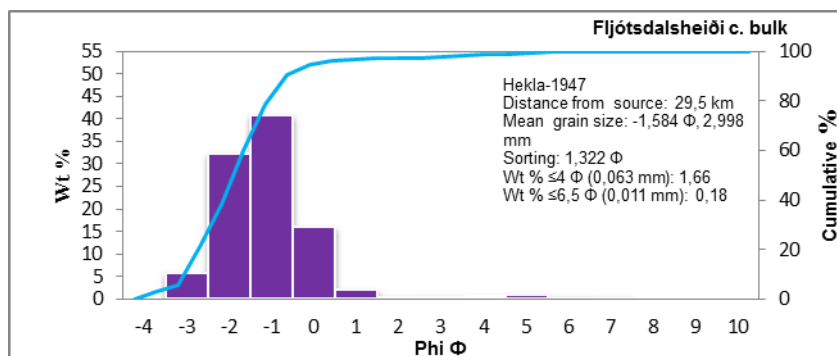
* Vent location is set at the top crater of Hekla volcano.

Tephra layer Hekla 1947
Grain size distribution along axis of thickness
GPS coordinates: N63.72352° W19.72365°

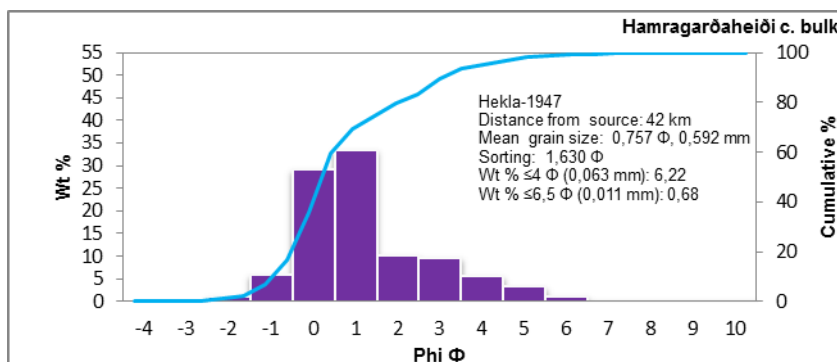
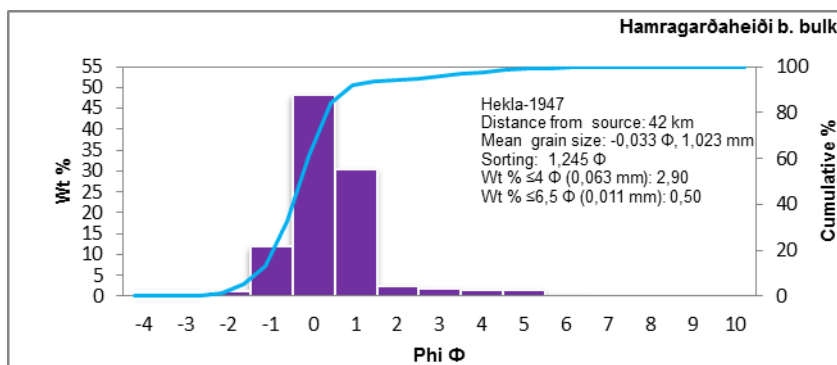
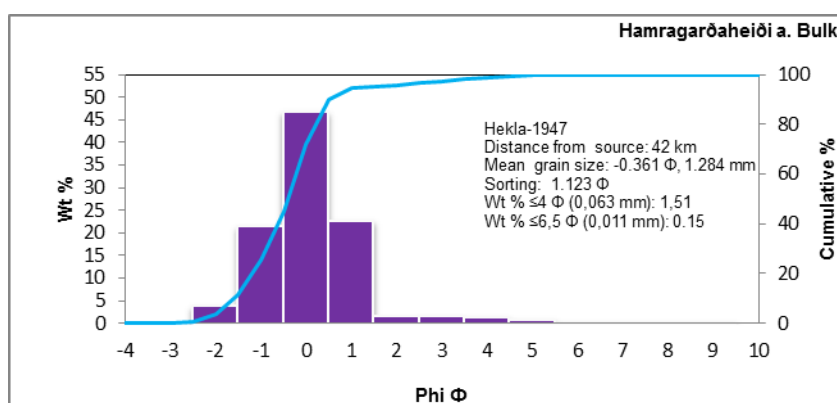


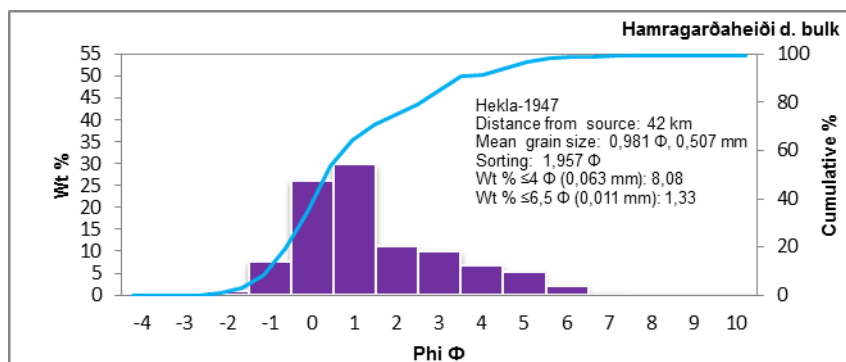
Tephra layer Hekla 1947
Grain size distribution along axis of thickness
GPS coordinates: N63.72352° W19.72365°





Tephra layer Hekla 1947
Grain size distribution along axis of thickness
GPS coordinates: N63.623758° W19.885576°





Appendix IV

Grain size results: raw data

Blágil SILK-LN

Millimeters	Phi	Weight g	Weight %	Cumulative %
16.0	-4	0.00	0.00	0.00
11.3	-3.5	0.00	0.00	0.00
8.0	-3	0.00	0.00	0.00
5.7	-2.5	0.00	0.00	0.00
4.0	-2	0.00	0.00	0.00
2.8	-1.5	0.02	0.10	0.10
2.0	-1	0.05	0.26	0.36
1.4	-0.5	0.20	1.04	1.40
1.0	0	0.74	3.84	5.24
0.710	0.5	0.09	0.47	5.70
0.500	1	1.84	9.54	15.24
0.354	1.5	1.90	9.85	25.09
0.250	2	1.98	10.26	35.36
0.177	2.5	0.68	3.53	38.88
0.125	3	2.82	14.62	53.50
0.088	3.5	2.16	11.20	64.70
0.063	4	0.91	4.70	69.40
0.044	4.5	1.74	9.04	78.44
0.031	5	1.64	8.50	86.94
0.022	5.5	1.13	5.85	92.79
0.0156	6	0.66	3.44	96.23
0.0110	6.5	0.24	1.22	97.45
0.0078	7	0.16	0.83	98.27
0.0055	7.5	0.01	0.04	98.31
0.0039	8	0.10	0.50	98.81
0.00276	8.5	0.13	0.68	99.49
0.00195	9	0.01	0.05	99.55
0.00138	9.5	0.01	0.05	99.60
0.00098	10	0.01	0.05	99.65
0.00069	10.5	0.01	0.05	99.70
0.00049	11	0.01	0.05	99.75
0.00035	11.5	0.01	0.05	99.81
0.00024	12	0.01	0.05	99.86
0.00017	12.5	0.01	0.05	99.91
0.00012	13	0.01	0.05	99.96
0.00009	13.5	0.01	0.05	100.00
0.00006	14	0.01	0.05	100.00

Geldingasker. SILK-LN middle unit

Millimeters	Phi	Weight g	Weight %	Cumulative %
16.0	-4	2.46	2.56	2.56
11.3	-3.5	0.00	0.00	2.56
8.0	-3	0.28	0.29	2.85
5.7	-2.5	0.72	0.75	3.60
4.0	-2	1.47	1.53	5.13
2.8	-1.5	2.23	2.32	7.45
2.0	-1	3.85	4.01	11.45
1.4	-0.5	4.03	4.19	15.65
1.0	0	4.51	4.69	20.34
0.710	0.5	4.14	4.31	24.65
0.500	1	4.34	4.52	29.16
0.354	1.5	18.91	19.67	48.83
0.250	2	2.01	2.09	50.93
0.177	2.5	4.18	4.35	55.27
0.125	3	7.12	7.41	62.68
0.088	3.5	8.09	8.42	71.10
0.063	4	1.75	1.82	72.92
0.044	4.5	5.01	5.21	78.13
0.031	5	5.37	5.59	83.72
0.022	5.5	4.12	4.29	88.01
0.0156	6	2.31	2.40	90.41
0.0110	6.5	1.11	1.16	91.57
0.0078	7	0.56	0.58	92.15
0.0055	7.5	0.28	0.29	92.44
0.0039	8	0.06	0.06	92.50
0.00276	8.5	0.19	0.20	92.70
0.00195	9	0.00	0.00	92.70
0.00138	9.5	0.08	0.09	92.78
0.00098	10	0.00	0.00	92.78
0.00069	10.5	0.85	0.88	93.67
0.00049	11	0.85	0.88	94.55
0.00035	11.5	0.85	0.88	95.43
0.00024	12	0.85	0.88	96.32
0.00017	12.5	0.85	0.88	97.20
0.00012	13	0.85	0.88	98.08
0.00009	13.5	0.85	0.88	98.97
0.00006	14	0.85	0.88	100.00

Geldingasker. SILK-LN bottom unit

Millimeters	phi	Weight g	Weight %	Cumulative %
16.0	-4	0.00	0.00	0.00
11.3	-3.5	0.00	0.00	0.00
8.0	-3	0.00	0.00	0.00
5.7	-2.5	0.29	0.34	0.34
4.0	-2	0.25	0.30	0.64
2.8	-1.5	0.75	0.89	1.53
2.0	-1	1.82	2.16	3.70
1.4	-0.5	2.94	3.49	7.19
1.0	0	3.80	4.52	11.71
0.710	0.5	3.68	4.37	16.08
0.500	1	4.68	5.56	21.65
0.354	1.5	9.64	11.46	33.10
0.250	2	6.13	7.29	40.39
0.177	2.5	7.38	8.77	49.16
0.125	3	10.02	11.91	61.07
0.088	3.5	7.59	9.02	70.09
0.063	4	2.35	2.80	72.89
0.044	4.5	5.69	6.77	79.66
0.031	5	6.23	7.40	87.06
0.022	5.5	4.35	5.17	92.24
0.0156	6	2.66	3.16	95.39
0.0110	6.5	1.49	1.77	97.17
0.0078	7	0.61	0.72	97.89
0.0055	7.5	0.48	0.57	98.46
0.0039	8	0.00	0.00	98.46
0.00276	8.5	0.10	0.12	98.58
0.00195	9	0.00	0.00	98.58
0.00138	9.5	0.05	0.06	98.64
0.00098	10	0.35	0.42	99.07
0.00069	10.5	0.10	0.12	99.18
0.00049	11	0.10	0.12	99.30
0.00035	11.5	0.10	0.12	99.41
0.00024	12	0.10	0.12	99.53
0.00017	12.5	0.10	0.12	99.64
0.00012	13	0.10	0.12	99.76
0.00009	13.5	0.10	0.12	99.88
0.00006	14	0.10	0.12	100.00

Grófará SILK-LN

Millimeters	Phi	Weight g	Weight %	Cumulative %
16.0	-4	0.00	0.00	0.00
11.3	-3.5	0.00	0.00	0.00
8.0	-3	0.00	0.00	0.00
5.7	-2.5	0.00	0.00	0.00
4.0	-2	0.00	0.00	0.00
2.8	-1.5	0.00	0.00	0.00
2.0	-1	0.00	0.00	0.00
1.4	-0.5	0.00	0.00	0.00
1.0	0	0.00	0.00	0.00
0.710	0.5	0.00	0.00	0.00
0.500	1	0.00	0.00	0.00
0.354	1.5	0.03	2.27	2.27
0.250	2	0.10	7.58	9.85
0.177	2.5	0.13	9.85	19.70
0.125	3	0.23	17.42	37.12
0.088	3.5	0.23	17.42	54.55
0.063	4	0.07	5.22	59.77
0.044	4.5	0.13	9.98	69.75
0.031	5	0.14	10.81	80.56
0.022	5.5	0.11	8.46	89.02
0.0156	6	0.03	1.94	90.96
0.0110	6.5	0.02	1.71	92.67
0.0078	7	0.00	0.14	92.81
0.0055	7.5	0.00	0.28	93.09
0.0039	8	0.00	0.14	93.23
0.00276	8.5	0.02	1.39	94.61
0.00195	9	0.00	0.00	94.61
0.00138	9.5	0.00	0.23	94.84
0.00098	10	0.00	0.00	94.84
0.00069	10.5	0.01	0.66	95.51
0.00049	11	0.01	0.66	96.17
0.00035	11.5	0.01	0.66	96.83
0.00024	12	0.01	0.66	97.49
0.00017	12.5	0.01	0.66	98.16
0.00012	13	0.01	0.66	98.82
0.00009	13.5	0.01	0.66	99.48
0.00006	14	0.01	0.66	100.00

Hvammur SILK-LN

Millimeters	Phi	Weight g	Weight %	Cumulative %
16.0	-4	0.00	0.00	0.00
11.3	-3.5	0.00	0.00	0.00
8.0	-3	0.00	0.00	0.00
5.7	-2.5	0.00	0.00	0.00
4.0	-2	0.00	0.00	0.00
2.8	-1.5	0.04	0.33	0.33
2.0	-1	0.09	0.75	1.08
1.4	-0.5	0.40	3.31	4.39
1.0	0	0.47	3.89	8.28
0.710	0.5	0.46	3.81	12.09
0.500	1	0.90	7.45	19.54
0.354	1.5	1.14	9.44	28.97
0.250	2	1.26	10.43	39.40
0.177	2.5	1.30	10.76	50.17
0.125	3	1.76	14.57	64.74
0.088	3.5	1.34	11.09	75.83
0.063	4	0.22	1.79	77.62
0.044	4.5	0.64	5.27	82.88
0.031	5	0.78	6.47	89.35
0.022	5.5	0.56	4.61	93.96
0.0156	6	0.28	2.33	96.29
0.0110	6.5	0.13	1.08	97.37
0.0078	7	0.08	0.64	98.00
0.0055	7.5	0.02	0.17	98.17
0.0039	8	0.03	0.22	98.40
0.00276	8.5	0.01	0.10	98.49
0.00195	9	0.00	0.00	98.49
0.00138	9.5	0.00	0.00	98.49
0.00098	10	0.00	0.00	98.49
0.00069	10.5	0.03	0.23	98.72
0.00049	11	0.03	0.23	98.95
0.00035	11.5	0.03	0.23	99.18
0.00024	12	0.03	0.23	99.40
0.00017	12.5	0.03	0.23	99.63
0.00012	13	0.03	0.23	99.86
0.00009	13.5	0.03	0.23	100.00
0.00006	14	0.03	0.23	100.00

Leiðólfssfell. SILK-LN top unit

Millimeters	Phi	Weight g	Weight %	Cumulative %
16.0	-4	0.00	0.00	0.00
11.3	-3.5	0.16	0.24	0.24
8.0	-3	0.16	0.24	0.49
5.7	-2.5	0.00	0.00	0.49
4.0	-2	0.31	0.47	0.96
2.8	-1.5	0.70	1.06	2.02
2.0	-1	2.78	4.22	6.24
1.4	-0.5	2.43	3.69	9.93
1.0	0	3.83	5.82	15.75
0.710	0.5	3.79	5.75	21.50
0.500	1	4.24	6.44	27.94
0.354	1.5	4.29	6.51	34.45
0.250	2	11.92	18.10	52.55
0.177	2.5	7.02	10.66	63.21
0.125	3	5.55	8.43	71.64
0.088	3.5	2.98	4.52	76.16
0.063	4	1.65	2.50	78.66
0.044	4.5	3.28	4.98	83.64
0.031	5	3.79	5.76	89.40
0.022	5.5	3.11	4.72	94.12
0.0156	6	1.96	2.97	97.09
0.0110	6.5	1.03	1.56	98.65
0.0078	7	0.37	0.57	99.22
0.0055	7.5	0.12	0.19	99.41
0.0039	8	0.39	0.59	100.00
0.00276	8.5	0.00	0.00	100.00
0.00195	9	0.00	0.00	100.00
0.00138	9.5	0.00	0.00	100.00
0.00098	10	0.00	0.00	100.00
0.00069	10.5	0.00	0.00	100.00
0.00049	11	0.00	0.00	100.00
0.00035	11.5	0.00	0.00	100.00
0.00024	12	0.00	0.00	100.00
0.00017	12.5	0.00	0.00	100.00
0.00012	13	0.00	0.00	100.00
0.00009	13.5	0.00	0.00	100.00
0.00006	14	0.00	0.00	100.00

Leiðólfssfell. SILK-LN middle unit

Millimeters	Phi	Weight g	Weight %	Cumulative %
16.0	-4	0.00	0.00	0.00
11.3	-3.5	0.00	0.00	0.00
8.0	-3	0.00	0.00	0.00
5.7	-2.5	0.01	0.05	0.05
4.0	-2	0.00	0.00	0.05
2.8	-1.5	0.07	0.32	0.36
2.0	-1	0.20	0.90	1.26
1.4	-0.5	0.55	2.48	3.75
1.0	0	1.09	4.92	8.67
0.710	0.5	1.02	4.60	13.27
0.500	1	1.03	4.65	17.92
0.354	1.5	1.12	5.06	22.98
0.250	2	1.34	6.05	29.03
0.177	2.5	1.76	7.95	36.98
0.125	3	3.74	16.88	53.86
0.088	3.5	1.44	6.50	60.36
0.063	4	0.84	3.78	64.14
0.044	4.5	1.87	8.44	72.58
0.031	5	2.14	9.68	82.26
0.022	5.5	1.68	7.57	89.83
0.0156	6	1.02	4.62	94.44
0.0110	6.5	0.53	2.39	96.83
0.0078	7	0.15	0.68	97.51
0.0055	7.5	0.10	0.44	97.95
0.0039	8	0.45	2.03	100.00
0.00276	8.5	0.00	0.00	100.00
0.00195	9	0.00	0.00	100.00
0.00138	9.5	0.00	0.00	100.00
0.00098	10	0.00	0.00	100.00
0.00069	10.5	0.00	0.00	100.00
0.00049	11	0.00	0.00	100.00
0.00035	11.5	0.00	0.00	100.00
0.00024	12	0.00	0.00	100.00
0.00017	12.5	0.00	0.00	100.00
0.00012	13	0.00	0.00	100.00
0.00009	13.5	0.00	0.00	100.00
0.00006	14	0.00	0.00	100.00

Leiðólfssfell. SILK-LN bottom unit

Millimeters	Phi	Weight g	Weight %	Cumulative %
16.0	-4	0.00	0.00	0.00
11.3	-3.5	0.00	0.00	0.00
8.0	-3	0.00	0.00	0.00
5.7	-2.5	0.00	0.00	0.00
4.0	2	0.00	0.00	0.00
2.8	-1.5	0.00	0.00	0.00
2.0	-1	0.08	0.43	0.43
1.4	-0.5	0.20	1.08	1.52
1.0	0	0.48	2.60	4.12
0.710	0.5	0.61	3.31	7.43
0.500	1	0.93	5.04	12.47
0.354	1.5	1.13	6.13	18.60
0.250	2	1.41	7.65	26.25
0.177	2.5	1.83	9.92	36.17
0.125	3	3.18	17.25	53.42
0.088	3.5	1.69	9.16	62.58
0.063	4	0.82	4.44	67.02
0.044	4.5	1.52	8.27	75.28
0.031	5	1.74	9.41	84.69
0.022	5.5	1.20	6.51	91.20
0.0156	6	0.71	3.86	95.07
0.0110	6.5	0.37	2.00	97.07
0.0078	7	0.54	2.93	100.00
0.0055	7.5	0.00	0.00	100.00
0.0039	8	0.00	0.00	100.00
0.00276	8.5	0.00	0.00	100.00
0.00195	9	0.00	0.00	100.00
0.00138	9.5	0.00	0.00	100.00
0.00098	10	0.00	0.00	100.00
0.00069	10.5	0.00	0.00	100.00
0.00049	11	0.00	0.00	100.00
0.00035	11.5	0.00	0.00	100.00
0.00024	12	0.00	0.00	100.00
0.00017	12.5	0.00	0.00	100.00
0.00012	13	0.00	0.00	100.00
0.00009	13.5	0.00	0.00	100.00
0.00006	14	0.00	0.00	100.00

Loðnugil. SILK-LN top unit

Millimeters	Phi	Weight g	Weight %	Cumulative %
16.0	-4	0.00	0.00	0.00
11.3	-3.5	1.48	1.60	1.60
8.0	-3	2.72	2.95	4.55
5.7	-2.5	2.53	2.74	7.29
4.0	-2	4.43	4.80	12.09
2.8	-1.5	4.46	4.83	16.92
2.0	-1	4.72	5.11	22.03
1.4	-0.5	5.37	5.82	27.85
1.0	0	5.12	5.55	33.39
0.710	0.5	2.63	2.85	36.24
0.500	1	3.15	3.41	39.66
0.354	1.5	3.78	4.09	43.75
0.250	2	5.32	5.76	49.51
0.177	2.5	5.57	6.03	55.55
0.125	3	6.96	7.54	63.08
0.088	3.5	7.14	7.73	70.82
0.063	4	3.20	2.00	72.82
0.044	4.5	5.98	6.48	79.30
0.031	5	5.96	6.45	85.75
0.022	5.5	4.63	5.02	90.77
0.0156	6	3.01	3.26	94.03
0.0110	6.5	1.81	1.97	95.99
0.0078	7	0.81	0.88	96.87
0.0055	7.5	0.22	0.23	97.11
0.0039	8	0.14	0.15	97.25
0.00276	8.5	0.24	0.26	97.52
0.00195	9	0.00	0.00	97.52
0.00138	9.5	0.00	0.00	97.52
0.00098	10	0.19	0.21	97.72
0.00069	10.5	0.10	0.11	97.83
0.00049	11	0.10	0.11	97.94
0.00035	11.5	0.10	0.11	98.04
0.00024	12	0.10	0.11	98.15
0.00017	12.5	0.10	0.11	98.26
0.00012	13	0.10	0.11	98.36
0.00009	13.5	0.10	0.11	98.47
0.00006	14	0.10	0.11	100.00

Loðnugil. SILK-LN upper middle unit

Millimeters	Phi	Weight g	Weight %	Cumulative %
22.6	-4.5	0.89	0.85	0.85
16.0	-4	2.64	2.51	3.36
11.3	-3.5	1.01	0.96	4.32
8.0	-3	2.41	2.29	6.62
5.7	-2.5	5.60	5.33	11.95
4.0	-2	6.60	6.28	18.23
2.8	-1.5	7.89	7.51	25.75
2.0	-1	7.49	7.13	32.88
1.4	-0.5	6.55	6.24	39.11
1.0	0	5.02	4.78	43.89
0.710	0.5	1.48	1.41	45.30
0.500	1	2.50	2.38	47.68
0.354	1.5	3.17	3.02	50.70
0.250	2	4.16	3.96	54.66
0.177	2.5	6.00	5.71	60.37
0.125	3	7.91	7.53	67.90
0.088	3.5	7.61	7.25	75.15
0.063	4	2.28	2.17	77.32
0.044	4.5	4.86	4.63	81.95
0.031	5	5.92	5.64	87.59
0.022	5.5	5.15	4.90	92.49
0.0156	6	3.53	3.36	95.85
0.0110	6.5	1.86	1.77	97.62
0.0078	7	0.82	0.78	98.41
0.0055	7.5	0.42	0.40	98.81
0.0039	8	0.19	0.18	98.99
0.00276	8.5	0.16	0.15	99.14
0.00195	9	0.00	0.00	99.14
0.00138	9.5	0.03	0.03	99.16
0.00098	10	0.00	0.00	99.16
0.00069	10.5	0.12	0.12	99.28
0.00049	11	0.12	0.12	99.40
0.00035	11.5	0.12	0.12	99.51
0.00024	12	0.12	0.12	99.63
0.00017	12.5	0.12	0.12	99.75
0.00012	13	0.12	0.12	99.86
0.00009	13.5	0.12	0.12	99.98
0.00006	14	0.12	0.12	100.00

Loðnugil. SILK-LN lower middle unit

Millimeters	Phi	Weight g	Weight %	Cumulative %
16.0	-4	0.58	0.46	0.46
11.3	-3.5	0.00	0.00	0.46
8.0	-3	0.76	0.61	1.07
5.7	-2.5	0.71	0.57	1.63
4.0	-2	1.36	1.08	2.72
2.8	-1.5	1.94	1.54	4.26
2.0	-1	2.98	2.37	6.63
1.4	-0.5	3.77	3.00	9.63
1.0	0	4.85	3.86	13.50
0.710	0.5	2.89	2.30	15.80
0.500	1	5.17	4.12	19.91
0.354	1.5	6.69	5.33	25.24
0.250	2	9.03	7.19	32.43
0.177	2.5	11.42	9.09	41.52
0.125	3	15.02	11.96	53.48
0.088	3.5	12.28	9.78	63.26
0.063	4	3.43	2.73	65.99
0.044	4.5	8.72	6.94	72.94
0.031	5	10.16	8.09	81.02
0.022	5.5	8.67	6.91	87.93
0.0156	6	6.21	4.95	92.88
0.0110	6.5	4.03	3.21	96.09
0.0078	7	2.41	1.92	98.01
0.0055	7.5	0.88	0.70	98.71
0.0039	8	0.46	0.37	99.08
0.00276	8.5	0.28	0.22	99.30
0.00195	9	0.00	0.00	99.30
0.00138	9.5	0.00	0.00	99.30
0.00098	10	0.88	0.70	100.00
0.00069	10.5	0.00	0.00	100.00
0.00049	11	0.00	0.00	100.00
0.00035	11.5	0.00	0.00	100.00
0.00024	12	0.00	0.00	100.00
0.00017	12.5	0.00	0.00	100.00
0.00012	13	0.00	0.00	100.00
0.00009	13.5	0.00	0.00	100.00
0.00006	14	0.00	0.00	100.00

Loðnugil. SILK-LN bottom unit

Millimeters	Phi	Weight g	Weight %	Cumulative %
16.0	-4	0.00	0.00	0.00
11.3	-3.5	0.13	0.17	0.17
8.0	-3	0.00	0.00	0.17
5.7	-2.5	0.38	0.51	0.68
4.0	-2	1.34	1.79	2.47
2.8	-1.5	1.39	1.86	4.33
2.0	-1	1.80	2.41	6.74
1.4	-0.5	2.46	3.29	10.03
1.0	0	3.32	4.44	14.47
0.710	0.5	2.15	2.88	17.34
0.500	1	3.76	5.03	22.37
0.354	1.5	4.97	6.65	29.02
0.250	2	5.53	7.40	36.41
0.177	2.5	5.99	8.01	44.42
0.125	3	8.96	11.98	56.41
0.088	3.5	7.07	9.45	65.86
0.063	4	2.19	2.93	68.79
0.044	4.5	5.01	6.70	75.49
0.031	5	5.88	7.87	83.36
0.022	5.5	4.77	6.39	89.74
0.0156	6	2.99	4.00	93.75
0.0110	6.5	1.96	2.62	96.37
0.0078	7	0.98	1.31	97.68
0.0055	7.5	0.46	0.62	98.30
0.0039	8	0.39	0.52	98.82
0.00276	8.5	0.10	0.14	98.96
0.00195	9	-0.23	0.00	98.96
0.00138	9.5	0.00	0.00	98.96
0.00098	10	0.70	0.93	99.89
0.00069	10.5	0.04	0.05	99.94
0.00049	11	0.04	0.05	100.00
0.00035	11.5	0.04	0.05	100.00
0.00024	12	0.04	0.05	100.00
0.00017	12.5	0.04	0.05	100.00
0.00012	13	0.04	0.05	100.00
0.00009	13.5	0.04	0.05	100.00
0.00006	14	0.04	0.05	100.00

Loðnugil. SILK-LN bulk sample

Millimeters	Phi	Weight g	Weight %	Cumulative %
16.0	-4	0.00	0.00	0.00
11.3	-3.5	0.00	0.00	0.00
8.0	-3	0.00	0.00	0.00
5.7	-2.5	0.28	0.30	0.30
4.0	-2	0.84	0.89	1.18
2.8	-1.5	1.38	1.46	2.64
2.0	-1	2.53	2.67	5.31
1.4	-0.5	5.12	5.41	10.72
1.0	0	9.46	9.99	20.71
0.710	0.5	6.63	7.00	27.71
0.500	1	8.01	8.46	36.17
0.354	1.5	6.89	7.28	43.44
0.250	2	6.77	7.15	50.59
0.177	2.5	7.37	7.78	58.37
0.125	3	7.61	8.04	66.41
0.088	3.5	7.26	7.67	74.08
0.063	4	2.91	3.08	77.15
0.044	4.5	5.25	5.55	82.70
0.031	5	5.88	6.21	88.91
0.022	5.5	4.46	4.71	93.61
0.0156	6	2.71	2.87	96.48
0.0110	6.5	1.57	1.66	98.13
0.0078	7	0.67	0.71	98.84
0.0055	7.5	0.52	0.55	99.40
0.0039	8	0.42	0.45	99.84
0.00276	8.5	0.01	0.01	99.86
0.00195	9	0.01	0.01	99.87
0.00138	9.5	0.01	0.01	99.88
0.00098	10	0.01	0.01	99.90
0.00069	10.5	0.01	0.01	99.91
0.00049	11	0.01	0.01	99.92
0.00035	11.5	0.01	0.01	99.94
0.00024	12	0.01	0.01	99.95
0.00017	12.5	0.01	0.01	99.96
0.00012	13	0.01	0.01	99.98
0.00009	13.5	0.01	0.01	99.99
0.00006	14	0.01	0.01	100.00

Strútur. SILK-LN bulk sample

Millimeters	Phi	Weight g	Weight %	Cumulative %
16.0	-4	0.00	0.00	0.00
11.3	-3.5	0.13	0.89	0.89
8.0	-3	0.00	0.00	0.89
5.7	-2.5	0.00	0.00	0.89
4.0	-2	0.37	2.55	3.44
2.8	-1.5	0.20	1.38	4.82
2.0	-1	0.49	3.37	8.19
1.4	-0.5	0.42	2.89	11.08
1.0	0	0.46	3.17	14.25
0.710	0.5	0.49	3.37	17.62
0.500	1	0.37	2.55	20.17
0.354	1.5	0.61	4.20	24.36
0.250	2	0.91	6.26	30.63
0.177	2.5	1.52	10.46	41.09
0.125	3	2.62	18.03	59.12
0.088	3.5	1.66	11.42	70.54
0.063	4	0.68	4.65	75.19
0.044	4.5	1.14	7.86	83.05
0.031	5	1.04	7.14	90.18
0.022	5.5	0.64	4.44	94.62
0.0156	6	0.36	2.46	97.08
0.0110	6.5	0.18	1.26	98.34
0.0078	7	0.04	0.30	98.64
0.0055	7.5	0.12	0.81	99.45
0.0039	8	0.08	0.57	100.00
0.00276	8.5	0.00	0.00	100.00
0.00195	9	0.00	0.00	100.00
0.00138	9.5	0.00	0.00	100.00
0.00098	10	0.00	0.00	100.00
0.00069	10.5	0.00	0.00	100.00
0.00049	11	0.00	0.00	100.00
0.00035	11.5	0.00	0.00	100.00
0.00024	12	0.00	0.00	100.00
0.00017	12.5	0.00	0.00	100.00
0.00012	13	0.00	0.00	100.00
0.00009	13.5	0.00	0.00	100.00
0.00006	14	0.00	0.00	100.00

Gully at Syðri Ófæra. SILK-LN bulk sample

Millimeters	Phi	Weight g	Weight %	Cumulative %
16.0	-4	0.00	0.00	0.00
11.3	-3.5	0.00	0.00	0.00
8.0	-3	0.04	0.14	0.14
5.7	-2.5	0.07	0.24	0.38
4.0	-2	0.24	0.83	1.22
2.8	-1.5	0.67	2.33	3.54
2.0	-1	0.86	2.99	6.53
1.4	-0.5	1.40	4.86	11.40
1.0	0	1.69	5.87	17.27
0.710	0.5	1.39	4.83	22.10
0.500	1	1.59	5.52	27.62
0.354	1.5	1.94	6.74	34.36
0.250	2	2.28	7.92	42.29
0.177	2.5	2.34	8.13	50.42
0.125	3	4.45	15.46	65.88
0.088	3.5	3.47	12.06	77.94
0.063	4	0.66	2.29	80.23
0.044	4.5	1.63	5.66	85.89
0.031	5	1.76	6.12	92.01
0.022	5.5	1.10	3.81	95.82
0.0156	6	0.54	1.89	97.71
0.0110	6.5	0.22	0.78	98.49
0.0078	7	0.04	0.16	98.65
0.0055	7.5	0.03	0.09	98.74
0.0039	8	0.10	0.36	99.09
0.00276	8.5	0.02	0.08	99.17
0.00195	9	0.02	0.08	99.25
0.00138	9.5	0.02	0.08	99.32
0.00098	10	0.02	0.08	99.40
0.00069	10.5	0.02	0.08	99.47
0.00049	11	0.02	0.08	99.55
0.00035	11.5	0.02	0.08	99.62
0.00024	12	0.02	0.08	99.70
0.00017	12.5	0.02	0.08	99.77
0.00012	13	0.02	0.08	99.85
0.00009	13.5	0.02	0.08	99.92
0.00006	14	0.02	0.08	100.00

Varmárfell. SILK-LN top unit

Millimeters	Phi	Weight g	Weight %	Cumulative %
16.0	-4	0.00	0.00	0.00
11.3	-3.5	0.00	0.00	0.00
8.0	-3	0.00	0.00	0.00
5.7	-2.5	0.00	0.00	0.00
4.0	-2	0.00	0.00	0.00
2.8	-1.5	0.04	0.08	0.08
2.0	-1	0.05	0.10	0.18
1.4	-0.5	0.13	0.26	0.45
1.0	0	0.52	1.05	1.50
0.710	0.5	0.93	1.88	3.38
0.500	1	2.59	5.25	8.63
0.354	1.5	5.90	11.95	20.58
0.250	2	8.09	16.39	36.97
0.177	2.5	8.47	17.16	54.13
0.125	3	11.3	22.89	77.03
0.088	3.5	6.10	12.36	89.38
0.063	4	1.66	3.37	92.75
0.044	4.5	1.84	3.72	96.47
0.031	5	0.89	1.79	98.26
0.022	5.5	0.28	0.57	98.83
0.0156	6	0.10	0.21	99.04
0.0110	6.5	0.19	0.38	99.42
0.0078	7	0.08	0.17	99.59
0.0055	7.5	0.01	0.03	99.62
0.0039	8	0.01	0.03	99.65
0.00276	8.5	0.01	0.03	99.68
0.00195	9	0.01	0.03	99.71
0.00138	9.5	0.01	0.03	99.74
0.00098	10	0.01	0.03	99.76
0.00069	10.5	0.01	0.03	99.79
0.00049	11	0.01	0.03	99.82
0.00035	11.5	0.01	0.03	99.85
0.00024	12	0.01	0.03	99.88
0.00017	12.5	0.01	0.03	99.91
0.00012	13	0.01	0.03	99.94
0.00009	13.5	0.01	0.03	99.97
0.00006	14	0.01	0.03	100.00

Varmárfell. SILK-LN middle unit

Millimeters	Phi	Weight g	Weight %	Cumulative %
16.0	-4	0.00	0.00	0.00
11.3	-3.5	0.00	0.00	0.00
8.0	-3	0.00	0.00	0.00
5.7	-2.5	0.00	0.00	0.00
4.0	-2	0.00	0.00	0.00
2.8	-1.5	0.01	0.02	0.02
2.0	-1	0.06	0.09	0.11
1.4	-0.5	0.29	0.44	0.55
1.0	0	1.21	1.86	2.41
0.710	0.5	2.41	3.70	6.11
0.500	1	4.43	6.80	12.90
0.354	1.5	5.23	8.02	20.93
0.250	2	5.4	8.28	29.21
0.177	2.5	6.28	9.63	38.85
0.125	3	8.36	12.83	51.67
0.088	3.5	7.16	10.98	62.66
0.063	4	1.62	2.49	65.15
0.044	4.5	5.02	7.70	72.84
0.031	5	6.02	9.24	82.09
0.022	5.5	4.62	7.09	89.18
0.0156	6	3.10	4.75	93.93
0.0110	6.5	1.75	2.68	96.61
0.0078	7	0.69	1.06	97.67
0.0055	7.5	0.52	0.79	98.46
0.0039	8	0.34	0.53	98.99
0.00276	8.5	0.66	1.02	100
0.00195	9	0.00	0.00	100
0.00138	9.5	0.00	0.00	100
0.00098	10	0.00	0.00	100
0.00069	10.5	0.00	0.00	100
0.00049	11	0.00	0.00	100
0.00035	11.5	0.00	0.00	100
0.00024	12	0.00	0.00	100
0.00017	12.5	0.00	0.00	100
0.00012	13	0.00	0.00	100
0.00009	13.5	0.00	0.00	100
0.00006	14	0.00	0.00	100

Varmárfell. SILK-LN bottom unit

Millimeters	Phi	Weight g	Weight %	Cumulative %
16.0	-4	0.00	0.00	0.00
11.3	-3.5	0.00	0.00	0.00
8.0	-3	0.00	0.00	0.00
5.7	-2.5	0.00	0.00	0.00
4.0	-2	0.00	0.00	0.00
2.8	-1.5	0.00	0.00	0.00
2.0	-1	0.07	0.25	0.25
1.4	-0.5	0.18	0.65	0.90
1.0	0	0.56	2.02	2.93
0.710	0.5	1.10	3.97	6.90
0.500	1	1.76	6.36	13.26
0.354	1.5	2.16	7.80	21.06
0.250	2	2.08	7.51	28.58
0.177	2.5	2.06	7.44	36.02
0.125	3	3.38	12.21	48.23
0.088	3.5	2.54	9.18	57.41
0.063	4	1.05	3.81	61.22
0.044	4.5	2.20	7.96	69.17
0.031	5	2.65	9.57	78.74
0.022	5.5	2.17	7.83	86.57
0.0156	6	1.46	5.29	91.86
0.0110	6.5	0.97	3.51	95.38
0.0078	7	0.39	1.40	96.78
0.0055	7.5	0.21	0.76	97.54
0.0039	8	0.12	0.42	97.96
0.00276	8.5	0.55	1.99	99.95
0.00195	9	0.01	0.04	100.00
0.00138	9.5	0.00	0.00	100.00
0.00098	10	0.00	0.00	100.00
0.00069	10.5	0.00	0.00	100.00
0.00049	11	0.00	0.00	100.00
0.00035	11.5	0.00	0.00	100.00
0.00024	12	0.00	0.00	100.00
0.00017	12.5	0.00	0.00	100.00
0.00012	13	0.00	0.00	100.00
0.00009	13.5	0.00	0.00	100.00
0.00006	14	0.00	0.00	100.00

Varmárfell. SILK-LN bulk sample

Millimeters	Phi	Weight g	Weight %	Cumulative %
16.0	-4	0.00	0.00	0.00
11.3	-3.5	0.00	0.00	0.00
8.0	-3	0.00	0.00	0.00
5.7	-2.5	0.00	0.00	0.00
4.0	-2	0.00	0.00	0.00
2.8	-1.5	0.08	0.11	0.11
2.0	-1	0.18	0.25	0.37
1.4	-0.5	0.44	0.62	0.98
1.0	0	1.89	2.66	3.64
0.710	0.5	2.32	3.26	6.91
0.500	1	5.33	7.50	14.40
0.354	1.5	5.81	8.17	22.57
0.250	2	6.04	8.50	31.07
0.177	2.5	5.86	8.24	39.31
0.125	3	9.83	13.83	53.14
0.088	3.5	7.10	9.99	63.12
0.063	4	1.76	2.47	65.59
0.044	4.5	5.82	8.19	73.78
0.031	5	6.82	9.59	83.37
0.022	5.5	4.9	6.93	90.30
0.0156	6	2.88	4.06	94.36
0.0110	6.5	1.63	2.29	96.64
0.0078	7	0.60	0.85	97.49
0.0055	7.5	0.45	0.63	98.12
0.0039	8	0.10	0.15	98.27
0.00276	8.5	1.08	1.51	99.78
0.00195	9	0.03	0.04	99.82
0.00138	9.5	0.01	0.02	99.83
0.00098	10	0.01	0.02	99.85
0.00069	10.5	0.01	0.02	99.87
0.00049	11	0.01	0.02	99.89
0.00035	11.5	0.01	0.02	99.91
0.00024	12	0.01	0.02	99.93
0.00017	12.5	0.01	0.02	99.94
0.00012	13	0.01	0.02	99.96
0.00009	13.5	0.01	0.02	99.98
0.00006	14	0.01	0.02	100.00

Framgil. SILK-UN bulk sample

Millimeters	Phi	Weight g	Weight %	Cumulative %
16.0	-4	0.00	0.00	0.00
11.3	-3.5	0.00	0.00	0.00
8.0	-3	0.22	0.32	0.32
5.7	-2.5	0.03	0.04	0.36
4.0	-2	0.78	1.13	1.50
2.8	-1.5	1.45	2.11	3.61
2.0	-1	3.42	4.98	8.58
1.4	-0.5	5.36	7.80	16.38
1.0	0	7.34	10.68	27.06
0.710	0.5	6.4	9.31	36.37
0.500	1	5.92	8.61	44.98
0.354	1.5	5.16	7.51	52.49
0.250	2	4.96	7.22	59.70
0.177	2.5	5.33	7.75	67.46
0.125	3	5.86	8.52	75.98
0.088	3.5	3.46	5.03	81.02
0.063	4	1.76	2.57	83.58
0.044	4.5	3.09	4.49	88.08
0.031	5	2.72	3.95	92.03
0.022	5.5	2.19	3.18	95.21
0.0156	6	1.43	2.08	97.30
0.0110	6.5	0.77	1.12	98.42
0.0078	7	0.32	0.46	98.88
0.0055	7.5	0.00	0.00	98.88
0.0039	8	0.20	0.29	99.17
0.00276	8.5	0.33	0.48	99.65
0.00195	9	0.02	0.03	99.68
0.00138	9.5	0.02	0.03	99.71
0.00098	10	0.02	0.03	99.74
0.00069	10.5	0.02	0.03	99.78
0.00049	11	0.02	0.03	99.81
0.00035	11.5	0.02	0.03	99.84
0.00024	12	0.02	0.03	99.87
0.00017	12.5	0.02	0.03	99.90
0.00012	13	0.02	0.03	99.94
0.00009	13.5	0.02	0.03	99.97
0.00006	14	0.02	0.03	100.00

Framgil. SILK-LN bulk sample

Millimeters	Phi	Weight g	Weight %	Cumulative %
16.0	-4	0.00	0.00	0.00
11.3	-3.5	0.00	0.00	0.00
8.0	-3	0.19	0.59	0.59
5.7	-2.5	0.53	1.65	2.24
4.0	-2	0.14	0.44	2.68
2.8	-1.5	0.84	2.61	5.29
2.0	-1	1.13	3.52	8.81
1.4	-0.5	1.37	4.26	13.07
1.0	0	1.59	4.95	18.02
0.710	0.5	1.97	6.13	24.15
0.500	1	2.25	7.00	31.15
0.354	1.5	2.09	6.50	37.66
0.250	2	2.46	7.66	45.31
0.177	2.5	2.5	7.78	53.10
0.125	3	3.1	9.65	62.74
0.088	3.5	4.07	12.67	75.41
0.063	4	0.50	1.57	76.98
0.044	4.5	1.42	4.43	81.40
0.031	5	1.84	5.72	87.12
0.022	5.5	1.66	5.17	92.30
0.0156	6	1.12	3.48	95.78
0.0110	6.5	0.59	1.84	97.62
0.0078	7	0.26	0.82	98.44
0.0055	7.5	0.12	0.37	98.81
0.0039	8	0.12	0.37	99.18
0.00276	8.5	-0.01	0.00	99.18
0.00195	9	-0.06	0.00	99.18
0.00138	9.5	0.09	0.27	99.46
0.00098	10	0.11	0.35	99.81
0.00069	10.5	0.02	0.05	99.86
0.00049	11	0.02	0.05	99.91
0.00035	11.5	0.02	0.05	99.96
0.00024	12	0.02	0.05	100.01
0.00017	12.5	0.02	0.05	100.06
0.00012	13	0.02	0.05	100.11
0.00009	13.5	0.02	0.05	100.16
0.00006	14	0.02	0.05	100

Framgil. SILK-N4 bulk sample

Millimeters	Phi	Weight g	Weight %	Cumulative %
16.0	-4	0.00	0.00	0.00
11.3	-3.5	0.00	0.00	0.00
8.0	-3	0.00	0.00	0.00
5.7	-2.5	0.00	0.00	0.00
4.0	-2	0.00	0.00	0.00
2.8	-1.5	0.00	0.00	0.00
2.0	-1	0.08	0.67	0.67
1.4	-0.5	0.18	1.51	2.18
1.0	0	0.25	2.09	4.27
0.710	0.5	0.38	3.18	7.44
0.500	1	0.29	2.42	9.87
0.354	1.5	0.28	2.34	12.21
0.250	2	0.33	2.76	14.97
0.177	2.5	0.33	2.76	17.73
0.125	3	0.83	6.94	24.67
0.088	3.5	1.43	11.98	36.65
0.063	4	0.71	5.91	42.56
0.044	4.5	1.69	14.11	56.66
0.031	5	1.88	15.70	72.36
0.022	5.5	1.43	11.95	84.31
0.0156	6	0.76	6.35	90.66
0.0110	6.5	0.33	2.80	93.46
0.0078	7	0.18	1.53	94.98
0.0055	7.5	0.08	0.64	95.62
0.0039	8	0.43	3.62	99.24
0.00276	8.5	0.01	0.06	99.30
0.00195	9	0.01	0.06	99.36
0.00138	9.5	0.01	0.06	99.43
0.00098	10	0.01	0.06	99.49
0.00069	10.5	0.01	0.06	99.55
0.00049	11	0.01	0.06	99.62
0.00035	11.5	0.01	0.06	99.68
0.00024	12	0.01	0.06	99.74
0.00017	12.5	0.01	0.06	99.80
0.00012	13	0.01	0.06	99.87
0.00009	13.5	0.01	0.06	99.93
0.00006	14	0.01	0.06	100.00

Framgil. SILK-N3 bulk sample

Millimeters	Phi	Weight g	Weight %	Cumulative %
16.0	-4	0.00	0.00	0.00
11.3	-3.5	0.00	0.00	0.00
8.0	-3	0.03	0.49	0.49
5.7	-2.5	0.06	0.97	1.46
4.0	-2	0.14	2.27	3.73
2.8	-1.5	0.34	5.50	9.23
2.0	-1	0.55	8.90	18.13
1.4	-0.5	0.68	11.00	29.13
1.0	0	0.73	11.81	40.94
0.710	0.5	0.61	9.87	50.81
0.500	1	0.48	7.77	58.58
0.354	1.5	0.11	1.78	60.36
0.250	2	0.51	8.25	68.61
0.177	2.5	0.23	3.72	72.33
0.125	3	0.77	12.46	84.79
0.088	3.5	0.15	2.43	87.22
0.063	4	0.10	1.65	88.87
0.044	4.5	0.20	3.29	92.17
0.031	5	0.18	2.99	95.16
0.022	5.5	0.10	1.60	96.76
0.0156	6	0.03	0.49	97.26
0.0110	6.5	0.03	0.42	97.67
0.0078	7	0.01	0.16	97.84
0.0055	7.5	-0.01	0.00	97.84
0.0039	8	0.00	0.00	97.84
0.00276	8.5	0.03	0.49	98.33
0.00195	9	-0.01	0.00	98.33
0.00138	9.5	-0.01	0.00	98.33
0.00098	10	0.04	0.59	98.92
0.00069	10.5	0.01	0.20	99.12
0.00049	11	0.01	0.20	99.33
0.00035	11.5	0.01	0.20	99.53
0.00024	12	0.01	0.20	99.73
0.00017	12.5	0.01	0.20	99.93
0.00012	13	0.01	0.20	100.00
0.00009	13.5	0.01	0.20	100.00
0.00006	14	0.01	0.20	100.00

Framgil. SILK-N2 bulk sample

Millimeters	Phi	Weight g	Weight %	Cumulative %
16.0	-4	0.00	0.00	0.00
11.3	-3.5	0.00	0.00	0.00
8.0	-3	0.00	0.00	0.00
5.7	-2.5	0.00	0.00	0.00
4.0	-2	0.00	0.00	0.00
2.8	-1.5	0.16	0.34	0.34
2.0	-1	0.43	0.91	1.25
1.4	-0.5	1.77	3.76	5.01
1.0	0	3.65	7.75	12.77
0.710	0.5	4.94	10.49	23.26
0.500	1	4.38	9.30	32.56
0.354	1.5	4.22	8.96	41.53
0.250	2	4.42	9.39	50.91
0.177	2.5	3.68	7.82	58.73
0.125	3	6.11	12.98	71.71
0.088	3.5	5.87	12.47	84.18
0.063	4	0.79	1.67	85.85
0.044	4.5	1.84	3.90	89.75
0.031	5	1.98	4.20	93.95
0.022	5.5	1.48	3.14	97.09
0.0156	6	0.73	1.54	98.64
0.0110	6.5	0.27	0.57	99.21
0.0078	7	0.12	0.25	99.46
0.0055	7.5	0.25	0.53	99.99
0.0039	8	0.01	0.02	100.00
0.00276	8.5	0.00	0.00	100.00
0.00195	9	0.00	0.00	100.00
0.00138	9.5	0.00	0.00	100.00
0.00098	10	0.00	0.00	100.00
0.00069	10.5	0.00	0.00	100.00
0.00049	11	0.00	0.00	100.00
0.00035	11.5	0.00	0.00	100.00
0.00024	12	0.00	0.00	100.00
0.00017	12.5	0.00	0.00	100.00
0.00012	13	0.00	0.00	100.00
0.00009	13.5	0.00	0.00	100.00
0.00006	14	0.00	0.00	100.00

Einhyrningur. SILK-N1 top unit

Millimeters	Phi	Weight g	Weight %	Cumulative %
16.0	-4	0.00	0.00	0.00
11.3	-3.5	0.00	0.00	0.00
8.0	-3	0.00	0.00	0.00
5.7	-2.5	0.00	0.00	0.00
4.0	-2	0.00	0.00	0.00
2.8	-1.5	0.00	0.00	0.00
2.0	-1	0.04	0.07	0.07
1.4	-0.5	0.02	0.03	0.10
1.0	0	0.36	0.63	0.73
0.710	0.5	1.17	2.04	2.78
0.500	1	2.89	5.05	7.83
0.354	1.5	3.51	6.13	13.96
0.250	2	3.32	5.80	19.76
0.177	2.5	3.33	5.82	25.58
0.125	3	5.63	9.84	35.42
0.088	3.5	9.71	16.97	52.39
0.063	4	2.37	4.13	56.52
0.044	4.5	5.34	9.32	65.84
0.031	5	6.63	11.58	77.42
0.022	5.5	5.34	9.32	86.74
0.0156	6	3.33	5.81	92.56
0.0110	6.5	1.87	3.27	95.82
0.0078	7	0.80	1.39	97.22
0.0055	7.5	0.50	0.86	98.08
0.0039	8	0.55	0.96	99.04
0.00276	8.5	0.05	0.08	99.12
0.00195	9	0.05	0.08	99.20
0.00138	9.5	0.05	0.08	99.28
0.00098	10	0.05	0.08	99.36
0.00069	10.5	0.05	0.08	99.44
0.00049	11	0.05	0.08	99.52
0.00035	11.5	0.05	0.08	99.60
0.00024	12	0.05	0.08	99.68
0.00017	12.5	0.05	0.08	99.76
0.00012	13	0.05	0.08	99.84
0.00009	13.5	0.05	0.08	99.92
0.00006	14	0.05	0.08	100.00

Einhyrningur. SILK-N1 middle unit

Millimeters	Phi	Weight g	Weight %	Cumulative %
16.0	-4	0.00	0.00	0.00
11.3	-3.5	0.00	0.00	0.00
8.0	-3	0.00	0.00	0.00
5.7	-2.5	0.00	0.00	0.00
4.0	-2	0.00	0.00	0.00
2.8	-1.5	0.00	0.00	0.00
2.0	-1	0.02	0.09	0.09
1.4	-0.5	0.15	0.64	0.73
1.0	0	0.48	2.05	2.77
0.710	0.5	1.26	5.38	8.15
0.500	1	1.89	8.07	16.22
0.354	1.5	2.4	10.24	26.46
0.250	2	1.9	8.11	34.57
0.177	2.5	1.65	7.04	41.61
0.125	3	2.58	11.01	52.62
0.088	3.5	2.07	8.83	61.46
0.063	4	1.32	5.62	67.08
0.044	4.5	2.01	8.60	75.67
0.031	5	2.22	9.49	85.16
0.022	5.5	1.46	6.24	91.40
0.0156	6	0.89	3.80	95.19
0.0110	6.5	0.47	2.01	97.21
0.0078	7	0.13	0.54	97.75
0.0055	7.5	0.09	0.39	98.14
0.0039	8	0.01	0.04	98.17
0.00276	8.5	0.26	1.12	99.30
0.00195	9	0.16	0.70	100.00
0.00138	9.5	0.00	0.00	100.00
0.00098	10	0.00	0.00	100.00
0.00069	10.5	0.00	0.00	100.00
0.00049	11	0.00	0.00	100.00
0.00035	11.5	0.00	0.00	100.00
0.00024	12	0.00	0.00	100.00
0.00017	12.5	0.00	0.00	100.00
0.00012	13	0.00	0.00	100.00
0.00009	13.5	0.00	0.00	100.00
0.00006	14	0.00	0.00	100.00

Einhyrningur. SILK-N1 bottom unit

Millimeters	Phi	Weight g	Weight %	Cumulative %
16.0	-4	0.00	0.00	0.00
11.3	-3.5	0.00	0.00	0.00
8.0	-3	0.00	0.00	0.00
5.7	-2.5	0.00	0.00	0.00
4.0	-2	0.00	0.00	0.00
2.8	-1.5	0.00	0.00	0.00
2.0	-1	0.01	0.13	0.13
1.4	-0.5	0.04	0.51	0.63
1.0	0	0.19	2.41	3.05
0.710	0.5	0.44	5.58	8.63
0.500	1	0.82	10.41	19.04
0.354	1.5	1.04	13.20	32.23
0.250	2	0.96	12.18	44.42
0.177	2.5	0.91	11.55	55.96
0.125	3	0.99	12.56	68.53
0.088	3.5	0.47	5.96	74.49
0.063	4	0.37	4.64	79.13
0.044	4.5	0.52	6.55	85.69
0.031	5	0.47	5.91	91.60
0.022	5.5	0.31	3.90	95.50
0.0156	6	0.14	1.72	97.22
0.0110	6.5	0.09	1.09	98.31
0.0078	7	0.12	1.49	99.80
0.0055	7.5	0.00	0.02	99.81
0.0039	8	0.00	0.02	99.83
0.00276	8.5	0.00	0.02	99.85
0.00195	9	0.00	0.02	99.87
0.00138	9.5	0.00	0.02	99.89
0.00098	10	0.00	0.02	99.90
0.00069	10.5	0.00	0.02	99.92
0.00049	11	0.00	0.02	99.94
0.00035	11.5	0.00	0.02	99.96
0.00024	12	0.00	0.02	99.98
0.00017	12.5	0.00	0.02	99.99
0.00012	13	0.00	0.02	100.00
0.00009	13.5	0.00	0.02	100.00
0.00006	14	0.00	0.02	100.00

Einhyrningur. SILK-A1 bulk sample

Millimeters	Phi	Weight g	Weight %	Cumulative %
16.0	-4	0.00	0.00	0.00
11.3	-3.5	0.00	0.00	0.00
8.0	-3	0.00	0.00	0.00
5.7	-2.5	0.00	0.00	0.00
4.0	-2	0.00	0.00	0.00
2.8	-1.5	0.00	0.00	0.00
2.0	-1	0.00	0.00	0.00
1.4	-0.5	0.04	0.16	0.16
1.0	0	0.30	1.20	1.35
0.710	0.5	0.34	1.35	2.71
0.500	1	1.09	4.34	7.05
0.354	1.5	2.10	8.37	15.42
0.250	2	2.74	10.92	26.33
0.177	2.5	2.51	10.00	36.33
0.125	3	3.09	12.31	48.65
0.088	3.5	2.76	11.00	59.64
0.063	4	0.76	3.04	62.68
0.044	4.5	1.63	6.48	69.16
0.031	5	2.06	8.23	77.39
0.022	5.5	1.82	7.25	84.64
0.0156	6	1.36	5.43	90.07
0.0110	6.5	0.79	3.16	93.23
0.0078	7	0.44	1.74	94.97
0.0055	7.5	0.19	0.77	95.74
0.0039	8	0.28	1.13	96.88
0.00276	8.5	0.02	0.08	96.96
0.00195	9	0.03	0.12	97.08
0.00138	9.5	0.08	0.32	97.40
0.00098	10	0.16	0.65	98.05
0.00069	10.5	0.06	0.24	98.30
0.00049	11	0.06	0.24	98.54
0.00035	11.5	0.06	0.24	98.78
0.00024	12	0.06	0.24	99.03
0.00017	12.5	0.06	0.24	99.27
0.00012	13	0.06	0.24	99.52
0.00009	13.5	0.06	0.24	99.76
0.00006	14	0.06	0.24	100.00

Einhyrningur. SILK-A5 bulk sample

Millimeters	Phi	Weight g	Weight %	Cumulative %
16.0	-4	0.00	0.00	0.00
11.3	-3.5	0.00	0.00	0.00
8.0	-3	0.00	0.00	0.00
5.7	-2.5	0.00	0.00	0.00
4.0	-2	0.00	0.00	0.00
2.8	-1.5	0.00	0.00	0.00
2.0	-1	0.00	0.00	0.00
1.4	-0.5	0.31	0.53	0.53
1.0	0	1.09	1.85	2.37
0.710	0.5	2.06	3.49	5.86
0.500	1	3.39	5.75	11.61
0.354	1.5	3.89	6.59	18.20
0.250	2	3.49	5.92	24.12
0.177	2.5	3.29	5.58	29.69
0.125	3	6.79	11.51	41.20
0.088	3.5	10.57	17.92	59.12
0.063	4	1.13	1.92	61.04
0.044	4.5	3.57	6.05	67.09
0.031	5	5.52	9.36	76.45
0.022	5.5	5.19	8.79	85.24
0.0156	6	3.69	6.25	91.50
0.0110	6.5	2.22	3.76	95.26
0.0078	7	1.04	1.76	97.02
0.0055	7.5	0.58	0.98	98.00
0.0039	8	0.27	0.45	98.45
0.00276	8.5	0.07	0.12	98.57
0.00195	9	0.00	0.00	98.57
0.00138	9.5	0.00	0.00	98.57
0.00098	10	0.31	0.53	99.10
0.00069	10.5	0.07	0.11	99.21
0.00049	11	0.07	0.11	99.33
0.00035	11.5	0.07	0.11	99.44
0.00024	12	0.07	0.11	99.55
0.00017	12.5	0.07	0.11	99.66
0.00012	13	0.07	0.11	99.77
0.00009	13.5	0.07	0.11	99.89
0.00006	14	0.07	0.11	100.00

Einhyrningur. SILK-A7 bulk sample

Millimeters	Phi	Weight g	Weight %	Cumulative %
16.0	-4	0.00	0.00	0.00
11.3	-3.5	0.00	0.00	0.00
8.0	-3	0.00	0.00	0.00
5.7	-2.5	0.00	0.00	0.00
4.0	-2	0.47	2.54	2.54
2.8	-1.5	1.20	6.48	9.02
2.0	-1	1.13	6.10	15.12
1.4	-0.5	1.29	6.97	22.08
1.0	0	1.33	7.18	29.27
0.710	0.5	1.20	6.48	35.75
0.500	1	1.16	6.26	42.01
0.354	1.5	1.07	5.78	47.79
0.250	2	1.19	6.43	54.21
0.177	2.5	1.43	7.72	61.93
0.125	3	2.00	10.80	72.73
0.088	3.5	1.62	8.75	81.48
0.063	4	0.40	2.15	83.63
0.044	4.5	0.87	4.72	88.36
0.031	5	0.94	5.06	93.41
0.022	5.5	0.56	3.02	96.43
0.0156	6	0.29	1.57	98.01
0.0110	6.5	0.12	0.67	98.68
0.0078	7	0.06	0.30	98.98
0.0055	7.5	0.01	0.06	99.04
0.0039	8	0.04	0.22	99.26
0.00276	8.5	0.00	0.00	99.26
0.00195	9	0.00	0.00	99.26
0.00138	9.5	0.05	0.24	99.50
0.00098	10	0.07	0.39	99.90
0.00069	10.5	0.00	0.01	99.91
0.00049	11	0.00	0.01	99.92
0.00035	11.5	0.00	0.01	99.94
0.00024	12	0.00	0.01	99.95
0.00017	12.5	0.00	0.01	99.96
0.00012	13	0.00	0.01	99.98
0.00009	13.5	0.00	0.01	99.99
0.00006	14	0.00	0.01	100.00

Einhyrningur. SILK-A8 bulk sample

Millimeters	Phi	Weight g	Weight %	Cumulative %
16.0	-4	0.00	0.00	0.00
11.3	-3.5	0.00	0.00	0.00
8.0	-3	0.00	0.00	0.00
5.7	-2.5	0.00	0.00	0.00
4.0	-2	0.00	0.00	0.00
2.8	-1.5	0.00	0.00	0.00
2.0	-1	0.01	0.01	0.01
1.4	-0.5	0.43	0.57	0.58
1.0	0	1.06	1.40	1.98
0.710	0.5	1.59	2.10	4.08
0.500	1	3.00	3.96	8.04
0.354	1.5	4.13	5.45	13.49
0.250	2	3.40	4.49	17.98
0.177	2.5	3.40	4.49	22.46
0.125	3	8.91	11.76	34.22
0.088	3.5	9.28	12.25	46.47
0.063	4	2.16	2.85	49.32
0.044	4.5	5.50	7.26	56.58
0.031	5	8.56	11.30	67.88
0.022	5.5	8.56	11.30	79.18
0.0156	6	6.48	8.55	87.73
0.0110	6.5	4.24	5.59	93.32
0.0078	7	2.08	2.74	96.07
0.0055	7.5	1.30	1.72	97.79
0.0039	8	0.45	0.59	98.38
0.00276	8.5	0.37	0.48	98.87
0.00195	9	0.04	0.05	98.92
0.00138	9.5	0.20	0.27	99.19
0.00098	10	0.61	0.81	100.00
0.00069	10.5	0.00	0.00	100.00
0.00049	11	0.00	0.00	100.00
0.00035	11.5	0.00	0.00	100.00
0.00024	12	0.00	0.00	100.00
0.00017	12.5	0.00	0.00	100.00
0.00012	13	0.00	0.00	100.00
0.00009	13.5	0.00	0.00	100.00
0.00006	14	0.00	0.00	100.00

Einhyrningur. SILK-A12 bulk sample

Millimeters	Phi	Weight g	Weight %	Cumulative %
16.0	-4	0.00	0.00	0.00
11.3	-3.5	0.00	0.00	0.00
8.0	-3	0.00	0.00	0.00
5.7	-2.5	0.00	0.00	0.00
4.0	-2	0.00	0.00	0.00
2.8	-1.5	0.00	0.00	0.00
2.0	-1	0.06	0.16	0.16
1.4	-0.5	1.11	2.97	3.13
1.0	0	1.33	3.56	6.69
0.710	0.5	1.80	4.82	11.51
0.500	1	2.31	6.18	17.69
0.354	1.5	2.59	6.93	24.63
0.250	2	2.69	7.20	31.83
0.177	2.5	2.79	7.47	39.29
0.125	3	5.02	13.44	52.73
0.088	3.5	4.78	12.79	65.52
0.063	4	1.36	3.64	69.16
0.044	4.5	2.96	7.94	77.10
0.031	5	3.27	8.74	85.83
0.022	5.5	2.32	6.22	92.06
0.0156	6	1.24	3.32	95.38
0.0110	6.5	0.67	1.78	97.16
0.0078	7	0.34	0.91	98.07
0.0055	7.5	0.05	0.14	98.21
0.0039	8	0.10	0.28	98.49
0.00276	8.5	0.16	0.42	98.91
0.00195	9	0.00	0.00	98.91
0.00138	9.5	0.03	0.07	98.98
0.00098	10	0.00	0.00	98.98
0.00069	10.5	0.05	0.13	99.11
0.00049	11	0.05	0.13	99.23
0.00035	11.5	0.05	0.13	99.36
0.00024	12	0.05	0.13	99.49
0.00017	12.5	0.05	0.13	99.61
0.00012	13	0.05	0.13	99.74
0.00009	13.5	0.05	0.13	99.87
0.00006	14	0.05	0.13	100.00

Vestan Hafrafells. Hekla 1947 bulk sample

Millimeters	Phi	Weight g	Weight %	Cumulative %
16.0	-4	2.94	12.18	12.18
11.3	-3.5	1.65	6.84	19.02
8.0	-3	1.25	5.18	24.20
5.7	-2.5	1.83	7.58	31.79
4.0	-2	1.33	5.51	37.30
2.8	-1.5	1.28	5.30	42.60
2.0	-1	0.9	3.73	46.33
1.4	-0.5	0.45	1.86	48.20
1.0	0	0.28	1.16	49.36
0.710	0.5	0.19	0.79	50.15
0.500	1	0.15	0.62	50.77
0.354	1.5	0.11	0.46	51.22
0.250	2	0.20	0.83	52.05
0.177	2.5	0.55	2.28	54.33
0.125	3	3.07	12.72	67.05
0.088	3.5	3.65	15.13	82.18
0.063	4	0.74	3.06	85.24
0.044	4.5	1.58	6.56	91.81
0.031	5	1.17	4.87	96.67
0.022	5.5	0.39	1.62	98.30
0.0156	6	0.07	0.29	98.58
0.0110	6.5	0.06	0.25	98.84
0.0078	7	0.11	0.47	99.31
0.0055	7.5	0.01	0.05	99.36
0.0039	8	0.01	0.05	99.41
0.00276	8.5	0.01	0.05	99.46
0.00195	9	0.01	0.05	99.51
0.00138	9.5	0.01	0.05	99.56
0.00098	10	0.01	0.05	99.61
0.00069	10.5	0.01	0.05	99.66
0.00049	11	0.01	0.05	99.71
0.00035	11.5	0.01	0.05	99.76
0.00024	12	0.01	0.05	99.81
0.00017	12.5	0.01	0.05	99.86
0.00012	13	0.01	0.05	99.91
0.00009	13.5	0.01	0.05	99.96
0.00006	14	0.01	0.05	100.00

Fljótalsdalsheiði. Hekla 1947 bulk sample (1)

Millimeters	Phi	Weight g	Weight %	Cumulative %
16.0	-4	1.32	1.16	1.16
11.3	-3.5	3.43	3.02	4.18
8.0	-3	5.93	5.22	9.41
5.7	-2.5	15.3	13.47	22.88
4.0	-2	15.16	13.35	36.23
2.8	-1.5	18.73	16.49	52.73
2.0	-1	18.45	16.25	68.97
1.4	-0.5	12.35	10.88	79.85
1.0	0	6.14	5.41	85.26
0.710	0.5	3.36	2.96	88.22
0.500	1	2.37	2.09	90.30
0.354	1.5	1.55	1.37	91.67
0.250	2	1.32	1.16	92.83
0.177	2.5	1.07	0.94	93.77
0.125	3	2.03	1.79	95.56
0.088	3.5	1.70	1.50	97.06
0.063	4	0.42	0.37	97.44
0.044	4.5	0.94	0.83	98.27
0.031	5	1.02	0.90	99.17
0.022	5.5	0.54	0.47	99.64
0.0156	6	0.19	0.16	99.81
0.0110	6.5	0.05	0.04	99.85
0.0078	7	0.00	0.00	99.85
0.0055	7.5	0.02	0.01	99.87
0.0039	8	0.02	0.02	99.89
0.00276	8.5	0.11	0.09	99.98
0.00195	9	0.00	0.00	99.98
0.00138	9.5	0.00	0.00	99.98
0.00098	10	0.00	0.00	99.98
0.00069	10.5	0.00	0.00	99.99
0.00049	11	0.00	0.00	99.99
0.00035	11.5	0.00	0.00	99.99
0.00024	12	0.00	0.00	99.99
0.00017	12.5	0.00	0.00	99.99
0.00012	13	0.00	0.00	99.99
0.00009	13.5	0.00	0.00	100.00
0.00006	14	0.00	0.00	100.00

Fljótisdalsheiði. Hekla 1947 bulk sample (2)

Millimeters	Phi	Weight g	Weight %	Cumulative %
16.0	-4	0.00	0.00	0.00
11.3	-3.5	2.53	4.79	4.79
8.0	-3	4.88	9.24	14.02
5.7	-2.5	6.49	12.28	26.31
4.0	-2	6.24	11.81	38.12
2.8	-1.5	5.67	10.73	48.85
2.0	-1	5.76	10.90	59.75
1.4	-0.5	4.00	7.57	67.32
1.0	0	2.44	4.62	71.93
0.710	0.5	1.75	3.31	75.25
0.500	1	1.59	3.01	78.26
0.354	1.5	1.75	3.31	81.57
0.250	2	1.74	3.29	84.86
0.177	2.5	2.84	5.37	90.23
0.125	3	3.54	6.70	96.93
0.088	3.5	1.13	2.14	99.07
0.063	4	0.05	0.10	99.17
0.044	4.5	0.15	0.28	99.45
0.031	5	0.14	0.26	99.71
0.022	5.5	0.05	0.09	99.80
0.0156	6	0.02	0.03	99.83
0.0110	6.5	0.01	0.02	99.84
0.0078	7	0.03	0.05	99.90
0.0055	7.5	0.00	0.00	99.90
0.0039	8	0.00	0.00	99.90
0.00276	8.5	0.00	0.01	99.90
0.00195	9	0.01	0.02	99.93
0.00138	9.5	0.01	0.02	99.95
0.00098	10	0.01	0.02	99.97
0.00069	10.5	0.00	0.00	99.97
0.00049	11	0.00	0.00	99.98
0.00035	11.5	0.00	0.00	99.98
0.00024	12	0.00	0.00	99.98
0.00017	12.5	0.00	0.00	99.99
0.00012	13	0.00	0.00	99.99
0.00009	13.5	0.00	0.00	99.99
0.00006	14	0.00	0.00	100.00

Fljótisdalsheiði. Hekla 1947 bulk sample (3)

Millimeters	Phi	Weight g	Weight %	Cumulative %
16.0	-4	0.00	0.00	0.00
11.3	-3.5	2.08	3.24	3.24
8.0	-3	1.59	2.47	5.71
5.7	-2.5	9.77	15.20	20.91
4.0	-2	10.97	17.06	37.97
2.8	-1.5	14.17	22.04	60.01
2.0	-1	12.05	18.74	78.75
1.4	-0.5	7.37	11.46	90.22
1.0	0	2.87	4.46	94.68
0.710	0.5	0.9	1.40	96.08
0.500	1	0.35	0.54	96.62
0.354	1.5	0.21	0.33	96.95
0.250	2	0.16	0.25	97.20
0.177	2.5	0.12	0.19	97.39
0.125	3	0.26	0.40	97.79
0.088	3.5	0.35	0.54	98.34
0.063	4	0.12	0.18	98.52
0.044	4.5	0.27	0.42	98.94
0.031	5	0.30	0.47	99.41
0.022	5.5	0.16	0.26	99.67
0.0156	6	0.10	0.15	99.82
0.0110	6.5	0.04	0.07	99.88
0.0078	7	0.07	0.11	100.00
0.0055	7.5	0.00	0.00	100.00
0.0039	8	0.00	0.00	100.00
0.00276	8.5	0.00	0.00	100.00
0.00195	9	0.00	0.00	100.00
0.00138	9.5	0.00	0.00	100.00
0.00098	10	0.00	0.00	100.00
0.00069	10.5	0.00	0.00	100.00
0.00049	11	0.00	0.00	100.00
0.00035	11.5	0.00	0.00	100.00
0.00024	12	0.00	0.00	100.00
0.00017	12.5	0.00	0.00	100.00
0.00012	13	0.00	0.00	100.00
0.00009	13.5	0.00	0.00	100.00
0.00006	14	0.00	0.00	100.00

Hamragarðaheiði. Hekla 1947 bulk sample (1)

Millimeters	Phi	Weight g	Weight %	Cumulative %
16.0	-4	0.00	0.00	0.00
11.3	-3.5	0.00	0.00	0.00
8.0	-3	0.00	0.00	0.00
5.7	-2.5	0.34	0.46	0.46
4.0	-2	2.43	3.32	3.79
2.8	-1.5	5.49	7.50	11.29
2.0	-1	10.14	13.86	25.14
1.4	-0.5	14.69	20.07	45.22
1.0	0	19.48	26.62	71.84
0.710	0.5	13.22	18.07	89.90
0.500	1	3.35	4.58	94.48
0.354	1.5	0.69	0.94	95.42
0.250	2	0.37	0.51	95.93
0.177	2.5	0.39	0.53	96.46
0.125	3	0.75	1.02	97.49
0.088	3.5	0.74	1.01	98.50
0.063	4	0.22	0.30	98.80
0.044	4.5	0.34	0.47	99.26
0.031	5	0.26	0.35	99.62
0.022	5.5	0.12	0.17	99.78
0.0156	6	0.05	0.07	99.86
0.0110	6.5	0.03	0.05	99.90
0.0078	7	0.06	0.08	99.98
0.0055	7.5	0.00	0.00	99.98
0.0039	8	0.00	0.00	99.98
0.00276	8.5	0.02	0.02	100.00
0.00195	9	0.00	0.00	100.00
0.00138	9.5	0.00	0.00	100.00
0.00098	10	0.00	0.00	100.00
0.00069	10.5	0.00	0.00	100.00
0.00049	11	0.00	0.00	100.00
0.00035	11.5	0.00	0.00	100.00
0.00024	12	0.00	0.00	100.00
0.00017	12.5	0.00	0.00	100.00
0.00012	13	0.00	0.00	100.00
0.00009	13.5	0.00	0.00	100.00
0.00006	14	0.00	0.00	100.00

Hamragarðaheiði. Hekla 1947 bulk sample (2)

Millimeters	Phi	Weight g	Weight %	Cumulative %
16.0	-4	0	0	0
11.3	-3.5	0	0	0
8.0	-3	0	0	0
5.7	-2.5	0	0	0
4.0	-2	0.39	1.23	1.23
2.8	-1.5	1.23	3.87	5.10
2.0	-1	2.53	7.96	13.06
1.4	-0.5	6.18	19.45	32.51
1.0	0	9.14	28.77	61.28
0.710	0.5	7.16	22.54	83.82
0.500	1	2.52	7.93	91.75
0.354	1.5	0.52	1.64	93.39
0.250	2	0.24	0.76	94.15
0.177	2.5	0.22	0.69	94.84
0.125	3	0.38	1.20	96.03
0.088	3.5	0.34	1.07	97.10
0.063	4	0.15	0.47	97.58
0.044	4.5	0.28	0.89	98.47
0.031	5	0.23	0.71	99.17
0.022	5.5	0.09	0.27	99.45
0.0156	6	0.02	0.06	99.50
0.0110	6.5	0.07	0.23	99.73
0.0078	7	0.01	0.04	99.77
0.0055	7.5	0.03	0.09	99.86
0.0039	8	0.02	0.05	99.91
0.00276	8.5	0.00	0.01	99.92
0.00195	9	0.00	0.01	99.93
0.00138	9.5	0.00	0.01	99.94
0.00098	10	0.00	0.01	99.94
0.00069	10.5	0.00	0.01	99.95
0.00049	11	0.00	0.01	99.96
0.00035	11.5	0.00	0.01	99.97
0.00024	12	0.00	0.01	99.97
0.00017	12.5	0.00	0.01	99.98
0.00012	13	0.00	0.01	99.99
0.00009	13.5	0.00	0.01	100.00
0.00006	14	0.00	0.01	100.00

Hamragarðaheiði. Hekla 1947 bulk sample (3)

Millimeters	Phi	Weight g	Weight %	Cumulative %
16.0	-4	0.00	0.00	0.00
11.3	-3.5	0.00	0.00	0.00
8.0	-3	0.00	0.00	0.00
5.7	-2.5	0.00	0.00	0.00
4.0	-2	0.20	1.06	1.06
2.8	-1.5	0.22	1.17	2.23
2.0	-1	0.88	4.68	6.91
1.4	-0.5	1.82	9.67	16.58
1.0	0	3.66	19.45	36.03
0.710	0.5	4.44	23.59	59.62
0.500	1	1.87	9.94	69.55
0.354	1.5	0.95	5.05	74.60
0.250	2	0.95	5.05	79.65
0.177	2.5	0.70	3.72	83.37
0.125	3	1.12	5.95	89.32
0.088	3.5	0.84	4.46	93.78
0.063	4	0.21	1.14	94.92
0.044	4.5	0.34	1.81	96.73
0.031	5	0.27	1.45	98.19
0.022	5.5	0.14	0.73	98.91
0.0156	6	0.08	0.41	99.33
0.0110	6.5	0.02	0.12	99.44
0.0078	7	0.03	0.14	99.58
0.0055	7.5	0.02	0.11	99.69
0.0039	8	0.00	0.02	99.71
0.00276	8.5	0.03	0.18	99.89
0.00195	9	0.00	0.01	99.90
0.00138	9.5	0.00	0.01	99.91
0.00098	10	0.00	0.01	99.92
0.00069	10.5	0.00	0.01	99.93
0.00049	11	0.00	0.01	99.94
0.00035	11.5	0.00	0.01	99.95
0.00024	12	0.00	0.01	99.97
0.00017	12.5	0.00	0.01	99.98
0.00012	13	0.00	0.01	99.99
0.00009	13.5	0.00	0.01	100.00
0.00006	14	0.00	0.01	100.00

Hamragarðaheiði. Hekla 1947 bulk sample (4)

Millimeters	Phi	Weight g	Weight %	Cumulative %
16.0	-4	0.00	0.00	0.00
11.3	-3.5	0.00	0.00	0.00
8.0	-3	0.00	0.00	0.00
5.7	-2.5	0.00	0.00	0.00
4.0	-2	0.08	0.77	0.77
2.8	-1.5	0.2	1.93	2.71
2.0	-1	0.57	5.51	8.22
1.4	-0.5	1.16	11.22	19.44
1.0	0	1.54	14.89	34.33
0.710	0.5	1.99	19.25	53.58
0.500	1	1.09	10.54	64.12
0.354	1.5	0.66	6.38	70.50
0.250	2	0.47	4.55	75.05
0.177	2.5	0.43	4.16	79.21
0.125	3	0.59	5.71	84.91
0.088	3.5	0.6	5.80	90.72
0.063	4	0.10	0.98	91.69
0.044	4.5	0.24	2.33	94.02
0.031	5	0.29	2.76	96.78
0.022	5.5	0.15	1.45	98.23
0.0156	6	0.06	0.57	98.80
0.0110	6.5	0.03	0.30	99.10
0.0078	7	0.01	0.12	99.23
0.0055	7.5	0.00	0.02	99.25
0.0039	8	0.01	0.09	99.34
0.00276	8.5	0.00	0.02	99.36
0.00195	9	0.00	0.00	99.36
0.00138	9.5	0.00	0.00	99.36
0.00098	10	0.03	0.28	99.64
0.00069	10.5	0.01	0.06	99.70
0.00049	11	0.01	0.06	99.76
0.00035	11.5	0.01	0.06	99.83
0.00024	12	0.01	0.06	99.89
0.00017	12.5	0.01	0.06	99.95
0.00012	13	0.01	0.06	100.00
0.00009	13.5	0.01	0.06	100.00
0.00006	14	0.01	0.06	100.00

Appendix V

Grain morphology results: raw data

Geldingasker SILK-LN. middle unit

	Area	Perim.	Long	Interm.	R1	R2	Circle	Elong	Facet	Roundn.
Mean	4.11	8.76	3.17	2.07	0.85	0.33	0.67	0.68	0.26	0.16
St. dev.	0.16	1.90	0.83	0.97	0.05	0.07	0.12	0.16	0.06	0.04

Geldingasker SILK-LN. bottom unit

	Area	Perim.	Long	Interm.	R1	R2	Circle	Elong	Facet	Roundn.
Mean	4.92	9.87	3.87	2.03	0.85	0.34	0.63	0.55	0.29	0.18
St. dev.	1.97	1.95	0.88	1.02	0.03	0.09	0.10	0.16	0.07	0.05

Varmárfell SILK-LN. middle unit

	Area	Perim.	Long	Interm.	R1	R2	Circle	Elong	Facet	Roundn.
Mean	0.02	0.68	0.27	0.12	0.85	0.43	0.57	0.51	0.40	0.19
St. dev.	0.01	0.20	0.10	0.05	0.05	0.11	0.19	0.24	0.09	0.07

Varmárfell SILK-LN. Bottom unit

	Area	Perim.	Long	Interm.	R1	R2	Circle	Elong	Facet	Roundn.
Mean	0.02	0.64	0.26	0.12	0.86	0.45	0.62	0.53	0.39	0.22
St. dev.	0.01	0.19	0.10	0.03	0.05	0.10	0.16	0.22	0.07	0.07

Einhyrningsflatir SILK-N1. middle unit

	Area	Perim.	Long	Interm.	R1	R2	Circle	Elong	Facet	Roundn.
Mean	0.02	0.62	0.23	0.15	0.88	0.40	0.73	0.69	0.33	0.21
St. dev.	0.01	0.13	0.06	0.04	0.04	0.08	0.12	0.19	0.07	0.06

Einhyrningsflatir SILK-N1. bottom unit

	Area	Perim.	Long	Interm.	R1	R2	Circle	Elong	Facet	Roundn.
Mean	0.02	0.65	0.25	0.14	0.86	0.41	0.66	0.58	0.34	0.21
St. dev.	0.01	0.21	0.10	0.03	0.06	0.11	0.13	0.16	0.09	0.08

Einhyrningsflatir SILK-A8. bulk sample

	Area	Perim.	Long	Interm.	R1	R2	Circle	Elong	Facet	Roundn.
Mean	0.02	0.49	0.18	0.12	0.89	0.42	0.74	0.69	0.38	0.24
St. dev.	0.01	0.14	0.05	0.04	0.05	0.07	0.10	0.16	0.06	0.08

Einhyrningsflatir SILK-A11. bulk sample

	Area	Perim.	Long	Interm.	R1	R2	Circle	Elong	Facet	Roundn.
Mean	0.02	0.60	0.21	0.16	0.90	0.35	0.78	0.78	0.28	0.20
St. dev.	0.01	0.12	0.04	0.04	0.03	0.06	0.05	0.11	0.08	0.05

Einhyrningsflatir SILK-A12. bulk sample

	Area	Perim.	Long	Interm.	R1	R2	Circle	Elong	Facet	Roundn.
Mean	0.02	0.63	0.25	0.12	0.87	0.42	0.65	0.52	0.35	0.21
St. dev.	0.01	0.16	0.07	0.03	0.04	0.10	0.12	0.16	0.08	0.07

Vestan Hafrafells Hekla 1947. bulk sample

	Area	Perim.	Long	Interm.	R1	R2	Circle	Elong	Facet	Roundn.
Mean	0.01	0.41	0.15	0.11	0.88	0.40	0.73	0.73	0.37	0.24
St. dev.	0.00	0.09	0.04	0.03	0.05	0.09	0.11	0.15	0.08	0.08

Hamragarðaheiði Hekla 1947. bulk sample

	Area	Perim.	Long	Interm.	R1	R2	Circle	Elong	Facet	Roundn.
Mean	0.02	0.52	0.19	0.14	0.89	0.41	0.75	0.73	0.35	0.24
St. dev.	0.01	0.11	0.05	0.03	0.05	0.10	0.11	0.11	0.08	0.08

Appendix VI

Grain morphology results: shadow images

Shadow images of grains from SILK-N1 tephra layer. middle unit
(mixture from 3 and 3.5 Φ grain size categories)



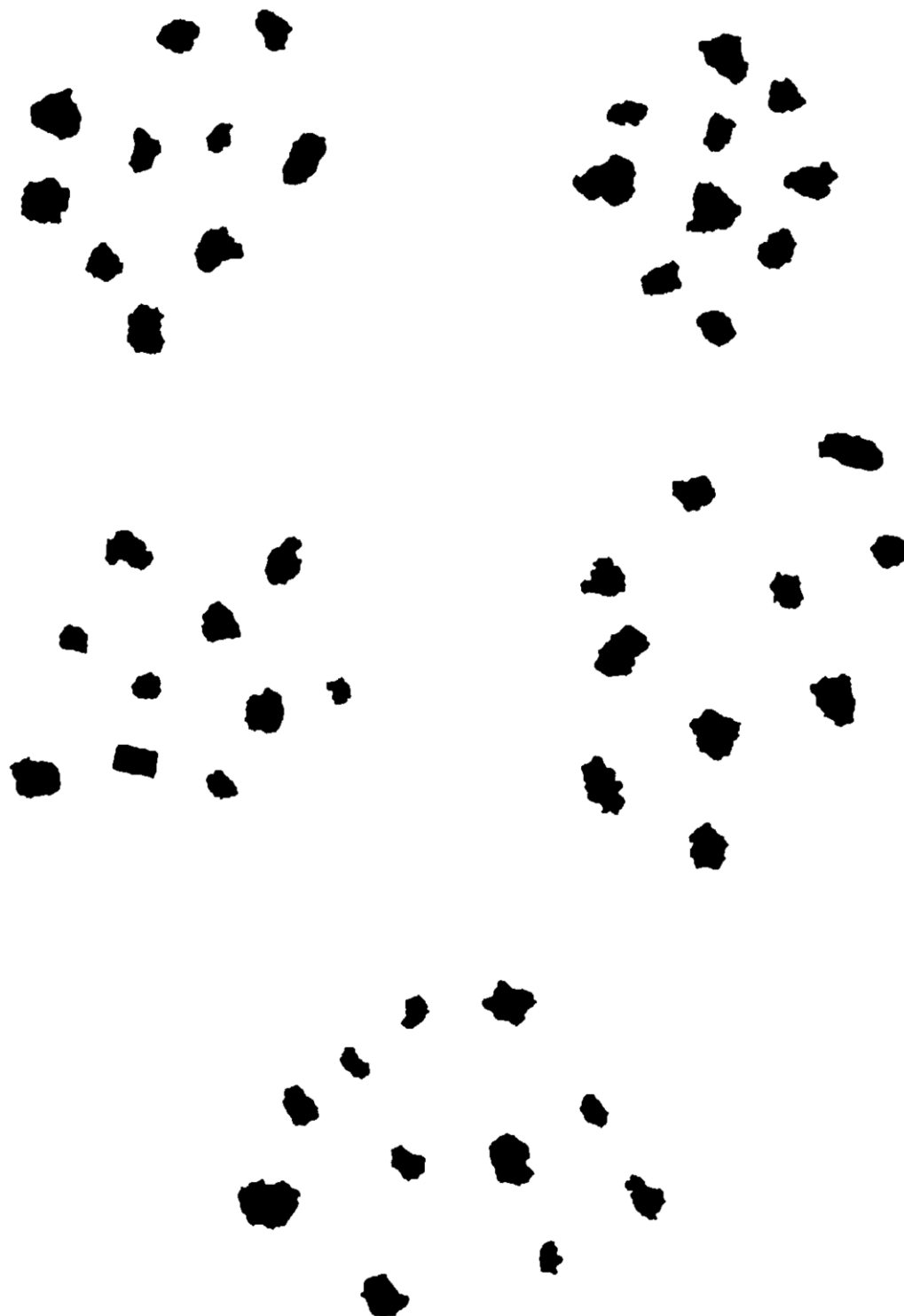
Shadow images of grains from SILK-N1 tephra layer. bottom unit
(mixture from 3 and 3.5 Φ grain size categories)



Shadow images of grains from SILK-A8 tephra layer. bulk sample
(mixture from 3 and 3.5 Φ grain size categories)



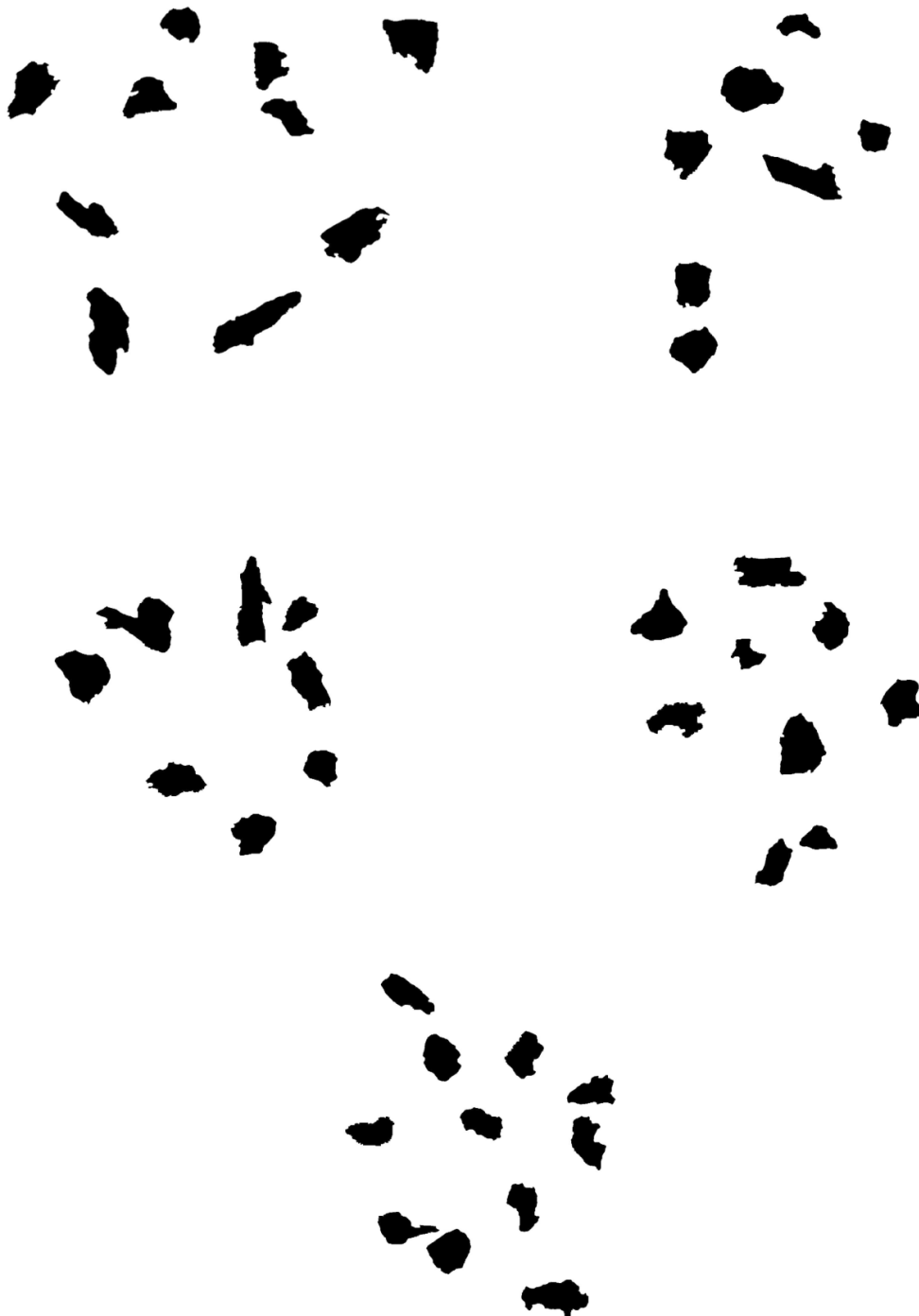
Shadow images of grains from SILK-A11 tephra layer. bulk sample
(mixture from 3 and 3.5 Φ grain size categories)



Shadow images of grains from SILK-A12 tephra layer. bulk sample
(mixture from 3 and 3.5 Φ grain size categories)

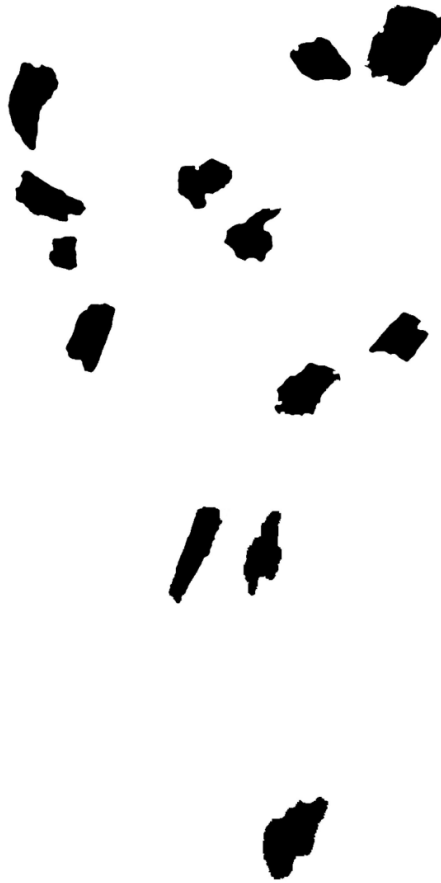


Shadow images of grains from SILK-LN tephra layer, middle unit in Geldingasker
(mixture from 3 and 3.5 Φ grain size categories)



Shadow images of grains from SILK-LN tephra layer. bottom unit in Geldingasker
(mixture from 3 and 3.5 Φ grain size categories)





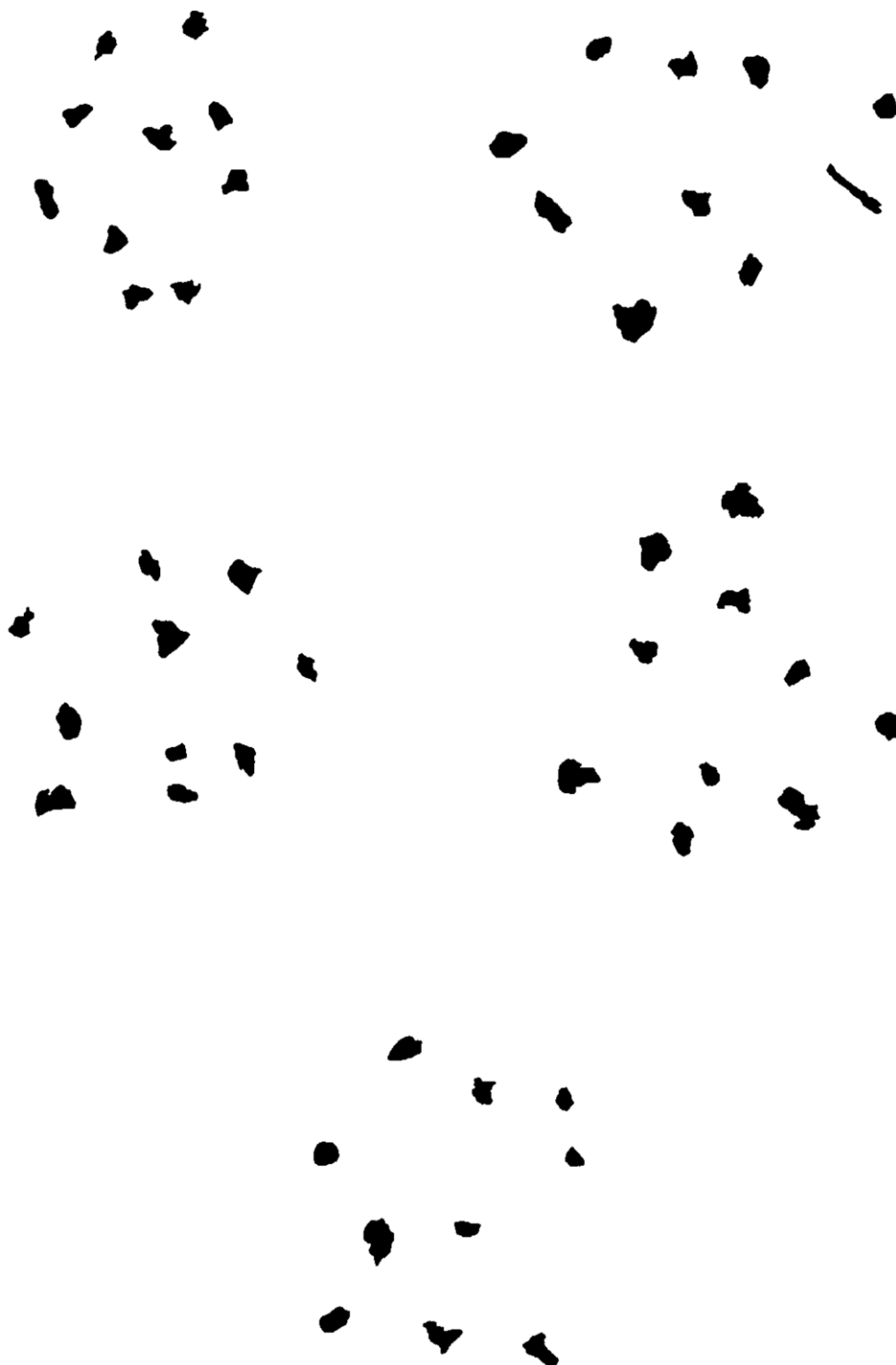
Shadow images of grains from SILK-LN tephra layer. middle unit in Varmárfell
(mixture from 3 and 3.5 Φ grain size categories)



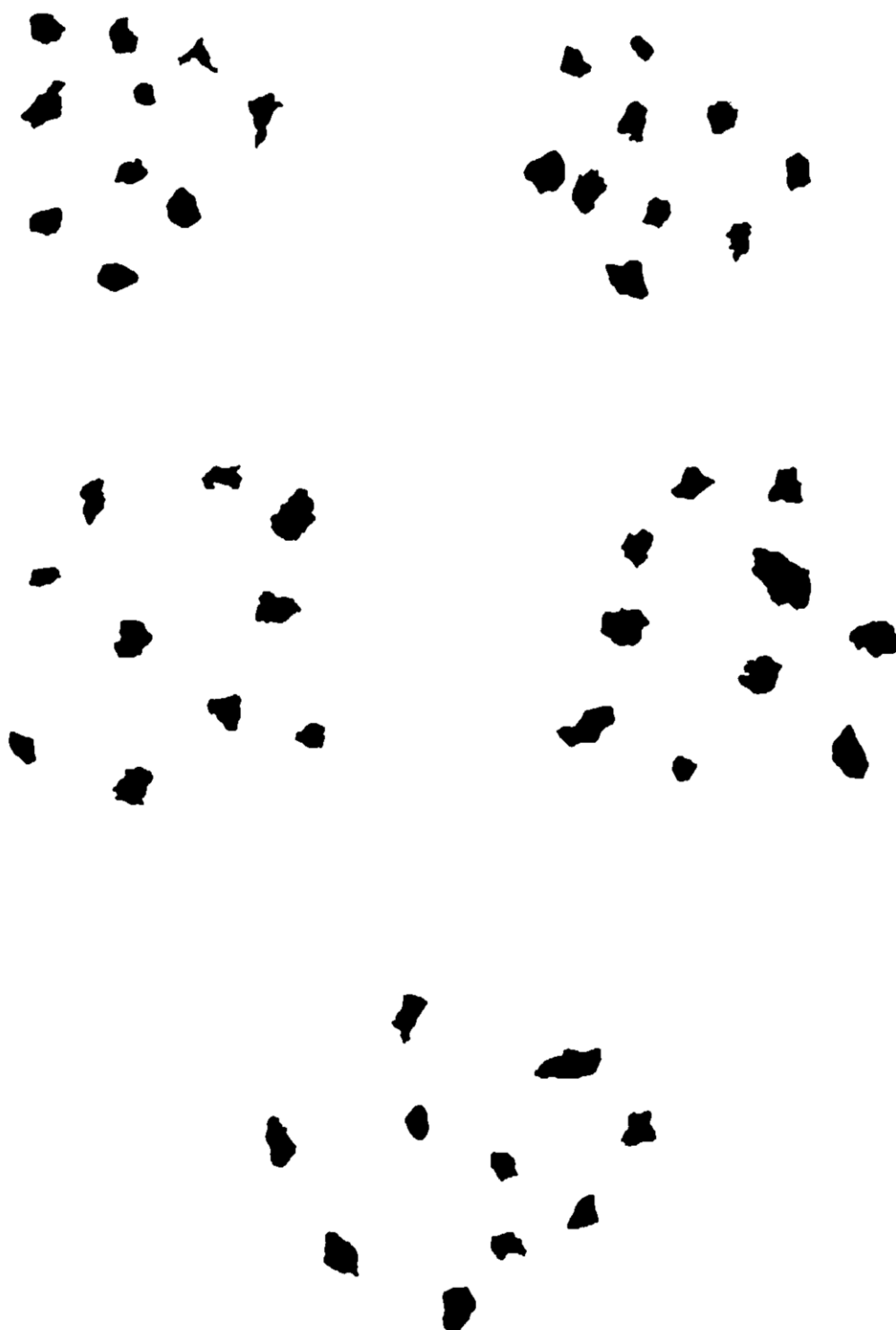
Shadow images of grains from SILK-LN tephra layer. bottom unit in Varmárfell
(mixture from 3 and 3.5 Φ grain size categories)



Shadow images of grains from Hekla 1947 tephra layer. bulk sample from Vestan
Hafrafells (mixture from 3 and 3.5 Φ grain size categories)



Shadow images of grains from Hekla 1947 tephra layer. bulk sample from Hamrgarðaheiði
(mixture from 3 and 3.5 Φ grain size categories)



Appendix VII

Major element composition for SILK-LN and Hekla 1947

Katla SILK tephra layers

Tephra	SiO ₂	TiO ₂	Al ₂ O ₃	FeO	MnO	MgO	CaO	Na ₂ O	K ₂ O	Total
SILK-YN	66.39	0.98	14.07	5.52	0.18	0.84	2.38	4.78	3.00	98.14
	65.90	1.27	14.01	6.17	0.21	1.07	2.86	4.37	2.63	98.49
	65.64	1.1	14.46	6.16	0.15	1.02	2.97	4.24	2.58	98.32
	65.61	1.19	14.33	5.99	0.16	1.11	3.09	4.51	2.73	98.72
	65.50	1.24	14.40	5.71	0.19	0.96	2.90	4.66	2.72	98.28
	65.5	1.11	14.10	6.18	0.18	1.10	2.95	4.66	2.71	98.49
	64.78	1.28	13.99	6.20	0.19	1.10	3.00	4.76	2.54	97.84
	64.66	1.25	13.94	6.16	0.19	1.23	3.25	4.66	2.74	98.08
	64.54	1.31	14.04	6.13	0.25	1.09	3.02	4.67	2.72	97.77
	64.53	1.19	14.16	6.14	0.17	1.11	2.97	4.18	2.60	97.05
Average	65.31	1.19	14.15	6.04	0.19	1.06	2.94	4.55	2.70	98.12

Tephra	SiO ₂	TiO ₂	Al ₂ O ₃	FeO	MnO	MgO	CaO	Na ₂ O	K ₂ O	Total
SILK-UN	64.97	1.4	14.05	5.81	0.19	1.34	3.43	4.11	2.65	97.95
	64.55	1.37	13.83	5.96	0.22	1.40	3.31	4.54	2.30	97.48
	64.36	1.31	14.36	5.85	0.18	1.47	3.62	4.13	2.62	97.90
	64.22	1.43	14.01	5.67	0.16	1.29	3.50	4.49	2.63	97.40
	64.21	1.27	13.89	6.19	0.17	1.32	3.34	4.10	2.60	97.09
	64.09	1.38	14.11	6.04	0.19	1.36	3.38	4.54	2.57	97.66
	64.02	1.28	13.98	5.24	0.20	1.19	3.17	4.53	2.70	96.31
	63.93	1.26	13.92	6.14	0.20	1.47	3.50	4.64	2.58	97.64
	63.66	1.29	13.43	6.25	0.25	1.36	3.44	4.35	2.68	96.71
	63.59	1.32	13.93	6.26	0.23	1.36	3.28	4.30	2.60	96.86
Average	64.16	1.33	13.95	5.94	0.20	1.36	3.40	4.37	2.59	97.30

Tephra	SiO ₂	TiO ₂	Al ₂ O ₃	FeO	MnO	MgO	CaO	Na ₂ O	K ₂ O	Total
SILK-MN	66.43	1.05	14.30	5.38	0.17	1.08	2.86	4.01	2.44	97.72
	65.82	1.16	14.33	5.63	0.27	1.11	3.03	4.53	2.50	98.38
	65.72	1.16	14.34	5.47	0.21	1.19	3.06	4.05	2.69	97.89
	65.45	1.25	13.96	5.58	0.23	1.22	2.98	4.24	2.70	97.61
	65.13	1.24	14.20	5.82	0.20	1.20	2.88	4.35	2.82	97.84
	64.92	1.22	14.07	5.51	0.18	1.09	2.89	4.48	2.58	96.94
	64.85	1.25	14.47	5.50	0.21	1.11	3.09	4.01	2.49	96.98
	64.77	1.20	13.97	5.43	0.22	1.06	2.92	4.10	2.78	96.45
Average	65.39	1.19	14.21	5.54	0.21	1.13	2.96	4.22	2.63	97.48

Tephra	SiO ₂	TiO ₂	Al ₂ O ₃	FeO	MnO	MgO	CaO	Na ₂ O	K ₂ O	Total
SILK-LN	65.93	1.25	14.32	5.83	0.20	1.12	3.06	4.51	2.91	99.13
	65.84	1.26	14.34	5.80	0.18	1.09	3.15	4.45	2.83	98.94
	65.63	1.27	14.09	5.48	0.20	1.09	3.02	4.54	2.86	98.18
	65.58	1.12	14.38	5.73	0.23	1.18	2.95	4.40	2.74	98.31
	65.34	1.24	14.29	5.69	0.10	1.14	3.06	4.51	2.76	98.31
	65.3	1.20	14.19	5.38	0.15	1.12	3.08	4.28	2.79	97.49
	65.01	1.23	14.45	5.42	0.18	1.19	2.90	4.09	2.64	97.11
	64.28	1.14	14.03	5.65	0.20	1.08	3.03	4.49	2.60	96.50
	64.12	1.22	14.13	5.60	0.25	1.11	2.92	4.54	2.71	96.60
Average	65.23	1.21	14.25	5.62	0.19	1.12	3.02	4.42	2.76	97.84

Tephra	SiO ₂	TiO ₂	Al ₂ O ₃	FeO	MnO	MgO	CaO	Na ₂ O	K ₂ O	Total
SILK-N4	67.25	1.19	14.2	4.96	0.18	1.03	2.71	4.57	2.95	99.04
	66.66	1.30	14.10	5.98	0.17	1.07	3.07	4.23	2.79	99.37
	66.62	1.32	14.13	5.35	0.19	1.12	2.79	4.42	2.81	98.75
	66.39	1.22	13.98	5.94	0.17	1.12	2.92	4.63	2.79	99.16
	66.18	1.26	14.08	5.58	0.16	1.19	2.83	4.69	2.80	98.77
	66.12	1.19	14.25	5.72	0.20	1.13	2.95	4.41	2.73	98.70
	65.84	1.12	14.08	5.55	0.20	1.05	2.93	4.40	2.67	97.84
	65.70	1.22	14.15	5.60	0.17	1.15	2.91	4.29	2.87	98.06
	65.61	1.28	14.13	5.45	0.13	1.41	2.81	4.64	2.83	98.29
	65.57	1.23	13.87	5.55	0.22	1.13	3.08	4.73	2.74	98.12
Average	66.19	1.23	14.10	5.57	1.79	1.14	2.90	4.50	2.80	98.61

Tephra	SiO ₂	TiO ₂	Al ₂ O ₃	FeO	MnO	MgO	CaO	Na ₂ O	K ₂ O	Total
SILK-N3	65.50	1.37	14.32	5.96	0.18	1.33	3.51	4.35	2.55	99.07
	65.39	1.45	14.07	6.03	0.18	1.33	3.26	4.36	2.63	98.70
	65.17	1.47	14.30	5.84	0.23	1.33	3.45	4.35	2.50	98.64
	65.02	1.53	14.03	6.09	0.24	1.39	3.43	3.94	2.62	98.29
	64.91	1.50	14.06	4.74	0.15	1.30	3.38	4.31	2.68	97.03
	64.67	1.48	14.43	6.12	0.25	1.38	3.33	4.30	2.49	98.45
	64.40	1.35	14.17	6.03	0.21	1.40	3.37	4.25	2.71	97.89
	64.18	1.58	13.96	6.02	0.20	1.39	3.23	4.17	2.62	97.35
	63.84	1.49	14.08	6.07	0.23	1.38	3.27	4.07	2.58	97.01
	63.77	1.59	14.06	6.66	0.15	1.28	3.24	4.42	2.64	97.81
Average	64.69	1.48	14.15	5.96	2.02	1.35	3.35	4.25	2.60	98.02

Tephra	SiO ₂	TiO ₂	Al ₂ O ₃	FeO	MnO	MgO	CaO	Na ₂ O	K ₂ O	Total
SILK-N2	64.31	1.50	14.07	6.23	0.23	1.35	3.53	4.39	2.52	98.13
	64.26	1.49	13.98	6.24	0.21	1.46	3.79	4.36	2.72	98.51
	63.95	1.49	14.14	6.47	0.25	1.35	3.58	4.57	2.47	98.27
	63.72	1.51	13.98	6.17	0.23	1.50	3.51	4.01	2.54	97.17
	63.63	1.67	14.03	6.16	0.14	1.44	3.47	4.23	2.55	97.32
	63.51	1.53	13.97	6.20	0.24	1.36	3.51	4.44	2.51	97.27
	63.41	1.36	13.79	6.44	0.19	1.47	3.61	4.21	2.44	96.92
	63.36	1.49	13.75	6.51	0.20	1.55	3.87	4.67	2.55	97.95
	63.26	1.50	13.70	6.50	0.19	1.37	3.53	4.30	2.56	96.91
	62.49	1.63	13.95	6.61	0.20	1.52	3.56	4.04	2.46	96.46
Average	63.59	1.52	13.94	6.35	0.21	1.44	3.60	4.32	2.53	97.49

Tephra	SiO ₂	TiO ₂	Al ₂ O ₃	FeO	MnO	MgO	CaO	Na ₂ O	K ₂ O	Total
SILK-N1	66.08	1.30	13.71	5.30	0.21	1.04	2.76	4.27	2.75	97.42
	65.73	1.37	13.79	5.71	0.18	1.15	3.02	4.07	2.72	97.74
	65.65	1.33	13.54	5.79	0.18	1.19	3.14	4.56	2.70	98.08
	65.49	1.44	13.45	5.81	0.18	1.17	2.97	4.65	2.83	97.99
	65.31	1.42	13.81	5.47	0.18	1.25	3.17	4.43	2.58	97.62
	65.22	1.36	13.87	5.92	0.13	1.23	3.05	4.49	2.94	98.21
	65.20	1.40	13.97	5.85	0.18	1.18	2.92	4.53	2.94	98.17
	65.08	1.32	13.60	6.12	0.28	1.22	3.03	4.75	2.80	98.20
	64.73	1.39	13.65	6.13	0.22	1.22	3.46	4.70	2.82	98.32
	64.69	1.35	13.26	5.66	0.18	1.22	2.82	4.70	2.71	96.59
Average	65.34	1.37	13.67	5.78	0.19	1.19	3.03	4.52	2.78	97.83

Tephra	SiO ₂	TiO ₂	Al ₂ O ₃	FeO	MnO	MgO	CaO	Na ₂ O	K ₂ O	Total
SILK-A1	67.55	1.14	14.01	5.28	0.16	1.14	2.69	4.50	2.89	99.63
	66.07	1.16	14.20	5.30	0.19	1.12	3.16	4.51	2.83	98.54
	65.73	1.12	14.26	5.44	0.17	1.21	3.01	4.36	2.78	98.08
	65.59	1.25	13.92	5.82	0.19	1.18	3.05	4.53	2.86	98.39
	65.55	1.22	14.09	5.64	0.15	1.21	3.15	4.24	2.69	97.94
	65.24	1.28	14.60	5.64	0.17	1.18	3.13	4.26	2.83	98.33
	65.23	1.27	14.07	5.55	0.21	1.11	3.19	4.49	2.75	97.87
	65.69	1.24	14.03	5.49	0.17	1.06	3.16	4.37	2.75	96.96
Average	65.83	1.21	14.15	5.52	0.18	1.15	3.07	4.41	2.80	98.22
	72.46	0.12	13.34	2.24	0.07	0.10	0.38	5.08	4.64	98.43
	72.15	0.12	13.30	2.32	0.06	0.08	0.40	4.93	4.88	98.24
	69.48	0.26	13.33	3.93	0.16	0.23	1.33	4.80	3.57	97.09
Average	71.36	0.17	13.32	2.83	0.10	0.14	0.70	4.94	4.36	97.92
	49.87	3.81	12.95	12.17	0.26	3.82	8.00	3.54	1.22	95.64
	48.24	4.12	12.40	13.91	0.24	4.49	8.80	3.37	0.93	96.50
	47.25	4.51	12.66	14.18	0.22	5.10	9.15	3.22	0.85	97.14
	47.24	4.72	12.40	14.96	0.23	4.76	9.35	3.11	0.76	97.53
Average	48.15	4.29	12.60	13.81	0.24	4.54	8.83	3.31	0.94	96.7

Tephra	SiO ₂	TiO ₂	Al ₂ O ₃	FeO	MnO	MgO	CaO	Na ₂ O	K ₂ O	Total
SILK-A8	66.13	1.08	14.04	5.19	0.18	0.95	2.76	4.54	2.89	97.76
	65.38	1.29	14.24	5.81	0.15	1.22	3.19	4.67	2.61	98.56
	65.12	1.10	13.42	5.82	0.14	1.18	3.42	4.59	2.74	97.53
	64.47	1.20	14.25	5.56	0.23	1.20	3.36	4.61	2.49	97.37
	64.39	1.26	13.95	5.86	0.19	1.30	3.33	4.73	2.70	97.71
	64.23	1.24	13.97	5.91	0.14	1.22	3.29	4.50	2.67	97.17
	63.88	1.32	14.22	6.07	0.18	1.32	3.54	4.68	2.43	97.64
	63.75	1.29	13.89	5.88	0.19	1.31	3.64	4.68	2.65	97.28
	63.56	1.31	13.84	5.72	0.19	1.23	3.34	4.76	2.59	96.54
	63.44	1.44	14.13	5.95	0.15	1.34	3.53	4.34	2.75	97.07
Average	64.44	1.25	14.00	5.78	0.17	1.23	3.34	4.61	2.65	97.46

Tephra	SiO₂	TiO₂	Al₂O₃	FeO	MnO	MgO	CaO	Na₂O	K₂O	Total
SILK-A9	65.73	1.08	14.05	5.30	0.12	1.14	2.84	4.54	2.65	97.45
	65.54	1.22	14.39	5.53	0.21	1.17	3.19	4.44	2.72	98.41
	65.47	1.19	14.09	5.56	0.23	1.16	3.22	4.44	2.65	98.01
	65.07	1.05	13.85	5.59	0.18	1.11	3.19	4.66	2.70	97.40
	64.89	1.14	14.04	5.33	0.16	1.15	3.26	4.46	2.70	97.13
	64.63	1.10	13.83	5.45	0.16	1.13	3.07	4.55	2.81	96.73
	64.54	1.20	14.04	5.48	0.16	1.16	3.15	4.75	2.68	97.16
	64.22	1.20	13.87	5.52	0.16	1.16	2.91	4.83	2.62	96.49
	63.86	1.12	13.74	5.27	0.15	1.09	3.08	4.72	2.75	95.78
Average	64.88	1.14	14.00	5.45	0.14	1.14	3.10	4.60	2.70	97.17

Tephra	SiO₂	TiO₂	Al₂O₃	FeO	MnO	MgO	CaO	Na₂O₃	K₂O	Total
SILK-A11	69.48	0.83	13.98	4.26	0.21	0.80	2.14	4.43	3.23	99.36
	69.08	0.92	13.76	4.18	0.17	0.73	2.00	4.59	3.19	98.62
	68.92	0.98	13.77	4.14	0.11	0.76	2.08	4.71	3.15	98.62
	68.62	0.91	13.81	4.53	0.14	0.71	2.18	3.94	3.02	97.86
	68.13	0.89	14.13	4.22	0.20	0.77	2.10	4.93	3.17	98.70
	67.30	0.76	13.74	4.21	0.17	0.68	2.06	5.10	3.03	97.15
Average	68.59	0.88	13.86	4.26	0.17	0.74	2.09	4.41	3.13	98.38

Tephra	SiO₂	TiO₂	Al₂O₃	FeO	MnO	MgO	CaO	Na₂O₃	K₂O	Total
SILK-A12	69.71	0.73	13.74	4.28	0.10	0.84	2.06	5.20	3.06	99.91
	69.70	0.95	14.05	4.22	0.09	0.89	2.06	4.87	3.04	99.99
	69.17	0.90	13.95	4.22	0.16	0.80	2.05	5.08	3.05	99.49
	69.07	0.84	14.23	4.02	0.16	0.76	2.00	5.14	3.24	99.68
	68.89	0.82	14.01	4.20	0.20	0.71	2.05	4.97	3.09	99.06
	68.79	0.90	13.77	4.31	0.19	0.82	2.18	5.11	3.09	99.25
	68.77	0.81	14.06	4.20	0.16	0.72	2.08	5.11	3.18	99.34
	68.47	0.84	14.03	4.23	0.11	0.82	2.07	4.74	3.06	98.47
Average	69.07	0.85	13.98	4.21	0.15	0.80	2.07	5.03	3.10	99.40

Hekla 1947

Tephra	SiO ₂	TiO ₂	Al ₂ O ₃	FeO	MnO	MgO	CaO	Na ₂ O	K ₂ O	Total
Hekla 1947	63.91	1.03	15.12	7.80	0.21	1.25	4.17	4.18	1.66	99.33
	63.34	0.98	14.96	7.46	0.22	1.23	4.30	4.27	1.75	98.51
	62.97	0.92	15.34	7.72	0.24	1.25	4.42	4.83	1.88	99.50
	62.56	1.03	15.13	8.12	0.27	1.36	4.66	4.25	1.71	99.08
	62.51	0.88	15.30	8.09	0.20	1.14	4.54	4.77	1.65	99.08
	62.14	0.96	15.02	7.88	0.24	1.18	4.28	3.95	1.73	97.39
	62.01	0.91	15.28	7.99	0.20	1.32	4.40	4.26	1.77	98.13
	61.03	0.92	15.11	8.12	0.22	1.31	4.52	4.59	1.66	97.49
	60.07	1.33	15.13	8.63	0.26	1.73	5.15	2.88	1.61	96.76
	59.09	1.15	15.19	8.98	0.24	1.71	4.99	4.52	1.69	97.48
Average	62.15	0.98	15.13	8.01	0.22	1.28	4.46	4.38	1.73	98.48